The Synthesis and Reactivity of Main Group Heterocycles via Frustrated Lewis Pair Chemistry

by

Lauren Elizabeth Longobardi

A thesis submitted in conformity with the requirements
for the degree of Doctor of Philosophy

Department of Chemistry
University of Toronto

The Synthesis and Reactivity of Main Group Heterocycles via Frustrated Lewis Pair Chemistry

Lauren Elizabeth Longobardi

Doctor of Philosophy

Department of Chemistry
University of Toronto

2017

Abstract

Combinations of sterically encumbered Lewis acids and bases, now referred to as a frustrated Lewis pair (FLP), have been shown to have a rich and diverse chemistry. Their advent led to the development of hydrogenation catalysis and other important transformations based on metal-free systems. This thesis investigates the chemistry of main group heterocycles, specifically those bearing phosphorus and/or boron atoms, within the realm of frustrated Lewis pair chemistry.

Investigations of nitrogen Lewis bases included bulky anilines substituted with *para*-methoxy groups, which were found to undergo a tandem aromatic hydrogenation/transannulation reaction to yield bicyclic ammonium hydridoborate salts. Alkenyl- and alkynyl-tethered N-heterocycles were found to undergo intramolecular ring closure across the C–C π-bond when treated with $B(C_6F_5)_3$.

Frustrated Lewis pairs were found to undergo 1,3-addition to N-sulfinylamines, which generated phosphinimine-borane and phosphinimine-alane adducts of sulfur monoxide. The activated species were found to oxidize triphenylphosphine and transfer sulfur monoxide to Wilkinson's complex and N-heterocyclic carbenes.

Triphosphabenzene was shown to activate H_2 independently, and the mechanism of this reaction was investigated. Phosphaalkynes did not react with prototypical phosphine-borane FLPs, however they were amenable to hydroboration with Piers' borane, which resulted in an unexpected regiochemical outcome. The reactivity of the dimeric P_2B_2 heterocycles was examined.

Aliphatic ketones were demonstrated to undergo stoichiometric reduction to the corresponding borinic esters when exposed to one equivalent of $B(C_6F_5)_3$ and H_2. This methodology was applied to polycyclic aromatic diones, which resulted in formation of neutral borocyclic radicals. The chemical properties of the radicals were examined, and their reactivity with phosphorus, carbon, and nitrogen nucleophiles was explored.

Acknowledgments

I would not have accomplished the work in this thesis without the support and guidance from my supervisor Prof. Doug Stephan. You have been an invaluable mentor to me, you've showed me that it's possible to love what you do for a living, and always reminded me that Ph.D. research is supposed to be fun. I am eternally grateful to have worked in your lab; I believe that I am a better scientist, a better teacher, and a better person because of it. I would also like to acknowledge my committee members, Prof. Bob Morris and Prof. Datong Song, for their advice, feedback, and encouragement throughout my Ph.D.

I would like to thank the PIs who have collaborated on my projects: Professors Todd Marder, Chris Russell, John McGrady, Simon Duckett, and Stefan Grimme. Thank you to my collaborators from the Stephan laboratory over the years: Tayseer Mahdi, Connie Tang, Vanessa Wolter, Julian Heck, Tim Johnstone, Roman Korol, Pavel Zatsepin, and Karlee Bamford. I consider myself very lucky to have had the chance to work with such a talented group of people. I would also like to thank Tyler Schon and Eli Carrera for their help with CV and UV/vis.

I feel spoiled to have worked in a department with such exceptional support staff. Giant thank yous go out to NMR experts Darcy Burns, Sergiy Nokhrin, Dimity Pichugin, and Jack Sheng, you guys are VITAL to the synthetic groups at UofT! Thank you to Alan Lough, Rose Balazs, Matt Forbes, Chung Fung, John Ford, Jack O'Donnell, Ken Greaves, and Anna Liza Villavelez for all of your help and assistance over the years.

To the Stephan lab, past and present: you have been the best group of people to work with every day. Thank you for your support and your friendship. Special thanks to team X-ray: Boone, Chris, Fatme, Conor, Ian, Eliar, Judy, Alex, Kevin, and Tim. Thanks to my cubicle mates over the years, Boone, Rashi, and Jolie, it was a pleasure getting to know all of you.

To my best friend Emily Gosine, thank you for your love and support. Thank you for inspiring me to travel. Thank you for always being there for me.

To Dad, Mom, and Patrick, thank you for always believing in me and supporting me throughout my education. I hope I have made you proud.

Lastly, to Sean: you have been my #1 fan, my confidant, my shoulder to cry on, and brain to pick. You supported me when I needed it most, and celebrated every highlight and milestone with me. Without you, none of this would have been possible. Thanks for the best 4 years.

Table of Contents

List of Schemes

List of Figures

List of Tables

List of Abbreviations

Å	angstrom
°	degrees
°C	degrees Celsius
η	eta (bonding mode)
μ	bridging
δ	chemical shift
$\Delta\delta_{m\text{-}p}$	*meta-para* chemical shift separation
Δ	heat
ν	wavenumber
$\nu_{½}$	frequency difference at half height
δ	chemical shift
μL	microlitre
aq.	aqueous
Ar	aryl
Ad	adamantyl
atm	atmospheres
BINAP	2,2'-bis(diphenylphosphino)-1,1'-binaphthyl
Bn	benzyl
Boc	*tert*-butyloxycarbonyl
br	broad
Bz	benzoyl
C_6D_6	deuterated benzene
C_6D_5Br	deuterated bromobenzene
C_6F_5	pentafluorophenyl
CAAC	cyclic (alkyl)(amino)carbene
Cat	catechol
calcd	calculated
$CDCl_3$	deuterated chloroform
CD_2Cl_2	deuterated dichloromethane
CF_3	trifluoromethyl

$CHCl_3$	chloroform
CO	carbon monoxide
COD	1,5-cyclooctadiene
conv.	conversion
Cp	cyclopentadienide anion
Cp^*	1,2,3,4,5-pentamethylcyclopentadienide anion
Cy	cyclohexyl
d	doublet
d_6-DMSO	deuterated dimethylsulfoxide
d_8-THF	deuterated THF
d_8-toluene	deuterated toluene
DABCO	1,4-diazabicyclo[2.2.2]octane
DART	direct analysis in real time
dba	dibenzylideneacetone
DBU	1,8-diazabicycloundec-7-ene
d_{calc}	calculated density
DCE	1,2-dichloroethane
DCM	dichloromethane
dd	doublet of doublets
ddd	doublet of doublet of doublets
DFT	density functional theory
Dipp	2,6-diisopropylphenyl
DMF	*N,N*-dimethylformamide
ee	enantiomeric excess
EI	electron ionization
equiv.	equivalents
ESI	electrospray ionization
Et	ethyl
Et_2O	diethyl ether
EtOAc	ethyl acetate
F_c	calculated structure factor
Fc	ferrocene

FLP	frustrated Lewis pair
fMes	1,3,5-tris(trifluoromethyl)benzene
F_o	observed structure factor
g	grams
GOF	goodness of fit
h	hours
HOMO	highest occupied molecular orbital
HRMS	high resolution mass spectrometry
Hz	hertz
i	ipso
ICP-MS	Inductively coupled plasma – mass spectrometry
IDipp	1,3-Bis(2,6-diisopropylphenyl)-1,3-dihydro-2*H*-imidazol-2-ylidene
i-Pr	isopropyl
IMes	1,3-bis(2,4,6-trimethylphenyl)-1,3-dihydro-2*H*-imidazol-2-ylidene
IR	infrared
I(*t*-Bu)	1,3-Bis(*tert*-butyl)-1,3-dihydro-2*H*-imidazol-2-ylidene
$^{n}J_{xy}$	n-bond scalar coupling constant between x and y atoms
K	Kelvin
kcal	kilocalories
kHz	kilohertz
kJ	kilojoule
LUMO	lowest unoccupied molecular orbital
M	molarity
m	meta
m	multiplet
MAO	methylaluminoxane
Me	methyl
MeCN	acetonitrile
MeOH	methanol
Mes	mesityl, 2,4,6-trimethylphenyl
mg	milligram
MHz	megahertz

min	minutes
mL	millilitre
mmol	millimole
Ms	mesylate, methanesulfonate
m/*z*	mass to charge ratio
n-Bu	normal butyl
NBO	Natural Bond Orbital
NHC	N-heterocyclic carbene
NICS	nucleus independent chemical shift
nm	nanometre
NMR	Nuclear Magnetic Resonance
Np	neopentyl
o	ortho
OAc	acetate
OTf	trifluoromethylsulfonate, aka triflate
OTMS	trimethylsilyloxy
p	para
p-H_2	para hydrogen
p-Tolyl	4-methylphenyl
PES	potential energy surface
Ph	phenyl
POV-ray	Persistence of Vision Raytracer
ppm	parts per million
pTLC	preparative thin layer chromatography
py	pyridine
q	quartet
quant.	quantitative
quat	quaternary
rac	racemic
recrys.	recrystallize
rt	room temperature
R_w	weighted residual

s	singlet
sat.	saturated
S_EAr	electrophilic aromatic substitution
SIMes	1,3-bis(2,4,6-trimethylphenyl)-2-imidazolidinylidene
S_NAr	nucleophilic aromatic substitution
SO	sulfur monoxide
SO_2	sulfur dioxide
t	triplet
t-Bu	tertiary-butyl
TBS	tertiary-butyldimethylsilyl
Temp.	temperature
tert	tertiary
THF	tetrahydrofuran
TLC	thin layer chromatography
TMP	2,2,6,6-tetramethylpiperidine
TMS	trimethylsilyl
tol	toluene
o-Tolyl	2-methylphenyl
p-Tolyl	4-methylphenyl
trityl	triphenylmethyl
UV/vis	ultraviolet/visible
vt	virtual triplet
VT	variable temperature

Chapter 1
Introduction

1.1 Chemistry in a Global Context

Scientific advances have impacted nearly every aspect of modern human life. For example, we are able to grow enough food to supply the earth's growing population thanks to the Haber Bosch process.[1] Plastics continue to dominate as a preferred material in modern society due to Ziegler Natta catalyst development.[2–4] In addition, the life expectancy of both men and women in Canada is considerably longer than it was 100 years ago[5] owing to advances in medicine and pharmaceuticals. Despite the monumental impact that science has on daily life, there is a persistent distrust in the general public with regards to the opinions, and sometimes the general consensus, of scientists on certain topics. Chemicals in particular seem to be viewed by some as inherently toxic and dangerous substances that need to be avoided. Indeed, the marketing of chemical-free food, chemical-free sunscreen, chemical-free dry cleaning, and so on, has become commonplace. 2016 has been the hottest year ever recorded,[6] yet the veracity of anthropogenic global warming is still challenged. Some view vaccines as toxins instead of recognizing the number of lives vaccines have saved over decades of consistent administration. The author's hope for science in a global context is that the significant advances in communications (over 67% of Canadians owned a smartphone in 2014)[7] will lead to increased access to *accurate* information. This will hopefully lead to a global community that is more scientifically aware and is more educated when forming opinions with regards to scientific research.

While advances in science and technology have shaped 21st century life, in recent years there has been a decline in the support and funding opportunities for fundamental research.[8] The emphasis on applicable and interdisciplinary science is reflected in the availability of grants from national funding agencies. While application-driven research has certainly led to monumental discoveries, the development of fundamental science remains of the utmost importance because unexpected and unprecedented findings can lead to phenomena that can greatly impact the world. The discovery of phosphorus,[9] X-rays,[10] and penicillin[11] were all unanticipated findings. The work outlined in this thesis is predominantly focused on fundamental main group chemistry, and the exploration of novel compounds and their reactivity. In particular, examining how frustrated

Lewis pair (FLP) chemistry can be used to activate small molecules and generate new compounds with interesting and unexpected properties will be detailed.

1.2 Inorganic Chemistry – the Application of Transition Metals in Catalysis

The chemistry of the metallic elements is rich, well established, and broadly applied across synthetic academic and industrial chemistry. The motivation behind the rapid development of transition metal chemistry and the naissance of organometallic chemistry can be traced back to the seminal works of Grignard and Sabatier in the early 20th century, for which they shared the Nobel Prize awarded in 1912. Sabatier discovered that transition metals can effect the hydrogenation of C–C π-bonds,[12] and Grignard uncovered his eponymous reagents and their application in forming C–C bonds.[13] The monumental impact of Sabatier and Grignard's work on synthetic chemistry cannot be overemphasized. The 1960s saw the pioneering works of: Halpern, who disclosed the homogeneous Ru-catalyzed hydrogenation of olefins;[14] Wilkinson, who famously reported the synthesis of $RhCl(PPh_3)_3$ and proposed a catalytic hydrogenation mechanism based on rhodium hydrides;[15,16] and the independently published reports by Knowles[17] and Horner[18] on the development of Rh-catalyzed asymmetric hydrogenation of olefins. A list of hydrogenation milestones would be incomplete without the Haber-Bosch process, which generates the ammonia (NH_3) feedstock for fertilizers responsible for half of the world's food production, making it "the detonator of the population explosion."[1] The development of new catalysts and investigations into hydrogenation reactions have been ongoing, which may explain why hydrogenation is now referred to as "the most important catalytic method in synthetic organic chemistry both on the laboratory and the production scale."[19]

Beyond hydrogenation, metals are responsible for a number of other important transformations. Examples include the industrial bulk syntheses of rubber and silicone products mediated by a Pt-catalyzed hydrosilylation reaction,[20] the Monsanto acetic acid process facilitated by a rhodium catalyst,[21] the hydroformylation reaction using Rh and Co catalysts, which generates >10 million metric tons of product annually,[22] and more recently, olefin metathesis and ring opening metathesis polymerization (ROMP) catalyzed by W or Ru catalysts.[23] Transition metals are also now routinely employed in the industrial synthesis of fine chemicals; the development of Pd-catalyzed C–C[24–27] and C–N[28,29] cross coupling reactions has made them an indispensable

tool for medicinal and pharmaceutical chemistry. The applications of transition metals in catalysis are clearly immense and broadly ranging, and have drastically impacted chemical industry.

1.3 The Renaissance of Main Group Chemistry

Metal chemistry is not free from drawbacks; several examples of catalysis discussed above are facilitated by expensive, rare, and toxic transition metals, and the application of transition metal catalysis in the production of fine chemicals has led to complex ligand designs that are also costly to produce. Even with the inherent disadvantages of metals, the chemistry of main group elements has certainly lagged behind that of their transition metal neighbours. This could be due to the significant advances in the field of transition metal chemistry highlighted above, making it a popular and lucrative field of research, which led to an overshadowing of the main group elements. Additionally, early fundamental work on the heavier main group elements led to conclusions that they did not have distinct chemistry from their lighter counterparts, and certainly did not possess the rich chemistry of the transition metals.[30] Fortuitously (especially for the author), this is a naïve assumption.

1.3.1 Lewis' Theory

The concept of electron pair acceptors and electron pair donors, now commonly referred to as Lewis acids and bases, respectively, was put forth by Gilbert Lewis in 1916.[31] Seven years later, he published a textbook on his theory devoted to the valence of atoms and molecules.[32] These seminal reports laid the foundation for understanding how atoms bond and how molecules form. The so-called classical Lewis adduct is the product of combining a Lewis acid and a Lewis base (Scheme 1.1). A common example of a Lewis adduct is ammonia-borane ($H_3N–BH_3$). The Lewis base donates its electron pair to the Lewis acid, forming a dative bond; this is the same concept behind transition metal phosphine coordination complexes.

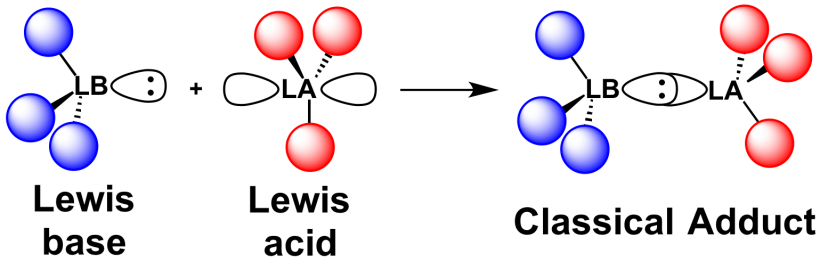

Scheme 1.1 – Cartoon depiction of a classical Lewis adduct.

1.3.2 Anomalies and Exceptions to Lewis Acid/Base Theory

There are several notable examples of exceptions to Lewis' theory, some of which are highlighted in Scheme 1.2. In 1942, Brown and co-workers found that, while BMe_3 forms classical adducts with pyridine and trimethylamine, it did not form an adduct with 2,6-lutidine, purportedly due to steric interference between the substituents (Scheme 1.2a).[33] Wittig also reported some key anomalies to Lewis' theory. In 1950, he observed ring opening of the THF–BPh_3 adduct when it was exposed to trityl anion instead of Ph_3C–BPh_3 adduct formation (Scheme 1.2b).[34] Wittig also found that PPh_3 and BPh_3 undergo 1,2-addition to benzyne, as opposed to Ph_3P–BPh_3 adduct formation (Scheme 1.2c).[35] Tochtermann reported that trityl anion and 2,3-dimethyl-1,3-butadiene do not react unless BPh_3 is present, which results in 1,4-addition to the diene (Scheme 1.2d). He proposed that this might be due to BPh_3 forming a π-complex with the butadiene.[36] The Stephan group expanded upon Wittig's 1950 report and found that THF adducts of $B(C_6F_5)_3$ undergo ring opening when subjected to a variety of phosphines and phosphides, instead of generating the classical Lewis adduct (Scheme 1.2f).[37] Erker discovered that treating $B(C_6F_5)_3$ with phosphorus ylide Ph_3P=CHPh leads to adduct formation at low temperature, but with prolonged heating a nucleophilic aromatic substitution occurs at the *para* position of a C_6F_5 ring to generate a phosphonium fluoroborate (Scheme 1.2e).[38] The Stephan group has subsequently reported similar *para*-attack products on $B(C_6F_5)_3$ using bulky phosphines as nucleophiles (Scheme 1.2g).[39] Similar reactivity is also observed when trityl cation is subjected to bulky phosphines (Scheme 1.2h).[40] It is now understood that these observations can be described as frustrated Lewis pair chemistry.

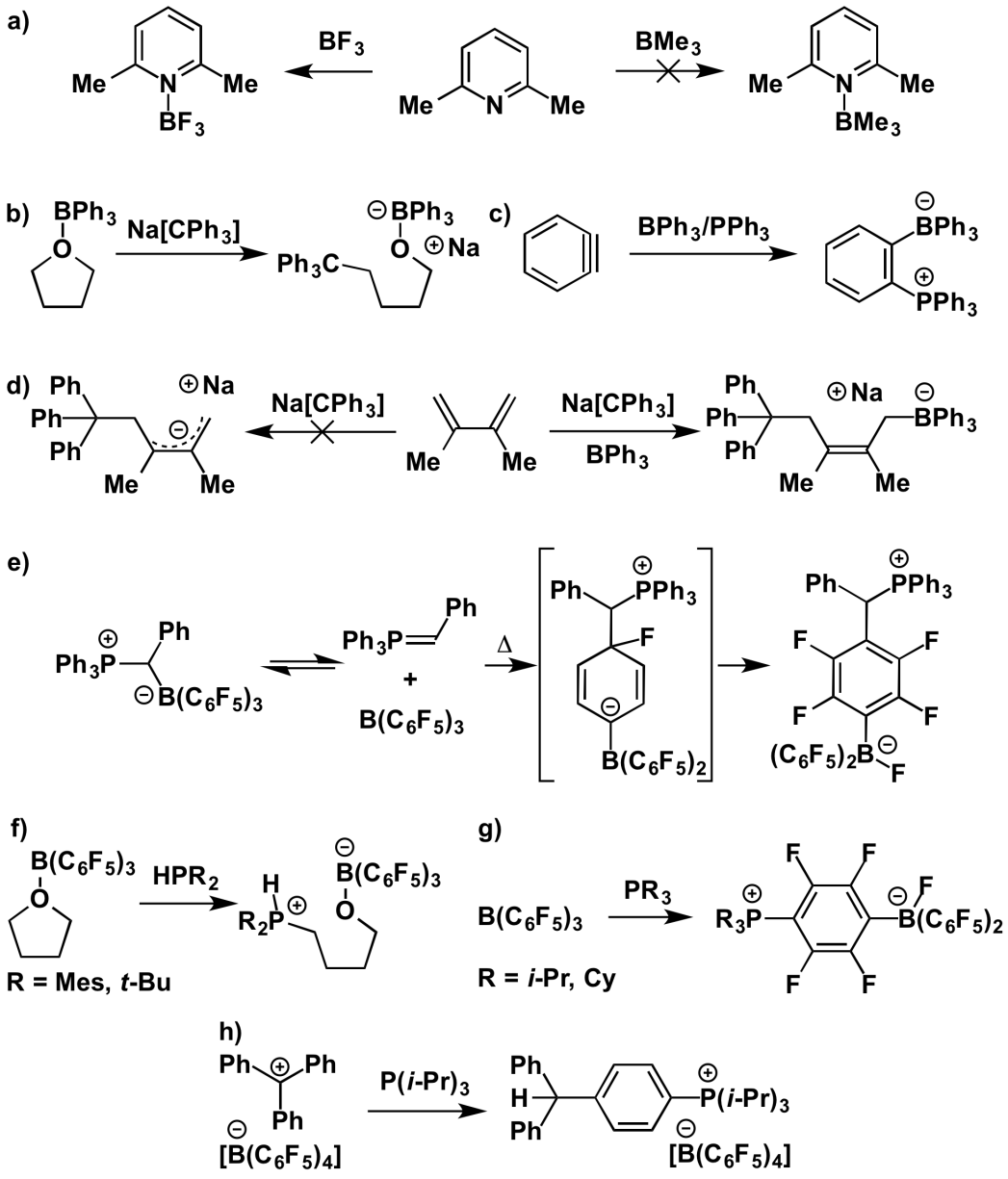

Scheme 1.2 – Examples where classical Lewis adduct formation does not prevail.

1.4 Frustrated Lewis Pair Chemistry

1.4.1 $B(C_6F_5)_3$ – The (not-so-little) Lewis Acid that Could

Throughout each chapter of this thesis, $B(C_6F_5)_3$ is omnipresent. Its role in these research projects ranges from a minor additive with little influence, to a key component for reactivity. It is commercially available, is soluble in organic solvents, and its reactivity can be monitored by both ^{11}B and ^{19}F NMR spectroscopy. It is a remarkable molecule that has recently found broad

application in frustrated Lewis pair (FLP) chemistry (*vide infra*), but also has a well-established domain in transition metal chemistry, specifically in olefin polymerization catalysis.

$B(C_6F_5)_3$ was first prepared by Massey in 1963.[41,42] The solid state structure of $B(C_6F_5)_3$ has remained elusive for over 50 years, however its minimum energy structure has been computed using DFT calculations.[43] The B–C bonds are 1.57 Å and the aryl substituents adopt a propeller-like configuration, with torsion angles of 40° between the C_6F_5 rings and the $B(C_6F_5)_2$ units (Figure 1.1a). It has good solubility in organic solvents, and is thermally robust (sublimation occurs at 80 °C under vacuum). The most notable feature of $B(C_6F_5)_3$ is its high Lewis acidity, as measured by the Gutmann-Beckett and Childs methods (Figure 1.1b).[43]

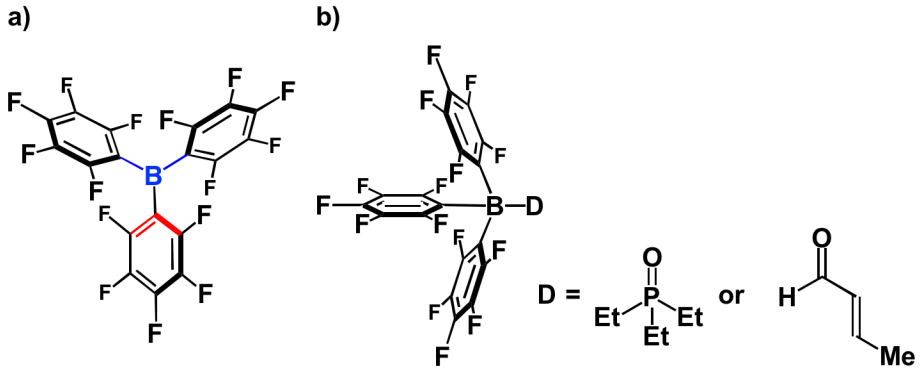

Figure 1.1 – a) Schematic depiction of $B(C_6F_5)_3$, with torsion angles highlighted in colour, and b) the classical Lewis adducts of $B(C_6F_5)_3$ with $Et_3P{=}O$ (Gutmann-Beckett)[44] and *trans*-crotonaldehyde (Childs).[45] D = donor.

$B(C_6F_5)_3$ has historically been used as an activator for olefin polymerization catalysis. In the early 1990s Marks reported that $B(C_6F_5)_3$ abstracts a methyl group from various zirconocene dialkyl complexes, generating species $[L_2ZrCH_3][CH_3B(C_6F_5)_3]$, where L = Cp, Cp^*, etc. (Scheme 1.3a).[46,47] These species were characterized through X-ray diffraction, and were found to be highly active homogeneous catalysts for the polymerization of ethylene, rivaling those activated by MAO. Erker also used $B(C_6F_5)_3$ to activate his zirconocene butadiene structures, generating $Cp_2Zr\text{-}C_4H_6\text{-}B(C_6F_5)_3$ (Scheme 1.3c), which is a highly active olefin polymerization catalyst that enabled the spectroscopic observation of an alkene-insertion product.[48] The Stephan group contributed to this field of research by applying phosphinimide ligands as mimics for Cp^* ligands; $B(C_6F_5)_3$ was successful in activating $[Cp^*((t\text{-}Bu)_3P{=}N)ZrMe_2]$ through abstraction of a

methyl group, and the resulting complex was demonstrated to be catalytically active for ethylene polymerization (Scheme 1.3b).[49]

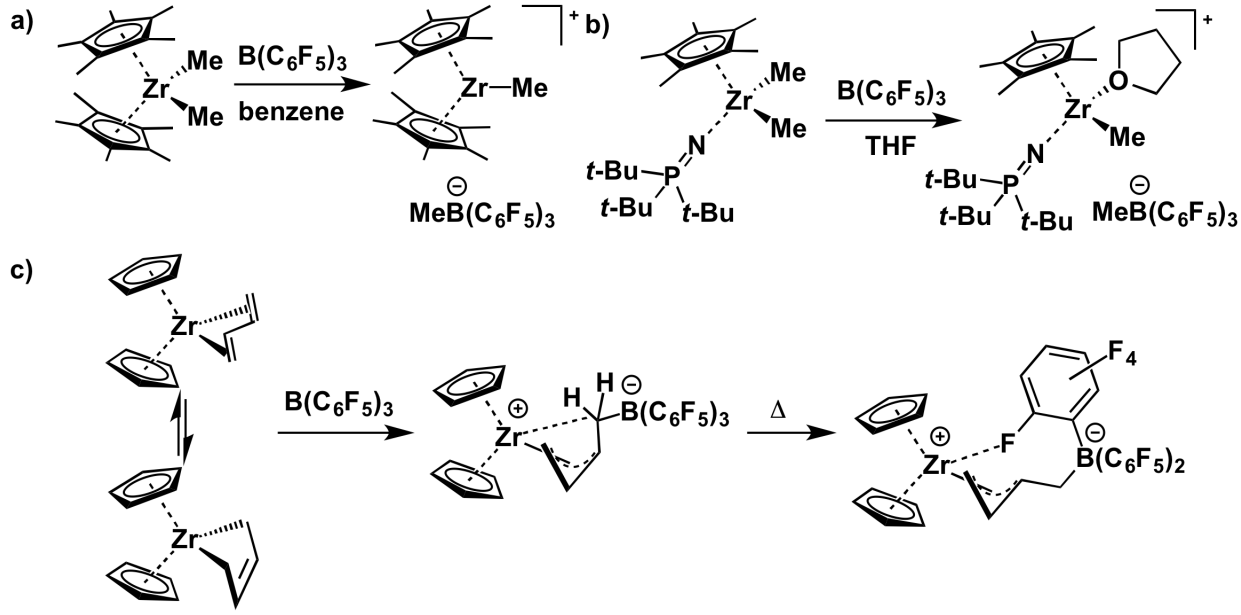

Scheme 1.3 – Examples of activation of olefin polymerization catalyst precursors using $B(C_6F_5)_3$.

$B(C_6F_5)_3$ has also been reported to be an active Lewis acid catalyst for transformations like aldol reactions[50] and Michael additions.[51] It was found to be an ideal Lewis acid because of its air stability and relative moisture tolerance. Piers also extensively applied $B(C_6F_5)_3$ as a catalyst for the hydrosilylation of carbonyl functional groups,[52,53] alcohols,[54] and imines,[55] and developed the proposed mechanism of activation.

1.4.2 Initial Reports of Frustrated Lewis Pairs

The propensity of $B(C_6F_5)_3$ to undergo *para*-attack when subjected to bulky nucleophiles was established by Erker in the 1990s.[38] The Stephan lab, when exploring analogous reactivity with phosphine nucleophiles, found that zwitterionic phosphonium fluoroborate Mes_2PH-(C_6F_4)-$BF(C_6F_5)_2$ reacts readily with Me_2SiHCl to generate the corresponding phosphonium borohydride (Scheme 1.4). The phosphonium borohydride was found to thermally liberate H_2 at temperatures >100 °C and, remarkably, this process was reversible, with the neutral phosphine borane activating H_2 at room temperature.[56] This report from 2006 was the

first example of a main group molecule that could *reversibly* activate H_2, and this initial discovery led to the rapid growth of this field of chemistry.

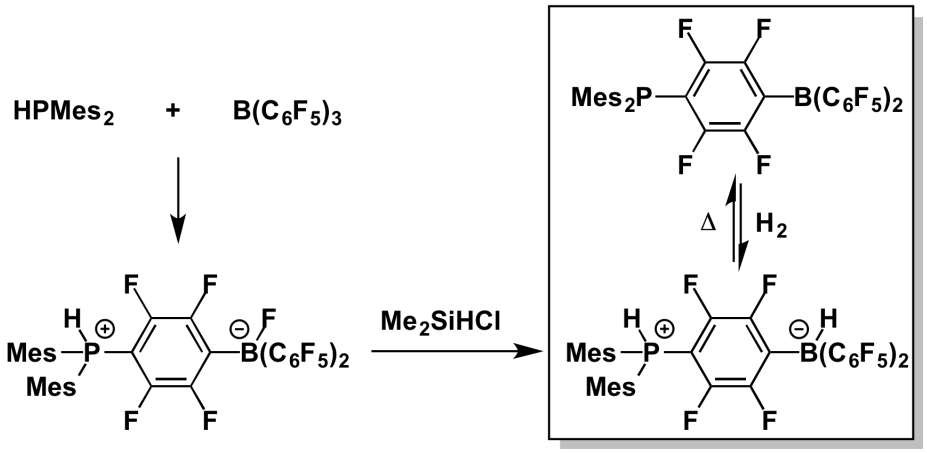

Scheme 1.4 – The first example of a main group species capable of reversible H_2 activation.

The ability of main group molecules to activate H_2 was not limited to intramolecular systems. In 2007, it was reported that combinations of $B(C_6F_5)_3$ with $P(t\text{-Bu})_3$ or $PMes_3$ could facilitate H_2 activation to generate $[R_3PH][HB(C_6F_5)_3]$ salts.[57] Unlike the intramolecular system (Scheme 1.4), this was not a reversible process. It was also found that BPh_3 could activate H_2 in combination with $P(t\text{-Bu})_3$, although this activation required longer reaction times and suffered lower yields than the analogous reaction with $B(C_6F_5)_3$.

The Erker laboratory also investigated phosphine-borane systems capable of effecting H_2 activation. They synthesized an intramolecular species by hydroboration of a vinylphosphine using Piers' borane, $HB(C_6F_5)_2$ (Scheme 1.5).[58] Spectroscopic evidence and DFT calculations suggest that this phosphine-borane forms an intramolecular adduct, but was still capable of activating H_2 at room temperature to yield the corresponding phosphonium hydridoborate salt.

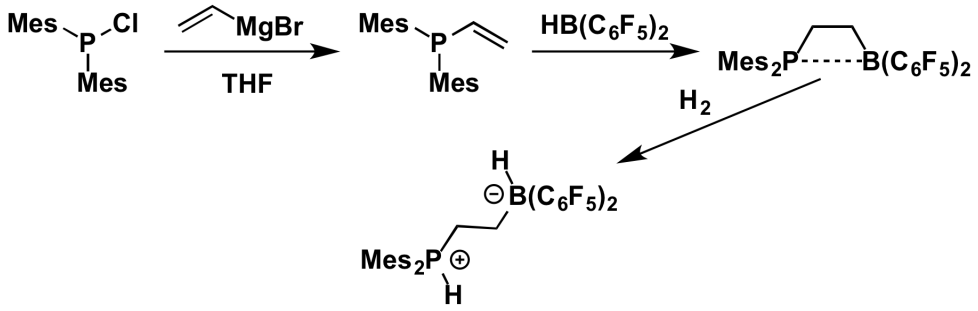

Scheme 1.5 – Synthesis and H_2 activation of Erker's phosphine-borane.

The mechanism by which these systems activate H_2 was difficult to investigate experimentally, as the uptake of H_2 is rapid even at low temperatures and pressures, and was further complicated by the difficulty to control the concentration of H_2 in solution.[59] There were examples from the literature detailing weak borane–H_2 complexes,[60–63] but no spectroscopic evidence of a $B(C_6F_5)_3$–H_2 complex was obtained.[57] There were also earlier reports describing the interaction of phosphines with H_2 in an argon matrix.[64] Computational investigations by Pápai[65] suggested the activation occurs via an "encounter complex" where P(*t*-Bu)$_3$ and $B(C_6F_5)_3$ form a unit held together by non-covalent H--F interactions, thus creating a binding pocket for H_2. This type of encounter complex was also proposed by Tamm using NHCs and $B(C_6F_5)_3$ to activate H_2.[66] Grimme later reevaluated this activation and proposed a non-linear transition state for both $B(C_6F_5)_3$/P(*t*-Bu)$_3$ and Erker's linked system, which generate an electric field where the H_2 molecule is polarized for subsequent activation.[67] This is the currently accepted model for the FLP activation of H_2.

1.4.3 Small Molecule Activations using Phosphine-Borane Combinations

1.4.3.1 Activation of C–C π-Bonds

Combinations of sterically encumbered phosphines and boranes which do not form classical Lewis adducts, and can effect H_2 activation, were first coined as "frustrated Lewis pairs" in 2007 (Scheme 1.6) when the Stephan laboratory reported the reactivity of P(*t*-Bu)$_3$ with $B(C_6F_5)_3$ and olefins.[68] The FLP was found to undergo 1,2-addition to ethylene, propylene, and 1-hexene, generating phosphonium borate zwitterions (Scheme 1.7a). While no interaction between the olefins and $B(C_6F_5)_3$ was observed, spectroscopic studies of a borane with a tethered olefin revealed evidence of a van der Waals complex (Scheme 1.7b).[69] This observation suggested that FLP activation of π-bonds may proceed initially by Lewis acid activation.

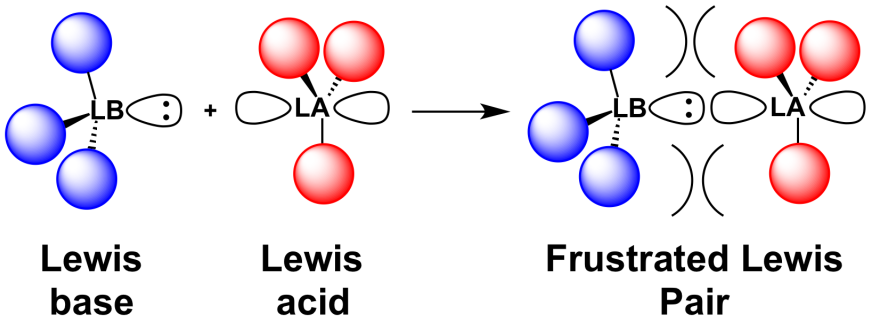

Scheme 1.6 – Cartoon depiction of a frustrated Lewis pair.

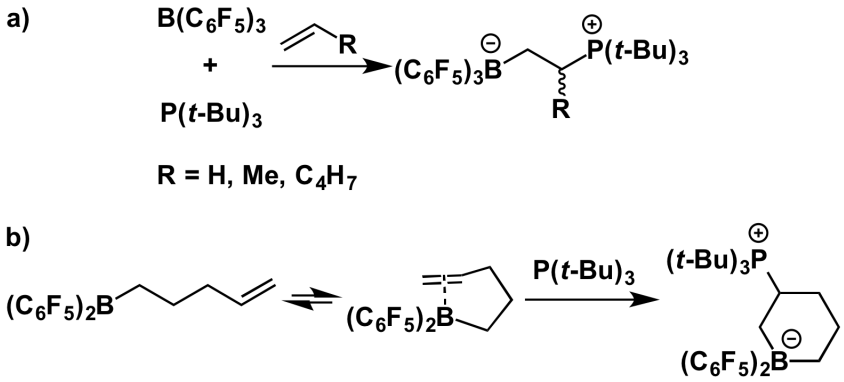

Scheme 1.7 – a) olefin activation by an FLP, and b) evidence for an olefin-borane interaction.

Frustrated Lewis pairs were also found to activate alkynes, although the outcome varied depending on the Lewis basic phosphine. Combinations of weakly basic phosphines (PPh_3 or P(*o*-Tolyl)$_3$) with $B(C_6F_5)_3$ or $Al(C_6F_5)_3$·tol in the presence of terminal alkynes led to zwitterionic 1,2-addition products (Scheme 1.8).[70] When the Lewis base was exchanged for the more strongly basic P(*t*-Bu)$_3$, the alkyne underwent deprotonation to form the phosphonium alkynyl borate. This reaction was later expanded to include nitrogen, carbon, and sulfur Lewis bases.[71]

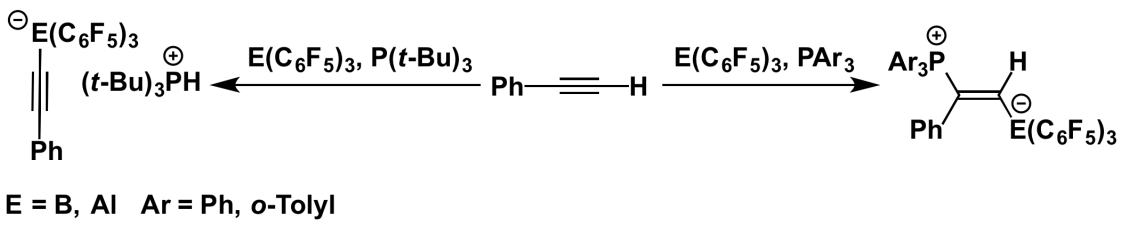

Scheme 1.8 – Activation of terminal alkynes by frustrated Lewis pairs.

1.4.3.2 Activation of CO_2, CO, and N_2O

The first example of CO_2 sequestration using an FLP was a collaborative effort between the Stephan and Erker laboratories.[72] The prototypical inter- and intramolecular FLPs $B(C_6F_5)_3/P(t\text{-}Bu)_3$ (Scheme 1.9a) and $Mes_2PCH_2CH_2B(C_6F_5)_2$ (Scheme 1.9b) were shown to sequester CO_2 via a reversible 1,2-addition across a C=O bond. The related system $ClB(C_6F_5)_2/P(t\text{-}Bu)_3$, which sequesters CO_2 reversibly, was investigated using microfluidic technology.[73] Recently, the Dielmann group reported that highly electron-rich phosphines are able to reversibly activate CO_2 without a Lewis acid additive.[74]

There are also examples describing the reactivity of CO with FLPs. The Erker group reported that the exposure of an intramolecular FLP to CO and $HB(C_6F_5)_2$ resulted in the formation of a formyl group that is side-on bound to boron (Scheme 1.9c).[75,76] The Stephan group described the reactivity of intermolecular FLPs with syngas (CO + H_2), which forms an epoxy borate that can undergo further reactivity with CO or H_2 (Scheme 1.9d).[77]

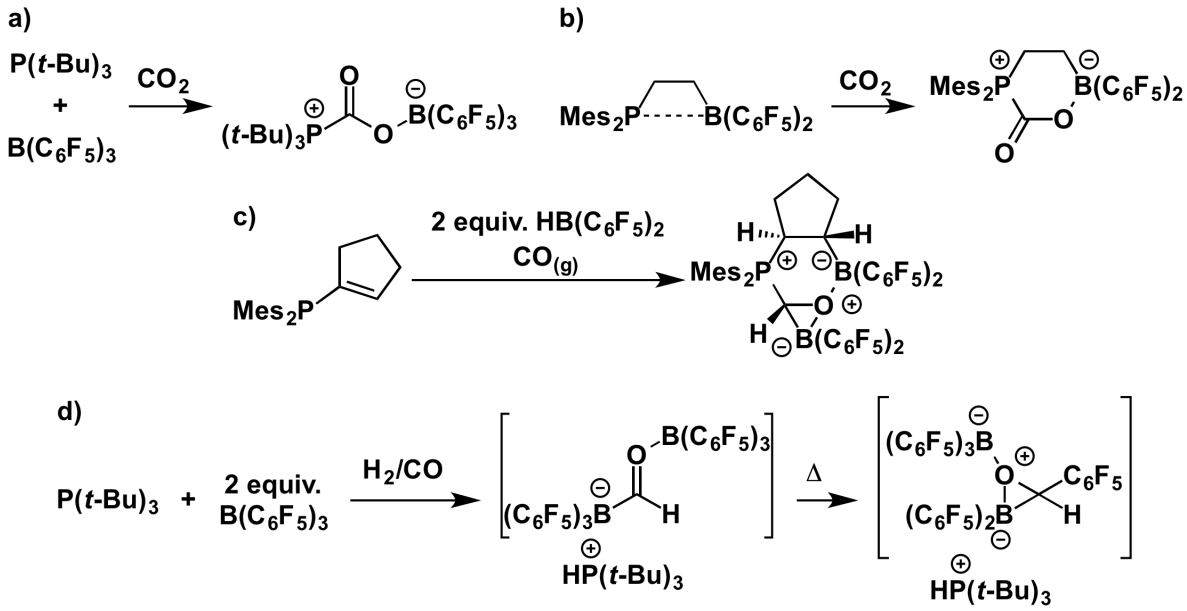

Scheme 1.9 – Examples of CO_2 and CO reactivity with inter- and intramolecular FLPs.

The reactivity of N_2O has also been evaluated with several different FLP combinations. The first report described the sequestration of N_2O with combinations of $P(t\text{-}Bu)_3$ and highly electrophilic boranes (Scheme 1.10a).[78] This capture is not reversible, and the activated species undergoes thermal liberation of N_2 to form a phosphine oxide-borane adduct, which is reminiscent of the

Staudinger oxidation process.[79] Subsequent studies found that strong Lewis acids such as $[CPh_3]^+$ and zirconocenium successfully captured N_2O with phosphines in a 1,3-addition process.[80] It was later found that N_2O activation by P(*t*-Bu)$_3$ and Al(C_6F_5)$_3$ leads to the formation of a "frustrated radical pair" when the adduct is exposed to additional Al(C_6F_5)$_3$[81] (see Chapter 6). Recently, Aldridge achieved the first reversible FLP activation of N_2O using a conformationally rigid phosphine-borane based on a dimethylxanthene backbone (Scheme 1.10b). With this system, clean liberation of N_2O was observed with no phosphine oxide formation. This rigid FLP was also found to catalytically dehydrogenate ammonia-borane and amine-boranes to generate B–N heterocycles.[82]

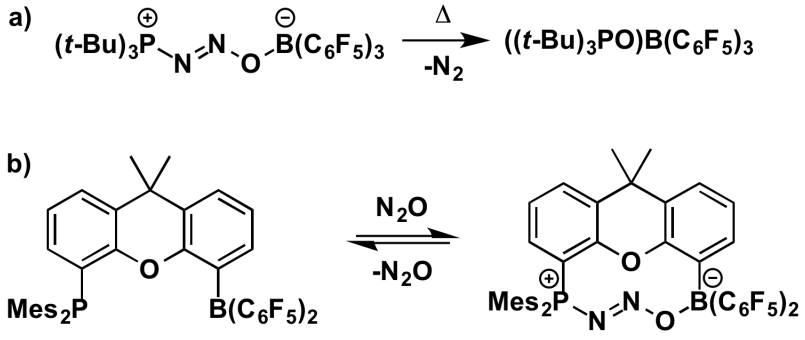

Scheme 1.10 – a) Irreversible FLP activation of N_2O, and b) reversible FLP N_2O activation.

1.4.4 Beyond Phosphine Lewis Bases and B(C_6F_5)$_3$

1.4.4.1 Group XIV, XV, and XVI Lewis Bases

The field of FLP chemistry quickly moved beyond the classic phosphine-borane combinations to accommodate other Lewis basic components. Early investigations of carbon-based Lewis bases, like NHCs, found that sufficient steric bulk was needed to preclude adduct formation with B(C_6F_5)$_3$. IDipp formed a classical Lewis adduct with B(C_6F_5)$_3$, which did not heterolytically cleave H_2.[83] Exchanging IDipp for I(*t*-Bu) led to the clean, quantitative formation of the corresponding imidazolium hydridoborate salt (Scheme 1.11a).[66,83] Krempner achieved H_2 activation using a sterically encumbered carbanion with weaker boron Lewis acids.[84] These representative examples of carbon Lewis bases in FLP chemistry activate H_2 irreversibly with boranes.

A variety of N-based Lewis bases, such as imines, amines, and N-heterocycles, have also been shown to activate numerous small molecules, including H_2, when combined with $B(C_6F_5)_3$ (see Chapter 2 for a more detailed overview).[59]

More recent FLP chemistry has delved into chalcogen-based Lewis bases. Repo reported in 2012 that ketones and aldehydes activate H_2 in combination with $B(C_6F_5)_3$ at elevated temperatures (see Chapters 5&6 for FLP carbonyl chemistry).[85] A remarkable discovery in 2013 was the combination of $B(C_6F_5)_3$ with Et_2O, which was found to form a sufficiently labile adduct such that H_2 was activated under mild conditions.[86] Inter- and intramolecular borane-thioether combinations were found to activate alkynes (Scheme 1.11b).[71,87] The Erker group explored sulfur Lewis bases in the 1,1-carboboration of thioalkynes to generate an intramolecular borane-thioether FLP (Scheme 1.11c)[88] and thiophenes.[89] The Stephan group investigated tellurium Lewis bases for 1,1-carboboration reactions of tellurium alkynes with $B(C_6F_5)_3$,[90] and the FLP reactivity of the resulting borane-telluroether FLP (Scheme 1.11c).[91]

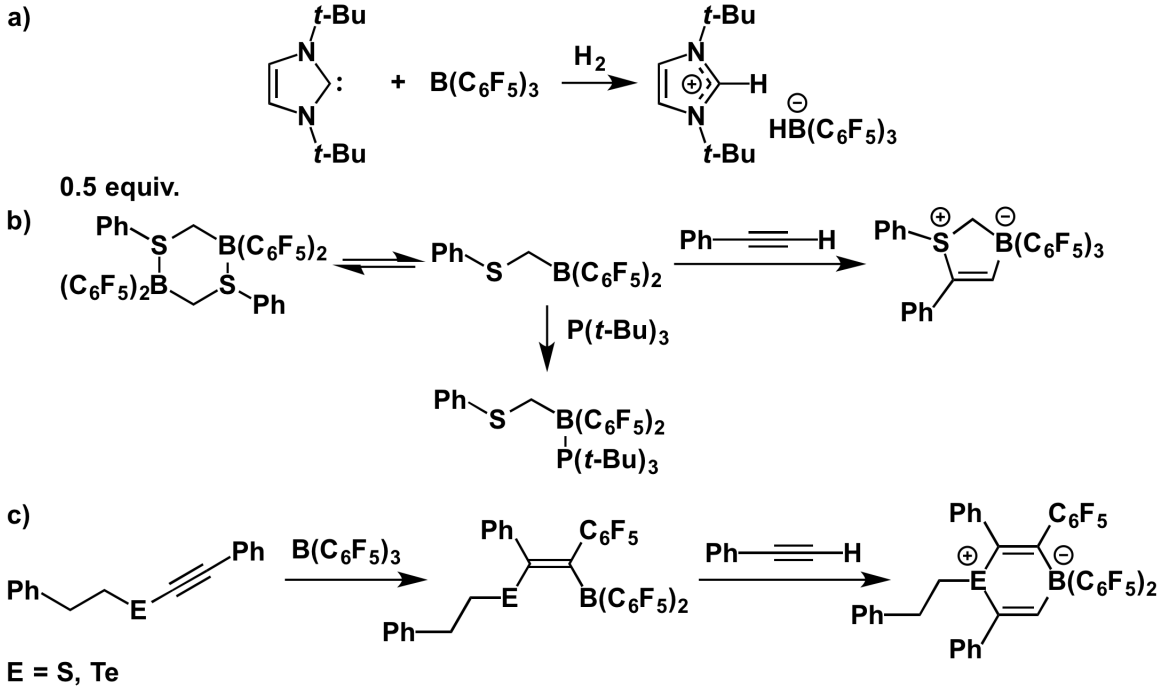

Scheme 1.11 – Examples of the reactivity of a) carbon Lewis bases, b) sulfur Lewis bases, and c) sulfur and tellurium Lewis bases in FLP chemistry.

1.4.4.2 Alternative Boron Lewis Acids in FLP Chemistry

Boranes that are less Lewis acidic than $B(C_6F_5)_3$ have been used in concert with stronger Lewis bases to effect FLP activation of H_2 (such as $BPh_3/P(t\text{-}Bu)_3$, see section 1.4.2). Tamm used $B(3,5\text{-}(CF_3)_2C_6H_3)_3$ in combination with I(*t*-Bu) to effect small molecule activations.[92] Arduengo demonstrated that less Lewis acidic boranes, such as trialkylboranes, could heterolytically cleave H_2 in combination with NHCs, which then undergo reduction by the borohydride to generate aminals.[93] Krempner has achieved the activation of H_2 with weakly acidic boranes by using protected carbanions[84] and Verkade's base.[94]

The synthetic challenges associated with C_6F_5-substituted boranes,[95] along with their intolerance of many functional groups,[96] led to the application of borenium cations in FLP chemistry. To this effect, NHC-stabilized 9-BBN cations with non-coordinating anions were shown to activate H_2 with phosphorus and nitrogen Lewis bases at room temperature, albeit at elevated H_2 pressures (Scheme 1.12).[97,98] This chemistry was later expanded to include triazole-stabilized borenium cations.[99]

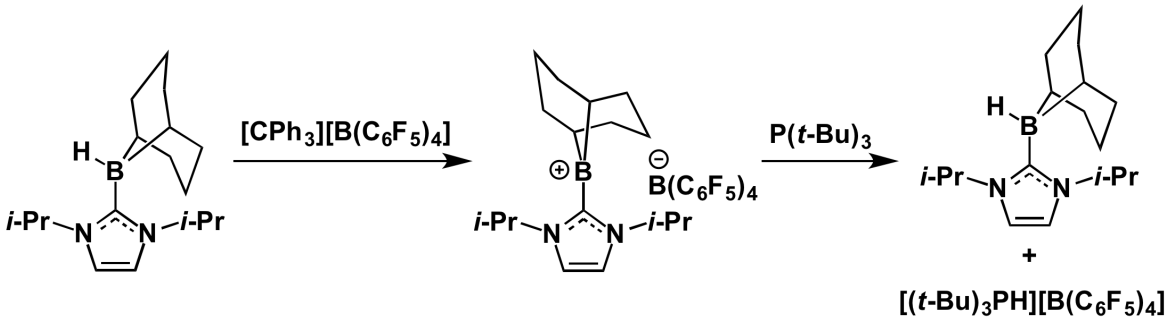

Scheme 1.12 – Generation of an NHC-stabilized borenium cation, and subsequent H_2 activation with $P(t\text{-}Bu)_3$.

1.4.5 Frustrated Lewis Pairs in Catalysis

Catalysis is not a prominent feature of this thesis, however the significant advances of FLP hydrogenation catalysis are worth highlighting. Many of the FLP examples presented in this chapter have been found to hydrogenate polarized substrates. The first report used the original linked FLP system (Scheme 1.4) to hydrogenate imines, protected nitriles, and aziridines.[100] It was later discovered that imines could behave as the Lewis basic component, and $B(C_6F_5)_3$ was exploited as the catalyst.[101] Erker's linked system (Scheme 1.5) is a notable hydrogenation

catalyst for imines and enamines,[102] and using a naphthalene-tethered diphosphine in combination with $B(C_6F_5)_3$ enabled the hydrogenation of silyl enol ethers.[103] There are now FLP systems capable of hydrogenating organic substrates like olefins,[86,104,105] alkynes,[106] oximes,[107] hydrazones,[108] ketones,[109] and aldehydes.[110] NHC-stabilized borenium cations remain the most active FLP hydrogenation catalysts.[98] Beyond hydrogenation, other notable examples of FLP catalysis include the $B(C_6F_5)_3$-catalyzed hydroamination of alkynes,[111] and the elegant recent work by Fontaine detailing C–H borylation using an intramolecular FLP.[112]

The majority of the FLP systems discussed in Section 1.4 require a judicious choice of solvent, as the unquenched empty and filled orbitals of the Lewis acid and base, respectively, are vital for small molecule activation. Polar, aprotic solvents like C_6D_5Br and DCM are generally compatible, given that they do not quench either FLP component and can solubilize the FLP adducts of small molecules. Ethereal solvents, while initially believed to be detrimental to FLP chemistry, have recently been demonstrated to behave as Lewis bases for the FLP activation of H_2.[86,109,110,113] Polar, protic solvents like MeOH and H_2O are generally incompatible with FLP systems, as they typically form irreversible adducts with the Lewis acidic component, or the Lewis acids are prone to degradation by protonolysis and B–O bond formation.

1.5 Heterocyclic Chemistry at a Glance

A unifying theme of this thesis is investigating the synthesis and reactivity of heterocycles. Heterocycles are omnipresent in natural products: many alkaloids are based on an N-heterocyclic scaffold, and this enormous class of molecules can display a wide range of pharmacological activity. Commonly cited examples include nicotine, morphine, and quinine. While nitrogen-containing rings are the most prevalent in pharmaceuticals, drugs that incorporate elements such as boron have garnered increased interest. The drugs Kerydin and Crisaborole, which are prescribed to treat fungal infections and atopic dermatitis, respectively, each contain a five-membered boron heterocycle (Figure 1.2).[114]

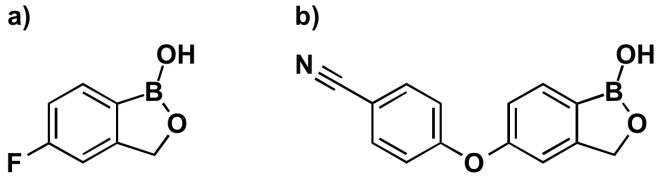

Figure 1.2 – Structures of a) Kerydin (tradename Tavaborole) and b) Crisaborole.

Cyclic molecules can have dissimilar properties to their acyclic counterparts. An example of this is cyclic peptides. Linear peptides can display poor stability and are prone to degradation under biological conditions, however cyclic analogues have improved metabolic stability and membrane permeability, and thus have been targeted for pharmaceutical treatments.[115,116]

When introduced into an all-carbon ring, heteroatoms can impose new chemical properties. For example, benzene is a non-polar molecule with D_{6h} symmetry, its ^{1}H NMR chemical shift ($CDCl_3$) is 7.36 ppm,[117] and it is reactive in S_EAr reactions. Pyridine, where one carbon atom is replaced with nitrogen, is a polar molecule with C_{2v} symmetry, has ^{1}H NMR ($CDCl_3$) resonances at 8.62, 7.29, and 7.68 ppm, and is less reactive in S_EAr reactions. These properties are indicative of a less electron-rich π-system due to the electron-withdrawing ability of nitrogen.

The geometrical constraints associated with heterocycles can bestow unique chemical properties on the molecule. For example, Radosevich has developed heterocyclic phosphines capable of catalyzing the transfer hydrogenation of diazo compounds,[118] and oxidatively adding E–H bonds (E = O, N),[119] both reactions that are not observed for classic acyclic phosphines. Some other examples of main group heterocycles that have shown exceptional reactivity are Piers' antiaromatic boroles that undergo H_2 activation,[120] and Stephan's B/Te heterocycle that undergoes alkyne exchange,[121] a transformation reminiscent of Le Floch and Mathey's diazaphosphinines (Scheme 1.13).[122] Their rich, diverse, and sometimes unexpected chemistry makes studying the synthesis and reactivity of heterocycles a fascinating research topic.

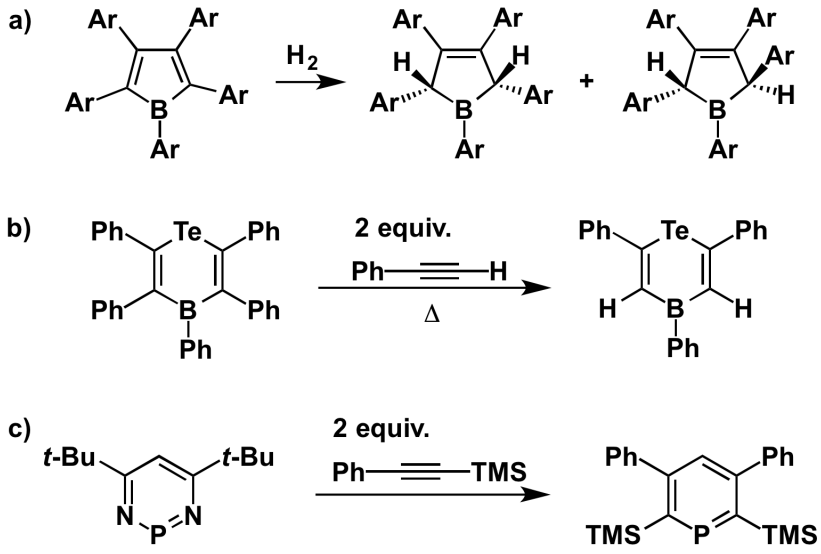

Scheme 1.13 – Examples of the reactivity of heterocycles: a) borole H_2 activation, and alkyne exchange by b) a B/Te heterocycle and c) a 1,3,2-diazaphosphinine.

1.6 Scope of Thesis

The objective of the author's graduate work was to investigate the role of heterocycles in FLP chemistry: heterocycles as substrates for FLP-mediated transformations, heterocyclic products generated by FLP chemistry, or heterocycles as a masked FLP. The projects presented in this thesis cover a wide range of synthetic chemistry. Chapter 2 focuses on nitrogen Lewis bases in FLP chemistry, and discusses two main projects: the $B(C_6F_5)_3$-mediated hydrogenation of *para*-substituted anilines to yield bicyclic products, and the addition of N-heterocycles to tethered alkenes and alkynes with $B(C_6F_5)_3$. Chapter 3 explores the activation of N-sulfinylamines by FLPs, and the reactivity of NSO-containing heterocycles. Chapter 4 details work in low coordinate phosphorus chemistry, including the reactivity of triphosphabenzene with H_2 and hydroborations of phosphaalkynes. Chapters 5 & 6 explore the reactivity of $B(C_6F_5)_3$ with carbonyl substrates: Chapter 5 presents the stoichiometric hydrogenation of ketones and aldehydes, and Chapter 6 presents the formation of borocyclic radicals through FLP hydrogenation, and their respective chemistry.

The project in Chapter 2 that investigates the hydrogenation of *para*-substituted anilines was performed in collaboration with Dr. Tayseer Mahdi, who discovered the reaction. The C–C π-bond addition project was started by Dr. Peter Dornan, who discovered the transformation, synthesized starting materials, and performed NMR scale reactions. All synthetic work presented

in the chapter was conducted by the author. Two visiting students from the University of Mainz, Ms. Vanessa Wolter and Mr. Julian Heck, worked on projects presented in Chapter 3 under the supervision of the author. Vanessa assisted in the synthesis of **3-1**, and grew crystals of **3-2** and **3-3** used for X-ray diffraction studies. Julian investigated sulfur diimine chemistry; while this is not discussed in great detail, his contribution is certainly acknowledged. The author performed all other synthetic chemistry. The chemistry in Chapter 4 was performed in collaboration with the Russell group at the University of Bristol. They synthesized **4-1** and **4-11**. The author performed all other synthetic work. DFT calculations were performed by Prof. John McGrady at the University of Oxford and Dr. Tim Johnstone at the University of Toronto. *Para*-hydrogen experiments were performed by Prof. Simon Duckett at the University of York. The ketone and aldehyde hydrogenation reactions in Chapter 5 were performed in collaboration with Ms. Connie Tang, an undergraduate student under the supervision of the author. The synthetic work surrounding boranes **5-6** and **5-7** was performed by the author. The DFT calculations in Chapter 6 were performed by Prof. Stefan Grimme and Dr. Lei Liu at the Universität Bonn. All synthetic work was performed by the author. Elemental analyses and high resolution mass spectrometry were performed by ANALEST and AIMS, respectively, at the University of Toronto.

Portions of each chapter have been published or drafted for publication at the time of writing: **Chapter 2**: **1)** Longobardi, L. E.; Mahdi, T.; Stephan, D. W. "$B(C_6F_5)_3$ Mediated Arene Hydrogenation/Transannulation of *para*-methoxyanilines." *Dalton Transactions* **2015**, *44*, 7114–7117. **2)** Dornan, P. K.; Longobardi, L. E.; Stephan, D. W. "Reversible Frustrated Lewis Pair Addition of N-Heterocycles to Unsaturated C–C bonds." *Synlett* **2014**, *25*, 1521–1524. **Chapter 3**: **1)** Longobardi, L. E.; Wolter, V.; Stephan, D. W. "Frustrated Lewis Pair Activation of an N-Sulfinylamine: A Source of Sulfur Monoxide." *Angewandte Chemie International Edition* **2015**, *54*, 809–812.

Chapter 4: **1)** Longobardi, L. E.; Russell, C. A.; Green, M.; Townsend, N. S.; Wang, K.; Holmes, A. J.; Duckett, S. B.; McGrady, J. E.; Stephan, D. W. "Hydrogen Activation by an Aromatic Triphosphabenzene." *Journal of the American Chemical Society* **2014**, *136*, 13453–13457. **2)** Longobardi, L. E.; Johnstone, T. C.; Falconer, R. L.; Russell, C. A.; Stephan, D. W. "Hydroboration of Phosphaalkynes by $HB(C_6F_5)_2$." *Chemistry – A European Journal* **2016**, *22*, 12665–12669.

Chapter 5: **1)** Longobardi, L. E.; Tang, C.; Stephan, D. W. "Stoichiometric Reductions of Alkyl-Substituted Ketones and Aldehydes to Borinic Esters." *Dalton Transactions* **2014**, *43*,

15723–15726. **2)** Zhang, Z.; Edkins, R. M.; Nitsch, J.; Fucke, K.; Steffen, A.; Longobardi, L. E.; Stephan, D. W.; Lambert, C.; Marder, T. B. "Optical and Electronic Properties of Air-Stable Organoboron Compounds with Strongly Electron-Accepting bis(fluoromesityl) Groups." *Chemical Science* **2015**, *6*, 308–321.

Chapter 6: **1)** Longobardi, L. E.; Liu, L.; Grimme, S.; Stephan, D. W. "Stable Borocyclic Radicals via Frustrated Lewis Pair Hydrogenations." *Journal of the American Chemical Society* **2016**, *138*, 2500–2503. **2)** Longobardi, L. E.; Zatsepin, P.; Korol, R.; Liu, L.; Grimme, S.; Stephan, D. W. "Reactions of Boron-Derived Radicals with Nucleophiles." *Journal of the American Chemical Society*, DOI: 10.1021/jacs.6b11190.

1.7 References

(1) Smil, V. *Nature* **1999**, *400*, 415.

(2) Ziegler, K.; Holzkamp, E.; Breil, H.; Martin, H. *Angewandte Chemie* **1955**, *67*, 541–547.

(3) Natta, G.; Pino, P.; Corradini, P.; Danusso, F.; Mantica, E.; Mazzanti, G.; Moraglio, G. *Journal of the American Chemical Society* **1955**, *77*, 1708–1710.

(4) Feature, N. *Nature* **2016**, *536*, 266–268.

(5) World Health Organization http://www.who.int/countries/can/en/ (accessed Aug 28, 2016).

(6) "NASA Analysis Finds July 2016 is Warmest on Record" http://data.giss.nasa.gov/gistemp/news/20160816/ (accessed Aug 28, 2016).

(7) Communications Monitoring Report 2015 - Canadian Radio-television and Telecommunications Commission.

(8) Manners, I. *Angewandte Chemie International Edition* **2016**, *55*, 3834–3835.

(9) Weeks, M. E. *Journal of Chemical Education* **1933**, *9*, 302–306.

(10) Glasser, O. *American Journal of Roentgenology* **1995**, *165*, 1033–1040.

(11) Bennett, J. W.; Chung, K.-T. *Advances in Applied Microbiology* **2001**, *49*, 163–184.

(12) Sabatier Paul. *Industrial and Engineering Chemistry* **1926**, *18*, 1005–1008.

(13) Grignard, V. *Comptes Rendus* **1900**, *130*, 1322–1324.

(14) Halpern, J.; Harrod, J. F.; James, B. R. *Journal of the American Chemical Society* **1961**, *83*, 753–754.

(15) Young, J. F.; Osborn, J. A.; Jardine, F. H.; Wilkinson, G. *Chemical Communications* **1965**, 131–132.

(16) Osborn, J. A.; Jardine, F. H.; Young, J. F.; Wilkinson, G. *Journal of the Chemical Society A* **1966**, 1711–1732.

(17) Knowles, W. S.; Sabacky, M. J. *Chemical Communications* **1968**, 1445–1446.

(18) Büthe, H.; Siegel, H.; Horner, L. *Angewandte Chemie International Edition* **1968**, *7*, 942.

(19) Blaser, H.-U.; Malan, C.; Pugin, B.; Spindler, F.; Steiner, H.; Studer, M. *Advanced Synthesis & Catalysis* **2003**, *345*, 103–151.

(20) Troegel, D.; Stohrer, J. *Coordination Chemistry Reviews* **2011**, *255*, 1440–1459.

(21) Le Berre, C.; Serp, P.; Kalck, P.; Torrence, G. P. In *Ullmann's Encyclopedia of Industrial Chemistry*; 2014; pp 1–34.

(22) Franke, R.; Selent, D.; Börner, A. *Chemical Reviews* **2012**, *112*, 5675–5732.

(23) Mol, J. C. *Journal of Molecular Catalysis A: Chemical* **2004**, *213*, 39–45.

(24) Miyaura, N.; Suzuki, A. *Chemical Reviews* **1995**, *95*, 2457–2483.

(25) Stille, J. K. *Angewandte Chemie International Edition* **1986**, *25*, 508–524.

(26) Knappke, C. E. I.; Jacobi von Wangelin, A.; von Wangelin, A. J. *Chemical Society Reviews* **2011**, *40*, 4948–4962.

(27) Corbet, J. P.; Mignani, G. *Chemical Reviews* **2006**, *106*, 2651–2710.

(28) Surry, D. S.; Buchwald, S. L. *Chemical Science* **2011**, *2*, 27–50.

(29) Hartwig, J. F. *Nature* **2008**, *455*, 314–322.

(30) Power, P. P. *Nature* **2010**, *463*, 171–177.

(31) Lewis, G. N. *Journal of the American Chemical Society* **1916**, *38*, 762–785.

(32) Lewis, G. N. *Valence and the Structure of Atoms and Molecules*; The Chemical Catalogue Company: New York, 1923.

(33) Brown, H. C.; Schlesinger, H. I.; Cardon, S. Z. *Journal of the American Chemical Society* **1942**, *64*, 325–329.

(34) Wittig, G.; Rückert, A. *Justus Liebigs Annalen Der Chemie* **1950**, *566*, 101–113.

(35) Wittig, G.; Benz, E. *Chemische Berichte* **1959**, *92*, 1999–2013.

(36) Tochtermann, W. *Angewandte Chemie International Edition* **1966**, *5*, 351–371.

(37) Welch, G. C.; Masuda, J. D.; Stephan, D. W. *Inorganic Chemistry* **2006**, *45*, 478–480.

(38) Döring, S.; Erker, G.; Frölich, R.; Meyer, O.; Bergander, K. *Organometallics* **1998**, *17*, 2183–2187.

(39) Welch, G. C.; Cabrera, L.; Chase, P. A.; Hollink, E.; Masuda, J. D.; Wei, P.; Stephan, D. W. *Dalton Transactions* **2007**, 3407–3414.

(40) Cabrera, L.; Welch, G. C.; Masuda, J. D.; Wei, P.; Stephan, D. W. *Inorganica Chimica Acta* **2006**, *359*, 3066–3071.

(41) Massey, A. G.; Park, A. J.; Stone, F. G. A. *Proceedings of the Chemical Society* **1963**, 212.

(42) Massey, A. G.; Park, J. *Journal of Organometallic Chemistry* **1964**, *2*, 245–250.

(43) Ashley, A. E.; Herrington, T. J.; Wildgoose, G. G.; Zaher, H.; Thompson, A. L.; Rees, N. H.; Krämer, T.; O'Hare, D. *Journal of the American Chemical Society* **2011**, *133*, 14727–14740.

(44) Viktor Gutmann. *Coordination Chemistry Reviews* **1976**, *18*, 225–255.

(45) Childs, R. F.; Mulholland, D. L.; Nixon, A. *Canadian Journal of Chemistry* **1982**, *60*, 801–808.

(46) Yang, X.; Stern, C. L.; Marks, T. J. *Journal of the American Chemical Society* **1991**, *113*, 3623–3625.

(47) Yang, X.; Stern, C. L.; Marks, T. J. *Journal of the American Chemical Society* **1994**, *116*, 10015–10031.

(48) Erker, G. *Accounts of Chemical Research* **2001**, *34*, 309–317.

(49) Stephan, D. W. *Organometallics* **2005**, *24*, 2548–2560.

(50) Ishihara, K.; Funahashi, M.; Hanaki, N.; Miyata, M.; Yamamoto, H. *Synlett* **1994**, 963–964.

(51) Ishihara, K.; Hananki, N.; Yamamoto, H. *Synlett* **1993**, 577–579.

(52) Parks, D. J.; Piers, W. E. *Journal Of The American Chemical Society* **1996**, *118*, 9440–9441.

(53) Parks, D. J.; Blackwell, J. M.; Piers, W. E. *The Journal of Organic Chemistry* **2000**, *65*, 3090–3098.

(54) Blackwell, J. M.; Foster, K. L.; Beck, V. H.; Piers, W. E. *The Journal of Organic Chemistry* **1999**, *64*, 4887–4892.

(55) Blackwell, J. M.; Sonmor, E. R.; Scoccitti, T.; Piers, W. E. *Organic Letters* **2000**, *2*, 3921–3923.

(56) Welch, G. C.; San Juan, R. R.; Masuda, J. D.; Stephan, D. W. *Science* **2006**, *314*, 1124–1126.

(57) Welch, G. C.; Stephan, D. W. *Journal of the American Chemical Society* **2007**, *129*, 1880–1881.

(58) Spies, P.; Erker, G.; Kehr, G.; Bergander, K.; Fröhlich, R.; Grimme, S.; Stephan, D. W. *Chemical Communications* **2007**, *2*, 5072–5074.

(59) Stephan, D. W.; Erker, G. *Angewandte Chemie International Edition* **2010**, *49*, 46–76.

(60) Jursic, B. S. *Journal of Molecular Structure (Theochem)* **1999**, *492*, 97–103.

(61) Watts, J. D.; Bartlett, R. J. *Journal of the American Chemical Society* **1995**, *117*, 825–826.

(62) Schreiner, P. R.; Schaefer III, H. F.; von Ragué Schleyer, P. *The Journal of Chemical Physics* **1994**, *101*, 7625–7632.

(63) Tague, T. J.; Andrews, L. *Journal of the American Chemical Society* **1994**, *116*, 4970–4976.

(64) Moroz, A.; Sweany, R. L.; Whittenburg, S. L. *The Journal of Physical Chemistry* **1990**, *94*, 1352–1357.

(65) Rokob, T. A.; Hamza, A.; Stirling, A.; Soós, T.; Pápai, I. *Angewandte Chemie International Edition* **2008**, *47*, 2435–2438.

(66) Holschumacher, D.; Bannenberg, T.; Hrib, C. G.; Jones, P. G.; Tamm, M. *Angewandte Chemie International Edition* **2008**, *47*, 7428–7432.

(67) Grimme, S.; Kruse, H.; Goerigk, L.; Erker, G. *Angewandte Chemie International Edition* **2010**, *49*, 1402–1405.

(68) McCahill, J. S. J.; Welch, G. C.; Stephan, D. W. *Angewandte Chemie International Edition* **2007**, *46*, 4968–4971.

(69) Zhao, X.; Stephan, D. W. *Journal of the American Chemical Society* **2011**, *133*, 12448–12450.

(70) Dureen, M. A.; Stephan, D. W. *Journal of the American Chemical Society* **2009**, *131*, 8396–8397.

(71) Dureen, M. A.; Brown, C. C.; Stephan, D. W. *Organometallics* **2010**, *29*, 6594–6607.

(72) Mömming, C. M.; Otten, E.; Kehr, G.; Fröhlich, R.; Grimme, S.; Stephan, D. W.; Erker, G. *Angewandte Chemie International Edition* **2009**, *48*, 6643–6646.

(73) Voicu, D.; Abolhasani, M.; Choueiri, R.; Lestari, G.; Seiler, C.; Ménard, G.; Greener, J.; Guenther, A.; Stephan, D. W.; Kumacheva, E. *Journal of the American Chemical Society* **2014**, *136*, 3875–3880.

(74) Bußß, F.; Mehlmann, P.; Mück-Lichtenfeld, C.; Bergander, K.; Dielmann, F. *Journal of the American Chemical Society* **2016**, *138*, 1840–1843.

(75) Sajid, M.; Elmer, L. M.; Rosorius, C.; Daniliuc, C. G.; Grimme, S.; Kehr, G.; Erker, G.

Angewandte Chemie International Edition **2013**, *52*, 2243–2246.

(76) Sajid, M.; Kehr, G.; Daniliuc, C. G.; Erker, G. *Angewandte Chemie International Edition* **2014**, *53*, 1118–1121.

(77) Dobrovetsky, R.; Stephan, D. W. *Journal of the American Chemical Society* **2013**, *135*, 4974–4977.

(78) Otten, E.; Neu, R. C.; Stephan, D. W. *Journal of the American Chemical Society* **2009**, *131*, 9918–9919.

(79) Staudinger, H.; Hauser, E. *Helvetica Chimica Acta* **1921**, *4*, 861–886.

(80) Neu, R. C.; Otten, E.; Lough, A.; Stephan, D. W. *Chemical Science* **2011**, *2*, 170.

(81) Ménard, G.; Hatnean, J. A.; Cowley, H. J.; Lough, A. J.; Rawson, J. M.; Stephan, D. W. *Journal of the American Chemical Society* **2013**, *135*, 6446–6449.

(82) Mo, Z.; Rit, A.; Campos, J.; Kolychev, E. L.; Aldridge, S. *Journal of the American Chemical Society* **2016**, *138*, 3306–3309.

(83) Chase, P. A.; Stephan, D. W. *Angewandte Chemie International Edition* **2008**, *47*, 7433–7437.

(84) Li, H.; Aquino, A. J. a; Cordes, D. B.; Hung-Low, F.; Hase, W. L.; Krempner, C. *Journal of the American Chemical Society* **2013**, *135*, 16066–16069.

(85) Lindqvist, M.; Sarnela, N.; Sumerin, V.; Chernichenko, K.; Leskelä, M.; Repo, T. *Dalton Transactions* **2012**, *41*, 4310–4312.

(86) Hounjet, L. J.; Bannwarth, C.; Garon, C. N.; Caputo, C. B.; Grimme, S.; Stephan, D. W. *Angewandte Chemie International Edition* **2013**, *52*, 7492–7495.

(87) Tanur, C. A.; Stephan, D. W. *Organometallics* **2011**, *30*, 3652–3657.

(88) Eller, C.; Kehr, G.; Daniliuc, C. G.; Fröhlich, R.; Erker, G. *Organometallics* **2013**, *32*, 384–386.

(89) Eller, C.; Kehr, G.; Daniliuc, C. G.; Stephan, D. W.; Erker, G. *Chemical Communications* **2015**, *51*, 7226–7229.

(90) Tsao, F. A.; Stephan, D. W. *Dalton Transactions* **2014**, *44*, 71–74.

(91) Tsao, F. A.; Lough, A. J.; Stephan, D. W. *Chemical Communications* **2015**, *51*, 4287–4289.

(92) Kolychev, E. L.; Bannenberg, T.; Freytag, M.; Daniliuc, C. G.; Jones, P. G.; Tamm, M. *Chemistry - A European Journal* **2012**, *18*, 16938–16946.

(93) Runyon, J. W.; Steinhof, O.; Dias, H. V. R.; Calabrese, J. C.; Marshall, W. J.; Arduengo,

A. J. *Australian Journal of Chemistry* **2011**, *64*, 1165–1172.

(94) Mummadi, S.; Unruh, D. K.; Zhao, J.; Li, S.; Krempner, C. *Journal of the American Chemical Society* **2016**, *138*, 3286–3289.

(95) Parks, D. J.; Spence, R. E. von H.; Piers, W. E. *Angewandte Chemie International Edition* **1995**, *34*, 809–811.

(96) Stephan, D. W.; Greenberg, S.; Graham, T. W.; Chase, P.; Hastie, J. J.; Geier, S. J.; Farrell, J. M.; Brown, C. C.; Heiden, Z. M.; Welch, G. C.; Ullrich, M. *Inorganic Chemistry* **2011**, *50*, 12338–12348.

(97) Farrell, J. M.; Hatnean, J. A.; Stephan, D. W. *Journal of the American Chemical Society* **2012**, *134*, 15728–15731.

(98) Farrell, J. M.; Posaratnanathan, R. T.; Stephan, D. W. *Chemical Science* **2015**, *6*, 2010–2015.

(99) Eisenberger, P.; Bestvater, B. P.; Keske, E. C.; Crudden, C. M. *Angewandte Chemie International Edition* **2015**, *54*, 2467–2471.

(100) Chase, P. A.; Welch, G. C.; Jurca, T.; Stephan, D. W. *Angewandte Chemie International Edition* **2007**, *46*, 8050–8053.

(101) Chase, P. A.; Jurca, T.; Stephan, D. W. *Chemical Communications* **2008**, *2*, 1701–1703.

(102) Spies, P.; Schwendemann, S.; Lange, S.; Kehr, G.; Fröhlich, R.; Erker, G. *Angewandte Chemie International Edition* **2008**, *47*, 7543–7546.

(103) Wang, H.; Fröhlich, R.; Kehr, G.; Erker, G. *Chemical Communications* **2008**, 5966–5968.

(104) Greb, L.; Oña-Burgos, P.; Schirmer, B.; Grimme, S.; Stephan, D. W.; Paradies, J. *Angewandte Chemie International Edition* **2012**, *51*, 10164–10168.

(105) Greb, L.; Daniliuc, C. G.; Bergander, K.; Paradies, J. *Angewandte Chemie International Edition* **2013**, *52*, 5876–5879.

(106) Chernichenko, K.; Madarász, A.; Pápai, I.; Nieger, M.; Leskelä, M.; Repo, T. *Nature Chemistry* **2013**, *5*, 718–723.

(107) Mohr, J.; Oestreich, M. *Angewandte Chemie International Edition* **2014**, *53*, 13278–13281.

(108) Mohr, J.; Porwal, D.; Chatterjee, I.; Oestreich, M. *Chemistry - A European Journal* **2015**, *21*, 17583–17586.

(109) Mahdi, T.; Stephan, D. W. *Journal of the American Chemical Society* **2014**, *136*, 15809–15812.

(110) Scott, D. J.; Fuchter, M. J.; Ashley, A. E. *Journal of the American Chemical Society* **2014**, *136*, 15813–15816.

(111) Mahdi, T.; Stephan, D. W. *Angewandte Chemie International Edition* **2013**, *52*, 12418–12421.

(112) Légaré, M.-A.; Courtemanche, M.-A.; Rochette, É.; Fontaine, F.-G. *Science* **2015**, *349*, 513–516.

(113) Scott, D. J.; Fuchter, M. J.; Ashley, A. E. *Angewandte Chemie International Edition* **2014**, *53*, 10218–10222.

(114) Kahlert, J.; Austin, C. J. D.; Kassiou, M.; Rendina, L. M. *Australian Journal of Chemistry* **2013**, *66*, 1118–1123.

(115) Yudin, A. K. *Chemical Science* **2015**, *6*, 30–49.

(116) Hickey, J. L.; Zaretsky, S.; St. Denis, M. A.; Kumar Chakka, S.; Morshed, M. M.; Scully, C. C. G.; Roughton, A. L.; Yudin, A. K. *Journal of Medicinal Chemistry* **2016**, *59*, 5368–5376.

(117) Fulmer, G. R.; Miller, A. J. M.; Sherden, N. H.; Gottlieb, H. E.; Nudelman, A.; Stoltz, B. M.; Bercaw, J. E.; Goldberg, K. I. *Organometallics* **2010**, *29*, 2176–2179.

(118) Dunn, N. L.; Ha, M.; Radosevich, A. T. *Journal of the American Chemical Society* **2012**, *134*, 11330–11333.

(119) Zhao, W.; Mccarthy, S. M.; Lai, T. Y.; Yennawar, H. P.; Radosevich, A. T. *Journal of the American Chemical Society* **2014**, *136*, 17634–17644.

(120) Fan, C.; Mercier, L. G.; Piers, W. E.; Tuononen, H. M.; Parvez, M. *Journal of the American Chemical Society* **2010**, *132*, 9604–9606.

(121) Tsao, F. A.; Cao, L.; Grimme, S.; Stephan, D. W. *Journal of the American Chemical Society* **2015**, *137*, 13264–13267.

(122) Avarvari, N.; Floch, P. Le; Mathey, F. *Journal of the American Chemical Society* **1996**, *118*, 11978–11979.

Chapter 2
FLP Ring Closing Reactions: Additions to C–C π-Bonds and Hydrogenation/Transannulation of *para*-Methoxyanilines

2.1 Introduction

2.1.1 Hydrogen Activation using Main Group Molecules

The notion that main group molecules could activate H_2, and even catalyze hydrogenation reactions, was not realized until the field of transition metal catalysis had been well established. An early report by Walling[1] discussed the reduction of benzophenone by H_2 using catalytic amounts of potassium *tert*-butoxide, which was proposed to occur via a mechanism analogous to Noyori's asymmetric ketone hydrogenation.[2] Seminal work by Power in the mid-2000s showed that heavier alkyne analogues, such as digermynes[3] and distannynes,[4] are capable of activating H_2, however this is an irreversible process and leads to a mixture of products. There have been recent notable publications highlighting the chemistry of heavier alkene analogues: Aldridge has achieved the synthesis of a germanium analogue of vinylidene ($H_2C{=}C$), which can activate H_2 to form a digermane,[5] and Tokitoh demonstrated the liberation of a doubly bonded Al=Al molecule from bicyclic precursors, which activates H_2 to yield aluminum hydride species.[6]

Bertrand's cyclic (alkyl)(amino)carbenes (CAACs), unlike Arduengo-type N-heterocyclic carbenes (NHCs), were reported to irreversibly react with H_2, generating the corresponding methylene product;[7] in a similar vein, Power later reported that germylenes[8] and stannylenes[9] react with H_2. Aldridge and co-workers have developed stable silylenes[10] and stannylenes[11] with strongly electron-donating boryl ligands capable of oxidatively adding H_2, forming stable R_2SiH_2 and R_2SnH_2 species, respectively. The proposed modes of H_2 activation are shown in Figure 2.1.

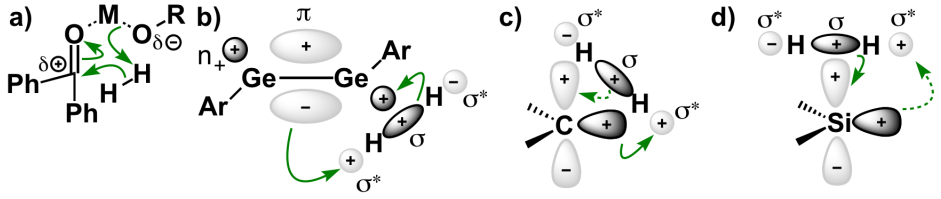

Figure 2.1 – H_2 activation modes by a) KO*t*-Bu, b) digermynes, c) (alkyl)(amino)carbenes, and d) silylenes.

The advent of the first reversible main group activation of H_2[12] enabled by a frustrated Lewis pair (FLP)[13] led to the growing field of metal-free hydrogenation catalysis.[14–17] A range of polar unsaturated substrates, such as imines, enamines, and silyl enol ethers, are amenable to FLP-catalyzed hydrogenation (Table 2.1). Substrates with C–C multiple bonds, such as 1,1-disubstituted olefins,[18] nitro-substituted olefins and acrylates,[19] enones,[20] and alkynes[21] have also been shown to be compatible with FLP hydrogenation catalysts. For a discussion of FLP reductions of carbonyl compounds, see Chapters 5 & 6.

Table 2.1 – Substrates amenable to FLP-catalyzed hydrogenation. PG = protecting group.

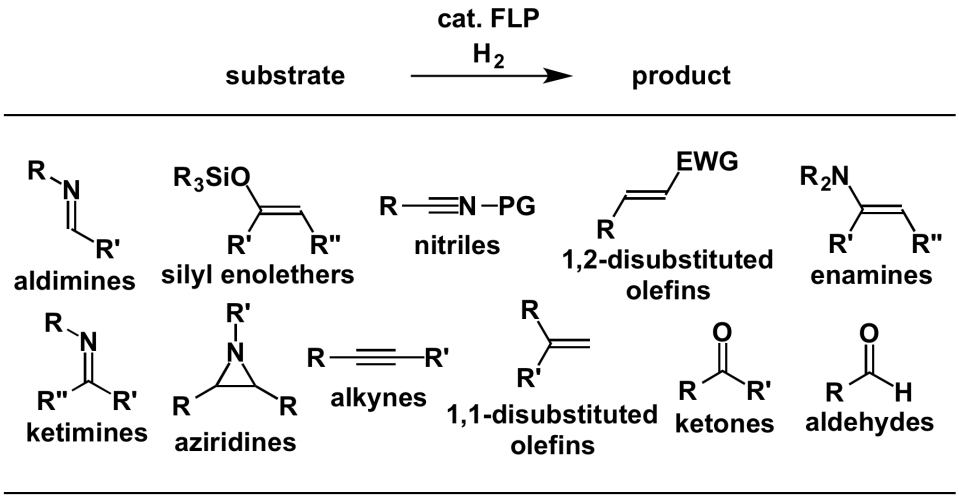

2.1.2 Catalytic Aromatic Hydrogenation

The field of catalytic hydrogenation is extremely well established, with a plethora of metals, and now main group species, capable of effecting cleavage of H_2. Despite these advances, aromatic rings remain a challenging substrate class for hydrogenation catalysts. Their inherent stability makes their reduction difficult, however a few transition metal systems are reported to facilitate aromatic hydrogenation. Homogeneous tantalum and niobium catalysts have been developed by Rothwell,[22,23] however most other systems rely on heterogeneous nickel, palladium, or rhodium catalysts, extremely high reaction temperatures, and high pressures of H_2.[24–30] In 2012, the Stephan group published the first example of a metal-free aromatic hydrogenation, mediated through H_2 activation by $B(C_6F_5)_3$ and bulky anilines (Scheme 2.1).[31] The reaction mechanism was calculated to proceed through a van der Waals complex of the borane and the *para*-position of the aniline. After complete reduction of the aromatic ring, the resulting cyclohexyl amine products irreversibly activate one equivalent of H_2 with $B(C_6F_5)_3$, rendering this method

non-catalytic. This protocol was also extended to the stoichiometric hydrogenation of a variety of N-heterocycles.[32] This reaction was later reported to be catalyzed by an *in situ*-generated borane under similar reaction conditions, and was applied in the total synthesis of isosolenopsin A (Scheme 2.2).[33] Related catalytic hydrogenations of polycyclic aromatic hydrocarbons have also been reported.[34]

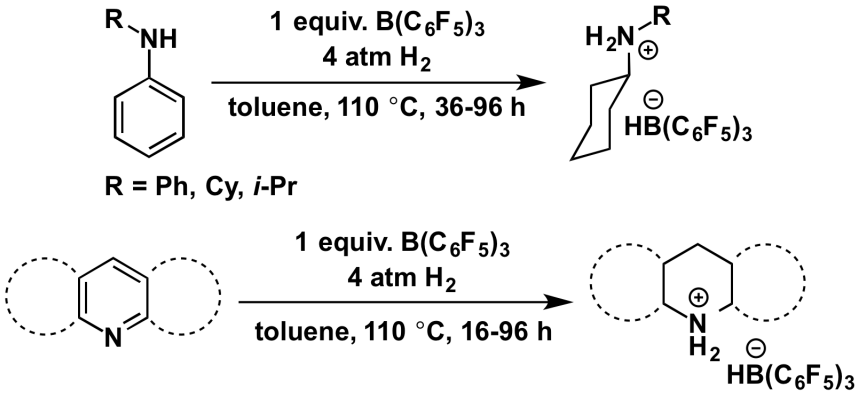

Scheme 2.1 – FLP-mediated aromatic reduction of anilines and N-heterocycles.

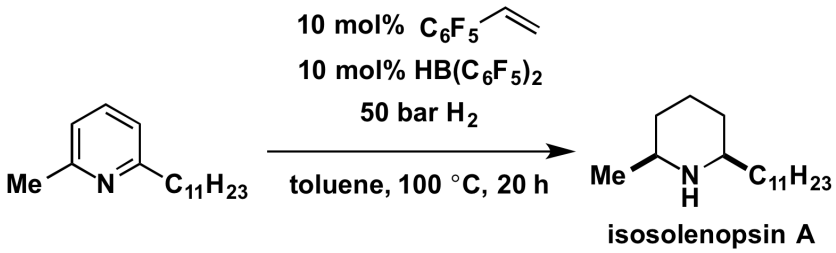

Scheme 2.2 – FLP-catalyzed aromatic hydrogenation and synthesis of isosolenopsin A.

2.1.3 FLP Addition Chemistry using Nitrogen Lewis Bases

While the first reports of small molecule activation by frustrated Lewis pairs focused on phosphines as the Lewis basic component,[14] the field has expanded to include other Lewis basic species, such as amines. Shortly after the Stephan group reported that combinations of bulky phosphines and boranes can activate H_2,[35] Repo and Rieger showed that amines, such as TMP, can heterolytically cleave H_2 in concert with $B(C_6F_5)_3$ to yield the corresponding ammonium hydridoborate salts (Figure 2.2a).[36] After these seminal reports, a variety of small molecules were shown to react with FLPs comprised of various different Lewis acids and bases. Focusing on combinations of nitrogen Lewis bases with $B(C_6F_5)_3$, these FLPs are able to activate H_2, CO_2

(Figure 2.2b & c), terminal and internal alkynes (Figure 2.2d & e), and alkenes.[37] Anilines with tethered alkenes and internal alkynes have also been reported to undergo ring closing reactions when treated with $B(C_6F_5)_3$ (Figure 2.2f).[38] Related ring closing reactions using N-heterocycles will be discussed in this chapter.

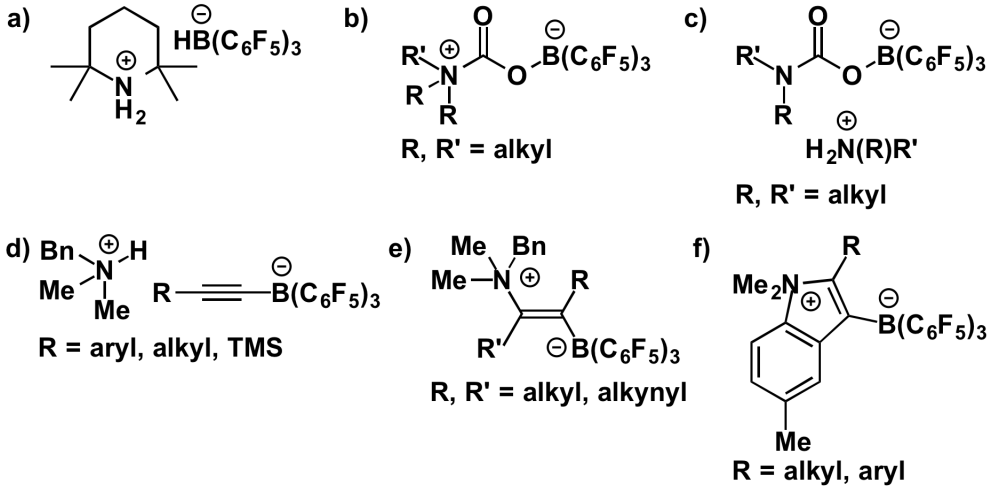

Figure 2.2 – Activation of a) H_2, b) & c) CO_2, d) terminal alkynes, and e) & f) internal alkynes by FLPs using amine Lewis bases.

The first section of this chapter focuses on our efforts towards an FLP-mediated tandem aromatic hydrogenation-transannulation reaction using *para*-substituted anilines, and the second section explores fundamental FLP C–C π-bond addition chemistry using N-heterocycles in concert with $B(C_6F_5)_3$, furnishing new heterocyclic products.

2.2 Results and Discussion

2.2.1 H_2 Activation, Hydrogenation, and Transannulation of *para*-Methoxyanilines

The application of FLP chemistry to organic synthesis was, and continues to be, of considerable interest to the Stephan research group. A significant accomplishment was the aromatic reduction of N-substituted anilines using $B(C_6F_5)_3$ and H_2.[31] This transformation had previously been limited to harsh reaction conditions, typically using alkali metal reductants,[39] which are intolerant of a variety of functional groups. My colleague Dr. Tayseer Mahdi had made an observation that, when substrate **2-1a** was exposed to the optimized reaction conditions for FLP aromatic hydrogenation, but the reaction time was increased from 24 to 48 h, the -OMe

substituent was not observed upon NMR spectroscopic analysis of the product. Recrystallization of the material and single crystal X-ray diffraction studies confirmed that ring closure had occurred and a new bicyclic ammonium salt **2-2a** was produced (Scheme 2.3), albeit in poor yield (<30%).

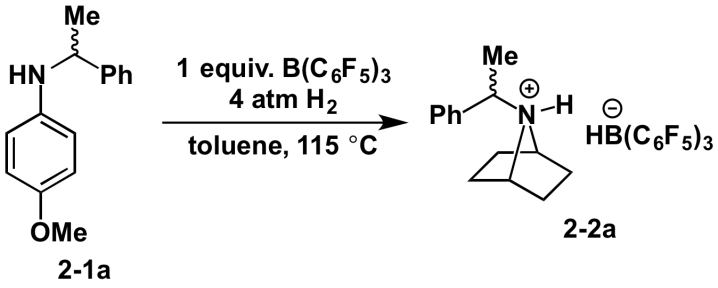

Scheme 2.3 – Preliminary finding of bicyclic product **2-1a** via hydrogenation of **2-2a**.

This reaction was interesting because of the occurrence of the 7-azabicyclo[2.2.1]heptane structure in the natural product epibatidine. This is a type of amphibian alkaloid,[40,41] and while numerous total syntheses have been reported,[42,43] they are plagued by difficult aromatic reductions or multi-step ring closing protocols. It was envisioned that, should this FLP-mediated reduction be a reasonably general method, epibatidine could be accessed through a tandem hydrogenation-transannulation. The author's role in this project was to develop a methodology and improve isolated yields, and to examine a variety of substrates to determine the functional group tolerance.

Pleasingly, it was found that a small family of bicyclic ammonium salts could be generated using this methodology, starting from the N-arylamine (**2-1a, 2-1b, 2-1c**) or the N-arylimine (**2-1a'**, **2-1c'**), as the N=C bond is hydrogenated under the reaction conditions.[44] Aniline substrates were synthesized using reductive amination or Pd-catalyzed C–N cross coupling methods. Imine substrates were made by condensation of *p*-anisidine with the appropriate ketone. The results are summarized in Table 2.2. The 7-azabicyclo[2.2.1]heptane salts were obtained in moderate to excellent yield, with all products isolated via recrystallization. Pleasingly, in the case of substrate **2-1c**, both of the N-bound aryl rings undergo aromatic hydrogenation under the reaction conditions. A comparison of the ^{1}H NMR spectra of **2-1c** and **2-2c** are shown in Figure 2.5, where the loss of aromatic resonances is apparent. All products were characterized spectroscopically, and their structures were confirmed by single crystal X-ray diffraction studies.

The solid state structures for **2-2b** and **2-2c** are shown in Figure 2.3 and Figure 2.4, respectively. This was the first synthesis of these complex bicyclic amine structures from relatively simple starting materials, using only H_2 and a strong Lewis acid to promote the transformation. Mechanistic studies were undertaken by Dr. Tayseer Mahdi and are therefore outside the scope of this dissertation.

Table 2.2 – Synthesis of **2-2a**, **2-2b**, and **2-2c** from the corresponding aniline or imine via an FLP-mediated hydrogenation-transannulation reaction.

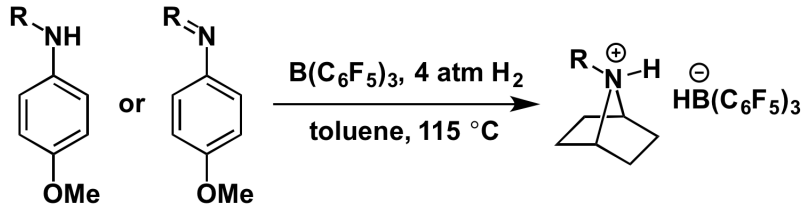

Entry	Substrate	Product	Isolated Yield
1	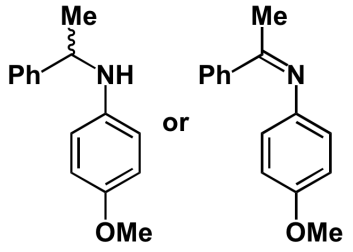 2-1a 2-1a'	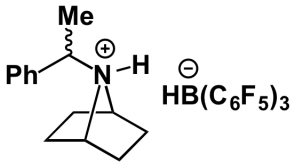 2-2a	51% (N-C) 63% (N=C)
2	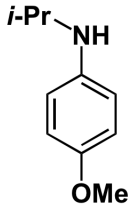 2-1b	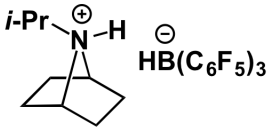 2-2b	87%
3	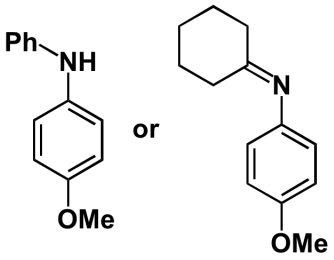 2-1c 2-1c'	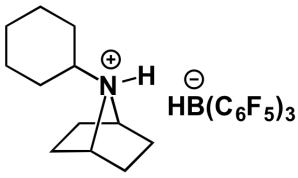 2-2c	36% (Ph) 56% (Cy)

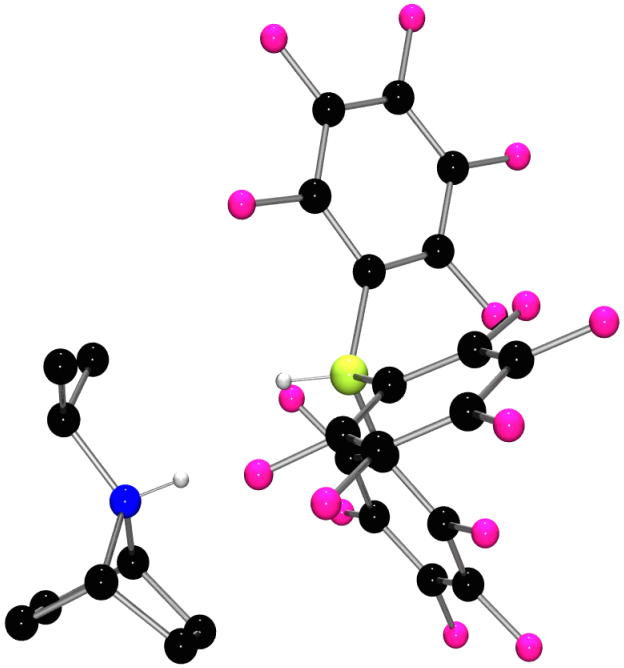

Figure 2.3 – POV-ray depiction of **2-2b**, with C–H atoms omitted for clarity. C: black; H: grey; B: yellow-green; F: pink; N: blue.

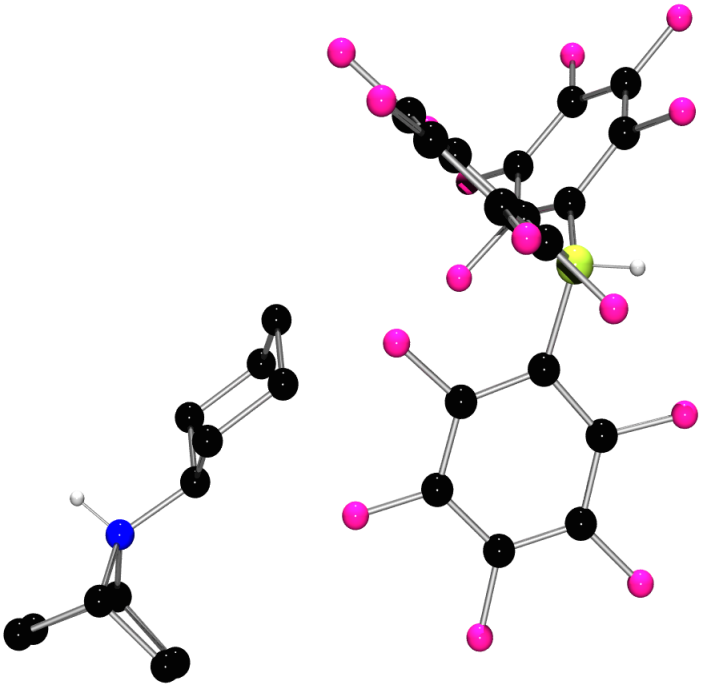

Figure 2.4 – POV-ray depiction of **2-2c**, with C–H atoms omitted for clarity. C: black; H: grey; B: yellow-green; F: pink; N: blue.

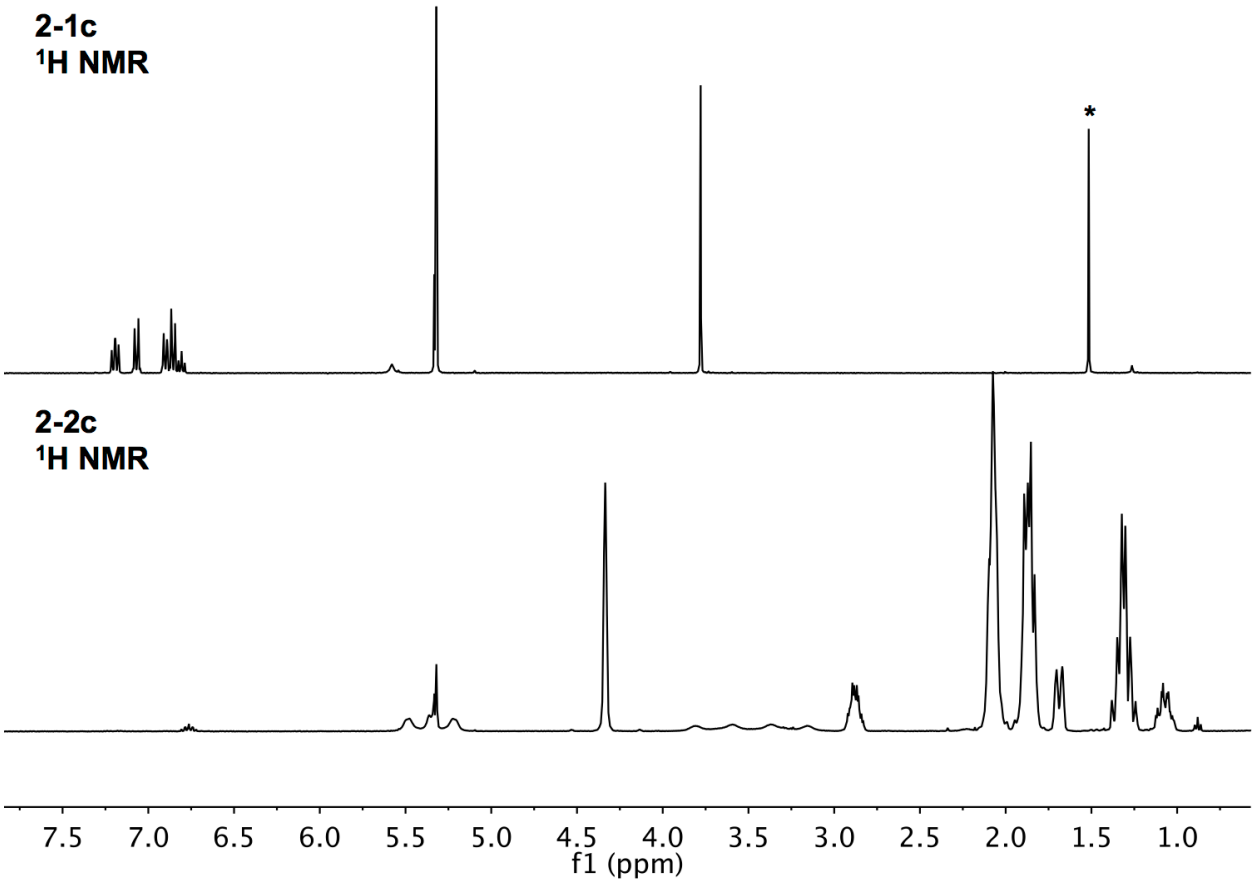

Figure 2.5 – ^{1}H NMR (400 MHz, 298 K, CD_2Cl_2) spectra of **2-1c** and **2-2c**. *H_2O peak.

2.2.2 Examining Alternate Substrates for the Hydrogenation/Transannulation Methodology

To test whether the *para*-methoxy substituent could be varied, a variety of sterically encumbered anilines bearing more traditional leaving groups at the *para* position were synthesized, with substrates shown in Table 2.3, row 1. Unfortunately, mesylate and triflate substituents were incompatible with the reaction conditions and only borane degradation was observed. A *para*-OH group formed an adduct with $B(C_6F_5)_3$ and no hydrogenation was observed. The *para*-OCF_3 substrate decomposed during the reaction, possibly due to C–F bond activation.[45] Nitrogen-based leaving groups were also found to be unsuitable, as the *para*-NH(*i*-Pr) group remains bound to the cyclohexyl ring following hydrogenation,[31] and the *para*-NHMe substrate formed a strong adduct with $B(C_6F_5)_3$ and no hydrogenation was observed.

Next, different N-substituents were investigated (Table 2.3, row 2), as a cleavable group would be essential for the synthesis of epibatidine. Unfortunately, substrates where the nitrogen was

protected using groups such as benzyl, Boc, and silanes of various sizes formed strong adducts with $B(C_6F_5)_3$, preventing H_2 activation. While this discovery made our method unsuitable for the synthesis of epibatidine, we nevertheless decided to explore the scope of the reaction within the limitations of this FLP H_2 activation.

Other *para*-methoxyanilines bearing additional substituents about the aromatic ring (Table 2.3, row 3) were examined, but they did not generate the desired ring-closed products. Hydrogen activation was achieved, but subsequent hydrogenation of the aromatic ring did not occur, as evidenced by ^{1}H NMR spectroscopy. When substrate **2-1d** was subjected to 4 atm of H_2, formation of the ammonium hydridoborate **2-1d(H_2)** was observed (Scheme 2.4). Upon heating, clean and complete consumption of the starting material was observed by multinuclear NMR spectroscopy, however by ^{1}H NMR spectroscopy it was evident that aromatic hydrogenation had not occurred. Two aromatic resonances were apparent by ^{1}H NMR spectroscopy, suggesting that the new product was symmetric, hinting at a *para*-substituted aromatic ring. This data, in combination with the ^{19}F and ^{11}B NMR resonances, suggested that a four-coordinate boron species had formed, leading us to assign the product as ammonium bromoborate **2-2d** (Scheme 2.4), which is the product of nucleophilic aromatic substitution (S_NAr). Upon H_2 activation, the bromo substituent is *ortho* to an electron-withdrawing ammonium group, and this allows the borohydride to undergo nucleophilic attack on the aromatic ring and eject the bromide, which complexes with $B(C_6F_5)_3$ to form the $[BrB(C_6F_5)_3]$ anion.

Table 2.3 – Substrates tested for aromatic hydrogenation/transannulation.

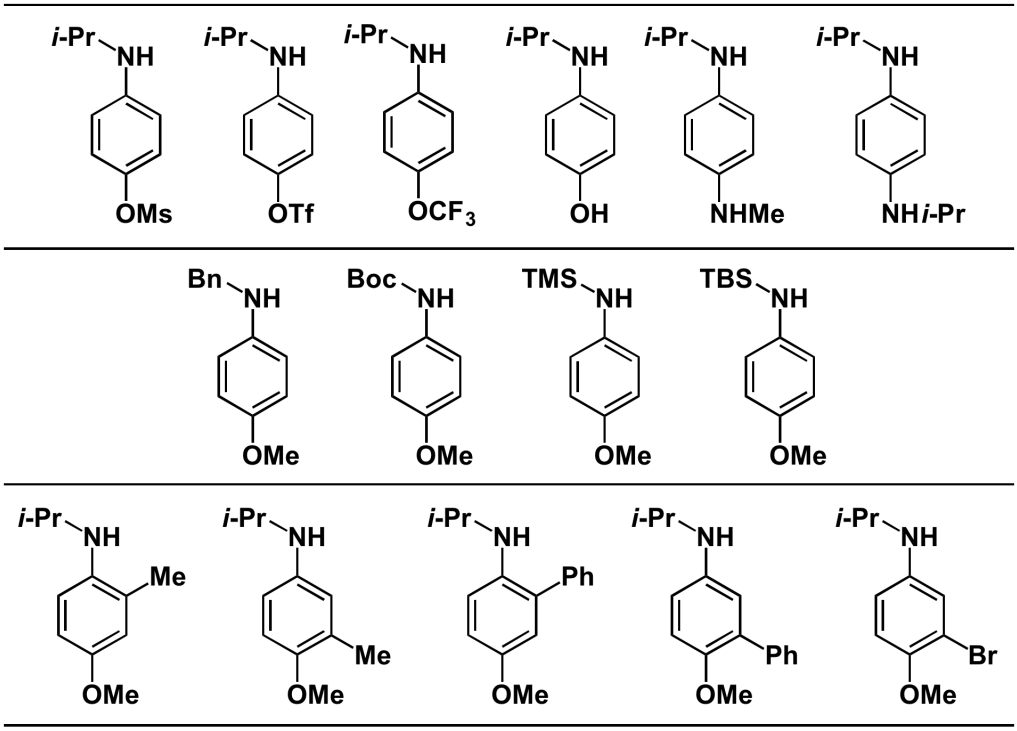

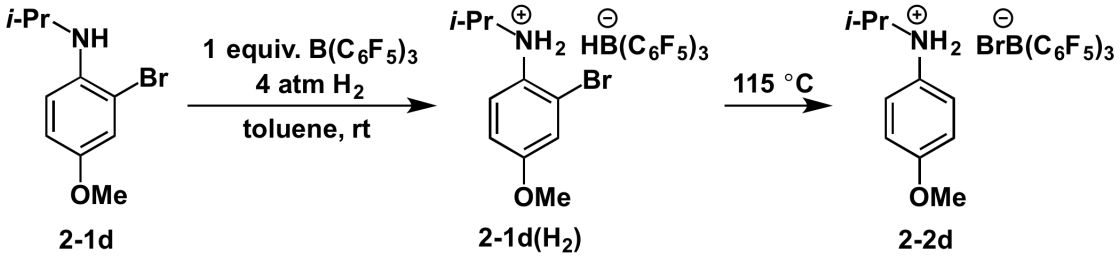

Scheme 2.4 – H_2 activation of **2-1d** with $B(C_6F_5)_3$ and subsequent S_NAr reaction upon heating.

H_2 activation and hydrogenation were observed for substrates **2-1e** and **2-1f** bearing *para*-phenoxy and *para*-ethoxy substituents, respectively (Scheme 2.5). After 96 h at 115 °C the cyclohexylammonium hydridoborate salts **2-2e** and **2-2f** were isolated in good yields, with the *para*-substituents intact, as evidenced by ^{1}H NMR spectroscopy. This is dramatically different from the *para*-methoxy substrate **2-1b**, and it was not fully understood why the *para*-ethoxy substrate **2-1f** does not undergo ring closure following aromatic hydrogenation, as neither steric nor electronic arguments are sufficient in distinguishing the two substituents. Examining the barrier of the ring flip may provide valuable insight, however this was not further explored due to the undesired reduction product.

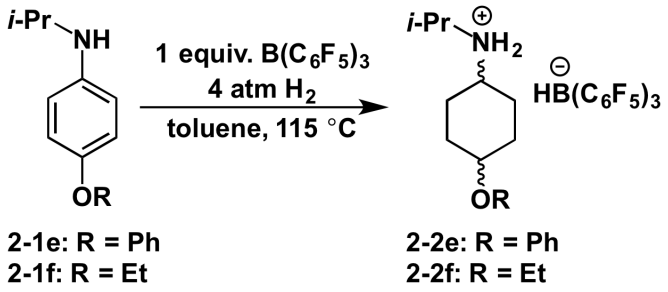

Scheme 2.5 – Reduction of aniline bearing *para*-phenoxy and ethoxy substituents to the corresponding cyclohexylammonium salts **2-2e** and **2-2f**.

2.2.3 N-heterocycles as Lewis Bases for FLP Additions to C–C π-Bonds

While our hydrogenation/transannulation methodology was not applicable to the synthesis of epibatidine, there was still interest in applying FLP chemistry to organic synthesis, and in particular, pursuing a total synthesis using an FLP-mediated reduction of an aromatic ring as the key step. A method for the reduction of quinolines to their corresponding decahydroquinolinium salts using $B(C_6F_5)_3$ had recently been established by the Stephan group,[32] therefore 2-substituted quinolines were targeted as precursors to decahydroquinoline natural products, which are a type of amphibian alkaloid.[40,46] Instead of aromatic hydrogenation, the treatment of **2-1g** with one equivalent of $B(C_6F_5)_3$ led to a new product with aromatic resonances but no olefinic resonances, as observed by my colleague Dr. Peter Dornan (Scheme 2.6). The product **2-2g** was proposed based on NMR spectroscopic data, and was unambiguously confirmed by a single crystal X-ray diffraction study.

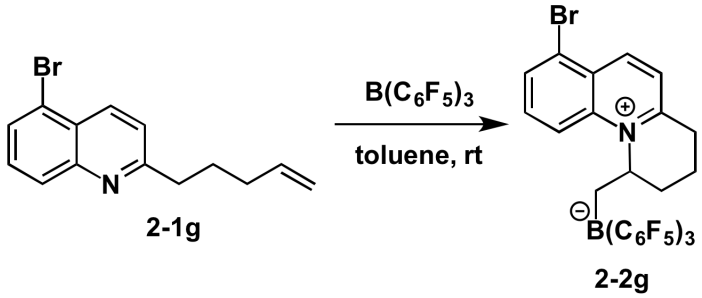

Scheme 2.6 - Ring closure of **2-1g** with $B(C_6F_5)_3$ to yield **2-2g**.

The substitution pattern of the N-heterocycle was shown to be critical for ring closure to prevail (Scheme 2.7). 2-Pentenylpyridine **2-1i**, in combination with $B(C_6F_5)_3$, cleanly forms a classic

Lewis adduct **2-1i'**. 2,6-Disubstituted pyridine **2-1h** reacted with one equivalent of $B(C_6F_5)_3$ to produce heterocycle **2-2h**. This was evident by ^1H NMR analysis of the reaction mixture; there were no olefinic resonances, and a peak at 4.64 ppm integrating to one proton was indicative of a methine group adjacent to the nitrogen centre (Figure 2.6). It was found that the alkene activation in **2-2h** is reversible, as treatment of a solution of **2-2h** with 4 atm H_2 at 115 °C led to the re-emergence of olefinic resonances in the ^1H NMR spectrum, as well as the diagnostic resonance for $[HB(C_6F_5)_3]$ in the ^{11}B NMR spectrum, leading us to assign the product as H_2 activated species **2-1h(H_2)**.

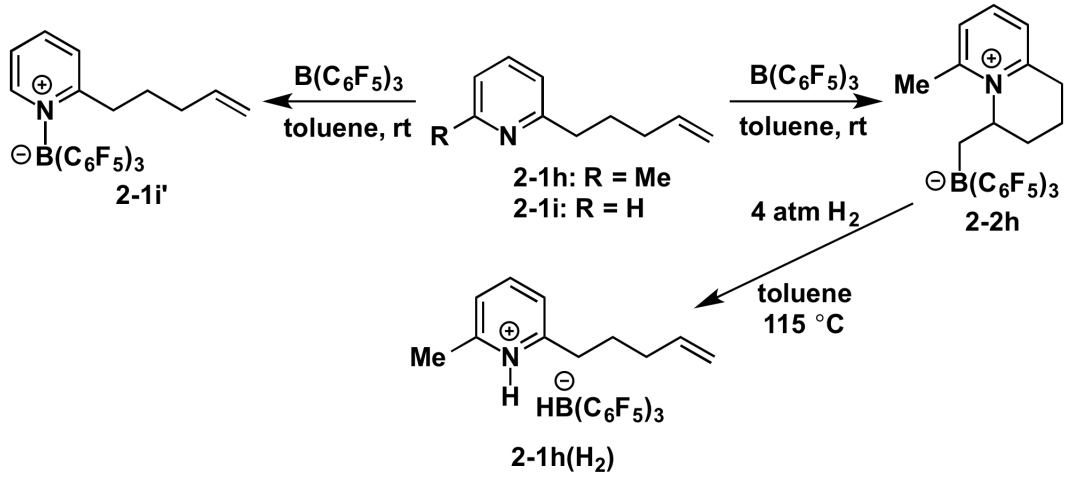

Scheme 2.7 – Adduct formation vs. ring closure for substituted pyridines **2-1h** and **2-1i**.

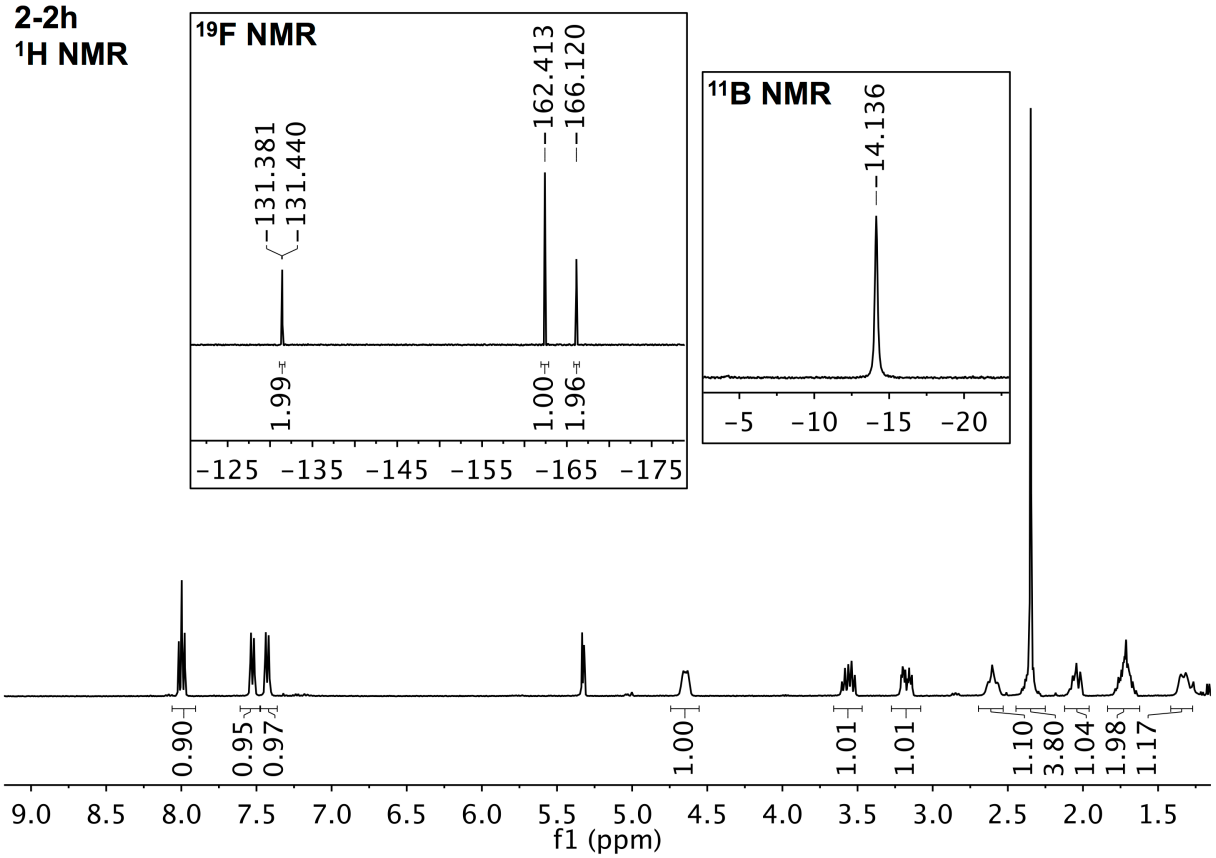

Figure 2.6 – ^{1}H, ^{19}F, and ^{11}B NMR spectra of **2-2h** (400 MHz, 298 K, CD_2Cl_2).

These reactions were intriguing, as amines[37,38] and imines[47] had been applied as the Lewis basic component for FLP additions to C–C π-bonds, but N-heterocycles had not been reported to undergo similar chemistry. A family of pyridines with tethered alkynes was generated to determine whether rings of different sizes could be generated, and whether tandem ring closures could be observed with multiple units of unsaturation incorporated into the substrate. To this end, substrates **2-1j**, **2-1k**, and **2-1l** were prepared and treated with $B(C_6F_5)_3$ at room temperature in toluene (Table 2.4). Terminal alkyne **2-1j** was shown to selectively and quantitatively form 5-membered ring **2-2j** when exposed to the strong Lewis acid; this was postulated based on the multinuclear NMR data and was unambiguously confirmed through X-ray diffraction analysis of single crystals of **2-2j** (Figure 2.7). The enyne **2-1k** was shown to generate a mixture of **2-2k** and **2-2k'** in a 1:1.9 ratio (determined by ^{1}H NMR spectroscopy) when exposed to $B(C_6F_5)_3$. When the mixture of products was heated to 115 °C for 13 h, the mixture isomerized and **2-2k** was the final product, which was isolated in 95% yield and crystallographically confirmed as the

6-membered ring (Figure 2.8). This data suggests that alkyne activation is reversible at elevated temperatures, and that **2-2k** is the thermodynamically favoured over 5-membered regioisomer **2-2k'**. Substrate **2-1l** was also shown to cleanly form the ring closed product **2-2l**, which was characterized crystallographically (Figure 2.9), confirming the formation of a new 6-membered ring. There was no observation of any activation of the terminal olefin in either **2-1k** or **2-1l** when they were exposed to $B(C_6F_5)_3$. This type of addition was recently achieved by the Melen group, who reported cascade FLP addition to diynes using boron and selenium Lewis acids.[48]

Table 2.4 – Reactivity of tethered terminal and internal alkynyl pyridines with $B(C_6F_5)_3$.

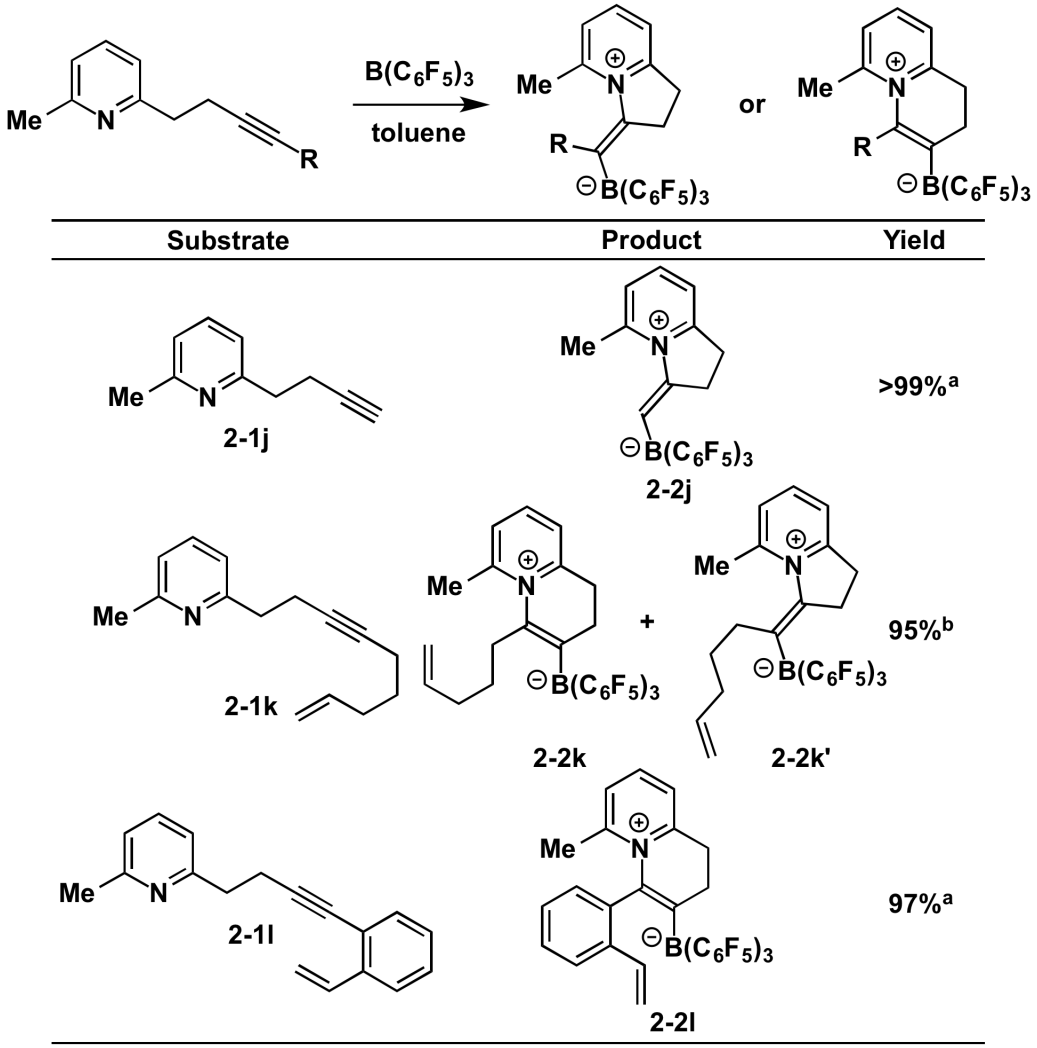

[a]Reaction conditions: toluene, rt, 13 h; [b]Reaction conditions: toluene, 115 °C, 13 h.

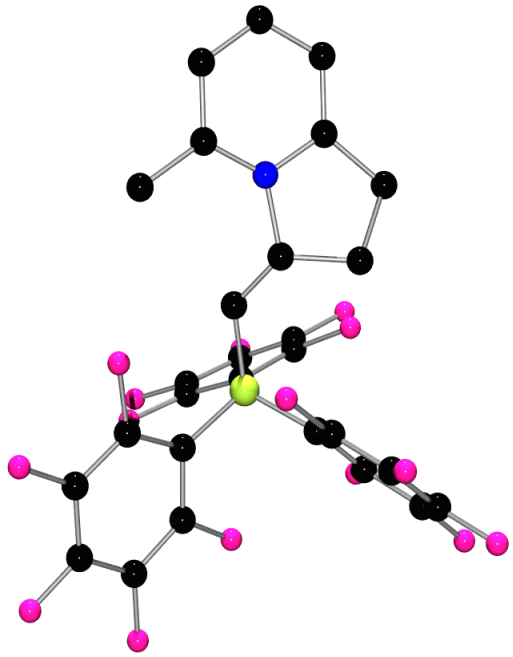

Figure 2.7 – POV-ray depiction of **2-2j**, with H atoms omitted for clarity. C: black; B: yellow-green; F: pink; N: blue.

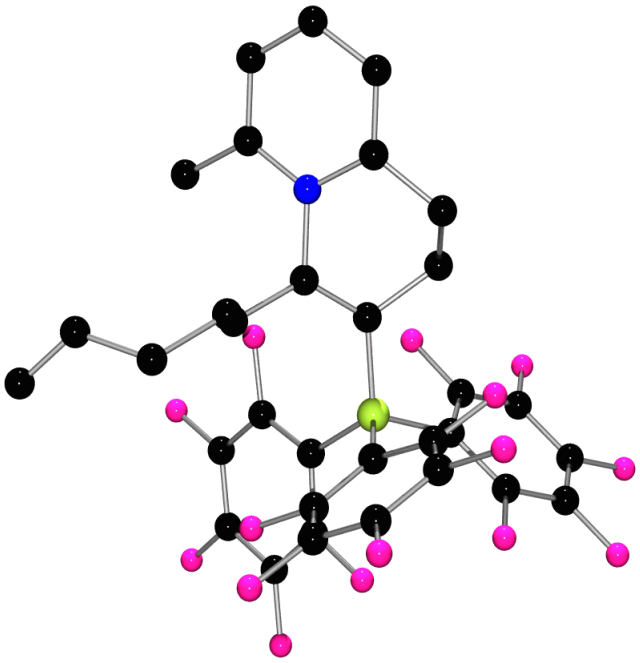

Figure 2.8 – POV-ray depiction of **2-2k**, with H atoms omitted for clarity. C: black; B: yellow-green; F: pink; N: blue.

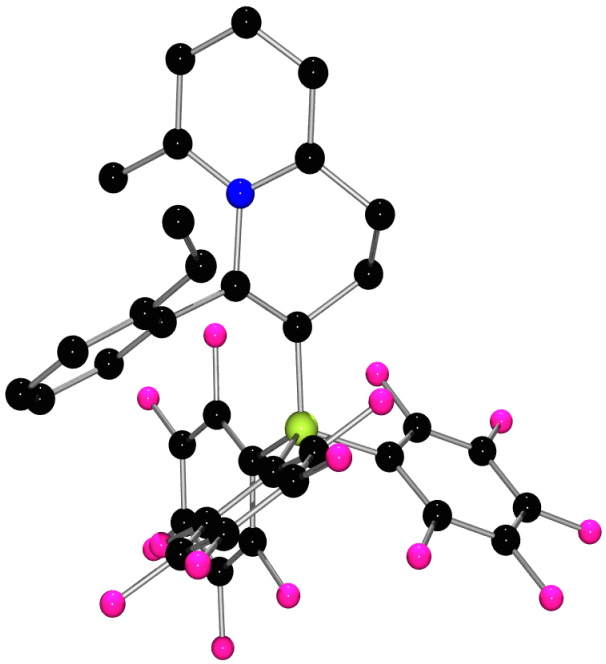

Figure 2.9 – POV-ray depiction of **2-2l**, with H atoms omitted for clarity. C: black; B: yellow-green; F: pink; N: blue.

2.3 Conclusions

This chapter has examined the application of FLP-mediated aromatic hydrogenation to the synthesis of complex organic products. The anilines **2-1a**, **2-1b**, and **2-1c** were shown to undergo an unprecedented aromatic hydrogenation/transannulation reaction to generate bicyclic ammonium hydridoborate products, of which the core scaffold is found in a natural product. While the scope is rather limited, the synthesis of the complex 7-azabicyclo[2.2.1]heptane ring, which typically requires complicated, multi-step syntheses, was achieved in a one-pot procedure starting from relatively simple starting materials. While aromatic hydrogenation of substrates **2-1g**, **2-1h**, **2-1j**, **2-1k**, and **2-1l** was not observed, we discovered a new ring closing methodology using the tethered C–C π-bonds. This had not previously been explored using N-heterocycles as the Lewis base. The alkene activation was shown to be reversible in the case of **2-1h**, and for substrates **2-1k** and **2-1l** it was shown that the addition reaction does not proceed in tandem, even in the presence of additional tethered π-systems.

2.4 Experimental Section

2.4.1 General Considerations

Manipulations were performed under an atmosphere of dry, oxygen-free N_2 by means of standard Schlenk or glovebox techniques (MBraun). $B(C_6F_5)_3$ was purchased from Boulder Scientific and used without purification. Anilines, amines, Pd_2dba_3, *rac*-BINAP and other reagents were purchased from Alfa Aesar, Sigma Aldrich, or TCI, and used as received. d_8-Toluene and CD_2Cl_2 were purchased from Cambridge Isotope Laboratories, degassed and stored over activated 4 Å molecular sieves in the glovebox prior to use. Toluene, pentane, and DCM were collected from a Grubbs-type column system manufactured by Innovative Technology, and stored over 4 Å molecular sieves. NMR spectra were recorded on a Bruker Avance III 400 MHz or an Agilent DD2 500 MHz spectrometer. Spectra were referenced to residual solvent of $CDCl_3$ (^1H = 7.16 ppm; ^{13}C = 77.2), CD_2Cl_2 (^1H = 5.32 ppm; ^{13}C = 53.8 ppm), d_8-toluene (^1H = 2.08 ppm (CH_3); ^{13}C = 20.4 ppm (CH_3)), or externally (^{19}F: $CFCl_3$, ^{11}B: $(Et_2O)BF_3$, ^{31}P: 85% H_3PO_4). Chemical Shifts (δ) are reported in ppm and the absolute values of the coupling constants (*J*) are in Hz. NMR assignments are supported by additional 2D experiments. Elemental analyses (C, H, N) and HRMS were performed in house. Hydrogen gas (Grade 5.0) was obtained from Linde and purified through a Matheson Model 450B or Matheson Nanochem WeldAssureTM gas purifier.

2.4.2 Syntheses and Characterizations

2.4.2.1 Synthesis and Characterization of Starting Materials

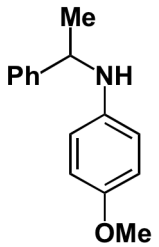

Synthesis of 2-1a

Following a literature procedure,[49] *p*-anisidine (2.95 g, 24 mmol) was dissolved in 12 mL dry toluene and quantitatively transferred to a flame-dried 100 mL round bottom flask equipped with a magnetic stir bar. Acetophenone (2.3 mL, 20 mmol) was added to the vessel, followed by ~3 g of activated 4 Å molecular sieves. The reaction was heated to reflux for 16 h. Once all of

the acetophenone was consumed (as determined by TLC analysis) the reaction was filtered and the solvent was removed *in vacuo* yielding an orange oil. The oil was dissolved in 22 mL dry THF and 2.5 g (21 mmol) benzoic acid was added to the solution. $NaBH_4$ (832 mg, 22 mmol) was added portion-wise to the reaction at room temperature, which was stirred for 24 h. Upon completion, the reaction was quenched with sat. $NaHCO_3$ and extracted in Et_2O. The organic layer was separated, dried over Na_2SO_4, filtered, and the solvent was removed *in vacuo*. Flash column chromatography (5% EtOAc in hexanes) recovered the pure product in 50% yield (2.3 g, 10.1 mmol). NMR data are consistent with literature reported values.[50]

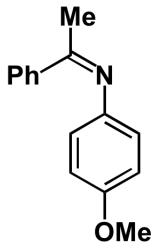

Synthesis of 2-1a'

Following a modified literature procedure,[51] *p*-anisidine (3.08 g, 25 mmol) was transferred to a flame-dried round bottom flask equipped with a magnetic stir bar and ~5 g of activated 4 Å molecular sieves. 10 mL of Et_2O was added to the flask, followed by acetophenone (2.9 mL, 25 mmol). The reaction was stirred vigorously under N_2 for 24 h, after which the reaction was filtered to remove the sieves and any precipitate. The filtrate was concentrated *in vacuo* to reveal faint yellow crystals, which were obtained in 45% yield (2.52 g, 11 mmol). NMR data are consistent with literature reported values.[51]

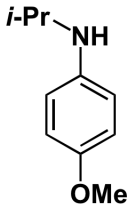

Synthesis of 2-1b

Following a modified literature procedure,[52] *p*-anisidine (2.2 g, 18 mmol) was dissolved in 30 mL acetone. The solution was stirred over ~20 g of 4 Å molecular sieves for 24 h. The solution was filtered and the acetone was removed *in vacuo*, yielding the imine as an orange oil. The imine was then redissolved in 30 mL of methanol in a round bottom flask and cooled to 0 °C in an ice bath. $NaBH_4$ (2.1 g, 55 mmol) was added portion-wise to the solution; upon complete

addition, the solution was allowed to slowly warm to room temperature. The reaction was quenched with 2 M NaOH, and the product was extracted into 100 mL DCM. The organic layer was separated and washed with 100 mL brine, dried over Na_2SO_4, filtered and the solvent was removed *in vacuo* to yield a yellow oil. The material was purified by flash column chromatography (5% EtOAc in hexanes) and isolated in 82% yield (2.5 g, 15.1 mmol) as a pale yellow oil. NMR data are consistent with literature reported values.[53]

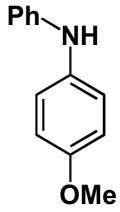

Synthesis of 2-1c

Following a literature procedure,[54] Pd_2dba_3 (28 mg, 0.03 mmol) was dissolved in 2 mL toluene. The solution was transferred to a vial containing *rac*-BINAP (56 mg, 0.09 mmol). The resulting catalyst mixture was transferred to a 100 mL Schlenk bomb, followed by NaO*t*-Bu (1.614 g, 16.8 mmol) and an additional 28 mL of toluene. 4-bromoanisole (1.50 mL, 12 mmol) and aniline (1.3 mL, 14.4 mmol) were then added to the reaction mixture. The bomb was sealed and heated to 100 °C for 24 h. The reaction mixture was then cooled to room temperature, filtered over Celite, and washed with EtOAc. The filtrate was washed with distilled water, dried over Na_2SO_4, and filtered. The solvent was removed *in vacuo* yielding a green-yellow solid. The material was purified by flash column chromatography (5% EtOAc in hexanes) recovering a yellow solid in 50% yield (1.2 g, 6.0 mmol). NMR data are consistent with reported values.[54]

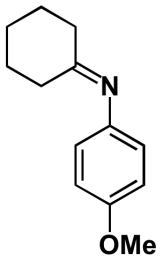

Synthesis of 2-1c'

Following a literature procedure,[55] *p*-anisidine (6.16 g, 50 mmol) was transferred to a 250 mL round bottom flask equipped with a stir bar. 100 mL of toluene was added to the flask, followed by cyclohexanone (5.2 mL, 50 mmol). The resulting mixture was refluxed for 12 h, during which time the water was removed azeotropically using a Dean-Stark apparatus. The reaction was

cooled to room temperature and all volatiles were removed *in vacuo*. The desired product was isolated as an orange oil in 60% yield (6.13 g, 30 mmol).

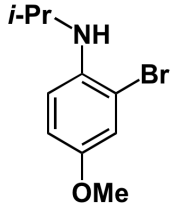

Synthesis of 2-1d

Following a modified literature procedure,[52] 2-bromo-N-isopropyl-4-methoxyaniline (500 mg, 2.5 mmol) was dissolved in 4.5 mL acetone and transferred to a 50 mL flame-dried Schlenk bomb equipped with a magnetic stir bar and ~3 g of 4 Å molecular sieves. The resulting red solution was vigorously stirred at room temperature for 24 h. The solution was then filtered and the acetone was removed *in vacuo*, yielding a red oil. The material was redissolved in 4.5 mL MeOH and cooled to 0 °C in an ice bath. $NaBH_4$ (284 g, 7.5 mmol) was added portion-wise to the solution; upon complete addition, the solution was allowed to slowly warm to room temperature. The reaction was quenched with 2 M NaOH, and the product was extracted in DCM. The organic layer was separated, dried over Na_2SO_4, filtered, and concentrated *in vacuo* to yield a red oil. The material was purified by flash column chromatography (5% EtOAc in hexanes) and isolated in 86% yield (524 mg, 2.1 mmol) as a light yellow oil.

^{1}H NMR (400 MHz, 298 K, $CDCl_3$): δ 7.05 (d, $^4J_{HH}$ = 2.8 Hz, 1H, 3-C<u>H</u>), 6.80 (dd, $^3J_{HH}$ = 9.2 Hz, $^4J_{HH}$ = 2.8 Hz, 1H, 5-C<u>H</u>), 6.62 (d, $^3J_{HH}$ = 9.2 Hz, 1H, 6-C<u>H</u>), 3.75 (br s, 1H, N<u>H</u>), 3.73 (s, 3H, OMe), 3.58 (br septet, $^3J_{HH}$ = 6.4 Hz, 1H, *i*-Pr C<u>H</u>), 1.23 (d, $^3J_{HH}$ = 6.4 Hz, 6H, *i*-Pr C<u>H</u>$_3$).

^{13}C{^{1}H} NMR (101 MHz, 298 K, $CDCl_3$): δ 151.5 (s, 4-<u>C</u>OMe), 139.1 (s, 1-<u>C</u>NH), 118.4 (s, 3-<u>C</u>H), 114.9 (s, 5-<u>C</u>H), 113.3 (s, 6-<u>C</u>H), 110.4 (s, 2-<u>C</u>Br), 56.2 (s, OMe), 45.3 (s, *i*-Pr <u>C</u>H), 23.2 (s, *i*-Pr <u>C</u>H$_3$).

HRMS (DART) calcd for $[C_{10}H_{15}BrNO]^+$ ($[M+H]^+$) 244.0337, found 244.0334.

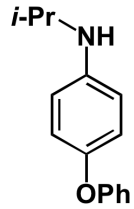

Synthesis of 2-1e

Following a literature procedure,[56] 4-phenoxyaniline (1.85 g, 10 mmol) was added to a 250 mL round bottom flash equipped with a magnetic stir bar, and was treated with 5 mL (70 mmol) acetone, 2.7 g (20 mmol) $NaOAc{\cdot}3H_2O$, 8.6 mL (150 mmol) glacial acetic acid, 25 mL distilled H_2O and 6 mL 95% EtOH. The reaction stirred at room temperature for 30 min, followed by slow addition of 1.9 g (50 mmol) $NaBH_4$. After the reaction was complete (determined by TLC analysis) the reaction was quenched with sat. $NaHCO_3$ and extracted into EtOAc. The organic layer was washed with 2 x 50 mL distilled water and then separated. It was subsequently dried over Na_2SO_4, filtered, and the solvent was removed *in vacuo*. Flash column chromatography (100% hexanes to 10% EtOAc in hexanes) recovered the material as a white solid in 65% yield (1.5 g, 6.5 mmol).

^{1}H NMR (400 MHz, 298 K, CD_2Cl_2): δ 7.28 (t, $^3J_{HH}$ = 8.0 Hz, 2H, *m*-OPh), 7.02–6.98 (m, 1H, *p*-OPh), 6.92–6.85 (m, 4H, *o*-OPh and N-Ar), 6.58 (d, $^3J_{HH}$ = 8.8 Hz, 2H, N-Ar), 3.63–3.55 (m, 1H, *i*-Pr C<u>H</u>), 3.45 (br s, 1H, NH), 1.21 (d, $^3J_{HH}$ = 6.4 Hz, 6H, *i*-Pr C<u>H</u>$_3$).

^{13}C{^{1}H} NMR (100 MHz, 298 K, CD_2Cl_2): δ 159.8 (s, Ar <u>C</u>-N), 147.6 (s, Ar O-<u>C</u>), 145.1 (s, Ar O-<u>C</u>), 130.0 (s, *m*-OPh), 122.4 (s, *p*-OPh), 121.8 (s, N-Ar), 117.5 (s, *p*-OPh), 114.6 (s, N-Ar), 45.2 (s, N-<u>C</u>H), 23.3 (s, *i*-Pr <u>C</u>H$_3$).

Elemental analysis calcd (%) for $C_{15}H_{17}NO$: C 79.26; H 7.54; N 6.16; Found: C 79.59; H 7.47; N 6.20.

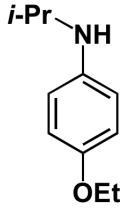

Synthesis of 2-1f

Following a literature procedure,[56] 4.9 mL (36 mmol) of 4-ethoxyaniline was added to a 250 mL round bottom flask equipped with a magnetic stir bar, and was treated with 19 mL (55 mmol) acetone, 10 g (73 mmol) $NaOAc{\cdot}3H_2O$, 31 mL (547 mmol) glacial acetic acid, 90 mL distilled

H_2O and 22 mL 95% EtOH. The reaction stirred at room temperature for 30 min, followed by slow addition of 6.9 g (182 mmol) $NaBH_4$. The reaction stirred for 24 h at room temperature. Upon completion, the reaction was extracted into 100 mL EtOAc and washed with 2 x 100 mL distilled water. The organic layer was separated, dried over Na_2SO_4, filtered, and the solvent was removed *in vacuo*. Flash column chromatography (20% EtOAc in hexanes) resulted in pure material isolated as a red oil in 45% yield (2.9 g, 16 mmol).

^{1}H NMR (400 MHz, 298 K, CD_2Cl_2): δ 6.75–6.71 (m, 2H, ArH), 6.55–6.51 (m, 2H, ArH), 3.93 (q, $^3J_{HH}$ = 7.0 Hz, 2H, OEt), 3.53 (septet, $^3J_{HH}$ = 6.3 Hz, 1H, *i*-Pr C<u>H</u>), 3.18 (br s, 1H, NH), 1.34 (t, $^3J_{HH}$ = 7.0 Hz, 3H, OEt), 1.17 (d, $^3J_{HH}$ = 6.3 Hz, 6H, *i*-Pr C<u>H</u>$_3$).

^{13}C{^{1}H} NMR (100 MHz, 298 K, CD_2Cl_2): δ 151.6 (s, Ar <u>C</u>-O), 142.6 (s, Ar <u>C</u>-N), 116.2 (s, Ar <u>C</u>H), 115.1 (s, Ar <u>C</u>H), 64.6 (s, O<u>C</u>H$_2$), 45.6 (s, N-<u>C</u>H), 23.4 (s, *i*-Pr <u>C</u>H$_3$), 15.4 (OCH$_2$<u>C</u>H$_3$).

Elemental analysis calcd (%) for $C_{11}H_{17}NO$: C 73.70; H 9.56; N 7.81; Found: C 73.68; H 9.32; N 7.75.

2.4.2.2 Synthesis and Characterization of Products

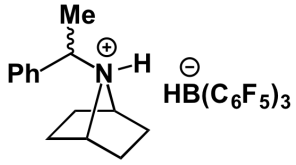

Synthesis of 2-2a

Method 1: In the glovebox, a Schlenk bomb (50 mL) was charged with a solution of **2-1a** (114 mg, 0.50 mmol) and $B(C_6F_5)_3$ (358 mg, 0.7 mmol) dissolved in toluene (4 mL). The Schlenk bomb was degassed three times through freeze-pump-thaw cycles on the vacuum/H_2 line and filled with H_2 (4 atm) at −196 °C. The reaction bomb was placed in a 115 °C oil bath for 48 hours. The toluene was then removed under reduced pressure, revealing a pale yellow oil. The oil was washed with pentane (2 x 10 mL) and the remaining material was purified via crystallization by slow diffusion of pentane into a DCM solution. The mother liquor was decanted from the crystals, which were dried under vacuum. The desired product was isolated in 51% yield (182 mg, 0.25 mmol). Crystals suitable for X-ray diffraction were obtained by slow diffusion of layered pentane into a DCM solution of **2-2a** at −35 °C.

Method 2: In the glovebox, a Schlenk bomb (50 mL) was charged with a solution of **2-1a'** (113 mg, 0.5 mmol) and $B(C_6F_5)_3$ (358 mg, 0.7 mmol) dissolved in toluene (4 mL). The Schlenk bomb was degassed three times through freeze-pump-thaw cycles on the vacuum/H_2 line and filled

with H_2 (4 atm) at −196 °C. The reaction bomb was placed in a 115 °C oil bath for 48 h. The toluene was then removed under reduced pressure, revealing a pale yellow oil. The oil was washed with pentane (2 x 10 mL) affording the product as a white powder. Compound **2-2a** was dried under vacuum and isolated in 63% yield (225 mg, 0.31 mmol). Crystals suitable for X-ray diffraction were obtained by slow diffusion of layered pentane into a DCM solution of **2-2a** at −35 °C.

^{1}H NMR (500 MHz, 298 K, CD_2Cl_2): δ 7.53–7.48 (m, 1H, *p*-C<u>H</u>), 7.47–7.42 (m, 2H, *m*-C<u>H</u>), 7.36–7.33 (m, 2H, *o*-C<u>H</u>), 5.72–5.46 (br m, 1H, NH), 4.45 (t, $^{3}J_{HH}$ = 4.8 Hz, 1H, bridgehead C<u>H</u>), 4.16–4.09 (m, 1H, C<u>H</u>(CH_3)Ph), 3.72 (t, $^{3}J_{HH}$ = 4.6 Hz, 1H, bridgehead C<u>H</u>), 3.92–3.26 (br m, 1H, BH), 2.34–2.10 (m, 4H, bicycle), 2.04–1.83 (m, 4H, bicycle), 1.76 (d, $^{3}J_{HH}$ = 6.8 Hz, 3H, C<u>H</u>$_3$).

^{19}F NMR (377 MHz, 298 K, CD_2Cl_2): δ −134.0 (d, $^{3}J_{FF}$ = 24 Hz, 2F, *o*-C_6F_5), −163.8 (t, $^{3}J_{FF}$ = 20 Hz, 1F, *p*-C_6F_5), −167.0 to −167.1 (m, 2F, *m*-C_6F_5).

^{11}B NMR (128 MHz, 298 K, CD_2Cl_2): δ −24.9 (d, $^{1}J_{BH}$ = 89 Hz, BH).

^{13}C{^{1}H} NMR (125 MHz, 298 K, CD_2Cl_2): δ 148.2 (dm, $^{1}J_{CF}$ ~ 236 Hz, C_6F_5), 137.8 (dm, $^{1}J_{CF}$ ~ 245 Hz, C_6F_5), 136.4 (dm, $^{1}J_{CF}$ ~ 249 Hz, C_6F_5), 134.6 (s, *i*-Ph), 130.8 (s, *p*-Ph), 130.1 (s, *m*-Ph), 126.6 (s, *o*-Ph), 124.6 (br s, *i*-C_6F_5), 65.2 (s, bridgehead), 64.7 (s, bridgehead), 58.6 (s, <u>C</u>H(CH_3)Ph), 27.7 (s, bicycle), 27.3 (s, bicycle), 25.4 (s, bicycle), 18.8 (s, <u>C</u>H$_3$).

Elemental analysis calcd (%) for $C_{32}H_{21}BF_{15}N$: C 53.73; H 2.96; N 1.96; Found: C 53.84; H 3.21; N 2.00

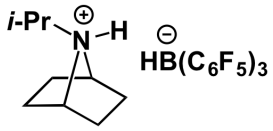

Synthesis of 2-2b

A Schlenk bomb (50 mL) was charged with a solution of **2-1b** (83 mg, 0.50 mmol) and $B(C_6F_5)_3$ (358 mg, 0.70 mmol) dissolved in toluene (4 mL). The Schlenk bomb was degassed three times through freeze-pump-thaw cycles on the vacuum/H_2 line and filled with H_2 (4 atm) at −196 °C. The reaction bomb was placed in a 115 °C oil bath for 48 h. The toluene was then removed under reduced pressure resulting in crude pale yellow oil. The oil was washed with pentane (3 x 2 mL) affording the product as a white powder. Compound **2-2b** was dried under vacuum and the product was isolated in 87% yield (285 mg, 0.44 mmol). Crystals suitable for X-ray diffraction were obtained by slow diffusion of layered pentane into a DCM solution of **2-2b** at −35 °C.

^{1}H NMR (400 MHz, 298 K, CD_2Cl_2): δ 5.53–5.23 (br m, 1H, NH), 4.29 (br s, 2H, bridgehead CH), 3.82–3.16 (br m, 1H, BH), 3.32–3.20 (m, 1H, *i*-Pr CH), 2.11–2.07 (m, 4H, bicycle), 1.96–1.82 (m, 4H, bicycle), 1.68 (dt, $^{2}J_{H\text{-}H}$ = 13.2 Hz, $^{3}J_{H\text{-}H}$ = 3.2 Hz, 1H), 1.38–1.23 (m, 4H), 1.38 (d, $^{3}J_{HH}$ = 6.4 Hz, 6H, *i*-Pr CH_3).

^{19}F NMR (377 MHz, 298 K, CD_2Cl_2, 298K): δ −134.2 (d, $^{3}J_{FF}$ = 21 Hz, 2F, *o*-C_6F_5), −163.6 (t, $^{3}J_{FF}$ = 21 Hz, 1F, *p*-C_6F_5), −166.8 to −167.0 (m, 2F, *m*-C_6F_5).

^{11}B NMR (128 MHz, 298 K, CD_2Cl_2): δ −24.8 (d, $^{1}J_{BH}$ = 88 Hz, HB).

^{13}C{^{1}H} NMR (100 MHz, 298 K, CD_2Cl_2): δ 148.5 (dm, $^{1}J_{CF}$ ~ 234 Hz, C_6F_5), 138.4 (dm, $^{1}J_{CF}$ ~ 243 Hz, C_6F_5), 137.0 (dm, $^{1}J_{CF}$ ~ 247 Hz, C_6F_5), 124.5 (br s, *i*-C_6F_5), 64.9 (s, bridgehead), 51.3 (s, *i*-Pr CH), 28.1 (s, bicycle), 26.0 (s, bicycle), 19.9 (s, *i*-Pr CH_3).

Elemental analysis calcd (%) for $C_{27}H_{19}BF_{15}N$: C 49.64; H 2.93; N 2.14; Found: C 49.30; H 3.03; N 2.20.

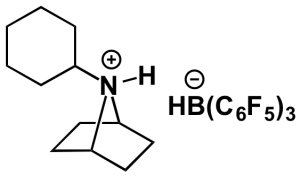

Synthesis of 2-2c

Method 1: A Schlenk bomb (50 mL) was charged with a solution of **2-1c** (100 mg, 0.50 mmol) and $B(C_6F_5)_3$ (256 mg, 0.50 mmol) dissolved in toluene (4 mL). The Schlenk bomb was degassed three times through freeze-pump-thaw cycles on the vacuum/H_2 line and filled with H_2 (4 atm) at −196 ºC. The reaction bomb was placed in a 115 °C oil bath for 48 h. The toluene was then removed under reduced pressure, revealing a yellow-green oil. The oil was washed with pentane (2 x 10 mL) and the remaining material was recrystallized via slow diffusion of pentane into dichloromethane at −35 °C, yielding compound **2-2c** in 36% yield (125 mg, 0.18 mmol). Crystals suitable for X-ray diffraction were obtained by slow diffusion of layered pentane into a DCM solution of **2-2c** at −35 °C.

Method 2: A Schlenk bomb (50 mL) was charged with a solution of **2-1c'** (102 mg, 0.50 mmol) and $B(C_6F_5)_3$ (358 mg, 0.70 mmol) dissolved in toluene (4 mL). The Schlenk bomb was degassed three times through freeze-pump-thaw cycles on the vacuum/H_2 line and filled with H_2 (4 atm) at −196 ºC. The reaction bomb was placed in a 115 °C oil bath for 48 h. The toluene was then removed under reduced pressure, revealing a yellow oil. The oil was washed with pentane (2 x 10 mL) affording the crude product as an off-white oil. The material was recrystallized via slow

diffusion of pentane into dichloromethane, yielding compound **2-2c** in 56% yield (194 mg, 0.28 mmol). Crystals suitable for X-ray diffraction were obtained by slow diffusion of layered pentane into a DCM solution of **2-2c** at −35 °C.

^{1}H NMR (400 MHz, 298 K, CD_2Cl_2): δ 5.50–5.21 (br m, 1H, NH), 4.33 (br s, 2H, bridgehead C<u>H</u>), 3.81–3.16 (br m, $^{1}J_{HB}$ = 89 Hz, BH), 2.93–2.83 (m, 1H, N-Cy), 2.10–2.02 (m, 6H), 1.91–1.82 (m, 6H), 1.71–1.66 (m, 1H), 1.38–1.23 (m, 4H), 1.12–1.02 (m, 1H).

^{19}F NMR (377 MHz, 298K, CD_2Cl_2): δ −134.2 (d, $^{3}J_{FF}$ = 23 Hz, 2F, *o*-C_6F_5), −163.6 (t, $^{3}J_{FF}$ = 20 Hz, 1F, *p*-C_6F_5), −166.9 to −167.0 (m, 2F, *m*-C_6F_5).

^{11}B NMR (128 MHz, 298K, CD_2Cl_2): δ −24.8 (d, $^{1}J_{BH}$ = 89 Hz, HB).

^{13}C{^{1}H} NMR (100 MHz, 298K, CD_2Cl_2): δ 148.5 (dm, $^{1}J_{CF}$ ~ 234 Hz, C_6F_5), 138.4 (dm, $^{1}J_{CF}$ ~ 243 Hz, C_6F_5), 137.0 (dm, $^{1}J_{CF}$ ~ 246 Hz, C_6F_5), 124.9 (br s, *i*-C_6F_5), 63.9 (s, bridgehead), 57.6 (s, N-Cy), 30.4 (s, Cy), 27.9 (s, bicycle), 26.1 (s, bicycle), 25.0 (s, Cy), 24.7 (s, Cy).

Elemental analysis calcd (%) for $C_{30}H_{23}BF_{15}N$: C 51.97; H 3.34; N 2.02; Found: C 51.56; H 3.42; N 2.30.

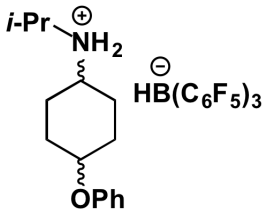

Synthesis of 2-2e

A Schlenk bomb (50 mL) was charged with a solution of **2-1e** (114 mg, 0.50 mmol) and $B(C_6F_5)_3$ (269 mg, 0.52 mmol) dissolved in toluene (1 mL). The Schlenk bomb was degassed three through a freeze-pump-thaw cycle on the vacuum/H_2 line and filled with H_2 (4 atm) at −196 °C. The reaction bomb was placed in a 115 °C oil bath for 4 days. The toluene was then removed under reduced pressure, revealing a white powder. The material was washed with pentane (3 x 2 mL) affording compound **2-2e** as a white solid in 48% yield (180 mg, 0.2 mmol).

^{1}H NMR (400 MHz, 298 K, CD_2Cl_2): δ 7.30–7.26 (m, 2H, *m*-Ph), 6.96 (t, $^{3}J_{HH}$ = 7.4 Hz, 1H, *p*-Ph), 6.88–6.84 (m, 2H, *o*-Ph), 5.93 (br s, 2H, NH_2), 4.59–4.56 (m, 0.4H, O-CH), 4.23–4.16 (m, 0.6H, O-CH), 3.74–3.10 (m, 3H, *i*-Pr C<u>H</u>, N-C<u>H</u>, B<u>H</u>), 2.27–2.06 (m, 3H, Cy), 1.90–1.81 (m, 2H, Cy), 1.70–1.48 (m, 3H, Cy), 1.42–1.37 (m, 6H, *i*-Pr C<u>H</u>$_3$).

^{19}F NMR (377 MHz, 298 K, CD_2Cl_2): δ −134.2 (d, $^{3}J_{FF}$ = 23 Hz, 2F, *o*-C_6F_5), −162.6 (t, $^{3}J_{FF}$ = 20 Hz, 1F, *p*-C_6F_5), −166.23 (td, $^{3}J_{FF}$ = 24 Hz, $^{4}J_{FF}$ = 8 Hz, 2F, *m*-C_6F_5).

^{11}B NMR (128 MHz, 298 K, CD_2Cl_2): δ −24.2 (d, $^{1}J_{BH}$ = 85 Hz, HB).

$^{13}C\{^{1}H\}$ NMR (100 MHz, 298 K, CD_2Cl_2): δ 157.7 (s, O-Ph), 157.2 (s, O-Ph), 148.6 (dm, $^{1}J_{CF}$ ~ 234 Hz, C_6F_5), 138.9 (dm, $^{1}J_{CF}$ ~ 245 Hz, C_6F_5), 137.3 (dm, $^{1}J_{CF}$ ~ 250 Hz, C_6F_5), 130.2 (s, *m*-Ph), 130.2 (s, *m*-Ph), 123.9 (br s, *i*-C_6F_5), 122.0 (s, *p*-Ph), 121.9 (s, *p*-Ph), 116.5 (s, *o*-Ph), 116.5 (s, *o*-Ph), 73.6 (s, O-CH), 69.2 (s, O-CH), 56.7 (s, N-*i*-Pr), 56.2 (s, N-*i*-Pr), 51.4 (s, N-CH), 50.9 (s, N-CH), 29.9 (s, Cy), 28.2 (s, Cy), 28.0 (s, Cy), 24.8 (s, Cy), 20.0 (s, *i*-Pr CH_3), 19.9 (s, *i*-Pr CH_3).

Elemental analysis calcd (%) for $C_{33}H_{25}BF_{15}NO$: C 53.03; H 3.37; N 1.87; Found: C 52.54; H 3.73; N 1.84.

Ratio of isomers = 1:1.4

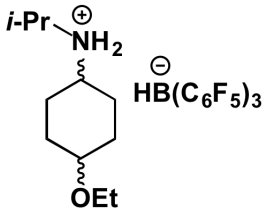

Synthesis of 2-2f

A Schlenk bomb (50 mL) was charged with a solution of **2-1f** (90 mg, 0.50 mmol) and $B(C_6F_5)_3$ (269 mg, 0.52 mmol) dissolved in toluene (1 mL). The Schlenk bomb was degassed three through a freeze-pump-thaw cycle on the vacuum/H_2 line and filled with H_2 (4 atm) at −196 °C. The reaction bomb was placed in a 115 °C oil bath for 4 days. The toluene was then removed under reduced pressure, revealing a yellow oil. The oil was washed with pentane (3 x 2 mL) affording the product as a yellow oil. The material was recrystallized via slow diffusion of pentane into a DCM solution of **2-2f**, yielding the product in 82% yield (287 mg, 0.41 mmol).

^{1}H NMR (400 MHz, 298K, CD_2Cl_2): δ 5.98 (br s, 2H, NH_2), 3.83–3.14 (m, 6H, BH, N-*i*-Pr, N-Cy, O-Cy, O-CH_2), 2.11–2.06 (m, 2H, Cy), 1.98–1.94 (m, 2H, Cy), 1.85–1.68 (m, 2H, Cy), 1.54–1.45 (m, 2H, Cy), 1.38 (d, $^{3}J_{HH}$ = 6.4 Hz, 6H, *i*-Pr CH_3), 1.14 (t, $^{3}J_{HH}$ = 7.0 Hz, 3H, Et).

^{19}F NMR (377 MHz, 298K, CD_2Cl_2): δ −134.2 (d, $^{3}J_{FF}$ = 23 Hz, 2F, *o*-C_6F_5), −163.0 (t, $^{3}J_{FF}$ = 20 Hz, 1F, *p*-C_6F_5), −166.5 (td, $^{3}J_{FF}$ = 22, 7 Hz, 2F, *m*-C_6F_5).

^{11}B NMR (128 MHz, 298K, CD_2Cl_2): δ −24.4 (d, $^{1}J_{BH}$ = 85 Hz, HB).

$^{13}C\{^{1}H\}$ NMR (100 MHz, 298K, CD_2Cl_2), partial: δ 148.5 (dm, $^{1}J_{CF}$ ~ 233 Hz, C_6F_5), 138.6 (dm, $^{1}J_{CF}$ ~ 243 Hz, C_6F_5), 137.1 (dm, $^{1}J_{CF}$ ~ 245 Hz, C_6F_5), 124.2 (br s, *i*-C_6F_5), 75.3 (s, OCH_2CH_3), 71.1 (s, OCH_2CH_3), 64.8 (s, OCH), 64.4 (s, OCH), 56.6 (s, N-*i*-Pr), 55.5 (s, N-*i*-Pr), 51.4 (s, N-CH), 50.4 (s, N-CH), 30.3 (s, Cy), 28.3 (s, Cy), 27.2 (s, Cy), 24.1 (s, Cy), 19.9 (s, Cy), 19.8 (s, Cy), 15.8 (s, OCH_2CH_3), 15.7 (s, OCH_2CH_3).

Elemental analysis calcd (%) for $C_{29}H_{25}BF_{15}NO$: C 49.81; H 3.60; N 2.00; Found: C 49.99; H 3.42; N 2.17.

Ratio of isomers = 3:1

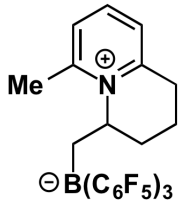

Synthesis of 2-2h

In a nitrogen-filled glovebox, alkene **2-1h** (16 mg, 0.1 mmol) was dissolved in 1 mL of toluene and transferred to a vial containing $B(C_6F_5)_3$ (51 mg, 0.1 mmol). After stirring for 13 h the reaction was concentrated *in vacuo* and the resulting precipitate was washed with 3 mL of hexanes. The wash was decanted and the remaining material was dried to yield **2-2h** as a white precipitate in 90% yield (61 mg, 0.09 mmol).

^{1}H NMR (400 MHz, 298K, CD_2Cl_2): δ 7.99 (t, $^3J_{HH}$ = 7.8 Hz, 1H, *p*-C<u>H</u>), 7.52 (d, $^3J_{HH}$ = 7.8 Hz, 1H, *m*-C<u>H</u>), 7.43 (d, $^3J_{HH}$ = 7.5 Hz, 1H, *m*-C<u>H</u>), 4.66–4.63 (m, 1H, N-C<u>H</u>), 3.60–3.52 (m, 1H, alkyl), 3.21–3.14 (m, 1H, alkyl), 2.63–2.56 (m, 1H, alkyl, B-C<u>H</u>$_2$), 2.40–2.32 (m, 1H, alkyl), 2.34 (s, 3H, Me), 2.09–2.01 (m, 1H, alkyl), 1.78–1.64 (m, 2H, alkyl), 1.34–1.26 (m, 1H, B-C<u>H</u>$_2$).

^{19}F NMR (377 MHz, 298K, CD_2Cl_2): δ −131.4 (d, $^3J_{FF}$ = 22 Hz, 2F, *o*-C_6F_5), −162.4 (t, $^3J_{FF}$ = 20 Hz, 1F, *p*-C_6F_5), −166.1 to −166.2 (m, 2F, *m*-C_6F_5).

^{11}B NMR (128 MHz, 298K, CD_2Cl_2): δ −14.2 (s).

^{13}C{^{1}H} NMR (101 MHz, 298K, CD_2Cl_2), partial: δ 157.8 (s, Ar <u>C</u>), 154.0 (s, <u>C</u>-Me), 143.0 (s, *p*-<u>C</u>H), 127.9 (s, *m*-<u>C</u>H), 127.4 (s, *m*-<u>C</u>H), 65.5 (s, N-<u>C</u>H), 29.1 (s, py-<u>C</u>H$_2$), 27.5 (br s, B-<u>C</u>H$_2$), 25.6 (s, <u>C</u>H$_2$), 20.4 (s, Me), 15.5 (s, <u>C</u>H$_2$).

Elemental analysis calcd (%) for $C_{29}H_{15}BF_{15}N$: C51.74; H 2.25; N 2.08; Found: C 50.58; H 2.17; N 1.98. Elemental analysis was consistently low on %carbon.

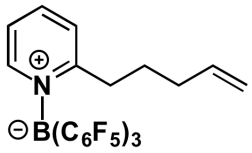

Synthesis of 2-1i'

In a nitrogen-filled glovebox, alkene **2-1i** (15 mg, 0.1 mmol) was dissolved in 1 mL toluene and transferred to a vial containing $B(C_6F_5)_3$ (51 mg, 0.1 mmol). After stirring for 13 h the reaction

was concentrated *in vacuo* yielding the desired product as a white precipitate in quantitative yield (66 mg, 0.1 mmol).

^{1}H NMR (400 MHz, 298 K, CD_2Cl_2): δ 8.66 (m, 1H, Ar C<u>H</u>), 8.16–8.08 (m, 1H, Ar C<u>H</u>), 7.59 (d, $^{3}J_{HH}$ = 8.0 Hz, 1H, Ar C<u>H</u>), 7.49 (t, $^{3}J_{HH}$ = 7.0 Hz, 1H, Ar C<u>H</u>), 5.68–5.58 (m, 1H, alkene C<u>H</u>), 4.95–4.90 (m, 2H, alkene C<u>H</u>$_2$), 3.06–2.83 (m, 2H, alkyl), 2.01–1.88 (m, 2H, alkyl), 1.51–1.40 (m, 1H, alkyl), 0.70–0.59 (m, 1H, alkyl).

^{19}F NMR (377 MHz, 298 K, CD_2Cl_2): δ −126.1 (t, $^{3}J_{FF}$ = 23 Hz, 1F, *o*-C_6F_5), −129.0 (s, 1F, *o*-C_6F_5), −131.8 (d, $^{3}J_{FF}$ = 24 Hz, 1F, *o*-C_6F_5), −132.8 (d, $^{3}J_{FF}$ = 24 Hz, 1F, *o*-C_6F_5), −133.1 to −133.6 (m, 1F, *o*-C_6F_5), −137.0 (td, $^{3}J_{FF}$ = 22, $^{4}J_{FF}$ = 9 Hz, 1F, *o*-C_6F_5), −156.3 to −156.6 (m, 1F, *p*-C_6F_5), −156.7 to −157.0 (m, 1F, *p*-C_6F_5), −158.5 to −159.0 (m, 1F, *p*-C_6F_5), −162.7 (td, $^{3}J_{FF}$ = 21 Hz, $^{4}J_{FF}$ = 8 Hz, 1F, *m*-C_6F_5), −163.3 to −163.6 (m, 1F, *m*-C_6F_5), −163.6 to −163.9 (m, 1F, *m*-C_6F_5), −164.3 to −164.7 (m, 1F, *m*-C_6F_5), −164.9 to −165.1 (m, 1F, *m*-C_6F_5), −165.1 to −165.3 (m, 1F, *m*-C_6F_5).

^{11}B NMR (128 MHz, 298 K, CD_2Cl_2): δ −3.7 (s, BH).

^{13}C{^{1}H} NMR (101 MHz, 298 K, CD_2Cl_2): δ 164.5 (s, Ar <u>C</u>), 147.9 (s, Ar <u>C</u>H), 143.1 (s, Ar <u>C</u>H), 137.3 (s, alkene <u>C</u>H), 128.3 (s, Ar <u>C</u>H), 123.0 (s, Ar <u>C</u>H), 116.0 (s, alkene <u>C</u>H$_2$), 34.2 (s, alkyl), 33.7 (s, alkyl), 29.9 (s, alkyl).

Elemental analysis calcd (%) for $C_{28}H_{13}BF_{15}N$: C 51.02; H 1.99; N 2.12; Found: C 51.30; H 2.42; N 2.56.

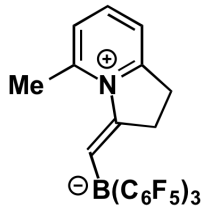

Synthesis of 2-2j

In a nitrogen-filled glovebox, alkyne **2-1j** (14 mg, 0.1 mmol) was dissolved in 1 mL of toluene and transferred to a vial containing $B(C_6F_5)_3$ (51 mg, 0.1 mmol). After stirring for 13 h the reaction was concentrated *in vacuo* and the resulting precipitate was washed with 3 mL of hexanes. The wash was decanted and the remaining material was dried to yield **2-2j** as a white powder in quantitative yield (66 mg, 0.1 mmol).

^{1}H NMR (400 MHz, 298 K, d_8-tol): δ 6.97 (br s, 1H, alkene C<u>H</u>), 6.54 (t, $^{3}J_{HH}$ = 7.8 Hz, 1H, *p*-C<u>H</u>), 6.08 (d, $^{3}J_{HH}$ = 7.7 Hz, 1H, *m*-C<u>H</u>), 5.93 (d, $^{3}J_{HH}$ = 7.8 Hz, 1H, *m*-C<u>H</u>), 2.29–2.54 (m, 2H, alkyl), 2.12–2.08 (m, 2H, alkyl), 2.11 (s, 3H, Me).

^{19}F NMR (377 MHz, 298 K, d_8-tol): δ −132.1 (d, $^3J_{FF}$ = 23 Hz, 2F, *o*-C_6H_5), −161.1 (t, $^3J_{FF}$ = 20 Hz, 1F, *p*-C_6H_5), −165.1 to −165.5 (m, 2F, *m*-C_6H_5).

^{11}B NMR (128 MHz, 298 K, d_8-tol): δ −16.1 (s).

^{13}C{^{1}H} NMR (101 MHz, 298 K, d_8-tol), partial: δ 156.4 (s, Ar C), 151.0 (s, C-Me), 148.9 (dm, $^1J_{CF}$ ~ 238 Hz, C_6F_5), 140.8 (s, *p*-CH), 139.2 (dm, $^1J_{CF}$ ~ 245 Hz, C_6F_5), 137.5 (s, *m*-CH), 137.4 (dm, $^1J_{CF}$ ~ 251 Hz, C_6F_5), 127.6 (s, *m*-CH), 120.9 (s, alkene C), 30.0 (s, CH_2), 27.5 (s, CH_2), 21.5 (s, Me).

Elemental analysis calcd (%) for $C_{28}H_{11}BF_{15}N$: C 51.17; H 1.79; N 2.07; Found: C 50.61; H 1.79; N 2.07.

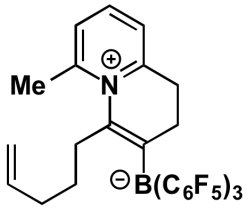

Synthesis of 2-2k

In a nitrogen-filled glovebox, alkyne **2-1k** (21 mg, 0.1 mmol) was dissolved in 1 mL of toluene and transferred to a vial containing $B(C_6F_5)_3$ (51 mg, 0.1 mmol). The resulting mixture was transferred to a Schlenk bomb equipped with a magnetic stir bar, which was sealed, removed from the glovebox, and heated to 115 °C. After 13 h the reaction was cooled to room temperature, concentrated *in vacuo* and the resulting material was washed with 3 mL of hexanes. The wash was decanted and the remaining material was dissolved in DCM, transferred to a tared vial, and dried *in vacuo* to yield **2-2k** as an off-white powder in 95% yield (69 mg, 0.09 mmol).

^{1}H NMR (400 MHz, 298 K, CD_2Cl_2): δ 7.99 (t, $^3J_{HH}$ = 7.8 Hz, 1H, *p*-CH), 7.56 (dd, $^3J_{HH}$ = 8.0 Hz, $^4J_{HH}$ = 1.7 Hz, 1H, *m*-CH), 7.48 (d, $^3J_{HH}$ = 7.6 Hz, 1H, *m*-CH), 5.48 (ddt, $^3J_{HH}$ = 17.0, 10.3, 6.8 Hz, 1H, alkene CH), 4.91–4.70 (m, 2H, alkene CH_2), 2.95–2.86 (m, 2H, alkyl), 2.85 (s, 3H, Me), 2.55–2.17 (m, 4H, alkyl), 1.70 (dd, $^3J_{HH}$ = 14.4, 6.8 Hz, 2H, alkyl), 0.52–0.41 (m, 1H, alkyl), 0.38–0.28 (m, 1H, alkyl).

^{19}F NMR (377 MHz, 298 K, CD_2Cl_2): δ −130.0 (s, 1F, *o*-C_6F_5), −130.8 to −130.9 (m, 2F, *o*-C_6F_5), −131.8 (d, $^3J_{FF}$ = 23 Hz, 1F, *o*-C_6F_5), −132.2 (br s, 1F, *o*-C_6F_5), −132.8 to −132.9 (m, 1F, *o*-C_6F_5), −161.55 to −162.64 (m, 3F, *p*-C_6F_5), −165.6 to −165.9 (m, 3F, *m*-C_6F_5), −166.2 to −166.5 (m, 3F, *m*-C_6F_5).

^{11}B NMR (128 MHz, 298 K, CD_2Cl_2): δ −14.4 (s).

$^{13}C\{^{1}H\}$ NMR (101 MHz, 298 K, CD_2Cl_2), partial: δ 159.8 (s, Ar C), 152.8 (s, C-Me), 149.0 (dm, $^{1}J_{CF}$ ~ 234 Hz, C_6F_5), 142.2 (s, *p*-CH), 137.7 (s, N-alkene), 137.4 (s, alkene CH), 137.1 (dm, $^{1}J_{CF}$ ~ 250 Hz, C_6F_5), 128.3 (s, *m*-CH), 123.6 (s, *m*-CH), 115.4 (s, alkene CH_2), 33.2 (s, CH_2), 32.0 (s, CH_2), 31.2 (s, CH_2), 26.5 (br s, CH_2), 26.2 (s, CH_2), 23.7 (s, Me).

Elemental analysis calcd (%) for $C_{33}H_{19}BF_{15}N$: C 54.65; H 2.65; N 1.93; Found: C 54.0; H 2.85; N 1.96.

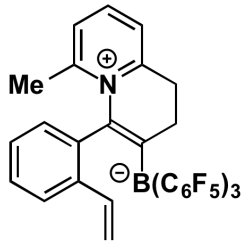

Synthesis of 2-2l

In a nitrogen-filled glovebox, alkyne **2-1l** (25 mg, 0.1 mmol) was dissolved in 1 mL of toluene and transferred to a vial containing $B(C_6F_5)_3$ (51 mg, 0.1 mmol). The resulting dark brown solution was stirred at room temperature for 13 h. The reaction was then concentrated *in vacuo* and the resulting precipitate was washed with 3 mL of hexanes. The wash was decanted and the remaining material was dried *in vacuo* to yield **2-2l** as a brown precipitate in 97% yield (74 mg, 0.1 mmol).

^{1}H NMR (400 MHz, 298 K, CD_2Cl_2): δ 7.89 (t, $^{3}J_{HH}$ = 7.7 Hz, 1H, py *p*-CH), 7.56–7.50 (m, 2H, py *m*-CH and Ph *o*-CH), 7.25 (d, $^{3}J_{HH}$ = 7.7 Hz, 1H, py *m*-CH), 7.16 (d, $^{3}J_{HH}$ = 7.7 Hz, 1H, Ph *m*-CH), 7.11–7.07 (m, 1H, Ph *m*-CH), 6.96 (d, $^{3}J_{HH}$ = 7.6 Hz, 1H, Ph *o*-CH), 5.66 (dd, $^{3}J_{HH}$ = 17.2, 11.0 Hz, 1H, alkene CH), 4.98 (d, $^{3}J_{HH}$ = 17.2 Hz, 1H, *trans* alkene CH_2), 4.66 (d, $^{3}J_{HH}$ = 11.0 Hz, 1H, *cis* alkene CH_2), 3.27–3.19 (m, 1H, alkyl), 3.13–3.08 (m, 1H, alkyl), 2.91–2.87 (m, 1H, alkyl), 2.75–2.67 (m, 1H, alkyl), 2.06 (s, 3H, Me).

^{19}F NMR (377 MHz, 298 K, CD_2Cl_2): δ −127.4 (s, 1F, *o*-C_6F_5), −127.9 (s, 1F, *o*-C_6F_5), −128.2 (s, 1F, *o*-C_6F_5), −123.0 (s, 1F, *o*-C_6F_5), −132.7 (s, 1F, *o*-C_6F_5), −134.4 (d, $^{3}J_{FF}$ = 23 Hz, 1F, *o*-C_6F_5), −161.5 (t, $^{3}J_{FF}$ = 20 Hz, 1F, *p*-C_6F_5), −162.0 (t, $^{3}J_{FF}$ = 20 Hz, 1F, *p*-C_6F_5), −163.5 (t, $^{3}J_{FF}$ = 20 Hz, 1F, *p*-C_6F_5), −165.4 (t, $^{3}J_{FF}$ = 22 Hz, 1F, *m*-C_6F_5), −166.1 (s, 1F, *m*-C_6F_5), −166.3 to −167.2 (m, 2F, *m*-C_6F_5), −167.4 (t, $^{3}J_{FF}$ = 22 Hz, 1F, *m*-C_6F_5), −168.0 (t, $^{3}J_{FF}$ = 23 Hz, 1F, *m*-C_6F_5).

^{11}B NMR (128 MHz, 298 K, CD_2Cl_2): δ −14.3 (s).

$^{13}C\{^{1}H\}$ NMR (101 MHz, 298 K, CD_2Cl_2), partial: δ 159.6 (s, py C), 154.2 (s, C-Me), 142.7 (s, py *p*-CH), 134.8 (s, Ph *o*-CH), 133.1 (s, alkene CH), 129.2 (s, py *m*-CH), 129.1 (s, Ph *m*-CH), 127.7 (s, Ph *m*-CH), 126.9 (s, Ph *o*-CH), 123.6 (s, py *m*-CH), 117.0 (s, alkene CH_2), 30.8 (s, CH_2), 27.8 (s, CH_2), 25.6 (s, Me).

Elemental analysis calcd (%) for $C_{36}H_{17}BF_{15}N$: C 56.94; H 2.26; N 1.84; Found: C 56.45; H 2.56; N 1.55.

2.4.3 X-ray Crystallography

2.4.3.1 X-ray Collection and Reduction

Crystals were coated in Paratone-N oil in the glovebox, mounted on a MiTegen Micromount and placed under an N_2 stream, thus maintaining a dry, O_2-free environment for each crystal. The data were collected on a Bruker Kappa Apex II diffractometer. Data collection strategies were determined using Bruker Apex 2 software and optimized to provide >99.5% complete data to a 2θ value of at least 55°. The data were collected at 150(±2) K for all. The data integration and absorption correction were performed with the Bruker Apex 2 software package.[57]

2.4.3.2 X-ray Solution and Refinement

Non-hydrogen atomic scattering factors were taken from the literature tabulations.[58] The heavy atom positions were determined using direct methods employing the SHELX-2013 direct methods routine. The remaining non-hydrogen atoms were located from successive difference Fourier map calculations. The refinements were carried out by using full-matrix least squares techniques on F^2. All non-hydrogen atoms were assigned anisotropic temperature factors in the absence of disorder or insufficient data. In the latter cases, atoms were treated isotropically. C-bound H atoms were placed at calculated positions and allowed to ride on the carbon to which they are bonded during refinement. H-atom temperature factors were fixed at 1.20 times (central, B–H, and N–H atoms) or 1.50 times (terminal CH_3 atoms) the isotropic temperature factor of the C-atom to which they are bonded. The locations of the largest peaks in the final difference Fourier map calculation as well as the magnitude of the residual electron densities in each case were of no chemical significance.

Table 2.5 – Select crystallographic data for **2-2b** and **2-2c**.

	2-2b	**2-2c**
Formula	$C_{27}H_{19}BF_{15}N$	$C_{30}H_{23}BF_{15}N$
Formula weight	653.26	693.32
Crystal System	Monoclinic	Orthorhombic
Space group	$P2_1/n$	$Pna2_1$
a (Å)	10.2625(4)	19.4606(10)
b (Å)	18.4212(7)	9.1786(4)
c (Å)	14.2535(5)	15.6625(8)
α (°)	90	90
β (°)	100.910(2)	90
γ (°)	90	90
V (Å^3)	2645.89(17)	2797.7(2)
Z	4	4
Temp. (K)	150	150
d_{calc} (gcm^{-1})	1.6397	1.6459
Abs. coeff. μ (mm^{-1})	0.169	0.166
Reflections Collected	24700	13394
Data $F_o^2>3\sigma(F_o^2)$	4654	4637
Variables	398	423
R	0.0368	0.0315
R_w	0.0929	0.0649
GOF	1.0542	1.0481

Table 2.6 - Select crystallographic data for **2-2j**, **2-2k**, and **2-2l**.

	2-2j·C_7H_8	**2-2k**	**2-2l**·CH_2Cl_2
Formula	$C_{35}H_{19}BF_{15}N$	$C_{33}H_{19}BF_{15}N$	$C_{37}H_{19}BCl_2F_{15}N$
Formula weight	749.32	725.30	844.24
Crystal System	Monoclinic	Monoclinic	Monoclinic
Space group	$P2_1/c$	$P2_1/c$	$P2_1/c$
a (Å)	15.7061(8)	10.4587(6)	17.0818(11)
b (Å)	11.9166(6)	18.042(1)	13.7984(8)
c (Å)	16.7185(8)	15.7100(8)	16.2764(9)
α (°)	90	90	90
β (°)	94.855(2)	102.256(2)	117.881(2)
γ (°)	90	90	90
V (Å^3)	3117.9(3)	2896.8(3)	3391.0(3)
Z	4	4	4
Temp. (K)	150	150	150
d_{calc} (gcm^{-1})	1.596	1.663	1.654
Abs. coeff. μ (mm^{-1})	0.156	0.164	0.306
Reflections collected	47567	26377	32238
Data $F_o^2>3\sigma(F_o^2)$	7136	6649	8979
Variables	463	452	506
R	0.0473	0.0420	0.0392
R_w	0.1264	0.0924	0.0913
GOF	1.034	1.028	1.060

2.5 References

(1) Walling, C.; Bollyky, L. *Journal of the American Chemical Society* **1961**, *83*, 2968–2969.

(2) Berkessel, A.; Schubert, T. J. S.; Müller, T. N. *Journal of the American Chemical Society* **2002**, *124*, 8693–8698.

(3) Spikes, G. H.; Fettinger, J. C.; Power, P. P. *Journal of the American Chemical Society* **2005**, *127*, 12232–12233.

(4) Peng, Y.; Brynda, M.; Ellis, B. D.; Fettinger, J. C.; Rivard, E.; Power, P. P. *Chemical Communications* **2008**, 6042–6044.

(5) Rit, A.; Campos, J.; Niu, H.; Aldridge, S. *Nature Chemistry* **2016**, *8*, 1022–1026.

(6) Nagata, K.; Murosaki, T.; Agou, T.; Sasamori, T.; Matsuo, T.; Tokitoh, N. *Angewandte Chemie International Edition* **2016**, *55*, 12877–12880.

(7) Frey, G. D.; Lavallo, V.; Donnadieu, B.; Schoeller, W. W.; Bertrand, G. *Science* **2007**, *316*, 439–441.

(8) Peng, Y.; Guo, J. D.; Ellis, B. D.; Zhu, Z.; Fettinger, J. C.; Nagase, S.; Power, P. P. *Journal of the American Chemical Society* **2009**, *131*, 16272–16282.

(9) Peng, Y.; Ellis, B. D.; Wang, X.; Power, P. P. *Journal of the American Chemical Society* **2008**, *130*, 12268–12269.

(10) Protchenko, A. V.; Birjkumar, K. H.; Dange, D.; Schwarz, A. D.; Vidovic, D.; Jones, C.; Kaltsoyannis, N.; Mountford, P.; Aldridge, S. *Journal of the American Chemical Society* **2012**, *134*, 6500–6503.

(11) Protchenko, A. V; Bates, J. I.; Saleh, L. M. A.; Blake, M. P.; Schwarz, A. D.; Kolychev, E. L.; Thompson, A. L.; Jones, C.; Mountford, P.; Aldridge, S. *Journal of the American Chemical Society* **2016**, *138*, 4555–4564.

(12) Welch, G. C.; San Juan, R. R.; Masuda, J. D.; Stephan, D. W. *Science* **2006**, *314*, 1124–1126.

(13) McCahill, J. S. J.; Welch, G. C.; Stephan, D. W. *Angewandte Chemie International Edition* **2007**, *46*, 4968–4971.

(14) Stephan, D. W.; Erker, G. *Angewandte Chemie International Edition* **2010**, *49*, 46–76.

(15) Stephan, D. W.; Erker, G. *Angewandte Chemie International Edition* **2015**, *54*, 6400–6441.

(16) Stephan, D. W. *Accounts of Chemical Research* **2015**, *48*, 306–316.

(17) Stephan, D. W. *Journal of the American Chemical Society* **2015**, *137*, 10018–10032.

(18) Greb, L.; Oña-Burgos, P.; Schirmer, B.; Grimme, S.; Stephan, D. W.; Paradies, J. *Angewandte Chemie International Edition* **2012**, *51*, 10164–10168.

(19) Greb, L.; Daniliuc, C. G.; Bergander, K.; Paradies, J. *Angewandte Chemie International Edition* **2013**, *52*, 5876–5879.

(20) Eros, G.; Mehdi, H.; Pápai, I.; Rokob, T. A.; Király, P.; Tárkányi, G.; Soós, T. *Angewandte Chemie International Edition* **2010**, *49*, 6559–6563.

(21) Chernichenko, K.; Madarász, A.; Pápai, I.; Nieger, M.; Leskelä, M.; Repo, T. *Nature Chemistry* **2013**, *5*, 718–723.

(22) Steffey, B. D.; Chesnut, R. W.; Kerschner, J. L.; Pellechia, P. J.; Fanwick, P. E.; Rothwell, I. P. *Journal of the American Chemical Society* **1989**, *111*, 378–380.

(23) P. Rothwell, I. *Chemical Communications* **1997**, 1331–1338.

(24) Hiroshi Hagihara and; Echigoya, E. *Bulletin of the Chemical Society of Japan* **1965**, *38*, 2094–2100.

(25) Echigoya, E.; Hagiwara, H.; Sakurai, A. *Bulletin of the Chemical Society of Japan* **1966**, *39*, 2527–2531.

(26) Ikedate, K.; Suzuki, S. *Bulletin of the Chemical Society of Japan* **1971**, *44*, 325–330.

(27) Sokolskii, D. V.; Ualikhanova, A.; Temirbulatova, A. E. *Reaction Kinetics and Catalysis Letters* **1982**, *20*, 35–37.

(28) Narayanan, S.; Sreekanth, G. *Reaction Kinetics and Catalysis Letters* **1993**, *51*, 449–458.

(29) Mink, G.; Horváth, L. *Reaction Kinetics and Catalysis Letters* **1998**, *65*, 59–65.

(30) Chatterjee, M.; Sato, M.; Kawanami, H.; Ishizaka, T.; Yokoyama, T.; Suzuki, T. *Applied Catalysis A: General* **2011**, *396*, 186–193.

(31) Mahdi, T.; Heiden, Z. M.; Grimme, S.; Stephan, D. W. *Journal of the American Chemical Society* **2012**, *134*, 4088–4091.

(32) Mahdi, T.; del Castillo, J. N.; Stephan, D. W. *Organometallics* **2013**, *32*, 1971–1978.

(33) Liu, Y.; Du, H. *Journal of the American Chemical Society* **2013**, *135*, 12968–12971.

(34) Segawa, Y.; Stephan, D. W. *Chemical Communications* **2012**, *48*, 11963–11965.

(35) Welch, G. C.; Stephan, D. W. *Journal of the American Chemical Society* **2007**, *129*, 1880–1881.

(36) Sumerin, V.; Schulz, F.; Nieger, M.; Leskelä, M.; Repo, T.; Rieger, B. *Angewandte Chemie International Edition* **2008**, *47*, 6001–6003.

(37) Voss, T.; Mahdi, T.; Otten, E.; Fro, R.; Kehr, G.; Stephan, D. W.; Erker, G. *Organometallics* **2012**, *31*, 2367–2378.

(38) Voss, T.; Chen, C.; Kehr, G.; Nauha, E.; Erker, G.; Stephan, D. W. *Chemistry - A European Journal* **2010**, *16*, 3005–3008.

(39) Birch, A. J. *Pure and Applied Chemistry* **1996**, *68*, 553–556.

(40) Daly, J. W.; Spande, T. F.; Garraffo, H. M. *Journal of Natural Products* **2005**, *68*, 1556–1575.

(41) Spande, T. F.; Garraffo, H. M.; Edwards, M. W.; Yeh, H. J. C.; Pannell, L.; Daly, J. W. *Journal of the American Chemical Society* **1992**, *114*, 3475–3478.

(42) Chen, Z.; Trudell, M. L. *Chemical Reviews* **1996**, *96*, 1179–1193.

(43) Bexrud, J.; Lautens, M. *Organic Letters* **2010**, *12*, 3160–3163.

(44) Chase, P. A.; Jurca, T.; Stephan, D. W. *Chemical Communications* **2008**, *2*, 1701–1703.

(45) Caputo, C. B.; Stephan, D. W. *Organometallics* **2012**, *31*, 27–30.

(46) Spande, T. F.; Jain, P.; Garraffo, H. M.; Pannell, L. K.; Yeh, H. J. C.; Daly, J. W.; Fukumoto, S.; Imamura, K.; Tokuyama, T.; Torres, J. A.; Snelling, R. R.; Jones, T. H. *Journal of Natural Products* **1999**, *62*, 5–21.

(47) Phillips, N.; Tirfoin, R.; Aldridge, S. *Dalton Transactions* **2014**, *43*, 15279–15282.

(48) Wilkins, L. C.; Günther, B. A. R.; Walther, M.; Lawson, J. R.; Wirth, T.; Melen, R. L. *Angewandte Chemie International Edition* **2016**, *55*, 11292–11295.

(49) Lai, P.-S.; Dubland, J. A.; Sarwar, M. G.; Chudzinski, M. G.; Taylor, M. S. *Tetrahedron* **2011**, *67*, 7586–7592.

(50) Wang, C.; Pettman, A.; Basca, J.; Xiao, J. *Angewandte Chemie International Edition* **2010**, *49*, 7548–7552.

(51) Pirovano, V.; Facoetti, D.; Acqua, M. D.; Fontana, E. Della; Abbiati, G.; Rossi, E.; Farmaceutiche, S.; Generale, C.; Marchesini, A.; Venezian, V. *Organic Letters* **2013**, *15*, 3812–3815.

(52) Weber, L.; Eickhoff, D.; Kahlert, J.; Böhling, L.; Brockhinke, A.; Stammler, H.-G.; Neumann, B.; Fox, M. A. *Dalton Transactions* **2012**, *41*, 10328–10346.

(53) Wahba, A. E.; Hamann, M. T. *The Journal of Organic Chemistry* **2012**, *77*, 4578–4585.

(54) MacNeil, S. L.; Wilson, B. J.; Snieckus, V. *Organic Letters* **2006**, *8*, 1133–1136.

(55) Anand, N.; Shah, B. A.; Kapoor, M.; Parshad, R.; Sharma, R. L.; Hundal, M. S.; Pannu, A. P. S.; Bharatam, P. V; Taneja, S. C. *The Journal of Organic Chemistry* **2011**, *76*, 5999–6006.

(56) Schellenberg, K. A. *The Journal of Organic Chemistry* **1963**, *28*, 3259–3261.

(57) *Bruker AXS Inc.*; 2013.

(58) Cromer, D. T.; Waber, J. T. In *International Tables for X-Ray Crystallography*; Kynoch Press: Birmingham, 1974; pp 71–147.

Chapter 3
Frustrated Lewis Pair Activation of an N-Sulfinylamine – A Source of Sulfur Monoxide

3.1 Introduction

3.1.1 Sulfur Monoxide – Occurrence, Properties, and Known Sources

Sulfur monoxide (SO) has been detected in the atmospheres of planets and comets in outer space[1–3] but is an unstable compound on earth.[4] Attempts to identify SO were first reported by Schenk in the 1930s.[5] Since then, chemists have exploited transition metal complexes to stabilize this reactive diatomic molecule,[6] although few examples have been crystallographically characterized (Figure 3.1).[7–15] The most common strategy for delivering SO has been extrusion from episulfoxides or trisulfide oxides, but most methods require elevated temperatures or suffer from low yields of the SO-trapped products.[16–22]

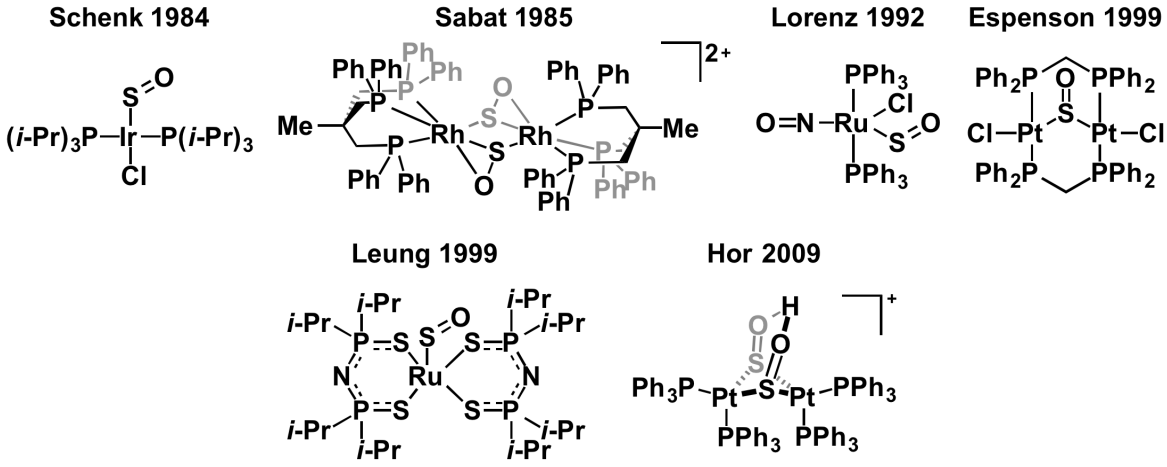

Figure 3.1 – Examples of crystallographically characterized transition metal complexes with SO ligands.

3.1.2 FLP Activation of SO_2 and Isocyanates

The advent of frustrated Lewis pair (FLP) H_2 activation, as discussed in Chapter 1, led to a substantial research effort investigating the activation of other small molecules by FLPs.[23,24] There are numerous reports detailing the reactivity of carbon and nitrogen oxides when subjected to an FLP,[25] however far less is known about the reactivity of sulfur oxides. A more recent report, which was a collaborative effort between the Stephan and Erker research groups,

discussed the activation of SO_2 with $B(C_6F_5)_3$ and phosphines.[26] It was shown that the borane and phosphine undergo a 1,2-addition across one of the S=O double bonds, generating a zwitterionic species with a B–O bond and a P–S bond (Scheme 3.1, top). These additions could be performed in an inter- or intramolecular fashion, and when treating SO_2 with an intramolecular FLP bearing a chiral centre, diastereomeric products were formed due to the chirality of the resulting sulfoxide.

Related work from the Erker laboratory in 2010 demonstrated the reactivity of phenyl isocyanate upon exposure to $Mes_2PCH_2CH_2B(C_6F_5)_2$.[27] The phosphine-borane was found to undergo a 1,2-addition across the C=O double bond, generating a new six-membered ring with an exocyclic imine functional group (Scheme 3.1, bottom). The structure of the zwitterionic product was confirmed crystallographically, with new P–C and B–O bonds identified.

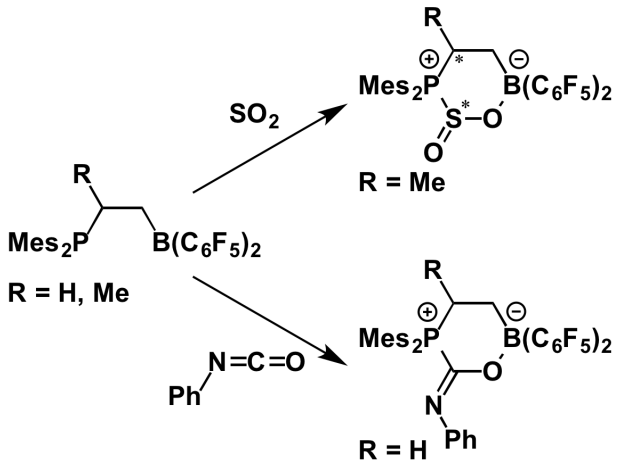

Scheme 3.1 – Reported FLP activation of SO_2 (top) and phenyl isocyanate (bottom).

3.1.3 N-Sulfinylamines

When examining the literature on FLP activation of small molecules in 2013, an absence of reactions involving N-sulfinylamines was noted. These molecules, bearing an R–N=S=O functional group, are fairly trivial to synthesize and derivatize. Treatment of a primary amine with $SOCl_2$ liberates two equivalents of HCl, which can be thermally extruded to yield the desired products in high yields (Scheme 3.2).[28] They are primarily used as building blocks for more complex organic molecules, as shown in Scheme 3.3. Treatment of R–N=S=O compounds with Grignard reagents forms sulfinamides,[28] the N=S bond can behave as a dienophile in Diels

Alder chemistry,[28] and reactions with intramolecular diamines leads to the formation of thiadiazoles.[29] N-Sulfinylamines are also known to ligate metal centres through a variety of coordination modes.[30] These compounds are trivial to prepare in large quantities and have a modular synthesis, thus their behaviour upon exposure to different FLPs was investigated and compared to the behaviour of isoelectronic SO_2.[31] The results will be presented and discussed in this chapter.

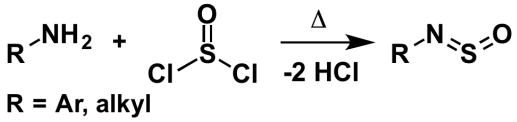

Scheme 3.2 – General synthesis of N-sulfinylamines from primary amines and thionyl chloride.

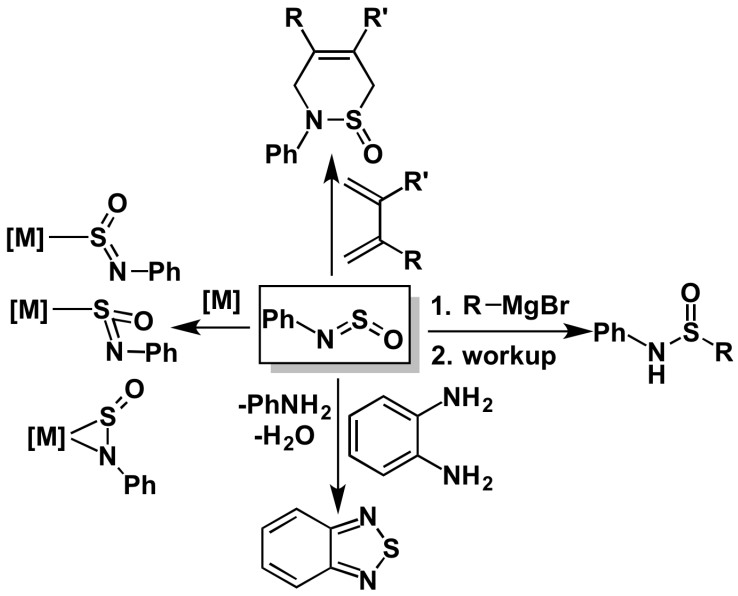

Scheme 3.3 – Reactivity of N-sulfinylamine towards dienes, Grignard reagents, diamines, and transition metal complexes.

3.2 Results and Discussion

3.2.1 Synthesis of N-Sulfinylamines

Initially, N-phenylsulfinylamine was prepared as a simple test substrate. Following a literature procedure,[29] the desired N-sulfinylamine was obtained in 77% yield. Unfortunately, any treatment of this compound with an FLP resulted in the precipitation of materials that were

sparingly soluble in organic solvents. The approach was adapted and a more soluble N-sulfinylamine **3-1**, bearing a *p*-Tolyl substituent, was synthesized following the same synthetic protocol. This material was isolated as a yellow oil in 84% yield (Scheme 3.4) and was the standard N-sulfinylamine used throughout this study.

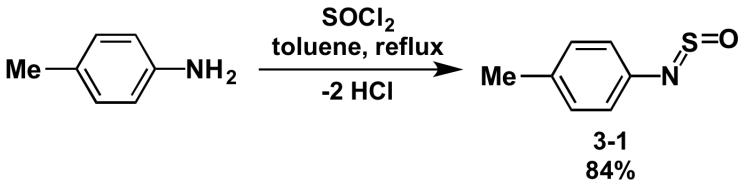

Scheme 3.4 – Synthesis of substrate **3-1**.

3.2.2 FLP Activation of N-Sulfinylamines

For an initial experiment, **3-1** was treated with the prototypical FLP used in the Stephan group, $B(C_6F_5)_3/P(t\text{-}Bu)_3$. NMR studies showed conversion to a single new product. A singlet at 83.8 ppm in the $^{31}P\{^1H\}$ NMR spectrum and a singlet at −2.1 ppm in the ^{11}B NMR spectrum (combined with sharper peaks and a smaller *meta-para* gap in the ^{19}F NMR spectrum)[32,33] led us to tentatively assign the product **3-2** as the 1,2-addition product across the S=O double bond (Figure 3.2b), analogous to the SO_2 activation by FLPs (Figure 3.2a).[26]

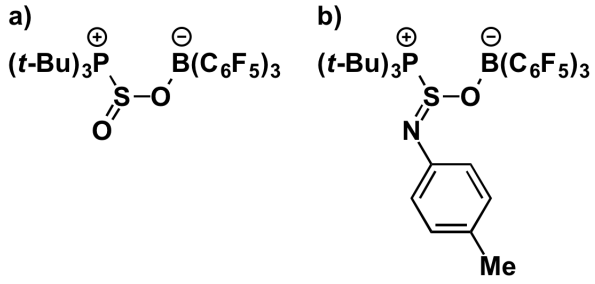

Figure 3.2 – a) SO_2 FLP activation product and b) initially proposed product of the FLP activation of **3-1**.

A complication with this project was the lack of NMR-active nuclei in the substrates; while ^{31}P, ^{19}F, and ^{11}B NMR spectra were practical for assessing the transformation of the FLP, they did not provide sufficient information regarding the transformation at the N, S, and O centres. It was essential to grow single crystals of each product to unambiguously determine the connectivity. The importance of solid state structural confirmation became even clearer when the molecular

structure of product **3-2** (Figure 3.3) was obtained, and it was not the anticipated 1,2-addition product across the S=O double bond, but the 1,3-addition product across the N=S=O functional group (Scheme 3.5). Select bond lengths and angles are shown in Table 3.1. The P–N bond length of 1.685(1) Å is similar to those of previously reported phosphinine borane adducts[34] and phosphinimine borane FLP CO_2 adducts.[35] The sum of the angles about N is 359.3°, and the N–S, S–O, and B–O bond lengths are indicative of single bond character. These data suggest that **3-2** can be viewed as a phosphinimine-borane FLP complex that is stabilizing a sulfur monoxide molecule.

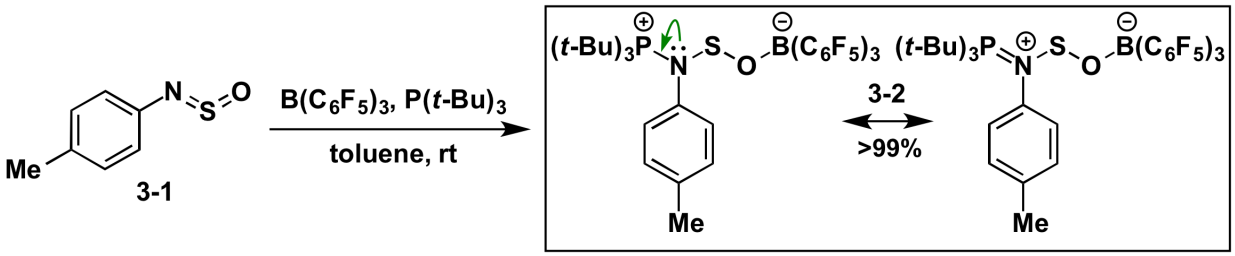

Scheme 3.5 – FLP 1,3-addition product **3-2**, with two resonance structures shown.

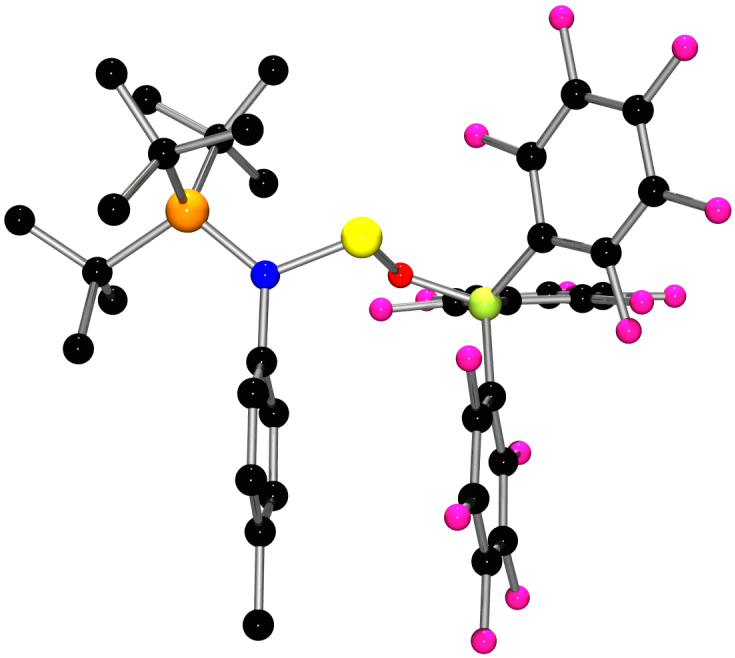

Figure 3.3 – POV-ray depiction of **3-2**, with H atoms omitted for clarity. C: black; B: yellow-green; F: pink; N: blue; O: red; P: orange; S: yellow.

The 1,3-addition reaction was found to occur when other Lewis acids were substituted for $B(C_6F_5)_3$. Exposure of **3-1** to an FLP comprised of $P(t\text{-Bu})_3$ with $Al(C_6F_5)_3$·tol (Scheme 3.6) led to similar changes in the ^{31}P and ^{19}F NMR spectra, and single crystal X-ray diffraction analysis confirmed the formation of analogous FLP 1,3-addition product **3-3** (Figure 3.4), which was isolated in 76% yield. Selected bond lengths and angles are reported in Table 3.1.

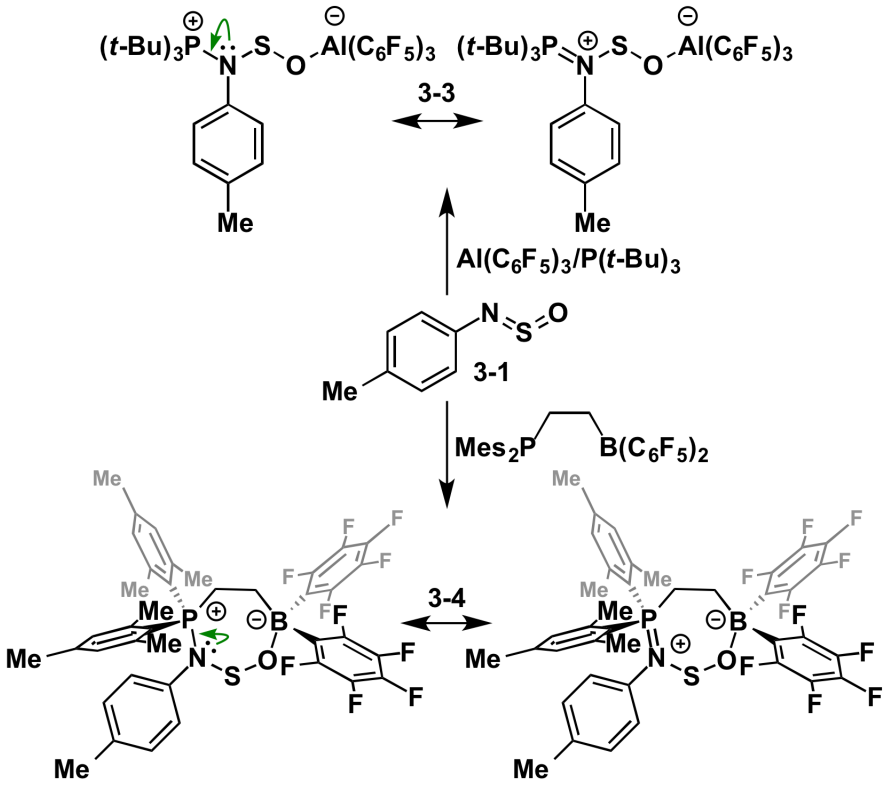

Scheme 3.6 – Synthesis of **3-3** and **3-4**.

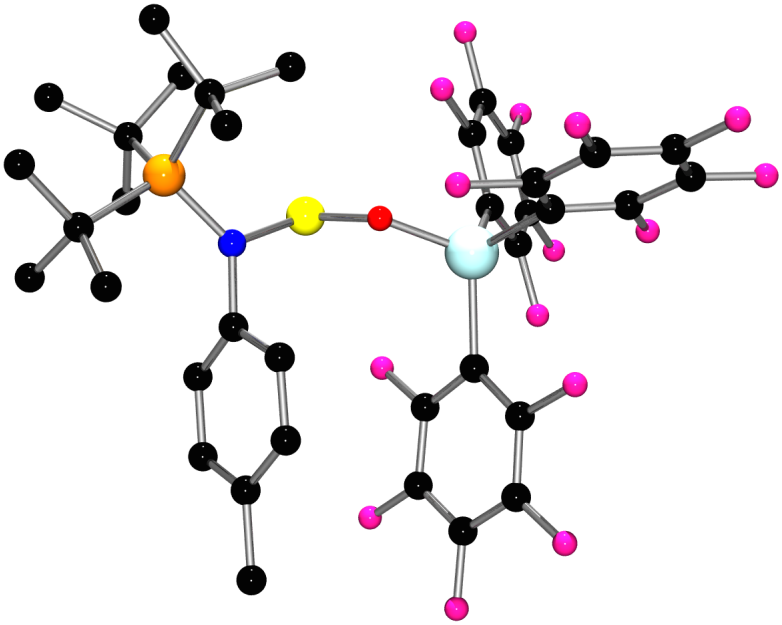

Figure 3.4 - POV-ray depiction of **3-3**, with H atoms omitted for clarity. C: black; Al: aquamarine; F: pink; N: blue; O: red; P: orange; S: yellow.

The possibility of making a heterocyclic product was intriguing, thus Erker's prototypical ethylene-linked FLP $Mes_2PCH_2CH_2B(C_6F_5)_2$[36] was treated with **3-1** (Scheme 3.6). This reaction cleanly produced 7-membered ring **3-4**, which was confirmed crystallographically (Figure 3.5). This unusual heterocycle is a rare, if not the only example of a seven-membered ring with 6 different elements linked contiguously. Selected bond lengths and angles are reported in Table 3.1, illustrating the crystallographic similarities of **3-4** to **3-2** and **3-3**.

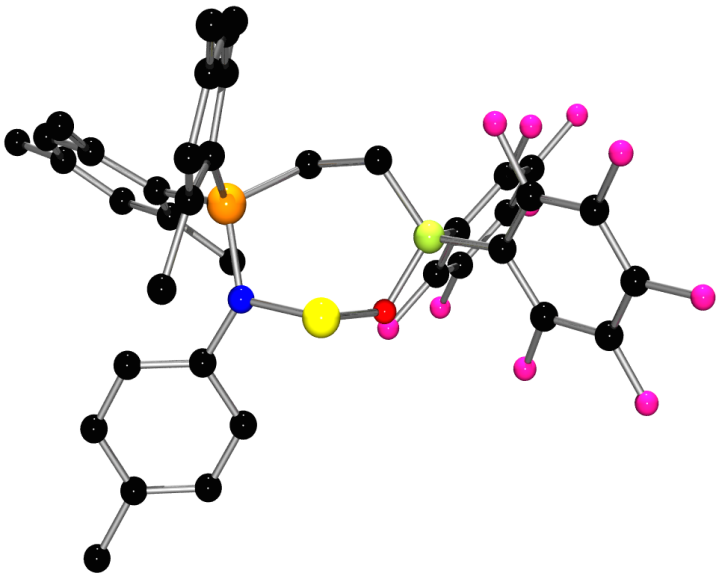

Figure 3.5 - POV-ray depiction of **3-4**, with H atoms omitted for clarity. C: black; B: yellow-green; F: pink; N: blue; O: red; P: orange; S: yellow.

Table 3.1 – Select bond lengths and angles for **3-2**, **3-3**, and **3-4**.

Product	P–N (Å)	N–S (Å)	S–O (Å)	O–B/Al (Å)	∢NSO (°)	∑∢N (°)
3-2	1.685(1)	1.712(2)	1.625(1)	1.509(2)	100.46(6)	359.3(2)
3-3	1.686(1)	1.708(1)	1.607(1)	1.767(1)	101.87(6)	359.7(2)
3-4	1.673(2)	1.713(2)	1.610(1)	1.528(3)	104.94(8)	359.6(2)

While this investigation was ongoing, a report from the Erker group discussed the reactivity of N-sulfinylamines with an intramolecular zirconocenium phosphine FLP.[37] Their system undergoes a 1,2-addition across the N=S bond, and the S=O unit binds η^2 to the metal centre (Scheme 3.7). It is an interesting contrast to the addition chemistry observed using boron and aluminum Lewis acids. Very recently, Schulz and co-workers were able to isolate the Lewis adduct of $B(C_6F_5)_3$ with H-N=S=O, the highly reactive parent N-sulfinylamine, which complexes though the nitrogen centre.[38]

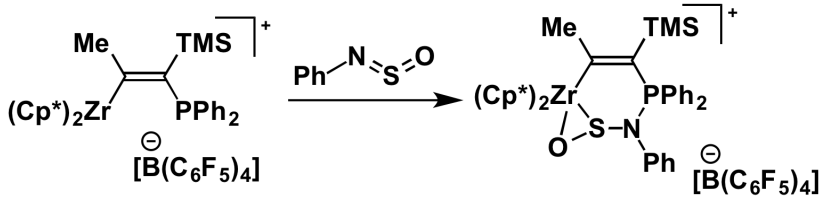

Scheme 3.7 – Reactivity of Erker's Zr^{+}/P FLP with an N-sulfinylamine.

3.2.3 Reactivity of FLP Adducts of N-Sulfinylamines

The formulation of **3-2**, **3-3**, and **3-4** as phosphinimine-borane adducts of sulfur monoxide prompted the investigation of their reactivity to determine whether they would transfer an SO molecule. Initially, **3-4** was treated with 2 equivalents of PPh_3 at 110 °C in d_8-toluene (Scheme 3.8). After 16 h, ^{31}P NMR spectroscopy showed that the 7-membered ring had been fully consumed, and 3 new products were formed. The peak at 24.2 ppm was assigned as $Ph_3P{=}O$, and the peak at 42.5 ppm was assigned as $Ph_3P{=}S$. These assignments were confirmed with authentic samples of both products. The peak at 53.2 ppm, which is close in chemical shift to that of **3-4** (50.8 ppm in d_8-toluene), was tentatively assigned as the 5-membered ring **3-5**, where the S and O atoms in **3-4** have been transferred to PPh_3. To confirm this assignment, the reaction was performed on a larger scale and the products were separated via column chromatography. The product **3-5** was isolated in 81% yield, and a single crystal X-ray diffraction study unambiguously confirmed that **3-5** is the 5-membered phosphinimine-borane adduct (Figure 3.6). This reaction was found to be kinetically favourable at room temperature, albeit with an extended reaction time of 72 h. It was also noted that treatment of **3-1** with 2 equivalents of PPh_3 at elevated temperature does not result in phosphine oxidation, as evidenced by ^{31}P NMR spectroscopy.

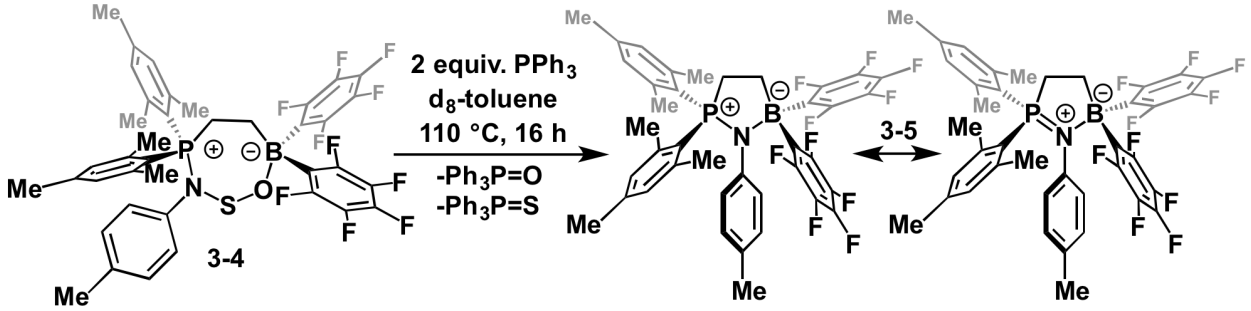

Scheme 3.8 - Reaction of **3-4** with 2 equivalents of PPh_3 to yield **3-5**.

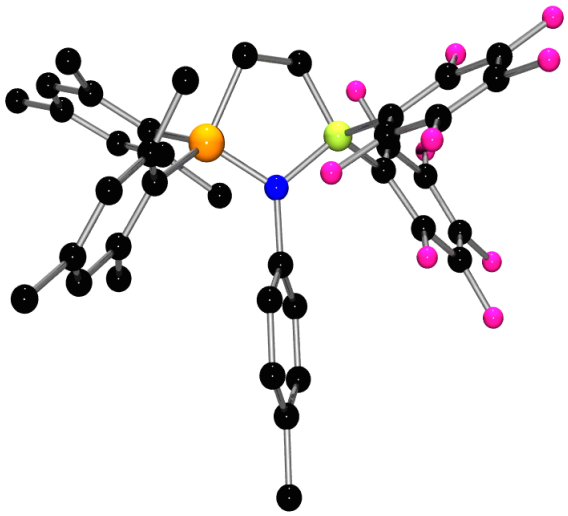

Figure 3.6 – POV-ray depiction of **3-5**, with H atoms omitted for clarity. C: black; B: yellow-green; F: pink; N: blue; P: orange.

Phosphine oxidation was also observed, and was a faster reaction, when **3-2** and **3-3** were treated with PPh_3, however their byproducts (presumably the phosphinimine-borane and phosphinimine-alane adducts, respectively) were not cleanly produced or isolable, therefore we chose to focus our reactivity studies on **3-4**.

When reading literature reports of SO transfer chemistry, an intriguing report from Agarwala in 1981 was discovered.[39] The authors treated stilbene episulfoxide with Wilkinson's complex $RhCl(PPh_3)_3$ in a 2:1 ratio in refluxing DCM, and they observed the formation of $Ph_3P{=}O$, $Ph_3P{=}S$, stilbene, and a new Rh-complex. They describe the Rh-complex as being soluble in a variety of organic solvents, diamagnetic, and air stable. Based on IR data they assigned the product as $[Rh(SO)Cl(PPh_3)]_2$, with bridging Cl ligands and terminal SO ligands. The product was not structurally characterized. **3-4** was therefore treated with $RhCl(PPh_3)_3$ in CD_2Cl_2 to determine whether the same product would be formed. The reaction was monitored by ^{31}P NMR spectroscopy and the formation of **3-5**, $Ph_3P{=}O$, $Ph_3P{=}S$, and a small amount of a product at 39.2 ppm (which was postulated to be the HCl salt of **3-5**)[34] was observed. No Rh-containing species were detected by multinuclear NMR spectroscopy, but a large amount of a new product **3-6** was formed, as evidenced by the orange crystals which grew in the NMR tube as the reaction progressed. While NMR spectroscopic analysis of the crystals was not feasible due to their insolubility in various organic solvents, a single crystal X-ray diffraction study confirmed the formulation of **3-6** as $[RhCl(\mu\text{-}\eta^1\eta^2\text{-}SO)(PPh_3)_2]_2$, a dimeric Rh complex with terminal Cl ligands

and bridging SO ligands (Figure 3.7). The Rh–S distances were found to be 2.271(2) Å and 2.327(1) Å, and the S–O and Rh–O distances were found to be 1.530(5) Å and 2.140(4) Å, respectively. **3-6** is structurally related to the dioxo compound $[RhCl(O_2)(PPh_3)_2]_2$ reported by Donaldson in 1977,[40] which was also described as an insoluble material. **3-6** represents a rare example of a [Rh(SO)] complex,[7,9,39,41–44] and is only the second example to be crystallographically characterized.[8] The overall reaction is shown in Scheme 3.9. Wilkinson's complex was also treated with **3-1** in refluxing toluene as a control reaction, and the crystals which grew from this mixture were found to be $[RhCl(PPh_3)_2]_2$,[45] confirming the prerequisite activation of the N-sulfinylamine **3-1** by an FLP in order to act as a source of sulfur monoxide.

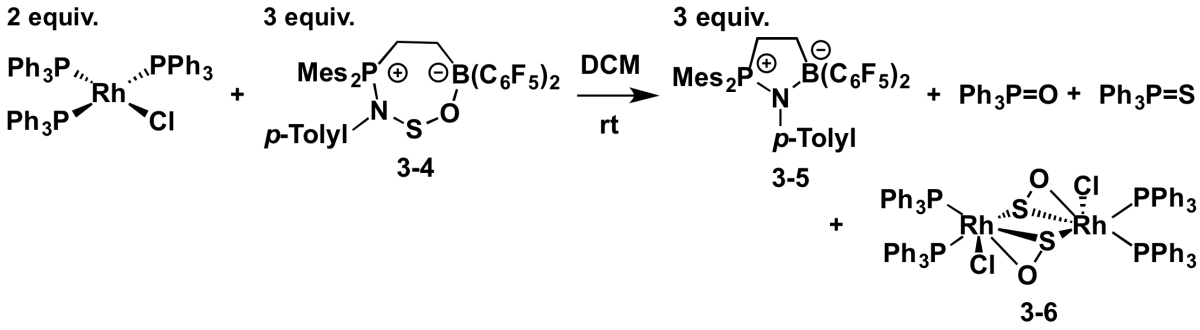

Scheme 3.9 – Reaction of **3-4** with Wilkinson's complex.

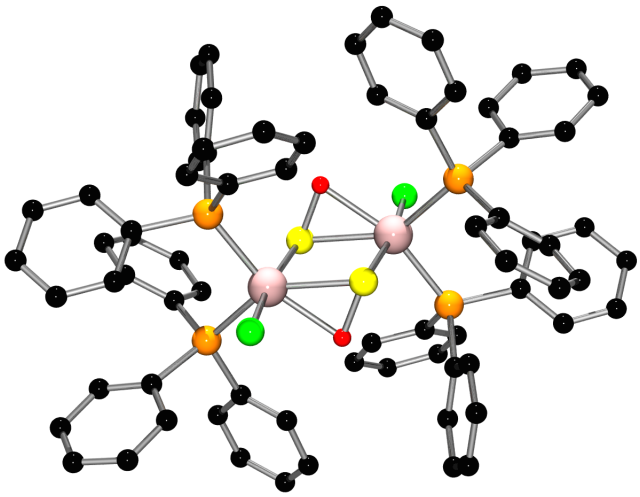

Figure 3.7 – POV-ray depiction of **3-6**, with H atoms omitted for clarity. C: black; Cl: green; O: red; P: orange; Rh: light pink; S: yellow.

Lastly, N-heterocyclic carbenes (NHCs) were reacted with the N-sulfinylamine FLP adducts. Treatment of **3-4** with one equivalent of SIMes in d_8-toluene led to the immediate formation of an off-white precipitate from a yellow solution (Scheme 3.10). Multinuclear NMR spectra showed clean formation of **3-5**. The precipitate was isolated and dissolved in CD_2Cl_2 for NMR spectroscopic analysis. The product **3-7** was ^{19}F, ^{31}P, and ^{11}B NMR silent, and the ^{1}H NMR spectrum showed resonances that appeared to match SIMes. The material was not stable in halogenated solvents for extended periods of time, and obtaining a clean $^{13}C\{^{1}H\}$ NMR spectrum proved difficult, however a resonance at 183.2 ppm was observed, which was attributed to a C=S fragment. Fortuitously, single crystals of **3-7** were grown by slowly concentrating a DCM solution of the material, which unambiguously confirmed its structure as the SIMes adduct of sulfur monoxide (Figure 3.8). To the best of our knowledge, this was the first example of NHCs acting as SO trapping agents. This provided a new route to thiourea S-oxides (also known as sulfines).[46–49]

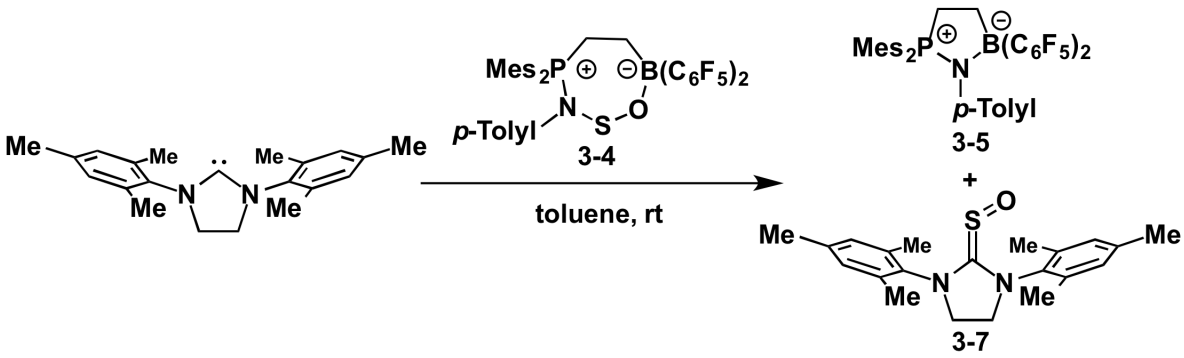

Scheme 3.10 – Reaction of **3-4** with SIMes.

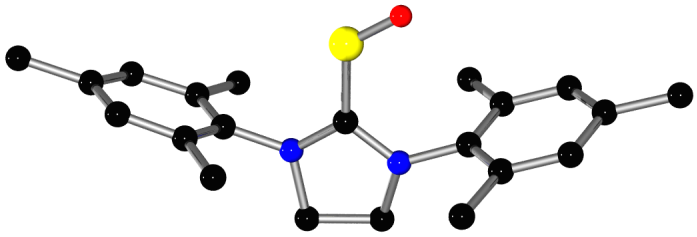

Figure 3.8 – POV-ray depiction of **3-7** (one orientation of two-fold disordered O atom is shown), with H atoms omitted for clarity. C: black; N: blue; O: red; S: yellow.

It was discovered that **3-1** also reacts with SIMes in a 1:2 ratio, generating **3-7** and a new organic product **3-8** (Scheme 3.11). Single crystals were grown from a cold, concentrated pentane solution of **3-8**, and X-ray diffraction analysis determined its structure to be a guanidine with *p*-Tolyl and SIMes substituents (Figure 3.9). It is evident that treatment of **3-1** with an NHC cleaves the N=S bond; however, when an FLP adduct of **3-1** (**3-4**) is treated with SIMes, only one equivalent of the NHC is consumed, and the resulting phosphinimine-borane adduct **3-5** is quite robust. To the best of our knowledge, this observed reactivity upon treating N-sulfinylamines with NHCs has not been reported, and this chemistry may be investigated at a later date.

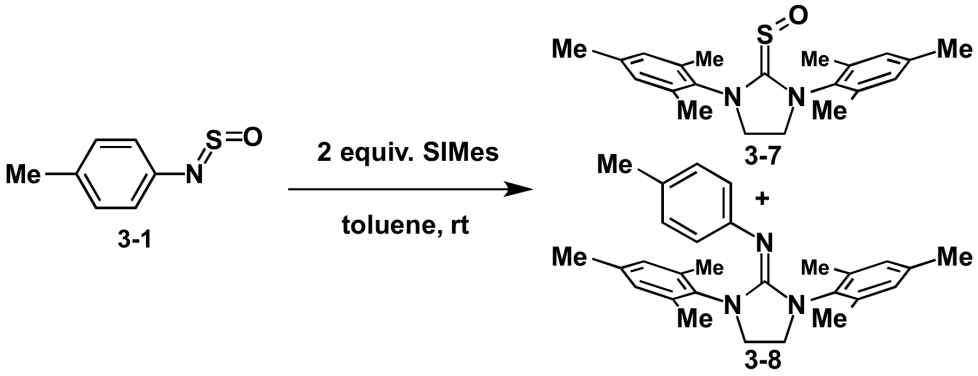

Scheme 3.11 – Reaction of **3-1** with 2 equivalents of SIMes.

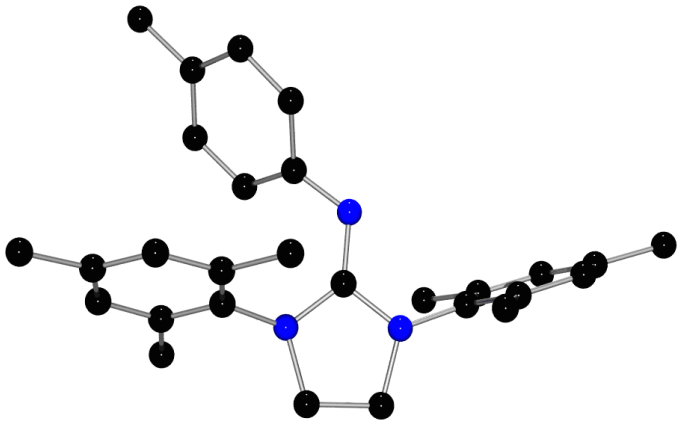

Figure 3.9 – POV-ray depiction of **3-8**, with H atoms omitted for clarity. C: black; N: blue.

3.2.4 Efforts towards SO Extrusion Chemistry

The majority of SO-transfer agents liberate sulfur monoxide at elevated temperatures through cycloreversion reactions, as discussed in section 3.1.1. It was pondered whether the FLP adducts of N-sulfinylamines were behaving in a similar fashion. After phosphinimine borane **3-5** had been fully characterized, a solution of **3-4** was heated to 110 °C to determine whether **3-5** could be observed, indicating that $SO_{(g)}$ had been extruded. Formation of **3-5** was observed, however it was an unselective reaction, and a variety of unidentified ^{31}P-containing products were also formed. Nevertheless, a large effort was focused on capturing SO from **3-4** with organic molecules, specifically dienes, as they are a commonly reported SO trapping agent.[20,21] Unfortunately, SO trapping with 2,3-dimethyl-1,3-butadiene was never observed, by either NMR spectroscopy or mass spectrometric methods. Changing the solvent and temperature did not result in SO trapping, and using a large excess of the diene also proved unsuccessful. **3-4** was the most robust of the FLP activation products, so **3-2** and **3-3** were also treated with 2,3-dimethyl-1,3-butadiene under a variety of different reaction conditions. What was observed, specifically when treating phosphine-alane NSO adduct **3-3** with butadiene at elevated temperatures, was the formation of **3-9** (Scheme 3.12), the product of a Diels Alder reaction, which was confirmed crystallographically (Figure 3.10). The same product was formed when **3-1** was treated with butadiene in refluxing toluene. It is postulated that, at elevated temperatures, **3-3** extrudes the N-sulfinylamine rather than SO, which can then undergo a [4+2] cycloaddition with 2,3-dimethyl-1,3-butadiene. Additionally, a sample of **3-4** was sent to the Cummins group at the Massachusetts Institute of Technology (MIT) to test using their Molecular Beam Mass Spectrometry (MBMS) instrumentation, which they have successfully employed to detect reactive intermediates such as P_2.[50] No sulfur monoxide was detected via MBMS, suggesting that these reactions do not proceed via loss of free $SO_{(g)}$. Instead, these reactions are believed to proceed by nucleophilic attack on the FLP NSO adduct, which then releases the SO-trapped material and **3-5**. Further work is needed to support these mechanistic predictions.

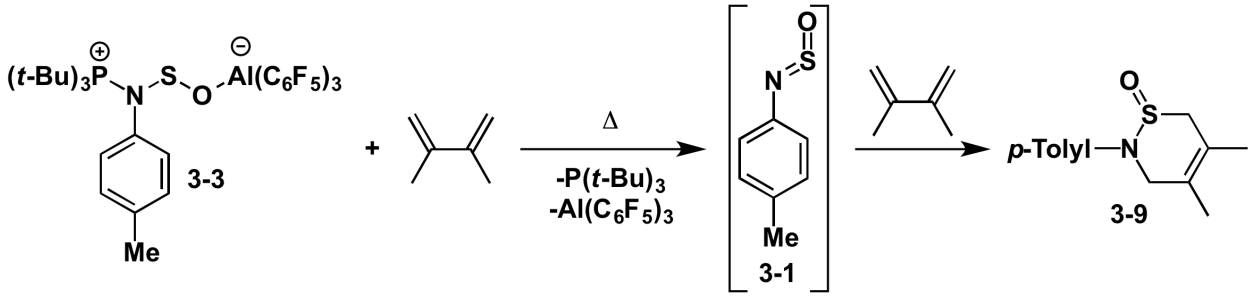

Scheme 3.12 – Proposed reaction, leading to the formation of **3-9** with prolonged heating of **3-3** in the presence of 2,3-dimethyl-1,3-butadiene.

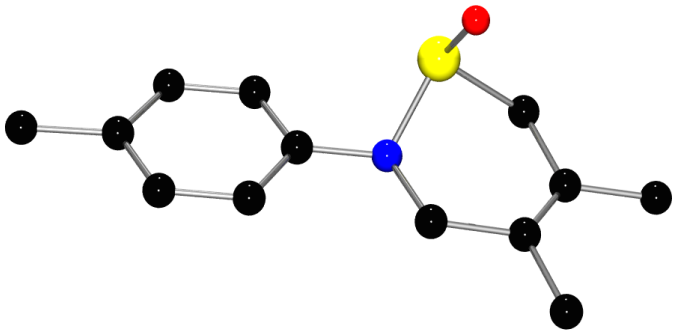

Figure 3.10 – POV-ray depiction of **3-9**, the Diels Alder product of **3-1** with 2,3-dimethyl-1,3-butadiene. H atoms are omitted for clarity. C: black; N: blue; O: red; S: yellow.

3.2.5 Sulfur Di-imine Reactivity

We were pleased to find that N-sulfinylamines, once activated by an FLP, showed interesting reactivity that the starting materials alone do no exhibit. Sulfur diimines were then sought as substrates for FLP activation, given their structural and electronic similarities with R–N=S=O compounds. Benzothiadiazole **3-10** was prepared first, which is a heterocyclic type of sulfur diimine, to test its behaviour upon exposure to an FLP (Scheme 3.13).

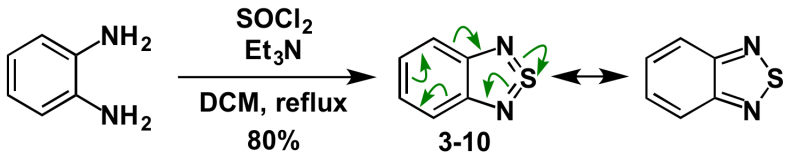

Scheme 3.13 – Formation of **3-10**, depicted by two resonance structures.

There was interest in generating a new heterocyclic product akin to **3-4**, therefore **3-10** was treated with one equivalent of Erker's linked P/B system[36] in CD_2Cl_2 at room temperature (Scheme 3.14). Multinuclear NMR spectroscopy provided evidence for the formation of a four-coordinate boron species, however the ^{31}P chemical shift of the product at −16.4 ppm indicated that a phosphinimine had not formed. X-ray diffraction analysis on single crystals grown from the NMR sample confirmed that the product was coordinated to boron through a nitrogen atom, however the phosphine arm was not bound to the substrate (Figure 3.11). Subsequent work with acyclic sulfur diimines revealed a lack of evidence for phosphine coordination when exposed to $B(C_6F_5)_3/P(t\text{-}Bu)_3$, therefore it was concluded that sulfur diimines are not amenable to FLP activation.

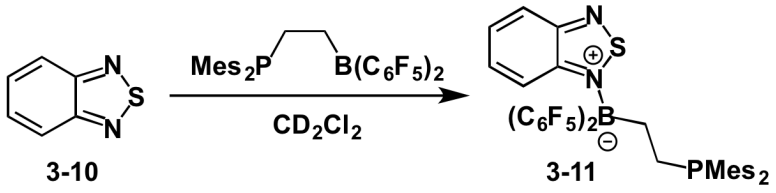

Scheme 3.14 – Synthesis of **3-11** by treatment of **3-10** with Erker's linked P/B system.

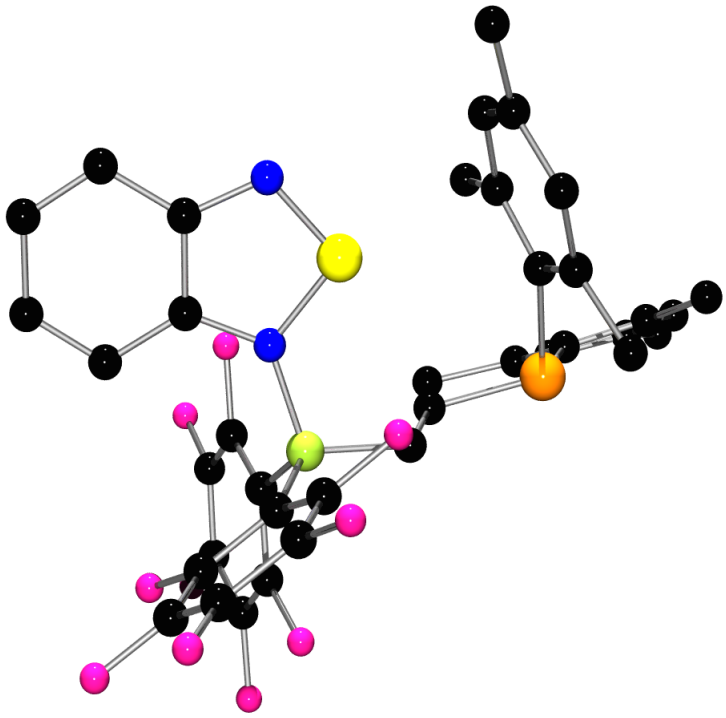

Figure 3.11 – POV-ray depiction of **3-11**, with H atoms omitted for clarity. C: black; B: yellow-green; F: pink; N: blue; P: orange; S: yellow.

3.3 Conclusions

This chapter has detailed investigations into N-sulfinylamines and related compounds as substrates for FLP activation. Inter- and intramolecular FLPs comprised of phosphine-boranes and phosphine-alanes were shown to react with N-sulfinylamine **3-1** in a 1,3-addition reaction to yield adducts **3-2**, **3-3**, and **3-4**. Crystallographic analysis confirmed the connectivity of these zwitterionic products. These materials were exploited as sources of sulfur monoxide, as evidenced by phosphine oxidation, formation of a [Rh(SO)] dimeric species, and generation of a carbene-SO adduct when **3-4** was treated with suitable substrates. This work represents the first examples of N-sulfinylamines behaving as precursors to SO, with prerequisite activation by an FLP. Preliminary investigations suggest that these reactions do no proceed via liberation of free $SO_{(g)}$. Sulfur diimines do not react with FLPs in an analogous fashion to the related N-sulfinylamines.

3.4 Experimental Section

3.4.1 General Considerations

All reactions and workup procedures were performed under an inert atmosphere of dry, oxygen-free N_2 using standard Schlenk techniques or a glovebox (MBraun, equipped with a −35 °C freezer). Hexanes, pentane, dichloromethane, and toluene (Aldrich) were dried using a Grubbs-type Innovative Technologies solvent system. Deuterated solvents (CD_2Cl_2, d_8-toluene) were purchased from Cambridge Isotope Laboratories, Inc. and stored over activated 4 Å molecular sieves prior to use. P(*t*-Bu)$_3$ and PPh_3 were purchased from Strem, Wilkinson's complex was gifted by Nova, *p*-toluidine, SIMes, and dimesitylchlorophosphine were purchased from Aldrich, thionyl chloride was purchased from BDH, and $B(C_6F_5)_3$ was purchased from Boulder Scientific. All were used without further purification. $Al(C_6F_5)_3$•tol,[51] Erker's ethylene-linked P/B system,[36] and benzothiadiazole **3-10**[52] were prepared according to literature procedures. Thin-layer chromatography (TLC) and preparative-TLC were performed on 0.5 mm EMD Silica Gel 60 F_{254} plates, with visualization of the developed plates under UV light (254 nm). Column chromatography was performed with Silicycle Silia-P Flash Silica Gel using glass columns.

IR spectra were recorded on a Perkin-Elmer Spectrum One FTIR instrument. NMR spectra were obtained on a Bruker Avance III 400 MHz, Varian Mercury 300 MHz, or Agilent DD2 500 MHz spectrometer, and spectra were referenced to residual solvent of d_8-toluene (^{1}H = 2.08 for CH_3; ^{13}C = 20.40 for CH_3), CD_2Cl_2 (^{1}H = 5.32; ^{13}C = 54.0), or externally (^{19}F: $CFCl_3$, ^{11}B: $(Et_2O)BF_3$, ^{31}P: 85% H_3PO_4). Chemical shifts are listed in ppm and coupling constants are listed in Hz. NMR assignments are supported by additional 2D experiments. Elemental analyses (C,H,N) were performed in house.

3.4.2 Syntheses and Characterizations

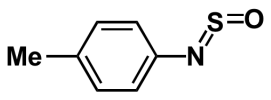

Synthesis of 3-1

Following a modified literature procedure,[28] *p*-toluidine (5.89 g, 55 mmol) was dissolved in 25 mL toluene, and to the mixture was added a solution of thionyl chloride (8.44 g, 71 mmol) in 25 mL toluene, dropwise, at room temperature. The resulting solution was heated to reflux for 16 h,

during which all the precipitate dissolved. The volatiles were removed *in vacuo*, and the remaining brown oil was purified by vacuum distillation. The desired product was obtained as a yellow oil (7.10 g, 84%). NMR data was consistent with previous literature reports.[53]

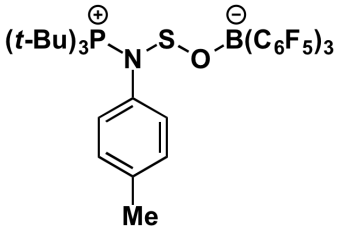

Synthesis of 3-2

A solution of P(*t*-Bu)$_3$ (101 mg, 0.5 mmol) in 1 mL of toluene was transferred to a vial containing B(C_6F_5)$_3$ (256 mg, 0.5 mmol). The resulting mixture was transferred quantitatively with an additional 1 mL toluene to a vial equipped with a magnetic stirring bar containing **3-1** (77 mg, 0.5 mmol) dissolved in 8 mL toluene. The reaction immediately turned dark red, then a cloudy peach color as the reaction progressed. The mixture was allowed to stir at room temperature for 1 h, after which the solvent was removed *in vacuo* and the resulting precipitate was stirred for 1 h over 10 mL hexanes. The solution was then decanted, yielding the desired product as a white powder (435 mg, quantitative yield). Crystals suitable for X-ray diffraction analysis were obtained through slow diffusion of hexanes into a DCM solution of **3-2** at −35 °C.

^{1}H NMR (400 MHz, 298 K, CD_2Cl_2): δ 6.96 (br s, 4H, ArH), 2.32 (s, 3H, N-*p*-Me), 1.64 (d, $^3J_{HP}$ = 14.8 Hz, 27 H, P(*t*-Bu)$_3$).

^{19}F NMR (377 MHz, 298 K, CD_2Cl_2): δ −132.0 to −132.1 (m, 2F, *o*-C_6F_5), −162.2 (t, $^3J_{FF}$ = 20 Hz, 1F, *p*-C_6F_5), −166.6 to −166.7 (m, 2F, *m*-C_6F_5).

^{31}P{^{1}H} NMR (162 MHz, 298 K, CD_2Cl_2): δ 83.8 (s).

^{11}B NMR (128 MHz, 298 K, CD_2Cl_2): δ −2.2 (s).

^{13}C{^{1}H} NMR (126 MHz, 298 K, CD_2Cl_2), partial: δ 148.2 (dm, $^1J_{CF}$ ~ 238 Hz, C_6F_5), 143.0 (d, $^2J_{CP}$ = 4 Hz, N-*i*-Ph), 139.8 (d, $^5J_{CP}$ = 1 Hz, N-*p*-Ph), 139.2 (dm, $^1J_{CF}$ ~ 244 Hz, C_6F_5), 137.0 (dm, $^1J_{CF}$ ~ 238 Hz, C_6F_5), 130.0 (br, *o*-Ph and *m*-Ph), 45.2 (d, $^1J_{CP}$ = 30 Hz, P-C), 31.4 (s, *t*-Bu), 21.1 (s, N-*p*-Me).

Elemental Analysis calcd (%) for $C_{37}H_{34}BF_{15}NOPS$: C 51.23; H 3.95; N 1.61; Found: C 50.73; H 4.34; N 1.82.

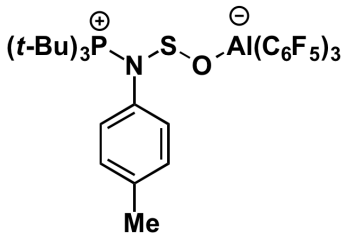

Synthesis of 3-3

A solution of P(*t*-Bu)$_3$ (82 mg, 0.41 mmol) in 1 mL of toluene was transferred to a vial containing Al(C_6F_5)$_3$•tol (252 mg, 0.41 mmol). The resulting solution was transferred quantitatively with an additional 1 mL toluene to a vial equipped with a magnetic stirring bar containing **3-1** (62 mg, 0.41 mmol) dissolved in 8 mL toluene. The solution immediately turned vivid red, then clear yellow as the reaction progressed. The mixture was allowed to stir at room temperature for 2 h, after which the solvent was removed *in vacuo* and the resulting precipitate was stirred for 1 h over 5 mL hexanes. The solution was then decanted, yielding the desired product as a white powder (275 mg, 76%). Crystals suitable for X-ray diffraction analysis were obtained through slow diffusion of cyclohexane into a DCM solution of **3-3** at room temperature.

^{1}H NMR (300 MHz, 298 K, CD_2Cl_2): δ 7.05 (d, $^3J_{HH}$ = 8.4 Hz, 2H, N-*m*-CH), 6.90 (br, N-*o*-CH), 2.24 (s, N-*p*-Me), 1.63 (d, $^3J_{HP}$ = 14.8 Hz, P-*t*-Bu).

^{19}F NMR (282 MHz, 298 K, CD_2Cl_2): δ −122.6 (dd, $^3J_{FF}$ = 28 Hz, $^4J_{FF}$ = 12 Hz, 2F, *o*-C_6F_5), −157.6 (t, $^3J_{FF}$ = 19 Hz, 1F, *p*-C_6F_5), −164.1 to −164.3 (m, 2F, *m*-C_6F_5).

^{31}P{^{1}H} NMR (121 MHz, 298 K, CD_2Cl_2): δ 82.4 (s).

^{27}Al NMR (104 MHz, 298 K, d_8-tol): δ 118 (br s, $\upsilon_{1/2}$ = ~ 1800 Hz).

^{13}C{^{1}H} NMR (101 MHz, 298 K, CD_2Cl_2), partial: δ 150.1 (dm, $^1J_{CF}$ ~ 232 Hz, C_6F_5), 143.0 (d, $^2J_{CP}$ = 5 Hz, N-*i*-Ph), 140.9 (dm, $^1J_{CF}$ ~ 251 Hz, C_6F_5), 139.4 (s, N-*p*-Ph), 136.8 (dm, $^1J_{CF}$ ~ 252 Hz, C_6F_5), 130.2 (br s, N-*o*-Ph), 129.7 (br s, N-*m*-Ph), 45.0 (d, $^1J_{CP}$ = 31 Hz, P-C), 31.3 (s, *t*-Bu), 21.0 (s, N-*p*-Me).

Elemental analysis calcd (%) for $C_{37}H_{34}AlF_{15}NOS$: C 50.29; H 3.88; N 1.59; Found: C 49.96; H 4.23; N 1.70.

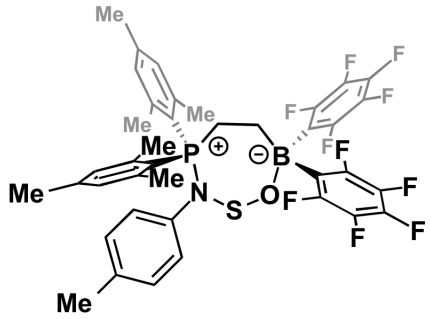

Synthesis of 3-4

Ethylene-linked P/B system (100 mg, 0.16 mmol) was dissolved in 1 mL toluene in a vial equipped with a magnetic stirring bar. **3-1** (24 mg, 0.16 mmol) was transferred to the FLP at once with 1 mL toluene. The solution immediately turned bright red, then became clear yellow as the reaction progressed. The mixture was allowed to stir at room temperature for 1 h, after which the toluene was removed *in vacuo* and the resulting yellow solid was stirred over 3 mL pentane for several hours. The pentane was decanted, yielding the desired product as a white powder (94 mg, 76% yield). Crystals suitable for X-ray diffraction analysis were obtained through slow diffusion of hexanes into a DCM solution of **3-4** at room temperature.

^{1}H NMR (400 MHz, 298 K, CD_2Cl_2): δ 7.16 (d, $^{3}J_{HH}$ = 8.0 Hz, 2H, N-*m*-CH), 6.95 (d, $^{3}J_{HH}$ = 8.4 Hz, 2H, N-*o*-CH), 6.95 (br s, 4H, Mes-*m*-CH), 3.21 (br s, 2H, P-CH_2), 2.29 (s, 6H, Mes-*p*-CH_3), 2.26 (br s, 12H, Mes-*o*-CH_3), 2.23 (s, 3H, N-*p*-CH_3), 1.60 (br d, $^{3}J_{HP}$ = 24.0 Hz, 2H, B-CH_2).

^{19}F NMR (377 MHz, 298 K, CD_2Cl_2): δ −134.6 (br s, 2F, *o*-C_6F_5), −162.1 (br s, 1F, *p*-C_6F_5), −166.1 (br s, 2F, *m*-C_6F_5).

^{31}P NMR (162 MHz, 298 K, CD_2Cl_2): δ 52.9 (br s).

^{11}B NMR (128 MHz, 298 K, CD_2Cl_2): δ 2.9 (s).

^{13}C{^{1}H} NMR (101 MHz, 298 K, CD_2Cl_2), partial: δ 148.4 (dm, $^{1}J_{CF}$ ~ 238 Hz, C_6F_5), 145.6 (d, $^{2}J_{CP}$ = 8 Hz, N-*i*-Ph), 145.1 (br s, Mes-*o*-Ph), 139.3 (dm, $^{1}J_{CF}$ ~ 246 Hz, C_6F_5), 137.4 (dm, $^{1}J_{CF}$ ~ 242 Hz, C_6F_5), 136.8 (s, N-*p*-Ph), 133.4 (br s, Mes-*m*-CH), 129.8 (s, N-*o*-CH), 124.9 (br s, N-*m*-CH), 120.3 (d, $^{1}J_{CP}$ = 92 Hz, Mes-*i*-Ph), 31.6 (d, $^{1}J_{CP}$ = 58 Hz, P-CH_2), 24.4 (br s, Mes-*o*-CH_3), 21.3 (d, $^{5}J_{CP}$ = 2 Hz, Mes-*p*-CH_3), 21.1 (s, N-*p*-CH_3), 16.6 (br s, B-CH_2).

Elemental analysis calcd (%) for $C_{39}H_{33}BF_{10}NOPS$: C 58.88; H 4.18; N 1.76; Found: C 58.61; H 4.36; N 1.73.

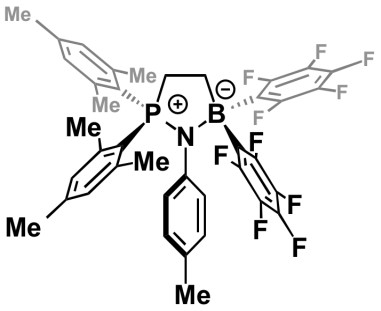

Synthesis of 3-5

Method 1: To a solution of **3-4** (100 mg, 0.13 mmol) dissolved in 2 mL toluene was added PPh_3 (68 mg, 0.26 mmol) dissolved in 1 mL toluene. The resulting faint yellow solution was quantitatively transferred to a 50 mL Schlenk bomb equipped with a magnetic stirring bar with an additional 2 mL toluene. The bomb was sealed and heated to 110 °C for 16 h, after which the volatiles were removed *in vacuo*. The remaining off-white solid, which was a mixture of the desired product, $Ph_3P{=}O$, and $Ph_3P{=}S$, was purified by flash column chromatography (100% hexanes to 1% EtOAc/hexanes), and the desired product was isolated as a crystalline white solid (76 mg, 81% yield). Crystals suitable for X-ray diffraction were obtained by cooling a saturated hexanes solution of **3-5** to −35 °C for several hours.

Method 2: To a 20 mL scintillation vial equipped with a magnetic stirring bar was added **3-4** (100 mg, 0.13 mmol). The material was dissolved in 3 mL toluene, after which PPh_3 (68 mg, 0.26 mmol) was transferred quantitatively to the solution with an additional 2 mL toluene. The resulting mixture was capped and allowed to stir at room temperature for 72 h. The volatiles were then removed *in vacuo*, and the resulting off-white solid, which was a mixture of the desired product, $Ph_3P{=}O$, and $Ph_3P{=}S$, was purified by flash column chromatography (100% hexanes to 1% EtOAc/hexanes). The product was isolated as a crystalline white solid (73 mg, 78% yield).

^{1}H NMR (400 MHz, 298 K, CD_2Cl_2): δ 6.85 (br s, 4H, Mes-*m*-CH), 6.70 (d, $^3J_{HH}$ = 8.4 Hz, 2H, N-*o*-CH), 6.48 (d, $^3J_{HH}$ = 8.0 Hz, 2H, N-*m*-CH), 2.90 (br s, 2H, P-CH_2), 2.29 (s, 6H, Mes-*p*-CH_3), 2.19 (s, 3H, N-*p*-Me), 2.14 (br s, 12H, Mes-*o*-CH_3), 1.83 (dt, $^3J_{HP}$ = 22.8 Hz, $^3J_{HH}$ = 6.0 Hz, 2H, B-CH_2).

^{19}F NMR (377 MHz, 298 K, CD_2Cl_2): δ −130.6 (br s, 2F, *o*-C_6F_5), −161.2 (br s, 1F, *p*-C_6F_5), −165.8 to −165.9 (m, 2F, *m*-C_6F_5).

^{31}P{^{1}H} NMR (162 MHz, 298 K, CD_2Cl_2): δ 54.0 (s).

^{11}B NMR (128 MHz, 298 K, CD_2Cl_2): δ −1.3 (s).

$^{13}C\{^{1}H\}$ NMR (126 MHz, 298 K, CD_2Cl_2), partial: δ 148.3 (dm, $^{1}J_{CF}$ ~ 239 Hz, C_6F_5), 143.2 (s, Mes-*p*-Ph), 142.0 (br s, Mes-*o*-Ph), 140.5 (s, N-*i*-Ph), 137.5 (dm, $^{1}J_{CF}$ ~ 244 Hz, C_6F_5), 135.3 (s, N-*p*-Ph), 132.0 (d, $^{3}J_{CP}$ = 11 Hz, Mes-*m*-CH), 129.6 (s, N-*m*-CH), 128.3 (s, N-*o*-CH), 125.4 (br s, Mes-*i*-Ph), 34.5 (d, $^{1}J_{CP}$ = 69 Hz, P-CH_2), 23.4 (br s, Mes-*o*-CH_3), 21.2 (s, Mes-*p*-CH_3), 21.0 (s, N-*p*-CH_3), 19.8 (br s, B-CH_2).

Elemental analysis calcd (%) for $C_{39}H_{33}BF_{10}NP$: C 62.67; H 4.45; N 1.87; Found: C 62.47, H 4.04, N 1.81.

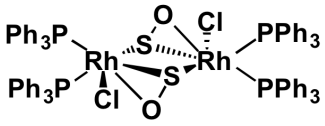

Synthesis of 3-6

To a 20 mL scintillation vial equipped with a magnetic stirring bar was added $RhCl(PPh_3)_3$ (130 mg, 0.14 mmol). The material was dissolved in 3 mL DCM, and to the resulting solution was added **3-4** (174 mg, 0.22 mmol) quantitatively with an additional 2 mL DCM. The reaction was allowed to stir at room temperature for 29 h, during which time a bright orange precipitate formed. The solution was decanted from the precipitate, which was washed with 2x1 mL DCM, yielding the product **3-6** in 46% yield (46 mg, 0.03 mmol). Crystals suitable for X-ray diffraction were grown from the above reaction when performed in a 5 mm NMR tube at room temperature. The recorded IR S=O stretching frequency is in accordance with a previously reported dimeric Rh-SO compound.[44]

IR (KBr): 874 cm^{-1}

Elemental Analysis calcd (%) for $C_{72}H_{60}Cl_2O_2P_4Rh_2S_2$: C 60.81; H 4.25; N 0.00; Found: C 60.38; H 4.36; N 0.02.

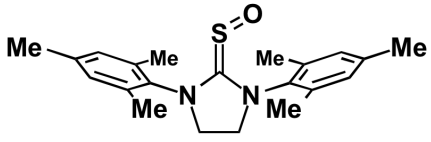

Synthesis of 3-7

To a solution of **3-4** (68 mg 0.09 mmol) dissolved in 1 mL toluene was added SIMes (26 mg, 0.09 mmol) dissolved in 1 mL toluene. The reaction stirred at room temperature for 2 h, during which a faint yellow precipitate formed. The solution was decanted from the precipitate, concentrated, redissolved in DCM, and filtered through a plug of silica, yielding **3-5** in quant. yield (64 mg, 0.09 mmol). The yellow precipitate was dissolved in minimal DCM and filtered over Celite, yielding SIMes=S=O **3-7** as an off-white powder in quant. yield (31 mg, 0.09

mmol). Crystals suitable for X-ray diffraction analysis were grown by slow concentration of a DCM solution of **3-7** at room temperature.

The carbene-SO adduct **3-7 is not stable in solution for extended periods of time, therefore only partial ^{13}C NMR data was recorded before decomposition was observed*

^{1}H NMR (400 MHz, 298 K, CD_2Cl_2): δ 6.92 (s, 4H, Mes-CH), 3.97 (s, 4H, CH_2-N), 2.38 (s, 12H, Mes *o*-CH_3), 2.29 (s, 6H, Mes *p*-CH_3).

^{13}C{^{1}H} NMR (101 MHz, 298 K, CD_2Cl_2), partial: δ 183.2 (s, C=S=O), 136.6 (br s, Mes), 129.6 (br s, *m*-CH), 48.2 (s, CH_2-N), 21.3 (s, *p*-CH_3), 18.1 (br s, *o*-CH_3).

Elemental Analysis calcd (%) for $C_{21}H_{26}N_2OS$: C 71.15; H 7.39; N 7.90; Found: C 71.41; H 7.23; N 8.12.

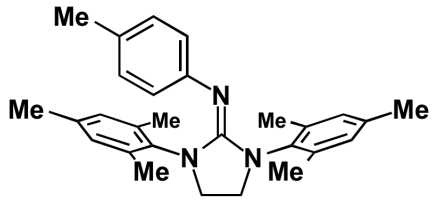

Synthesis of 3-8

A solution of **3-1** (8 mg, 0.05 mmol) in 1 mL toluene was transferred to a vial containing a solution of SIMes (31 mg, 0.1 mmol) in 1 mL toluene. The resulting yellow reaction mixture was cloudy, and was stirred with a magnetic stir bar for 30 min at ambient glovebox temperature (35 °C). The toluene was then removed *in vacuo*, and the remaining material was washed with pentane. The pentane wash was filtered to remove the insoluble **3-7** generated in the reaction, and the pentane was removed *in vacuo* to reveal **3-8** as a yellow oil, isolated in quant. yield (21 mg, 0.05 mmol).

^{1}H NMR (400 MHz, 298 K, CD_2Cl_2): δ 6.63 (br s, 4H, Mes-CH), 6.42–6.34 (m, 2H, *p*-Tolyl *m*-CH), 6.28–6.22 (m, 2H, *p*-Tolyl *o*-CH), 3.61 (s, 4H, CH_2-N), 2.20 (s, 12H, Mes *o*-CH_3), 2.07 (s, 6H, Mes *p*-CH_3), 1.90 (s, 3H, *p*-Tolyl CH_3).

^{13}C{^{1}H} NMR (101 MHz, 298 K, CD_2Cl_2): δ 149.7 (s, C=N), 147.2 (s, *p*-Tolyl *i*-C), 137.20 (s, Mes *i*-C), 137.16 (br s, Mes *o*-C), 136.5 (s, Mes *p*-C), 129.5 (s, Mes *m*-CH), 129.1 (s, *p*-Tolyl *p*-C), 128.1 (s, *p*-Tolyl *m*-CH), 121.6 (s, *p*-Tolyl *o*-CH), 47.5 (br s, CH_2-N), 21.1 (s, Mes *p*-CH_3), 20.7 (s, *p*-Tolyl CH_3), 18.5 (s, Mes *o*-CH_3).

HRMS (DART) calcd for $[C_{28}H_{34}N_3]^+$ ($[M+H]^+$) 412.2753, found 412.2760.

3.4.3 X-ray Crystallography

3.4.3.1 X-ray Collection and Reduction

Crystals were coated in Paratone-N oil in the glovebox, mounted on a MiTegen Micromount and placed under an N_2 stream, thus maintaining a dry, O_2-free environment for each crystal. The data were collected on a Bruker Kappa Apex II diffractometer. Data collection strategies were determined using Bruker Apex 2 software and optimized to provide >99.5% complete data to a 2θ value of at least 55°. The data were collected at 150(±2) K for all. The data integration and absorption correction were performed with the Bruker Apex 2 software package.[54]

3.4.3.2 X-ray Solution and Refinement

Non-hydrogen atomic scattering factors were taken from the literature tabulations.[55] The heavy atom positions were determined using direct methods employing the SHELX-2013 direct methods routine. The remaining non-hydrogen atoms were located from successive difference Fourier map calculations. The refinements were carried out by using full-matrix least squares techniques on F^2. All non-hydrogen atoms were assigned anisotropic temperature factors in the absence of disorder or insufficient data. In the latter cases, atoms were treated isotropically. C-bound H atoms were placed at calculated positions and allowed to ride on the carbon to which they are bonded during refinement. H-atom temperature factors were fixed at 1.20 times (central atoms) or 1.50 times (terminal CH_3 atoms) the isotropic temperature factor of the C-atom to which they are bonded. The locations of the largest peaks in the final difference Fourier map calculation as well as the magnitude of the residual electron densities in each case were of no chemical significance.

Table 3.2 – Selected crystallographic data for **3-2**, **3-3**, and **3-4**.

	3-2·CH_2Cl_2	**3-3**·CH_2Cl_2	**3-4**
Formula	$C_{38}H_{36}BCl_2F_{15}NOPS$	$C_{38}H_{36}AlCl_2F_{15}NOPS$	$C_{39}H_{33}BF_{10}NOPS$
Formula weight	952.42	968.59	795.50
Crystal System	triclinic	triclinic	triclinic
Space group	P-1	P-1	P-1
a (Å)	12.5907(5)	12.8518(15)	10.2018(6)
b (Å)	13.1192(5)	12.9801(16)	13.7459(8)
c (Å)	14.1964(5)	14.5667(16)	18.5545(12)
α (°)	81.895(2)	80.396(6)	72.294(2)
β (°)	73.253(2)	72.624(6)	85.469(3)
γ (°)	62.328(2)	63.046(6)	77.893(3)
V (Å^3)	1988.59(13)	2065.8(4)	2423.2(3)
Z	2	2	2
Temp. (K)	150	150	149
d_{calc} (gcm^{-1})	1.591	1.557	1.090
Abs. coeff. μ (mm^{-1})	0.361	0.369	0.164
Reflections Collected	42688	34889	40778
Data $F_o^2>3\sigma(F_o^2)$	9114	9449	11094
Variables	569	569	491
R	0.0342	0.0374	0.0511
R_w	0.0823	0.0963	0.1385
GOF	1.022	1.033	1.087

Table 3.3 – Selected crystallographic data for **3-5**, **3-6**, and **3-7**.

	3-5·CH_2Cl_2	½[**3-6**]·$2CH_2Cl_2$	**3-7**
Formula	$C_{40}H_{35}BCl_2F_{10}NP$	$C_{38}H_{34}Cl_5OP_2RhS$	$C_{21}H_{26}N_2OS$
Formula weight	832.37	880.81	354.50
Crystal System	Triclinic	Triclinic	Monoclinic
Space group	P-1	P-1	$P2_1/c$
a (Å)	10.101(3)	11.1280(12)	16.158(2)
b (Å)	11.024(3)	13.1241(14)	15.908(2)
c (Å)	17.741(5)	14.1582(14)	7.5200(11)
α (°)	82.869(14)	108.398(6)	90
β (°)	88.871(14)	105.816(6)	90.110(6)
γ (°)	79.587(14)	91.917(7)	90
V ($Å^3$)	1928.0(10)	1871.5(3)	1933.0(5)
Z	2	2	4
Temp. (K)	149	149	150
d_{calc} (gcm^{-1})	1.434	1.563	1.218
Abs. coeff. μ (mm^{-1})	0.289	0.986	0.178
Reflections Collected	27003	26904	14596
Data $F_o^2>3\sigma(F_o^2)$	6754	6570	3394
Variables	496	433	235
R	0.0769	0.0591	0.0726
R_w	0.2141	0.1384	0.1440
GOF	1.047	1.100	1.155

Table 3.4 – Selected crystallographic data for **3-8**, **3-9**, and **3-11**.

	3-8	**3-9**	**3-11**
Formula	$C_{28}H_{33}N_3$	$C_{13}H_{17}NOS$	$C_{38}H_{30}BF_{10}N_2PS$
Formula weight	411.57	235.33	778.48
Crystal System	Monoclinic	Monoclinic	Monoclinic
Space group	$P2_1/c$	$P2_1/c$	C2/c
a (Å)	12.9514(8)	4.5832(3)	28.847(3)
b (Å)	15.4049(8)	11.7755(6)	12.5107(13)
c (Å)	12.2454(7)	23.1294(15)	22.083(2)
α (°)	90	90	90
β (°)	101.223(3)	90.145(2)	117.803(5)
γ (°)	90	90	90
V ($Å^3$)	2396.4(2)	1248.28(13)	7049.6(13)
Z	4	4	8
Temp. (K)	150	150	150
d_{calc} (gcm^{-1})	1.141	1.252	1.467
Abs. coeff. μ (mm^{-1})	0.067	0.238	0.222
Reflections Collected	18678	8977	73650
Data $F_o^2>3\sigma(F_o^2)$	4213	2196	13545
Variables	280	145	479
R	0.0795	0.0445	0.0487
R_w	0.2047	0.1188	0.1355
GOF	1.022	1.042	1.030

3.5 References

(1) Despois, D. *Earth, Moon, Planets* **1997**, *79*, 103–124.

(2) Boissier, J.; Bockelee-Morvan, D.; Biver, N.; Crovisier, J.; Despois, D.; Marsden, B. G.; Moreno, R. *Astronomy & Astrophysics* **2007**, *475*, 1131–1144.

(3) Cherchneff, I.; Dwek, E. *The Astrophysical Journal* **2009**, *703*, 642–661.

(4) Greenwood, N. N.; Earnshaw, A. *Chemistry of the Elements*; Pergamon Press: New York, 1984.

(5) Schenk, P. W. *Zeitschrift für Anorganische und Allgemeine Chemie* **1933**, *211*, 150–160.

(6) Schenk, W. A. *Dalton Transactions* **2011**, *40*, 1209–1219.

(7) Schenk, W. A.; Leissner, J.; Burschka, C. *Angewandte Chemie International Edition* **1984**, *23*, 806–807.

(8) Bianchini, C.; Mealli, C.; Meli, A.; Sabat, M. *Journal of the Chemical Society, Chemical Communications* **1985**, 1024–1025.

(9) Schenk, W. A.; Leissner, J.; Burschka, C. *Zeitschrift für Naturforschung* **1985**, *40b*, 1264–1273.

(10) Heyke, O.; Beuter, G.; Lorenz, I.-P. *Journal of Organometallic Chemistry* **1992**, *440*, 197–205.

(11) Huang, R.; Guzei, I. A.; Espenson, J. H. *Organometallics* **1999**, *18*, 5420–5422.

(12) Leung, W.; Zheng, H.; Chim, J. L. C.; Chan, J.; Wong, W.; Williams, I. D. *Journal of the Chemical Society, Dalton Transactions* **2000**, 423–430.

(13) Böttcher, H.-C.; Graf, M.; Merzweiler, K.; Wagner, C. *Inorganica Chimica Acta* **2003**, *350*, 399–406.

(14) Li, J.; Koh, L. L.; Hor, T. S. A. *Chemical Communications* **2009**, 3416–3418.

(15) Tuong, C. M.; Hammons, W. K.; Howarth, A. L.; Lutz, K. E.; Maduvu, A. D.; Haysley, L. B.; Allred, B. R. T.; Hoyt, L. K.; Mashuta, M. S.; Noble, M. E. *Inorganic Chemistry* **2009**, *48*, 5027–5038.

(16) Hartzell, G. E.; Paige, J. N. *The Journal of Organic Chemistry* **1967**, *32*, 459–460.

(17) Dodson, R. M.; Sauers, R. F. *Chemical Communications* **1967**, 1189–1190.

(18) Abu-Yousef, I. A.; Harpp, D. N. *The Journal of Organic Chemistry* **1997**, *62*, 8366–8371.

(19) Abu-Yousef, I. A.; Harpp, D. N. *Tetrahedron Letters* **1995**, *36*, 201–204.

(20) Grainger, R. S.; Procopio, A.; Steed, J. W. *Organic Letters* **2001**, *3*, 3565–3568.

(21) Grainger, R. S.; Patel, B.; Kariuki, B. M.; Male, L.; Spencer, N. *Journal of the American Chemical Society* **2011**, *133*, 5843–5852.

(22) Nakayama, J.; Tajima, Y.; Xue-hua, P.; Sugihara, Y. *Journal of the American Chemical Society* **2007**, *129*, 7250–7251.

(23) Stephan, D. W.; Erker, G. *Angewandte Chemie International Edition* **2010**, *49*, 46–76.

(24) Stephan, D. W.; Erker, G. *Angewandte Chemie International Edition* **2015**, *54*, 6400–6441.

(25) Stephan, D. W.; Erker, G. *Chemical Science* **2014**, *5*, 2625.

(26) Sajid, M.; Klose, A.; Birkmann, B.; Liang, L.; Schirmer, B.; Wiegand, T.; Eckert, H.; Lough, A. J.; Fröhlich, R.; Daniliuc, C. G.; Grimme, S.; Stephan, D. W.; Kehr, G.; Erker, G. *Chemical Science* **2013**, *4*, 213.

(27) Spies, P.; Schwendemann, S.; Lange, S.; Kehr, G.; Fröhlich, R.; Erker, G. *Angewandte Chemie International Edition* **2008**, *47*, 7543–7546.

(28) Kresze, G.; Maschke, A.; Albrecht, R.; Bederke, K.; Patzschke, P.; Smalla, H.; Trede, A. *Angewandte Chemie International Edition* **1962**, *1*, 89–98.

(29) Lei, T.; Zhou, Y.; Cheng, C.; Cao, Y.; Peng, Y.; Bian, J.; Pei, J. *Organic Letters* **2011**, *13*, 2642–2645.

(30) Yeh, W.; Stern, C.; Shriver, D. F. *Inorganic Chemistry* **1996**, *35*, 7857–7862.

(31) Dahn, H.; Pechy, P.; Toama, V. Van; Bonini, B. F.; Lunazzi, L.; Mazzanti, G.; Cerioni, G.; Zwanenburg, B. *Journal of the Chemical Society, Perkin Transactions 2* **1993**, 1881–1885.

(32) Parks, D. J.; Blackwell, J. M.; Piers, W. E. *The Journal of Organic Chemistry* **2000**, *65*, 3090–3098.

(33) Blackwell, J. M.; Piers, W. E.; Parvez, M. *Organic Letters* **2000**, *2*, 695–698.

(34) Alhomaidan, O.; Hollink, E.; Stephan, D. W. *Organometallics* **2007**, *26*, 4301–4308.

(35) Jiang, C.; Stephan, D. W. *Dalton Transactions* **2013**, *42*, 630–637.

(36) Spies, P.; Erker, G.; Kehr, G.; Bergander, K.; Fröhlich, R.; Grimme, S.; Stephan, D. W. *Chemical Communications* **2007**, *2*, 5072–5074.

(37) Xu, X.; Kehr, G.; Daniliuc, C. G.; Erker, G. *Journal of the American Chemical Society* **2014**.

(38) Labbow, R.; Michalik, D.; Reiß, F.; Schulz, A.; Villinger, A. *Angewandte Chemie International Edition* **2016**, *55*, 7680–7684.

(39) Arulsamy, K. S.; Pandey, K. K.; Agarwala, U. C. *Inorganica Chimica Acta* **1981**, *54*, L51.

(40) Bennett, M. J.; Donaldson, P. B. *Inorganic Chemistry* **1977**, *16*, 1585–1589.

(41) Bianchini, C.; Mealli, C.; Meli, A.; Sabat, M. *Inorganic Chemistry* **1986**, *25*, 4617–4618.

(42) Schenk, W. A.; Leissner, J. *Zeitschrift für Naturforschung* **1987**, *42b*, 967–971.

(43) Schenk, W. A.; Johanna Leissner. *Zeitschrift für Naturforschung* **1987**, *42b*, 799–800.

(44) Neher, A.; Heyke, O.; Lorenz, I.-P. *Zeitschrift für Anorganische und Allgemeine Chemie* **1989**, *578*, 185–190.

(45) Osborn, J. A.; Jardine, F. H.; Young, J. F.; Wilkinson, G. *Journal of the Chemical Society*

A **1966**, 1711–1732.

(46) Zwanenburg, B. *Phosphorus, Sulfur, and Silicon and the Related Elements* **1989**, *43*, 1–24.

(47) Zwanenburg, B.; Damen, T. J. G.; Philipse, H. J. F.; De Laet, R. C.; Lucassen, A. C. B. *Phosphorus, Sulfur, and Silicon and the Related Elements* **1999**, *153*, 119–136.

(48) Zwanenburg, B. *Journal of Sulfur Chemistry* **2013**, *34*, 142–157.

(49) Sheppard, W. A.; Diekmann, J. *Journal of the American Chemical Society* **1964**, *86*, 1891–1892.

(50) Velian, A.; Nava, M.; Temprado, M.; Zhou, Y.; Field, R. W.; Cummins, C. C. *Journal of the American Chemical Society* **2014**, *136*, 13586–13589.

(51) Hair, G. S.; Cowley, A. H.; Jones, R. A.; McBurnett, B. G.; Voigt, A. *Journal of the American Chemical Society* **1999**, *121*, 4922–4923.

(52) DaSilveira Neto, B. A.; Lopes, A. S. A.; Ebeling, G.; Goncalves, R. S.; Costa, V. E. U.; Quina, F. H.; Dupont, J. *Tetrahedron* **2005**, *61*, 10975–10982.

(53) Braverman, S.; Cherkinsky, M. *Tetrahedron Letters* **1997**, *38*, 487–490.

(54) *Bruker AXS Inc.*; 2013.

(55) Cromer, D. T.; Waber, J. T. In *International Tables for X-Ray Crystallography*; Kynoch Press: Birmingham, 1974; pp 71–147.

Chapter 4
Investigations of P–C π-Bonds – H_2 Activation and Hydroboration

4.1 Introduction

4.1.1 A Brief History of Low Coordinate Phosphorus Compounds

Chemistry involving C=C, C=N, and C=O functional groups, where a π-bond exists between carbon and another second row element, has been investigated for over 150 years. The enormous amount of research discovering and developing the reactivity of these functional groups, and the scarcity of examples involving heavier p-block elements, cemented the dogma that (3p-2p) π-bonds are unstable.[1–4] This notion was perpetuated by the formation and detection of HC≡P[5] and CH_2=PH,[6] which were characterized spectroscopically in the gas phase, but could not be isolated. This view was challenged by the mid 1960s, when phosphinines[7] and phosphacyanines[8] were found to be the first stable and isolable examples of C–P π-bonds. This chapter will focus on the chemistry of phosphaalkenes, phosphaalkynes, phosphinines, and triphosphabenzenes.

4.1.1.1 Phosphaalkenes

The first example of an isolable, localized P=C bond was the phosphaalkene prepared by Becker in 1976 (Scheme 4.1a),[9] and the first example of an all-carbon substituted phosphaalkene was reported by Bickelhaupt in 1978 (Scheme 4.1b).[10] Since these seminal reports, phosphaalkenes have been applied as ligands in transition metal catalysis, as monomers for phosphorus-containing polymers, and as subunits in π-conjugated phosphorus-containing materials.[4,11–13]

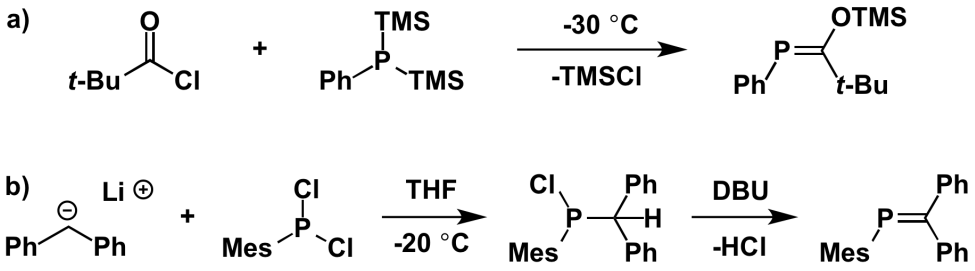

Scheme 4.1 – The first reports of localized P=C bonds by a) Becker and b) Bickelhaupt.

4.1.1.2 Phosphaalkynes

Stable phosphaalkynes were not reported until after the chemistry of phosphaalkenes and conjugated P-heterocycles had been established. In fact, 20 years passed after Gier's detection of HC≡P[5] before a kinetically stabilized phosphaalkyne, *t*-Bu-C≡P, was prepared and isolated.[14] This remarkable synthetic accomplishment was achieved by treating a Becker phosphaalkene[9] with NaOH (Scheme 4.2). This original synthesis has been further optimized, and has been applied to the synthesis of many different phosphaalkynes.[15]

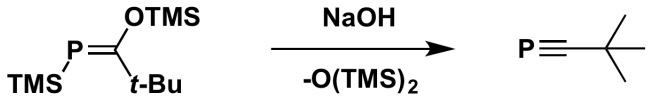

Scheme 4.2 – The first report detailing the preparation and isolation of a phosphaalkyne.

In 1992, Becker reported the first synthesis of $[O–C≡P]^-$,[16] the phosphorus analogue of cyanate; the groups of Grützmacher,[17] Cummins,[18] and Goicoechea[19] have recently modified the approach for the synthesis of $[OCP]^-$ with different countercations. The $[OCP]^-$ anion has been demonstrated to be a versatile building block for phosphaurea[20] and phosphorus-containing heterocycles.[21]

4.1.1.3 Phosphinines

Phosphinines, or monophosphabenzenes, were among the first isolable examples of low coordinate phosphorus species.[7] After Märkl's pioneering report in 1966 detailing the preparation of 2,4,6-triphenylphosphinine from 2,4,6-triphenylpyrylium tetrafluoroborate (Scheme 4.3), he expanded the synthetic scope and showed that $P(CH_2OH)_3$ could be replaced with $P(TMS)_3$ or PH_3, which eliminated the need of an external base (such as pyridine) to generate phosphinines.[22,23] Ashe was later able to synthesize the parent phosphinine PC_5H_5.[24]

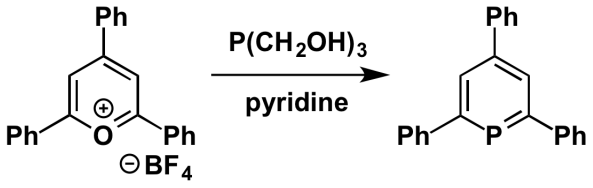

Scheme 4.3 – The first report by Märkl detailing the synthesis of 2,4,6-triphenylphosphinine.

4.1.1.4 1,3,5-Triphosphabenzene

1,3,5-Triphosphabenzene was first prepared in the coordination sphere of transition metals. Cowley described a triphosphabenzene-ligated molybdenum complex that arose by treating [$Mo(CO)_3$(η^6-cycloheptatriene)] with *tert*-butylphosphaalkyne.[25] In 1995, Binger was able to liberate 2,4,6-tri-*tert*-butyl-1,3,5-triphosphabenzene from a hafnium complex by treatment with C_2Cl_6.[26] While these reports represent the earliest evidence that the cyclotrimerization of phosphaalkynes using metals had synthetic value, they were not preparative methods for generating the desired P-heterocycle. The work by Preuss and Regitz detailing the reactivity of phosphaalkynes with vanadium species[27] became the first synthetically convenient route to appreciable quantities of triphosphabenzenes. They found that combining phosphaalkyne with $Cl_3V{=}N(t\text{-Bu})$ in a 4:1 ratio resulted in a cyclotrimerization reaction, and triphosphabenzenes were isolated in yields as high as 68%. This method is now the standard approach for synthesizing these P-heterocycles (Scheme 4.4).[28]

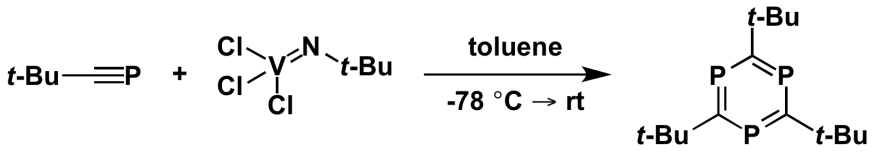

Scheme 4.4 – Synthesis of triphosphabenzene via cyclotrimerization of phosphaalkyne.

4.1.2 Reactivity of Phosphaalkynes

Phosphaalkynes demonstrate reactivity more akin to alkynes than nitriles, which is the inspiration for their name.[3,15] Their HOMO is associated with the P≡C triple bond, not the lone pair on phosphorus, in contrast to nitriles. When treated with HCl, a 1,2-addition is observed, generating new P–Cl and C–H bonds; protonation of the phosphorus centre does not occur. Many E–H 1,2-additions reactions to phosphaalkynes have been reported, including additions of germanes,[29] stannanes,[30] boranes,[31] and metal hydrides.[32–35] Most of these additions proceed with formation of a P–H bond, which is supported by the difference in electronegativity between phosphorus and carbon. The anomalous examples are the metal hydride addition reactions, specifically Ru–H additions to phosphaalkynes, where a C–H bond is formed. This contrasting reactivity is likely due to the steric bulk around the Ru centre, favouring bond formation with the less sterically encumbered site of the phosphaalkyne.

Phosphaalkynes undergo a variety of cycloadditions reactions, including [2+1], [3+2], and [4+2] cycloadditions.[3] A more recent example by the Martin group detailed the reaction of adamantylphosphaalkyne with a pentaarylborole; the mechanism was investigated using DFT calculations, which suggested that the reaction proceeded via a Diels Alder cycloaddition.[36]

4.1.3 Reactivity of P-Heterocycles

4.1.3.1 Phosphinines

The reactivity of phosphinines is dissimilar to their N-analogue, pyridine. The primary difference is that the HOMO of pyridine is the N lone pair, whereas the P lone pair in phosphinine is the HOMO^{-2}. The N lone pair orbital is computed to contain 29% s-orbital character, while the P lone pair orbital is computed to contain 64% s-orbital character, meaning phosphinines bear a lone pair that is more diffuse and less directional than pyridine.[37] This also means that phosphinines are very weak bases, and only recently was Reed able to successfully protonate 2,4,6-tri-*tert*-butylphosphinine using carborane acids.[38] Monophosphabenzenes are aromatic molecules;[39] their P-ring is planar, with NMR resonances in the same chemical shift regions as benzene, and they are computed to possess 88-90% of the aromatic stabilization of benzene.[40]

Phosphinines have been used as ligands for transition metals with applications in homogeneous catalysis. Major advances were the Fe-catalyzed cyclotrimerization of alkynes[41] and the Rh-catalyzed hydroformylation of olefins,[42] both using phosphinine ligands. Phosphinines are also suitable dienes for Diels Alder chemistry, and have been demonstrated to undergo [4+2] cyclizations to generate bicyclic phosphines with a variety of dienophiles (alkynes[43] and benzyne[44]).

4.1.3.2 Triphosphabenzene

Triphosphabenzenes are a class of phosphorus-containing heterocycles which have not been developed to the same extent as phosphinines, however their reactivity is similar in many ways. They are planar[45] and are calculated to have ~85% of the aromatic stability of benzene.[39] Russell and co-workers have also shown that deviations from planarity do not significantly perturb their aromaticity.[46]

Triphosphabenzenes, like phosphinines, are weak bases, and have only recently been reported to undergo protonation with strong carborane acids.[38] They are suitable dienes for Diels Alder

chemistry, and undergo [4+2] cycloadditions with alkenes, alkynes, and phosphaalkynes.[28] Triphosphabenzenes were also reported to undergo a [1+4] cycloaddition with a stable silylene, producing a bicyclic product with a bridging Si centre (Figure 4.1a).[47] Regitz and co-workers have shown that treatment of triphosphabenzene with Grignard reagents (Figure 4.1b)[48] or lithium alkoxides (Figure 4.1c)[49] results in nucleophilic attack at a P-centre, consistent with the electronegativity difference between carbon and phosphorus.

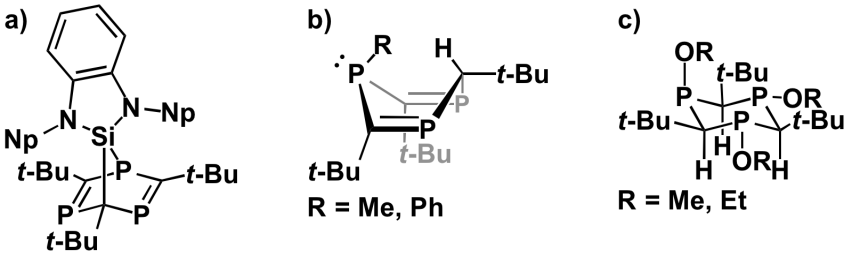

Figure 4.1 – Products from triphosphabenzene reactions with a) silylene, b) Grignard reagents, and c) lithium alkoxides.

Very recently, the Scheer group reported their synthesis of a silicon analogue of triphosphabenzene.[50] Computational studies suggest that these P_3Si_3 rings possess aromatic character, and while no reactivity was reported, it is anticipated that the chemistry of these heterocycles will be the subject of future reports.

4.2 Results and Discussion

4.2.1 Reduction of Triphosphabenzene

In Chapter 2, the advent of frustrated Lewis pair (FLP) aromatic hydrogenation[51] and its application in the reduction of N-heterocycles was discussed.[52,53] Given the propensity of 2,4,6-tri-*tert*-butyl-1,3,5-triphosphabenzene (**4-1**) to undergo aromatic reduction with reagents such as main group hydrides,[54] or upon hydrolysis of its Hf-complexes,[55] it was thought that **4-1** would also be amenable to FLP hydrogenation. We believed (naively) that this P-heterocycle would behave like a 2,6-disubstituted pyridine, and would activate H_2 in combination with $B(C_6F_5)_3$. We were hopeful that, given the weaker basicity of P-heterocycles compared to N-heterocycles,[40,56] an FLP-catalyzed aromatic reduction could be achieved.[57,58]

The initial experiment subjected a C_6D_5Br solution of **4-1** to 4 atm H_2 in the presence of 5 mol% $B(C_6F_5)_3$. The reaction proceeded, albeit slowly, at 60 °C and 80 °C, therefore subsequent hydrogenations were conducted at 110 °C. After 12 h (un-optimized), complete consumption of the starting material was observed by ^{31}P NMR spectroscopy, and the products of the reaction gave rise to 6 new resonances at 310.2, 287.5, −117.8, −128.9, −135.4, and −171.9 ppm. The wide range of chemical shifts suggested that both phosphaalkene- and phosphine-type centres had been generated. The relative integration of the ^{31}P NMR resonances led to the conclusion that two different products were generated in a 2.5:1 ratio. Single crystals grown by slow concentration of the C_6D_5Br reaction mixture confirmed the molecular structure of one product as the triphosphabicyclo[3.1.0]hexene species **4-2a** (Figure 4.2). Within the five-membered ring, the C=P bond length is 1.689(3) Å, C–P bond lengths are 1.850(4) Å, 1.832(2) Å, and 1.871(3) Å, and the P–P bond length is 2.196(1) Å. The three-membered ring has C–P bond lengths of 1.830(4) Å and 1.864(5) Å. This product was previously prepared and spectroscopically characterized by Binger,[55] and its diastereomer **4-2b** had been prepared and spectroscopically characterized by Jones,[54] which was proposed to be the second product from the hydrogenation of **4-1** with $B(C_6F_5)_3$.

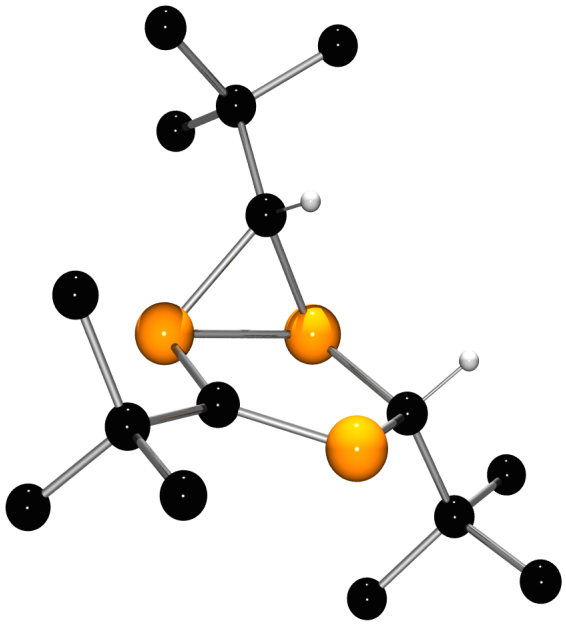

Figure 4.2 – POV-ray depiction of **4-2a**, with *t*-Bu H atoms omitted for clarity. C: black; H: grey; P: orange.

It was noted that increasing the catalyst loading from 5 mol% to 10 mol% resulted in poorer selectivity for product formation; the two diastereomers were generated in a 1.4:1 ratio (**4-2a**:**4-2b**). It was then postulated that decreasing the loading from 5 mol% to 1 mol% $B(C_6F_5)_3$ should result in better selectivity for the *syn* product. This was later confirmed, and the products **4-2a** and **4-2b** were produced in a 3.6:1 ratio. The more intriguing observation from that experiment was that the rate of product formation did not appear to be affected by the catalyst loading. Moreover, $B(C_6F_5)_3$ is prone to hydrolysis and is rarely reported at such low loadings in FLP catalysis, especially at such high reaction temperatures.[59] The $B(C_6F_5)_3$ had not been rigorously purified prior to use, so the observation that **4-1** was fully consumed when using only 1 mol% of catalyst was unexpected. **4-1** was then subjected to the same reaction conditions, but without the "catalyst". Much to our surprise, the reaction was complete after the same reaction time as when $B(C_6F_5)_3$ had been added, and the same products **4-2a** and **4-2b** were generated in a 4.3:1 ratio (Scheme 4.5).

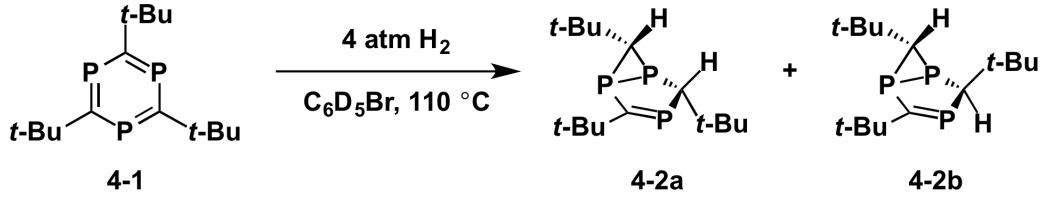

4-1 **4-2a** **4-2b**

Scheme 4.5 – Reaction of **4-1** with H_2 to form **4-2a** and **4-2b**.

This result led to a considerable effort towards disproving the influence of any trace metal contaminants. The J-Young NMR tube used for the hydrogenation had been washed with aqua regia prior to use; the reaction was repeated in a different tube, which had also been cleaned with aqua regia, and this had no effect on the outcome of the reduction. The synthesis of **4-1** was then evaluated to determine which contaminants may have been present in the sample and contributed to the observed reactivity. The final synthetic step in the preparation of **4-1** involves a cyclotrimerization using stoichiometric $Cl_3V{=}N\text{-}(t\text{-Bu})$. Trace metal analysis (ICP-MS) determined that the material contained 0.034 %W vanadium. In order to exclude the possibility that trace vanadium was responsible for the reaction, an authentic sample of $Cl_3V{=}N\text{-}(t\text{-Bu})$ was prepared following literature procedures.[60] The spectral data was consistent with previous literature reports,[61] as well as the molecular structure.[62] Three experiments under the same reaction conditions (4 atm H_2, C_6D_5Br, 110 °C) were monitored: one without any additive, one

with 10 mol% Cl_3V=N-(*t*-Bu), and one with 10 mol% $B(C_6F_5)_3$. The reductions were monitored over several hours by ^{31}P NMR spectroscopy and it was determined that the reaction rate was unaffected by the additives, and the only observable differences between the three reactions were the proportions of **4-2a** and **4-2b** produced.

It was also noticed, upon careful monitoring of the reduction of **4-1**, that a new species appeared during the course of the reduction (Figure 4.3), but was fully consumed by the time the reaction had reached completion. This led to the postulate that an intermediate en route to the final products **4-2a** and **4-2b** was being observed. The new species gave rise to two new ^{31}P resonances: a singlet at 240.0 ppm and a doublet centered at −24.8 ppm with a coupling constant of 227 Hz, integrating approximately 2:1, respectively. A new doublet of triplets centered at 6.40 ppm was observed by ^{1}H NMR spectroscopy, with coupling constants of 227 Hz and 6 Hz. These data support the formation of a symmetric species with two phosphaalkene centres and a phosphine centre bearing a P–H bond. This species was assigned as product **4-3**, where an H_2 molecule had undergone a 1,4-addition across the aromatic ring (Scheme 4.6). This species was previously prepared by Binger via hydrolysis of a Hf-complex, and the spectroscopic data are consistent with this previous literature report.[55] It was proposed that the distribution of products **4-2a** and **4-2b** arises from inversion of the P-centre in intermediate **4-3**. It is postulated that adding $B(C_6F_5)_3$ to the reaction mixture is influencing the P-centre inversion to intermediate **4-3b**, perhaps because the intermediates could transiently coordinate to $B(C_6F_5)_3$, and the phosphorus lone pair in **4-3b** may be less sterically hindered than that of **4-3a**. This is a potential explanation for why more of product **4-2b** was observed when $B(C_6F_5)_3$ had been added to the reaction.

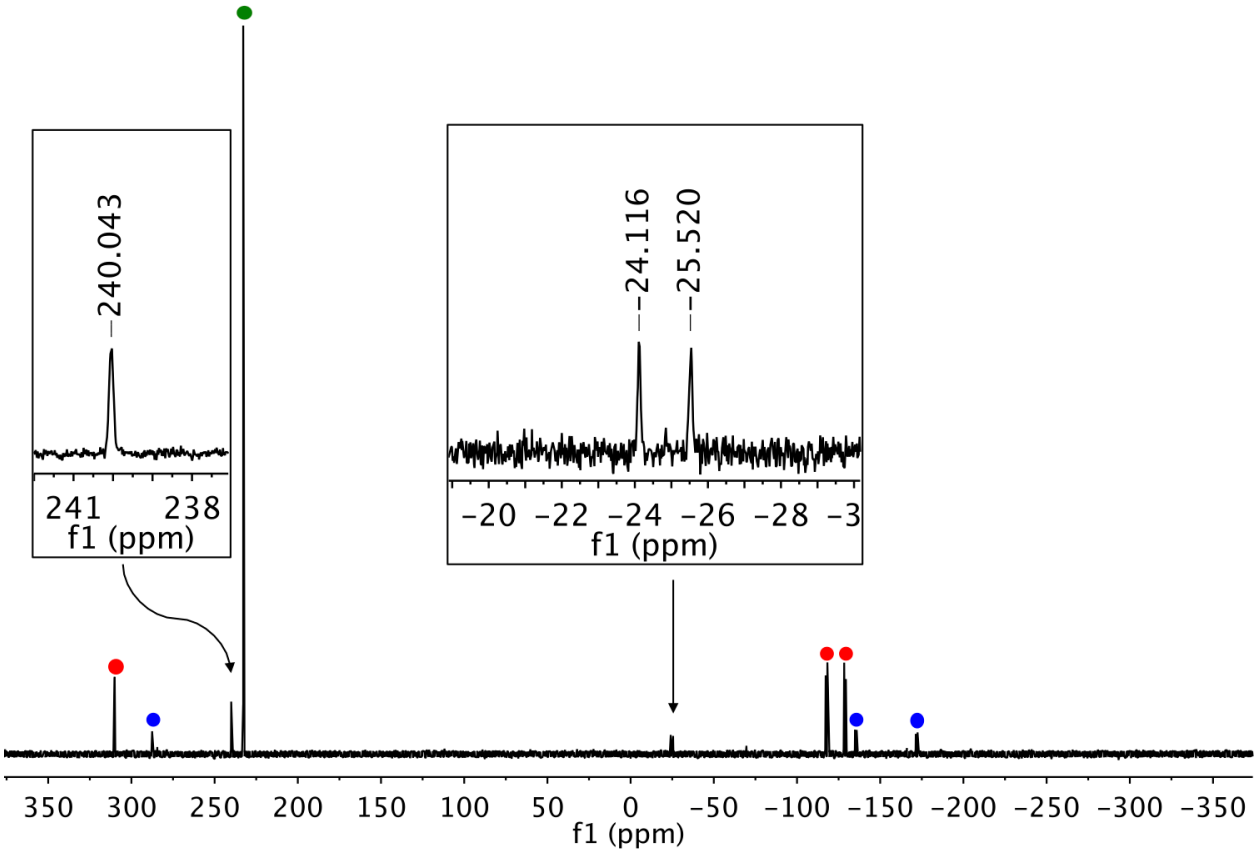

Figure 4.3 – ^{31}P NMR spectrum (162 MHz, 298 K, C_6D_5Br) of the reduction of **4-1** after 100 minutes. Green = **4-1**, red = **4-2a**, blue = **4-2b**.

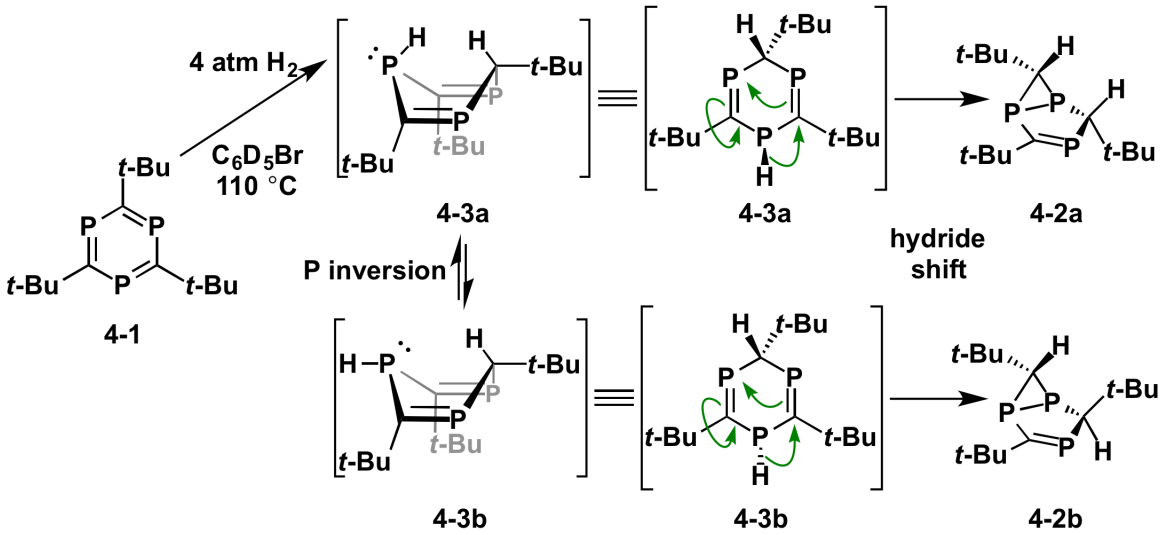

Scheme 4.6 – Formation of intermediate **4-3** and subsequent hydride shift to yield **4-2**.

This reduction was further studied using *para*-hydrogen (*p*-H_2),[63] and this work was conducted by our collaborator Prof. Simon Duckett at the University of York. His studies showed that treatment of **4-1** with *p*-H_2 and warming the solution to 110 °C led to the emergence of two polarized signals in the ^{1}H NMR spectrum at 6.4 ppm and 1.8 ppm, corresponding to the resonances for species **4-3**. The spin-encoding associated with *p*-H_2 was retained (Figure 4.4), supporting the proposed bimolecular activation mechanism where both H atoms arise from the same molecule of H_2. This technique has been employed to study hydrogen activation mechanisms for transition metal systems quite extensively,[64] however the application of *p*-H_2 to a non-metal system is rare, with the only other reported example being Koptyug's H_2 addition to Repo's amino-borane FLP.[65]

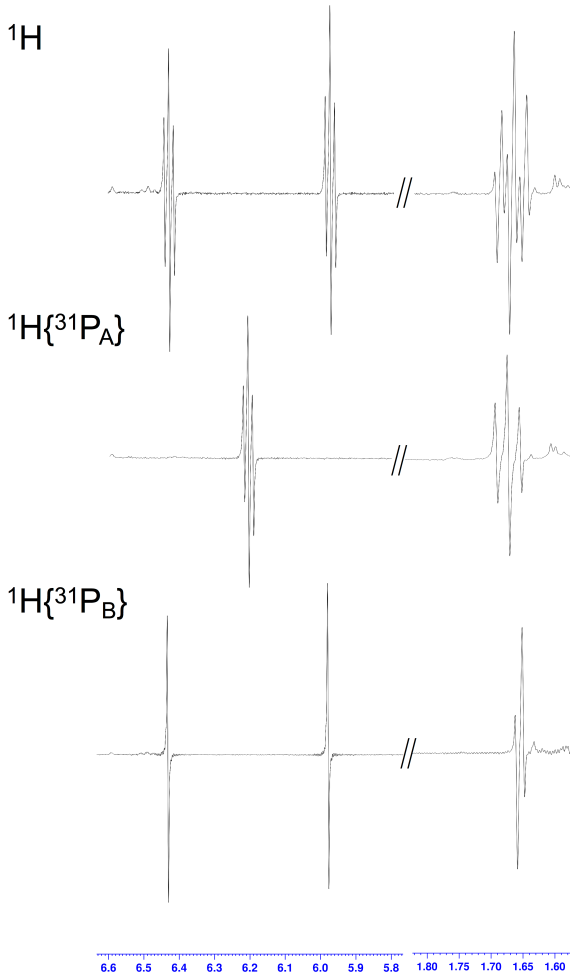

Figure 4.4 – 1D ^{1}H NMR spectra where **4-1** is exposed to *p*-H_2.

This unexpected reaction was further explored via DFT calculations by our collaborator Prof. John McGrady at the University of Oxford. Using a simplified model substrate $(PCMe)_3$ **4-1'**, he found that the key H_2 activation step involves 1,4-addition where the H–H vector is aligned parallel to the 1,4-axis of the aromatic ring (Scheme 4.7). The barrier for this activation was computed to be 28 kcal/mol, which is consistent with the elevated reaction temperature. The transition state (TS1') is comprised of a distorted C_3P_3 unit, where **4-1'** has adopted a boat conformation. The flexibility of triphosphabenzene has been previously observed and analyzed,[46] and is an important factor in the reactivity of the molecule. NBO analysis revealed that the dominant interactions in TS1' are donation of electron density from a C–P π-orbital localized on C to the H–H σ*-orbital, and from the H–H σ-bond to a C–P π*-orbital localized on P (Figure 4.5). This is very similar to the underlying principles for other main group H_2 activation modes discussed in Chapter 2.

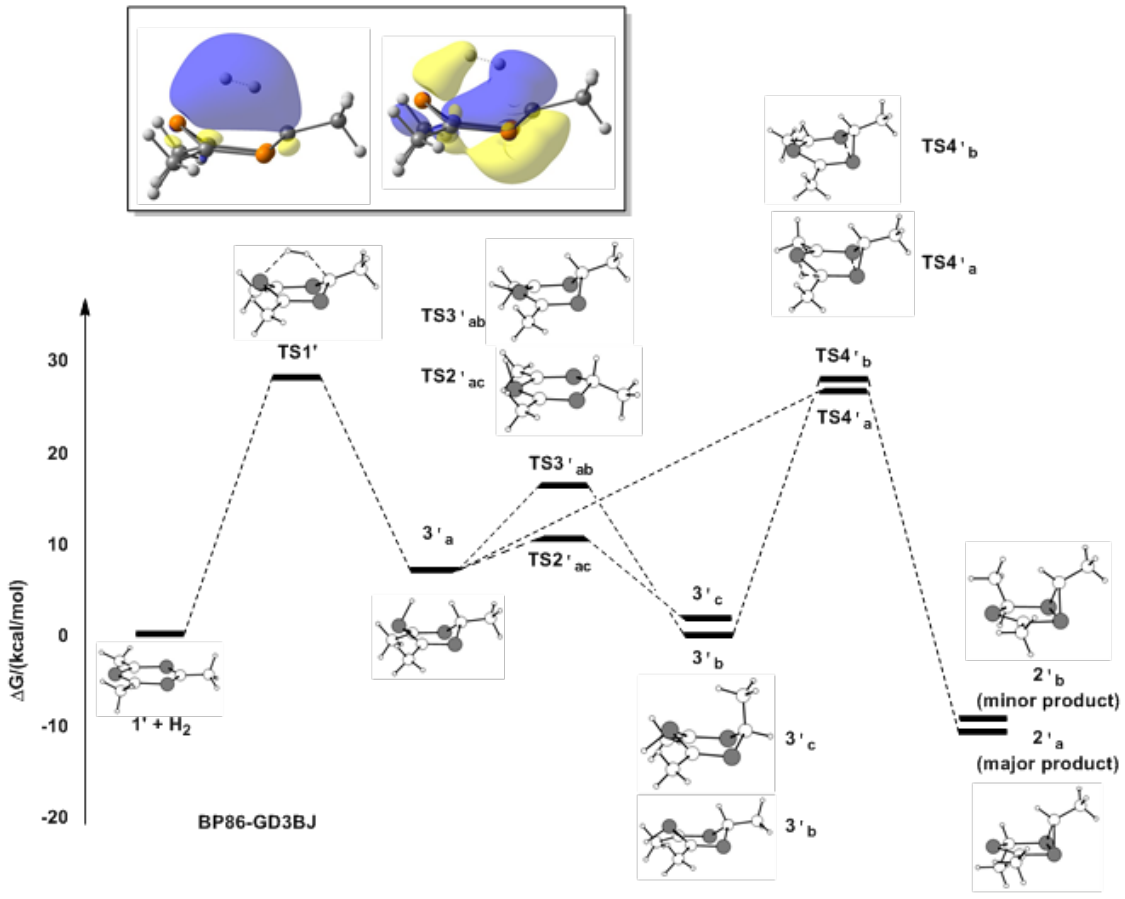

Scheme 4.7 – Reaction coordinate for the hydrogenation of **4-1'** (free energies at 298 K computed at BP86-GD3BJ level of theory).

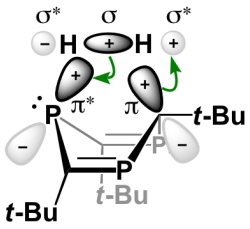

Figure 4.5 – Pictorial depiction of the FMO interactions of **4-1** with H_2.

4.2.2 Catalytic Hydrogenation Attempts with Triphosphabenzene

There was interest in using this H_2 activation by **4-1** as a new method for hydrogenation catalysis. The *p*-H_2 experiments performed by Prof. Simon Duckett suggested that the H_2 activation is reversible (the enhanced signal was apparent for several minutes), however efforts attempting to transfer H_2 from **4-3** were unsuccessful. The hydrogenation of **4-1** was attempted in the presence of N-benzylidene-*tert*-butylamine, 1,1-diphenylethylene, and cyclohexene, but no reduction of these substrates was detected, and only the triphosphabenzene ring was reduced. These catalytic runs were tried using 10 mol% **4-1** at room temperature and at 80 °C, at 4 atm H_2 and at 100 atm H_2. All of the experimental evidence suggested that **4-1** is not a hydrogenation catalyst.

4.2.3 Triphosphabenzene Activation of HD

The reduction of **4-1** was investigated using H_2, D_2, and HD, with the hope that these experiments would aid in the elucidation of the reaction mechanism, prior to the completion of DFT calculations. The ^{31}P NMR spectra of the three reactions upon completion are stacked in Figure 4.6 and Figure 4.7. Based on the hypothesis that the H_2 molecule undergoes a 1,4-addition across the triphosphabenzene (which was supported computationally, *vide supra*), it was anticipated that when **4-1** was reduced using HD, exclusive formation of the H–D addition product and the D–H addition product (Scheme 4.8) would be observed. However, when the ^{31}P NMR spectra of the HD, D_2, and H_2 reduction products were compared, it appeared that the H_2 and D_2 addition products were present in the sample that was reduced by HD. This is inconsistent with the proposed hydrogenation mechanism; even if the addition of HD is reversible, the release of H_2 or D_2 would not be expected. There was no apparent degradation of the *tert*-butyl groups, so a scrambling process involving the alkyl substituents on the heterocycle is unlikely. Possible explanations for this observation include further HD addition to the phosphaalkenes in

4-3a$_{HD}$/**4-3a$_{DH}$**, or the basic phosphine centre in **4-3a$_{HD}$**/**4-3a$_{DH}$** may react with another molecule of HD-activated product, deprotonating the C–H/C–D bond and facilitating a scrambling process.

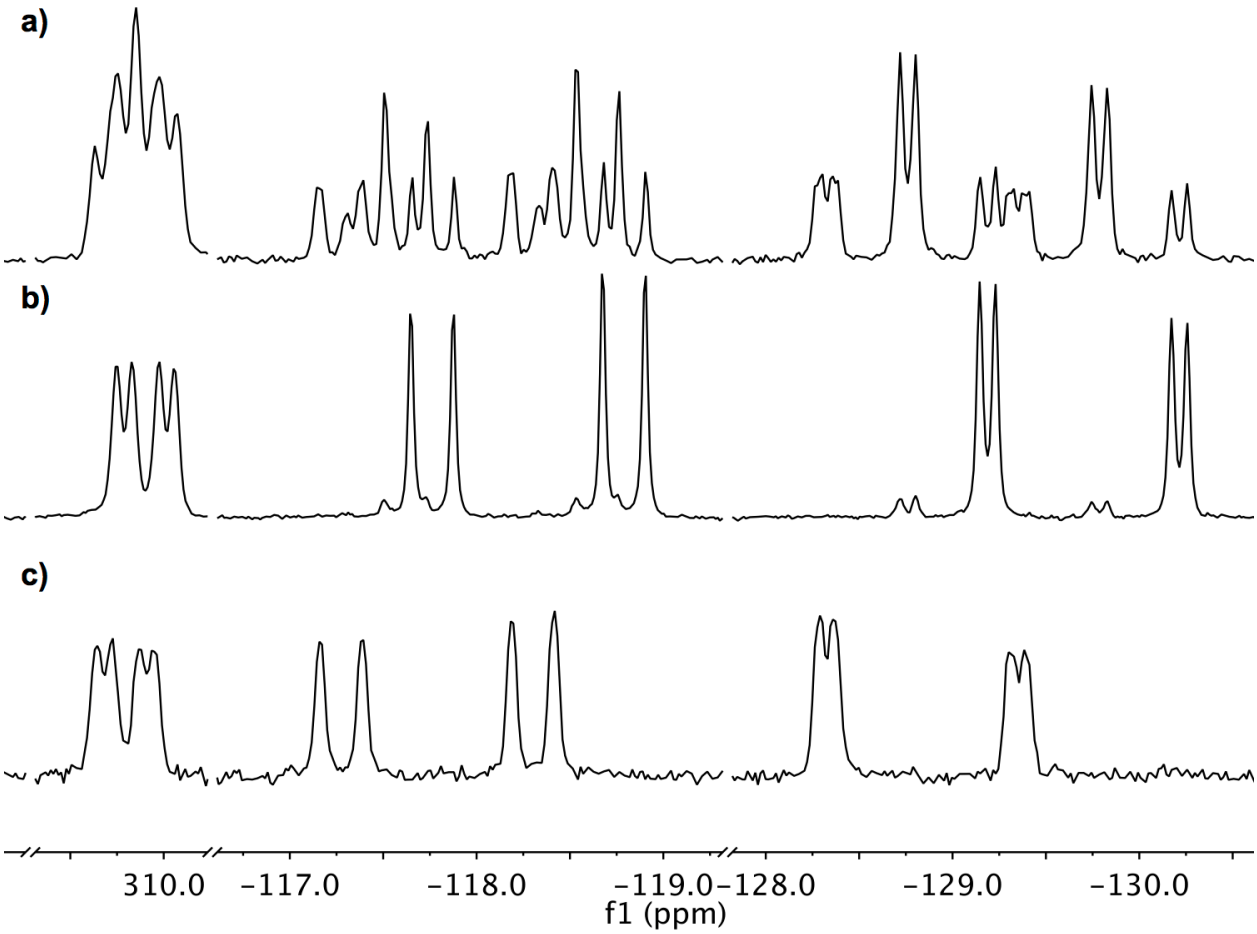

Figure 4.6 – Stacked ^{31}P NMR spectra for the reaction of **4-1** with a) HD, b) D_2, and c) H_2, focusing on the peaks attributed to **4-2a** (162 MHz, C_6D_5Br, 298 K).

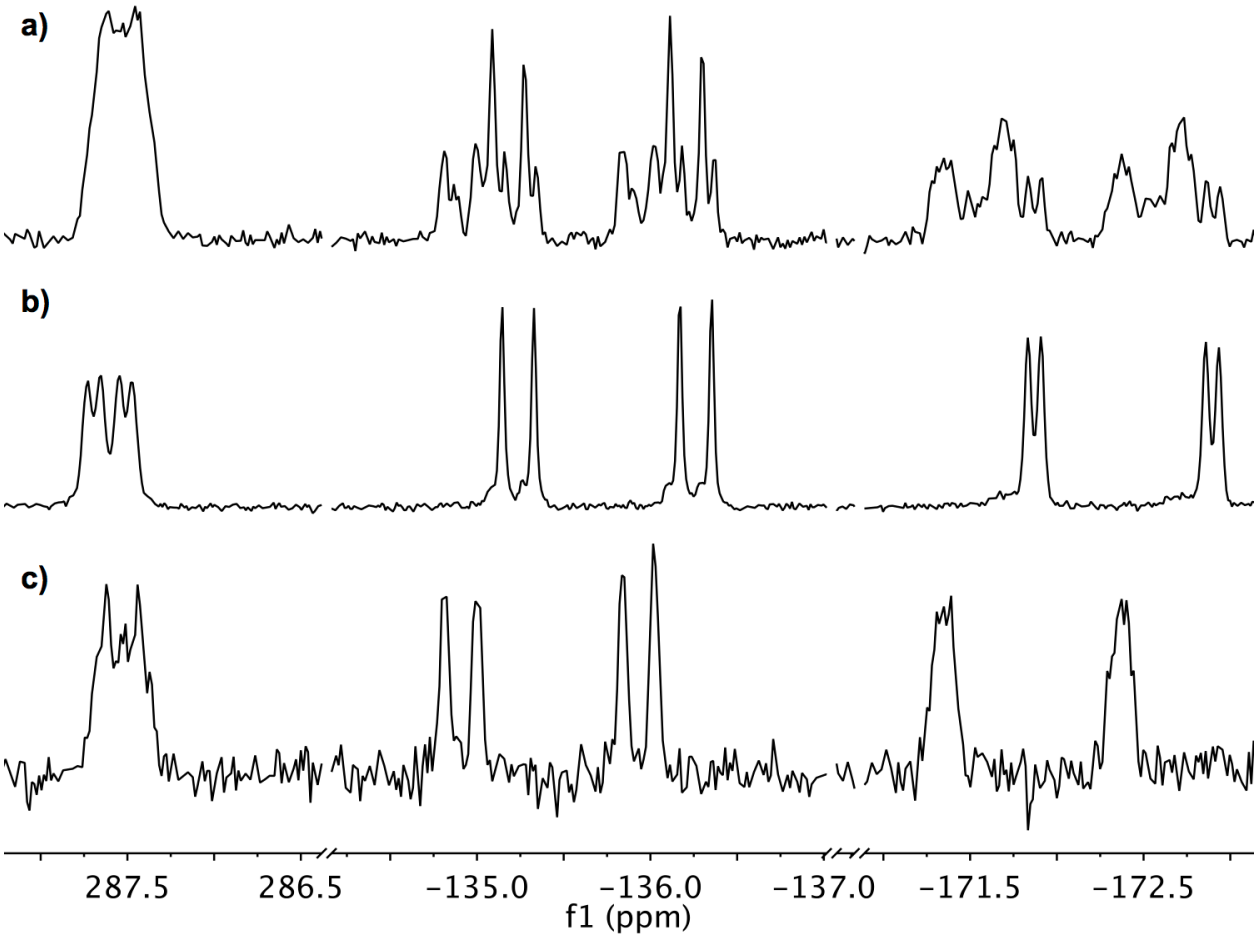

Figure 4.7 – Stacked ^{31}P NMR spectra for the reaction of **4-1** with a) HD, b) D_2, and c) H_2, focusing on the peaks attributed to **4-2b** (162 MHz, C_6D_5Br, 298 K).

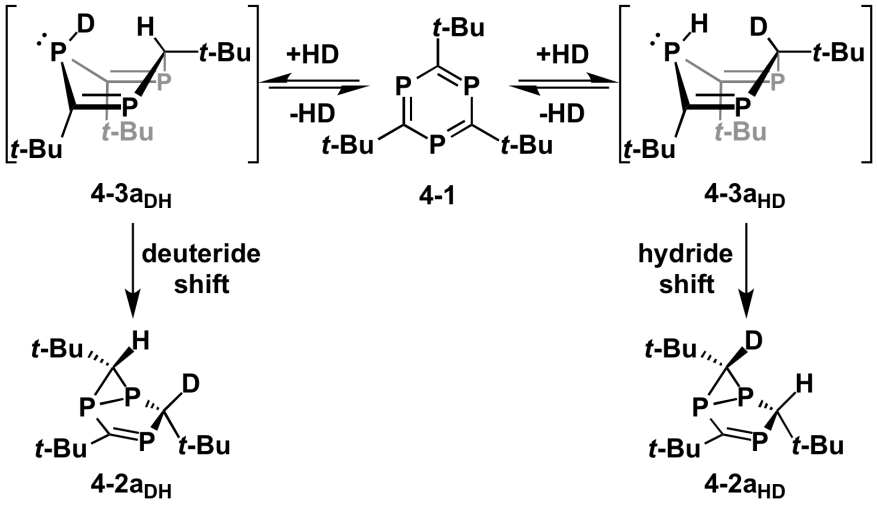

Scheme 4.8 – HD addition reactions to **4-1**, with the hypothesized products **4-2a$_{DH}$** and **4-2a$_{HD}$.**

Unfortunately, at the time our supply of **4-1** was dwindling and subsequent batches did not survive the trip across the Atlantic Ocean, so I was unable to repeat these experiments. Recently, a visiting student from the Russell laboratory, Ms. Rosalyn Falconer, has since been able to reproduce these results, and computations investigating this activation are ongoing.

4.2.4 Investigating Triazines and Phosphinines for Aromatic H_2 Activation

The unexpected reactivity of triphosphabenzene with H_2 prompted the examination of other related aromatic systems to determine whether they too could facilitate small molecule activation. The analogous 2,4,6-tri-*tert*-butyl-1,3,5-triazine **4-4** was prepared via the pathway outlined in Scheme 4.9.[66] This substrate did not activate H_2 under the optimized reaction conditions,[67] nor did it activate H_2 in concert with $B(C_6F_5)_3$, unlike related 2,6-disubstituted pyridines.[52] This robustness was attributed to the steric shielding of the nitrogen centres. The related substrate 2,4,6-tris(trifluoromethyl)-1,3,5-triazine **4-5** was also inactive when treated with $B(C_6F_5)_3$ and/or H_2.

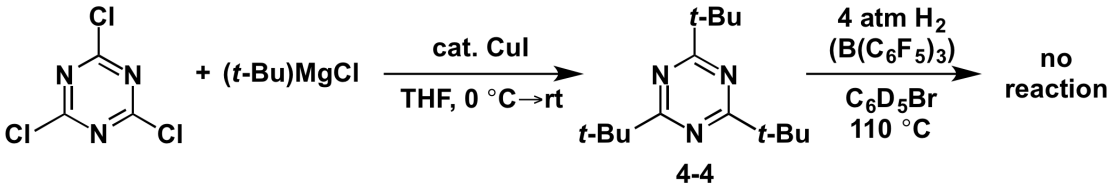

Scheme 4.9 – Synthesis of substrate **4-4** and attempted reductions with or without $B(C_6F_5)_3$.

Phosphinines were then tested to determine whether they can cleave H_2 in a 1,4-addition process like **4-1**. The investigation started with 2,4,6-triphenylphosphinine **4-6**, which was prepared from the corresponding pyrylium BF_4 salt as outlined in Scheme 4.10.[68]

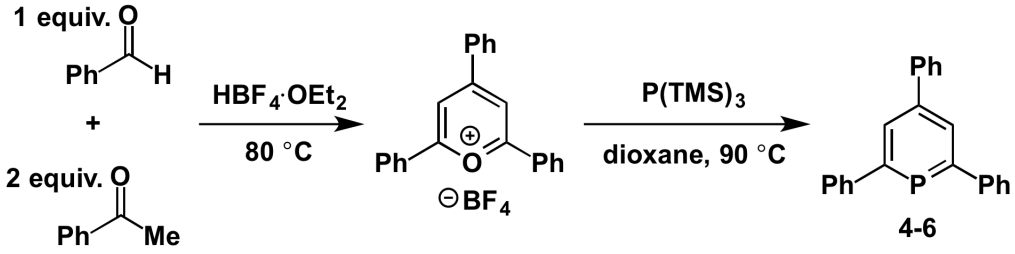

Scheme 4.10 – Preparation of substrate **4-6** via treatment of the corresponding pyrylium salt with $P(TMS)_3$.

Phosphinine **4-6** was unreactive towards H_2 under the reaction conditions optimized for **4-1**. There was also no observable reduction when the reaction was carried out in the presence of $B(C_6F_5)_3$. It was thought that increasing the dipole of the molecule might assist in the 1,4-addition reaction with H_2, so phosphinine **4-7** was also prepared. This required a modified synthetic route to isolate an appreciable quantity of the desired substrate, shown in Scheme 4.11. The synthesis of a phosphinine with a C_6F_5 substituent in the 4-position was also attempted, however the precursor pyrylium salt could not be generated cleanly. Treatment of **4-7** with 4 atm H_2 at room temperature, 110 °C, or 150 °C did not result in any observable reduction by multinuclear NMR spectroscopy.

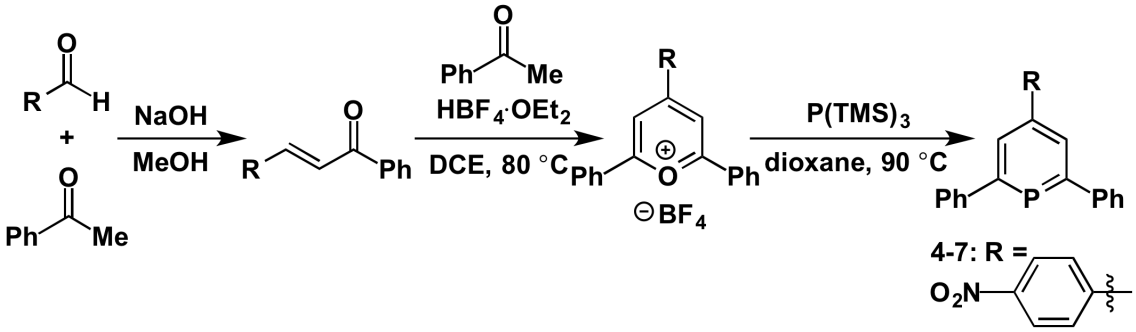

Scheme 4.11 – Synthesis of phosphinines **4-7**.

Lastly, in an effort to make the direct phosphinine analogue of **4-1**, the synthesis of 2,4,6-tri-*tert*-butylphosphinine **4-8** was attempted following the same synthetic route used to prepare **4-7**. Unfortunately, this method was unsuccessful for generating the desired pyrylium salt due to the cyclization reaction shown in Scheme 4.12 when the precursor enone is treated with $HBF_4{\cdot}OEt_2$.[69] When the enone was treated with 3,3-dimethylbutan-2-one in the presence of $HBF_4{\cdot}OEt_2$ the cyclization to the 5-membered carboxonium salt occurs preferentially and no pyrylium salt was detected. Therefore, 2,4,6-tri-*tert*-butylpyrylium tetrafluoroborate had to be prepared via an alternate route (Scheme 4.13).[70] Treatment of the enone with 3,3-dimethylbutan-2-one under basic conditions led to clean formation of the dione **4-9**, which was cyclized under acidic conditions to furnish pyrylium salt **4-10**. This was then converted to the desired phosphinine **4-8**. Unfortunately, this P-heterocycle was also unreactive towards H_2. It was postulated that the difference in reactivity between triphosphabenzene and phosphinines might be due to the heightened aromaticity of phosphinines (phosphinine NICS(1) = − 10.8, triphosphabenzene NICS(1) = −9.6, benzene NICS(1) = −11.3),[39] rendering them more stable.

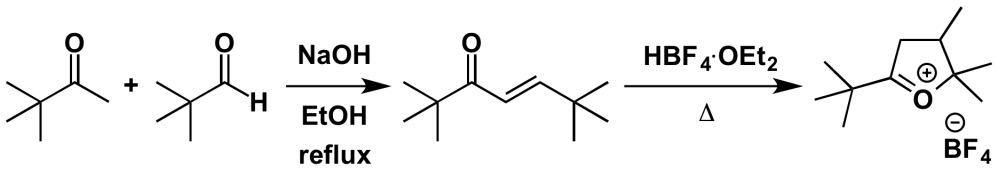

Scheme 4.12 – Base-mediated synthesis of 2,2,6,6-tetramethylhept-4-en-3-one and subsequent cyclization with acid.

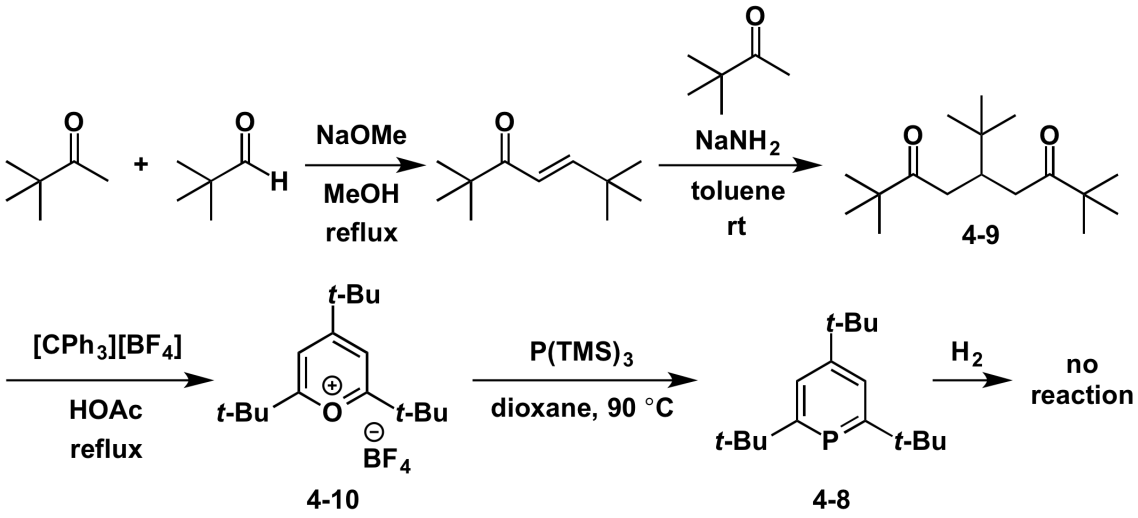

Scheme 4.13 – Synthesis of 2,4,6-tri-*tert*-butylphosphinine **4-8**.

4.2.5 FLP Chemistry of Phosphaalkynes

After testing the reactivity of a variety of N- and P-heterocycles with FLPs, the effect of FLPs on phosphaalkynes was explored. It is well established that they are more closely related to alkynes than nitriles,[3,15,71] and alkynes were among the first molecules discovered to undergo FLP activation.[72,73] Phosphaalkyne **4-11** was first combined with one equivalent of $B(C_6F_5)_3$. No interaction between the Lewis acid and **4-11** was observed by multinuclear NMR spectroscopy, and no carboboration was observed after prolonged heating.[74,75] This lack of interaction was attributed to the low basicity and nucleophilicity of the phosphaalkyne lone pair.[76,77] Similarly, treatment of **4-11** with FLPs $B(C_6F_5)_3/P(t\text{-}Bu)_3$ or $B(C_6F_5)_3/PPh_3$ at ambient or elevated temperature showed no evidence of addition across the C–P π-bonds, in contrast to the reported reactivity of FLPs with C–C π-bonds.[72,73]

4.2.6 Hydroboration of Phosphaalkynes

After confirming that phosphaalkynes do not parallel alkynes in FLP chemistry, other addition chemistry with **4-11** was investigated. While phosphaalkynes are known to undergo insertions into polyhedral boranes[78,79] and boroles,[36] a scarcity of hydroboration chemistry was noted; the only report found was from 1990, where the authors described a double hydroboration of **4-11** with HBCat to yield a primary phosphine with a *gem*-diboryl substituent (Figure 4.8a).[31] A related metalloboration reaction was reported by Erker, where treatment of a Ti-phosphaalkyne complex with $HBEt_2$ resulted in formation of a P–B bond and C–Ti bond (Figure 4.8b).[80] One report discussed the haloboration of **4-11** with BBr_3 (Figure 4.8c),[81] however no characterization data or experimental details were available.

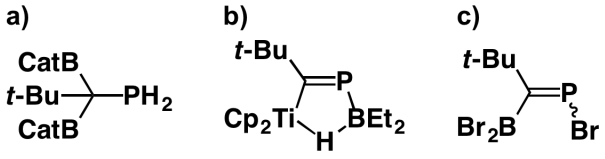

Figure 4.8 – Examples of boron-functionalized phosphaalkenes and phosphines originating from phosphaalkynes.

The hydroboration reaction of **4-11** was tested with Piers' borane, $HB(C_6F_5)_2$, which is a highly electrophilic borane known to undergo hydroboration reactions under mild conditions.[82] Pleasingly, an immediate reaction occurred when **4-11** was treated with one equivalent of $HB(C_6F_5)_2$; following workup, a colourless crystalline solid was isolated in 67% yield (Scheme 4.14). The solid state structure revealed that hydroboration of the phosphaalkyne had occurred, however, contrary to the innate polarity of the $^{\delta+}P{\equiv}C^{\delta-}$ bond, new P–B and C–H bonds were formed, generating a phosphaalkenylborane which dimerized to yield a new P_2B_2 four-membered heterocycle **4-12** (Figure 4.9). The hydroboration of the related 1-adamantylphosphaalkyne **4-13** was tested, and when it was treated with one equivalent of $HB(C_6F_5)_2$, B–H bond addition was observed with the same regiochemical outcome to yield P_2B_2 heterocycle **4-14** (Scheme 4.14), which was crystallographically characterized (Figure 4.10). Given the difference in the electronegativities of carbon and phosphorus, and the polar nature of the P≡C bond, it is interesting to note that the hydroboration occurs with formation of P–B and C–H bonds, as this pattern of reactivity stands in contrast to literature reports of B–H,[31] Ge–H,[29] and Sn–H[30] phosphaalkyne addition reactions. The formation of **4-12** and **4-14** is more akin to reactions of

phosphaalkynes with Ru–H species described by Hill, Jones[32,34,83] and Crossley,[35] where the regiochemical outcome was likely governed by steric congestion at the ruthenium centre. It was also noted that, unlike the previously reported double addition of HBCat to phosphaalkyne,[31] Piers' borane underwent a single 1,2-addition to **4-11,** and any excess borane remained unreacted in solution, as evidenced by multinuclear NMR spectroscopy.

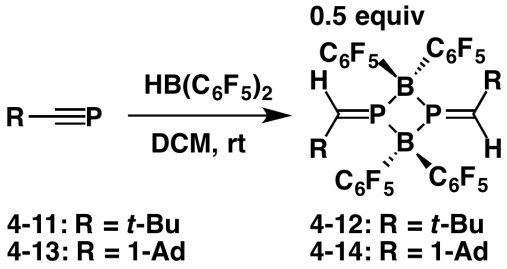

Scheme 4.14 – Hydroboration of phosphaalkynes **4-11** and **4-13**, yielding P_2B_2 heterocycles **4-12** and **4-14**.

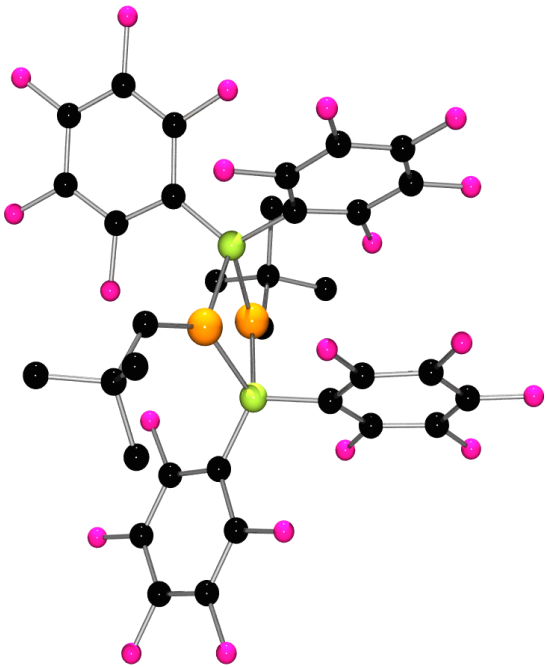

Figure 4.9 – POV-ray depiction of **4-12**, with H atoms omitted for clarity. C: black; B: yellow-green; F: pink; P: orange.

The P=C double bond lengths in **4-12** were 1.651(2) and 1.6470(19) Å. The P_2B_2 ring is distorted from planarity in a butterfly conformation featuring a dihedral angle of 23.315(82)°. P–B–P bond

angles of 81.14(8)° and 81.01(8)°, and B–P–B bond angles of 96.17(9)° and 96.24(9)° were found in the central ring. The P–B bond lengths in **4-12** ranged from 2.009(2) to 2.013(2) Å; these distances are shorter than those of phosphinoborane dimers $[R_2B–PR'_2]_2$, which range from 2.055(2) to 2.096(5) Å,[84,85] but are longer than those of P_2B_2 diradicaloids, which range from 1.8904(15) to 1.900(2) Å.[86–89] The short P–B distances in **4-12** are perhaps due to the reduced steric demands of the bridging phosphaalkene units or the hybridization of the P-centre.

Unlike **4-12**, the P_2B_2 unit of **4-14** is centrosymmetric in the solid state (Figure 4.10), with B–P distances of 2.021(3) and 2.023(4) Å. The B–P–B and P–B–P angles were found to be 98.5(1)° and 81.5(1)°, respectively, and the P=C double bond length is 1.649(3) Å, similar to that of **4-12**.

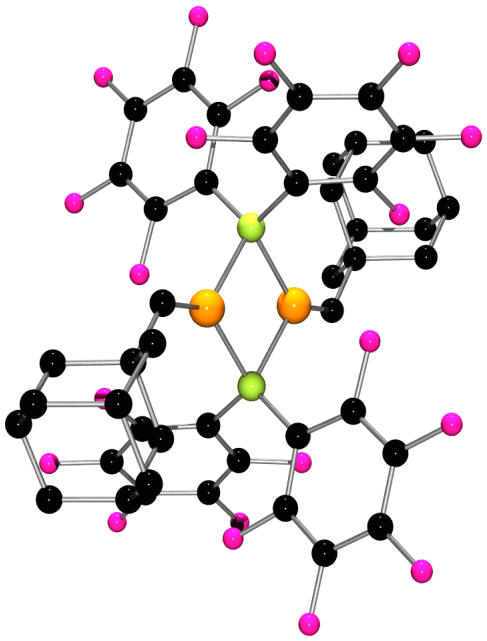

Figure 4.10 – POV-ray depiction of **4-14**, with H atoms omitted for clarity. C: black; B: yellow-green; F: pink; P: orange.

The ^{11}B NMR spectrum of **4-12** revealed a sharp singlet at −5.3 ppm and the ^{19}F NMR spectrum showed three resonances at − 127.3, − 153.3, and − 162.0 ppm. These data support the assignment of **4-12** as a four-coordinate boron species, suggesting that the dimeric structure remains intact in solution. ^{31}P NMR data revealed a broad singlet at 183.2 ppm, a drastic downfield change in chemical shift from that of phosphaalkyne **4-11** (−69 ppm),[15] consistent with the formation of a phosphaalkene. The ^{1}H NMR spectrum showed two resonances at 8.03 and 1.04 ppm, with relative integrations of 1:9, which were assigned as the olefinic and *tert*-butyl

resonances, respectively. Surprisingly, the resonance at 8.03 ppm appeared as a triplet with an apparent coupling constant of $J = 8.2$ Hz. The triplet resonance persisted even when recorded at different magnetic field strengths and temperatures (25 to −35 °C). The $^{1}H\{^{31}P\}$ spectrum, however, revealed this resonance as a singlet, indicating that the fine structure of the signal arose from coupling between the ^{1}H and ^{31}P nuclei (Figure 4.11). $^{13}C\{^{1}H\}$ NMR data showed resonances at 177.7, 40.7, and 29.9 ppm, all of which were also apparent triplets (Figure 4.12).

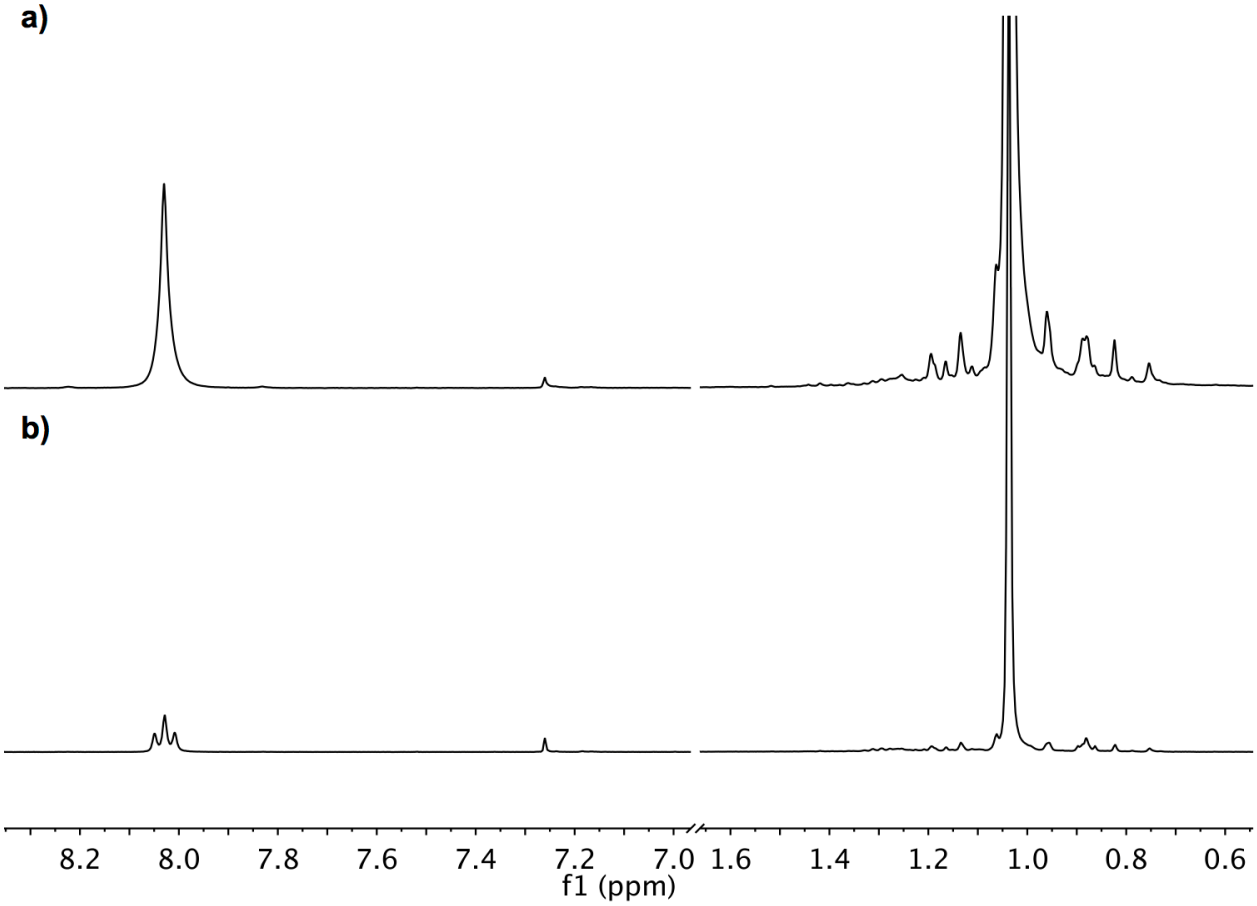

Figure 4.11 – a) $^{1}H\{^{31}P\}$ and b) ^{1}H NMR spectra of **4-12** (400 MHz, $CDCl_3$, 298 K).

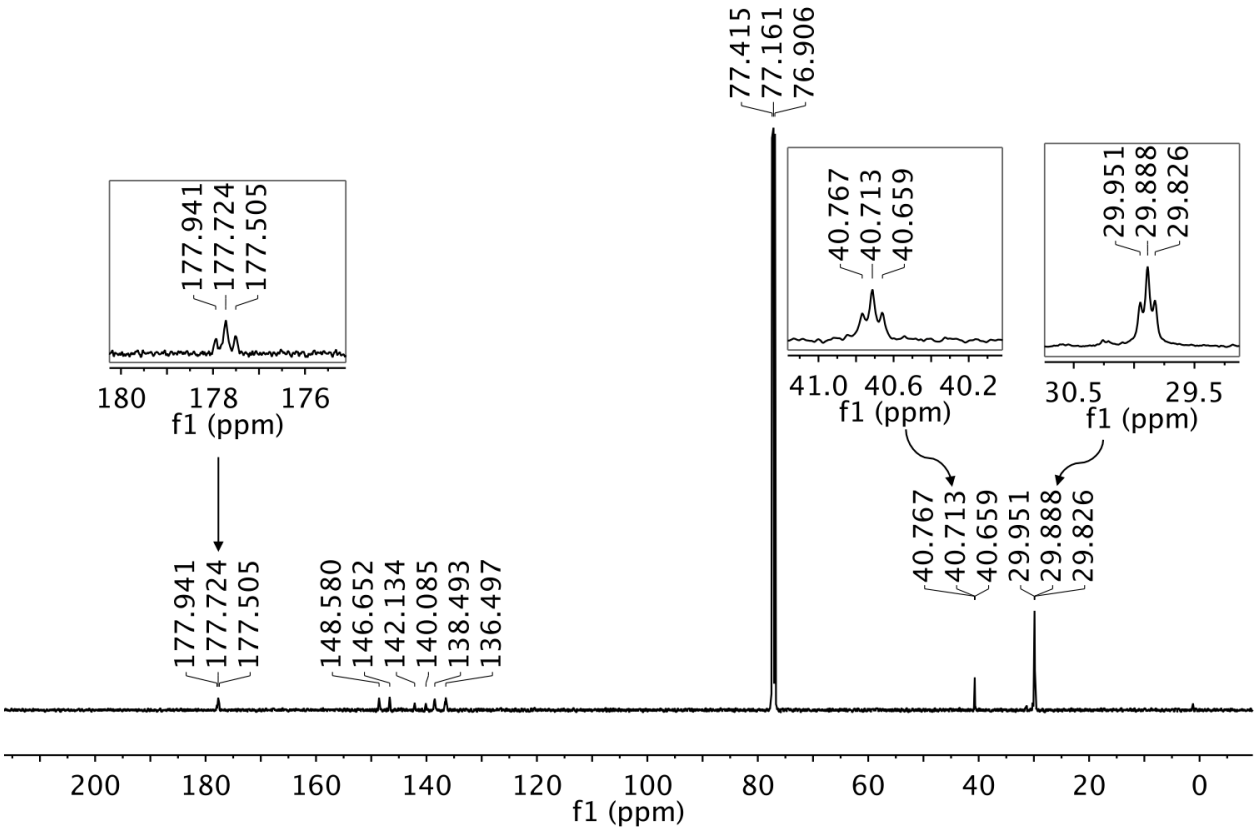

Figure 4.12 – $^{13}C\{^{1}H\}$ NMR spectrum of **4-12** (126 MHz, $CDCl_3$, 298 K).

The multiplicities of the ^{1}H and ^{13}C NMR signals are proposed to arise from virtual coupling to the pair of strongly coupled ^{31}P nuclei in **4-12.** A similar phenomenon has been observed for *trans*-diphosphine metal complexes,[90] and the structurally analogous dimeric four-membered heterocycle $[LiPPh_2]_2$.[91] The two putatively coupled phosphorus centres in **4-12** have identical chemical shifts in solution and thus do not exhibit any coupling to each other. Fortuitously, dimer **4-12** sits on a general position in the solid state and thus the two P-centres are crystallographically inequivalent. Consequently, the CP-MAS ssNMR $^{31}P\{^{1}H\}$ spectrum of **4-12** (Figure 4.18) exhibits two ^{31}P resonances (which partially overlap) that couple to each other with $^{2}J_{pp} \sim 1520$ Hz.

Dr. Timothy Johnstone performed DFT calculations to probe the mechanism of this reaction and explain the observed regiochemistry in the formation of **4-12**. Relaxed potential energy surface (PES) scans of the distance between the centre of the P≡C triple bond and the boron atom of either Piers' borane or $B(C_6F_5)_3$ revealed that the energy of the system experiences a minimum as Piers' borane approaches the triple bond. In contrast, the energy rises as $B(C_6F_5)_3$ and

phosphaalkyne approach one another. The latter result suggests that steric repulsion between the C_6F_5 rings and the *tert*-butyl group precludes approach of $B(C_6F_5)_3$ and the nucleophilic π-cloud of the phosphaalkyne. The minimum from the PES scan with Piers' borane was used as the starting point for a geometry optimization. In the optimized configuration, the B–H bond is directed towards the carbon atom of the phosphaalkyne (Figure 4.13). This configuration is favourable as it minimizes steric interactions between the C_6F_5 rings and the *tert*-butyl group. These results support the lack of reactivity of **4-11** with $B(C_6F_5)_3$ and the observed regiochemical outcome of the reaction with Piers' borane.

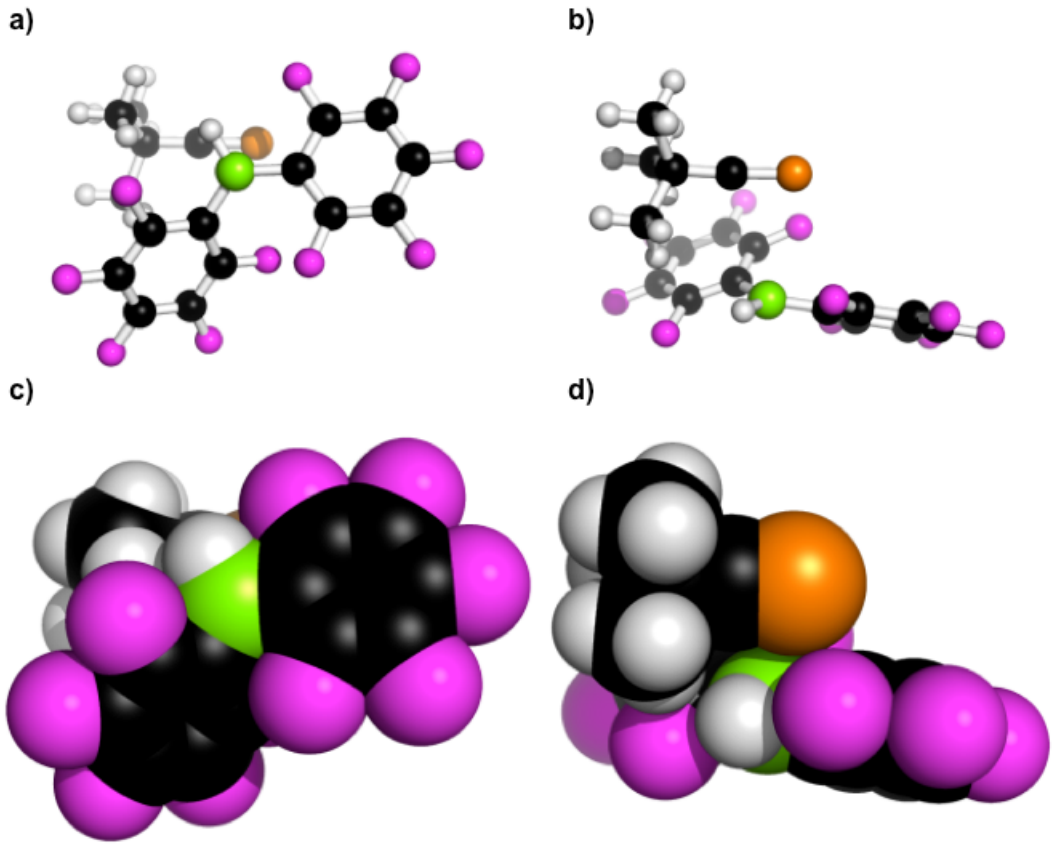

Figure 4.13 – Ball-and-stick (a and b) and space-filling (c and d) depictions of the optimized geometry of Piers' borane approaching **4-11** viewed from top (left) and side (right). H: white, C: black, B: yellow-green, F: pink, P: orange.

Investigations of the reactivity of dimers **4-12/4-14** revealed their thermal instability. Both decompose in C_6D_5Br with modest heat (60 °C) or upon standing at room temperature in halogenated solvents over several hours. Given the short P–B bond lengths and the strong NMR

spectroscopic coupling observed in **4-12** and **4-14**, the dimers were anticipated to be unreactive towards small molecules. Indeed, **4-12** shows no reactivity with H_2, CO_2, or CO. Upon treatment with *tert*-butylisocyanide, however, a rapid and clean reaction occurred, affording a new species **4-15**, which was proposed to be the monomeric phosphaalkenylborane adduct (Scheme 4.15). This assignment was supported by the loss of the virtual triplet of **4-12** in the ^{1}H NMR spectrum, and the appearance of a doublet at 8.75 ppm with $J = 23.6$ Hz. Compound **4-15** gives rise to a ^{19}F NMR spectrum with three resonances observed at −130.1, −157.1, and −163.1 ppm, and the ^{11}B NMR resonance appears at −22.5 ppm. The $^{31}P\{^{1}H\}$ NMR spectrum features a quintet at 265.9 ppm, with $J = 36$ Hz, while in the $^{31}P\{^{19}F\}$ spectrum, the resonance collapses to a doublet with $J = 24$ Hz (Figure 4.14). This evidence suggests that the phosphorus centre couples to both the olefinic proton and the four *ortho*-fluorines of the two C_6F_5 rings. This reactivity contrasts with that of phosphinoborane dimers $[(C_6F_5)_2B–PR_2]_2$ which proved unreactive toward donor molecules.[84,92] It is reminiscent of the chemistry of borane-thioether dimeric heterocycles, which form monomeric adducts when exposed to strong L-type donors.[93]

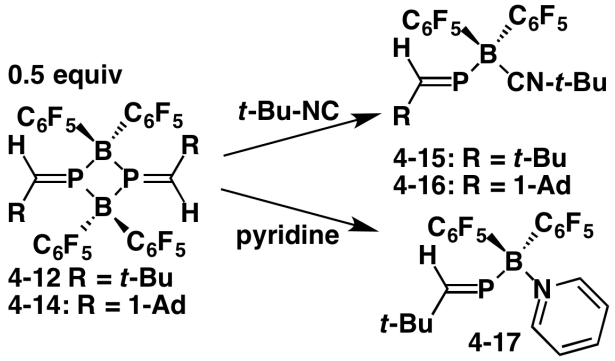

Scheme 4.15 – Reactions of dimers **4-12/4-14** with *tert*-butylisocyanide and pyridine to produce **4-15**, **4-16**, and **4-17**, respectively.

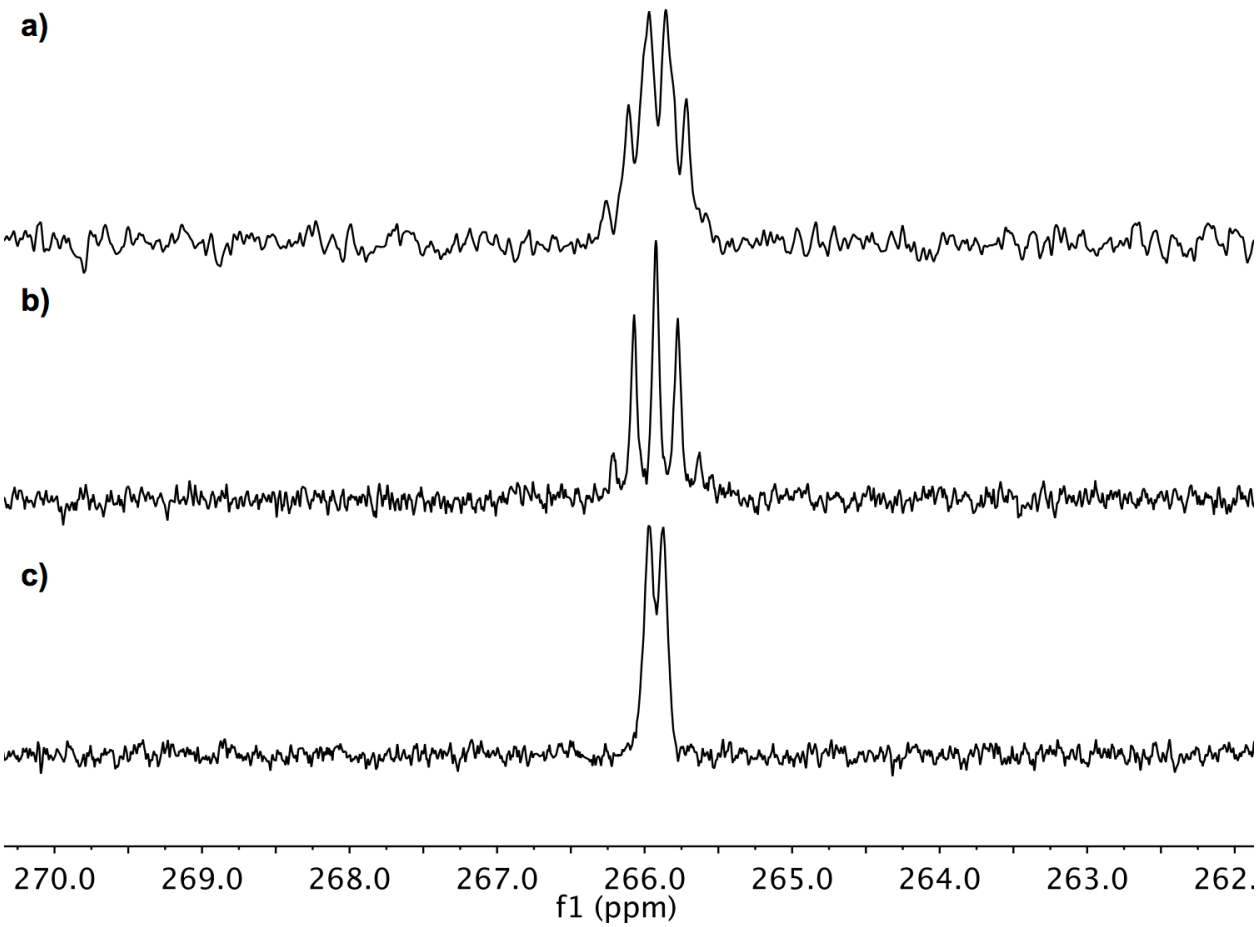

Figure 4.14 – a) ^{31}P, b) $^{31}P\{^{1}H\}$, and c) $^{31}P\{^{19}F\}$ NMR spectra of **4-15** (243 MHz, $CDCl_3$, 298 K).

The adduct **4-15** was isolated as a pale oil, so analogous chemistry with **4-14** was undertaken with the goal of obtaining crystallographic data. Compound **4-14** also reacted cleanly with *tert*-butylisocyanide, affording **4-16** (Scheme 4.15). Additionally, when **4-12** was treated with pyridine, the resulting adduct **4-17** could be isolated as a crystalline material (Scheme 4.15). Species **4-16** exhibits solution NMR spectra with similar properties to those of **4-15**, while **4-17** exhibits a ^{11}B NMR resonance at −0.8 ppm. X-ray diffraction data for both **4-16** and **4-17** confirmed the structural formulations (Figure 4.15 and Figure 4.16, respectively). For both molecules, the B-centre adopts a pseudo-tetrahedral geometry. The average $B–C_{isocyanide}$ bond distance of **4-16** is 1.61(1) Å, and the B–N bond distance of **4-17** is 1.612(3) Å. The P–B bond lengths average 2.040(7) Å in **4-16** and was found to be 2.029(2) Å in **4-17**. These P–B distances are significantly longer than those of $(C_6F_5)_2BPR_2$ (R = *t*-Bu, Cy),[92] which were found to be

1.786(4) Å and 1.762(4) Å, reflecting the π-donating ability of the phosphorus centres in monomeric $(C_6F_5)_2BPR_2$ molecules. The P=C bond lengths average 1.657(6) Å in **4-16** and 1.669(2) Å in **4-17**, with B–P–C average angles of 103.7(3)° and 105.1(1)°, respectively. The P=C bond lengths fall within the range typically observed for phosphaalkenes (1.661(6) to 1.694(2) Å).[29,94–98] These adducts represent the first examples of phosphaalkenylboranes to be synthesized, and to be crystallographically characterized.

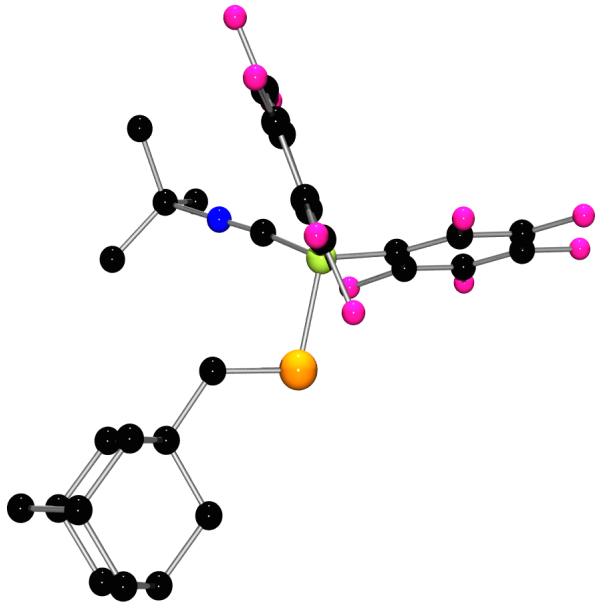

Figure 4.15 – POV-ray depiction of **4-16**, with H atoms omitted for clarity. C: black; B: yellow-green; F: pink; N: blue; P: orange.

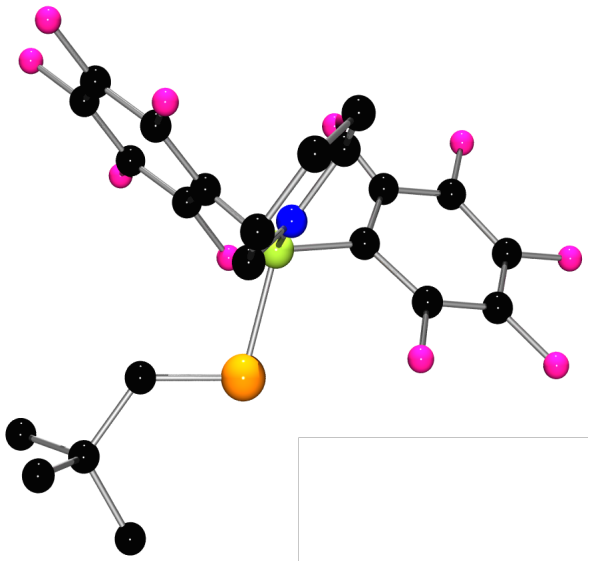

Figure 4.16 – POV-ray depiction of **4-17**, with H atoms omitted for clarity. C: black; B: yellow-green; F: pink; N: blue; P: orange.

4.3 Conclusions

The reactivity of P-heterocycles with H_2 was investigated, and it was determined that triphosphabenzene **4-1** reacts with H_2 via an uncatalyzed 1,4-addition to yield **4-3**, which undergoes a hydride shift to yield two stereoisomers of **4-2**. The analogous H_2 1,4-addition reaction with phosphinines and triazines was not observed. It was also discovered that, while FLPs do not undergo 1,2-addition reactions to phosphaalkynes, hydroboration of phosphaalkyne **4-11** proceeds with an unexpected regiochemical outcome, generating new phosphaalkenylborane dimers **4-12** and **4-14**. These dimers were shown to form ligated monomers **4-15**, **4-16**, and **4-17** when treated with *tert*-butylisocyanide or pyridine, whose structures were confirmed crystallographically.

4.4 Experimental Details

4.4.1 General Considerations

All reactions and workup procedures were performed under an inert atmosphere of dry, oxygen-free N_2 using standard Schlenk techniques or a glovebox (MBraun, equipped with a −35 °C freezer) unless otherwise specified. All glassware was oven-dried and cooled under vacuum before use. Pentane, dichloromethane, and toluene (Aldrich) were dried using a Grubbs-type Innovative Technologies solvent purification system and were stored over activated

4 Å molecular sieves. Chloroform was stirred over CaH_2 for several days, distilled under N_2, and stored in a nitrogen-filled glovebox. Deuterated solvents (C_6D_5Br, $CDCl_3$) were purchased from Cambridge Isotope Laboratories, Inc. degassed, and stored over activated 4 Å molecular sieves prior to use. 2,4,6-Tri-*tert*-butyl-1,3,5-triphosphabenzene **4-1**,[27] $Cl_3V{=}N(t\text{-Bu})$,[60] 2,4,6-tri-*tert*-butyl-1,3,5-triazine **4-4**,[66] 2,4,6-triphenylphosphinine **4-6**,[68] phosphinine **4-7**,[99] 2,4,6-tri-*tert*-butylphosphinine **4-8**,[70] dione **4-9**,[70] 2,4,6-tri-*tert*-butylpyrylium tetrafluoroborate **4-10**,[70] and *tert*-butylphosphaalkyne **4-11**[15] were prepared according to literature procedures. 1-Adamantylphosphaalkyne **4-13** was purchased from Santa Cruz Biotechnology and used as received. $B(C_6F_5)_3$ was purchased from Boulder Scientific and sublimed under vacuum at 85 °C prior to use. *tert*-Butylisocyanide, and 2,4,6-tri(trifluoromethyl)-1,3,5-triazine **4-5** were purchased from Alfa Aesar and used as received. Pyridine was purchased from Sigma Aldrich, degassed, and stored over activated 4 Å molecular sieves prior to use. Hydrogen gas (Grade 5.0) was obtained from Linde and purified through a Matheson Model 450B or Matheson Nanochem WeldAssureTM gas purifier.

Solution state NMR spectra were obtained on a Bruker Avance III 400 MHz, Agilent DD2 500 MHz, or Agilent DD2 600 MHz spectrometer and spectra were referenced to the residual solvent signals (C_6D_5Br: ^1H = 7.28 ppm for *meta* proton, ^{13}C = 122.4 ppm for *ipso* carbon; $CDCl_3$: ^1H = 7.26; ^{13}C = 77.2) or externally (^{19}F: $CFCl_3$, ^{11}B: $(Et_2O)BF_3$, ^{31}P: 85% H_3PO_4). Chemical shifts (δ) are reported in ppm and coupling constants are listed as absolute values in Hz. NMR assignments are supported by additional 2D experiments. The numbering system used for adamantyl substituents is shown in Figure 4.17. Elemental analyses (C,H,N) and high resolution mass spectrometry (HRMS) were performed in house.

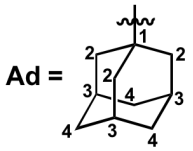

Figure 4.17 – Numbering system used for adamantyl substituents.

4.4.2 Syntheses and Characterizations

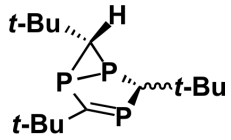

Synthesis of 4-2

In a 3 mL vial, **4-1** (15.0 mg, 0.05 mmol) was weighed and dissolved in C_6D_5Br (0.4 mL), generating a bright yellow solution. The solution was transferred to a J-Young NMR tube and sealed. The vessel was degassed three times through freeze-pump-thaw cycles and filled with H_2 (4 atm) at −196 °C. The J-Young NMR tube was then heated to 110 °C in an oil bath, and over five hours the reaction became a faint yellow solution. The C_6D_5Br was removed slowly under reduced pressure yielding diffraction-quality crystals of **4-2a** (13 mg). NMR data shows isomers **4-2a** and **4-2b** in a 4:1 ratio. **4-2a**[55] and **4-2b**[54] have been previously synthesized and their NMR characterization is reported in the literature.

^{1}H NMR (400 MHz, 298 K, C_6D_5Br): δ 2.98 (dd, $^2J_{PH}$ = 3.9, 1.7 Hz, 1H, **A** C2 H), 2.59 (t, $^2J_{PH}$ = 8.2 Hz, 1H, **B** C2 H), 1.49 (d, $^4J_{PH}$ = 1.6 Hz, 9H, **A** C1 *t*-Bu), 1.46 (d, $^4J_{PH}$ = 2 Hz, 9H, **B** C1 *t*-Bu), 1.28 (s, 9H, **B** C2 *t*-Bu), 1.13 (s, 9H, **A** C2 *t*-Bu), 0.93 (s, 9H, **B** C3 *t*-Bu), 0.92 (s, 9H, **A** C3 *t*-Bu).

^{31}P NMR (162 MHz, 298 K, C_6D_5Br): δ 310.2 (dd, $^2J_{PP}$ = 36, 13 Hz, **A** P1), 287.5 (d, $^2J_{PP}$ = 30 Hz, **B** P1), −117.8 (dd, $^1J_{PP}$ = 166 Hz, $^2J_{PP}$ = 36 Hz, **A** P2), −128.8 (ddd, $^1J_{PP}$ = 166 Hz, $^2J_{PP}$ = 13 Hz, $^2J_{P\text{-}H}$ = 3 Hz, **A** P3), −135.4 (dd, $^1J_{PP}$ = 167 Hz, $^2J_{PP}$ = 29 Hz, **B** P2), −171.9 (d, $^1J_{PP}$ = 167 Hz, **B** P3).

HRMS (DART) calcd. for $[C_{15}H_{30}P_3]^+$ ($[M+H]^+$) 303.1560, found 303.1562.

Synthesis of Piers' Borane, $HB(C_6F_5)_2$

Based on a modified literature procedure,[100] $B(C_6F_5)_3$ (5.0 g, 9.8 mmol) was slurried in 30 mL toluene in a wide-necked Schlenk bomb equipped with a magnetic stir bar. To this solution was added $HSiEt_3$ (1.6 mL, 9.8 mmol). The reaction flask was sealed and heated to 60 °C for 5 days. The volatiles were then removed *in vacuo* and the resulting material was stirred over ~15 mL pentane for several hours. The suspension was filtered, and the solid material was washed with additional pentane. The white precipitate was collected and any residual solvent removed *in vacuo* to yield the desired product $HB(C_6F_5)_2$ in 51% yield (1.6 g). NMR data are consistent with literature reported values.[82]

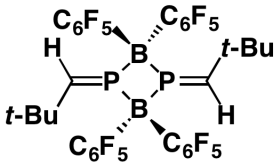

Synthesis of 4-12

In a nitrogen-filled glovebox, $HB(C_6F_5)_2$ (104 mg, 0.3 mmol) was weighed in a 20 mL scintillation vial equipped with a magnetic stir bar. The material was dissolved in 2.5 mL DCM. *tert*-Butylphosphaalkyne **4-11** was weighed in a 3 mL vial (30 mg, 0.3 mmol), dissolved in 0.5 mL DCM, and transferred to the solution of $HB(C_6F_5)_2$. The 3 mL vial was rinsed with 2 x 0.5 mL DCM, with washes added to the reaction mixture. The resulting homogeneous yellow solution was stirred vigorously at ambient glovebox temperature (35 °C) for 5 minutes. The volatiles were then removed *in vacuo* to yield a mixture of white precipitate and yellow oil. The material was vigorously stirred over 5 mL of pentane; the resulting yellow solution was decanted, and the material was stirred over an additional 5 mL of pentane. The second pentane wash was decanted and residual volatiles were removed *in vacuo*, yielding the dimeric phosphaalkenylborane **4-12** as a white powder in 67% yield (90 mg, 0.10 mmol). Single crystals suitable for X-ray diffraction studies were grown by layered diffusion of pentane into a DCM solution of **4-12** at −35 °C.

^{1}H NMR (500 MHz, 298 K, $CDCl_3$): δ 8.03 (vt, $^2J_{HP}$ = 16.5 Hz, 1H, phosphaalkene C<u>H</u>), 1.04 (s, 9H, phosphaalkene-*t*-Bu).

^{1}H{^{31}P} NMR (400 MHz, 298 K, $CDCl_3$): δ 8.03 (s, 1H, phosphaalkene C<u>H</u>), 1.04 (s, 9H, phosphaalkene-*t*-Bu).

^{19}F NMR (377 MHz, 298 K, $CDCl_3$): δ −127.3 (d, $^3J_{FF}$ = 21 Hz, 2F, *o*-C_6F_5), −153.3 (t, $^3J_{FF}$ = 20 Hz, 1F, *p*-C_6F_5), −161.9 to −162.0 (m, 2F, *m*-C_6F_5).

^{31}P NMR (162 MHz, 298 K, $CDCl_3$): δ 183.2 (s, phosphaalkene).

^{11}B NMR (128 MHz, 298 K, $CDCl_3$): δ −5.3 (s, borate).

^{13}C{^{1}H} NMR (126 MHz, 298 K, $CDCl_3$), partial: δ 177.7 (vt, $^1J_{CP}$ = 55 Hz, phosphaalkene <u>C</u>H), 147.6 (dm, $^1J_{CF}$ ~ 243 Hz, C_6F_5), 141.1 (dm, $^1J_{CF}$ ~ 258 Hz, C_6F_5), 137.5 (dm, $^1J_{CF}$ ~ 251 Hz, C_6F_5), 40.7 (vt, $^2J_{CP}$ = 14 Hz, phosphaalkene-<u>C</u>$(CH_3)_3$), 29.9 (vt, $^3J_{CP}$ = 16 Hz, phosphaalkene-C(<u>C</u>$H_3)_3$).

Elemental Analysis calcd (%) $C_{34}H_{20}B_2F_{20}P_2$: C 45.78; H 2.26; Found: C 45.35; H 2.20.

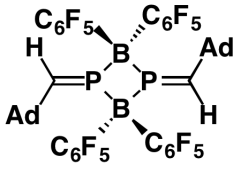

Synthesis of 4-14

In a nitrogen-filled glovebox, $HB(C_6F_5)_2$ (104 mg, 0.3 mmol) was weighed in a 20 mL scintillation vial equipped with a magnetic stir bar. The material was dissolved in 2.5 mL DCM. 1-Adamanylphosphaalkyne **4-13** was weighed in a 3 mL vial (54 mg, 0.3 mmol), dissolved in 0.5 mL DCM, and transferred to the solution of $HB(C_6F_5)_2$. The 3 mL vial was rinsed with 2 x 0.5 mL DCM, with washes added to the reaction mixture. The resulting homogeneous bright yellow solution was stirred vigorously at ambient glovebox temperature (35 °C) for 5 minutes. The volatiles were then removed *in vacuo* to yield a mixture of white precipitate and yellow oil. The material was vigorously stirred over 5 mL of pentane; the resulting yellow solution was decanted, and the material was stirred over an additional 5 mL of pentane. The second pentane wash was decanted and residual volatiles were removed *in vacuo*, yielding the dimeric phosphaalkenylborane **4-14** as a white powder in 68% yield (107 mg, 0.10 mmol). Single crystals suitable for X-ray diffraction studies were grown by layered diffusion of pentane into a DCM solution of **4-14** at −35 °C.

^{1}H NMR (500 MHz, 298 K, $CDCl_3$): δ 7.89 (vt, $^2J_{HP}$ = 15.9 Hz, 1H, sp^2 C<u>H</u>), 1.89 (br s, 3H, Ad C3), 1.66–1.64 (m, 3H, Ad C4), 1.53 (br d, $^4J_{HP}$ = 2.2 Hz, 6H, Ad C2), 1.46–1.44 (m, 3H, Ad C4).

^{19}F NMR (377 MHz, 298 K, $CDCl_3$): δ −126.9 (d, $^3J_{FF}$ = 21.5 Hz, 2F, *o*-C_6F_5), −153.7 (t, $^3J_{FF}$ = 20.5 Hz, 1F, *p*-C_6F_5), −162.0 to −162.2 (m, 2F, *m*-C_6F_5).

^{31}P NMR (162 MHz, 298 K, $CDCl_3$): δ 183.0 (br s, phosphaalkene).

^{11}B NMR (128 MHz, 298 K, $CDCl_3$): δ −5.2 (br s, borate).

^{13}C{^{1}H} NMR (126 MHz, 298 K, $CDCl_3$), partial: δ 177.1 (vt, $^1J_{CP}$ = 53.5 Hz, sp^2 <u>C</u>H), 147.6 (dm, $^1J_{CF}$ ~ 235 Hz, C_6F_5), 141.0 (dm, $^1J_{CF}$ ~ 259 Hz, C_6F_5), 137.5 (dm, $^1J_{CF}$ ~ 254 Hz, C_6F_5), 43.0 (vt, $^2J_{CP}$ = 14 Hz, Ad C1), 42.1 (vt, $^3J_{CP}$ = 15.0 Hz, Ad C2), 36.1 (s, Ad C4), 28.1 (s, Ad C3).

Elemental Analysis calcd (%) $C_{46}H_{32}B_2F_{20}P_2$: C 52.71; H 3.08; Found: C 51.81; H 3.27. Elemental analysis was consistently low on %carbon.

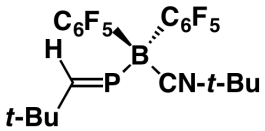

Synthesis of 4-15

In a nitrogen-filled glovebox, dimer **4-12** (18 mg, 0.02 mmol) was weighed in a 3 mL vial equipped with a magnetic stir bar and dissolved in 0.5 mL $CHCl_3$. *tert*-Butylisocyanide (3.4 mg, 0.04 mmol) was weighed in a 3 mL vial, dissolved in 0.25 mL $CHCl_3$, and transferred to the solution of **4-12**. The isocyanide vial was rinsed with 0.25 mL $CHCl_3$, and the rinse was added to the reaction mixture. The resulting solution was stirred at ambient glovebox temperature (35 °C) for 5 minutes, followed by concentration *in vacuo* to yield **4-15** as a faint yellow oil in 93% yield (20 mg, 0.038 mmol).

^{1}H NMR (400 MHz, 298 K, $CDCl_3$): δ 8.75 (d, $^2J_{HP}$ = 23.6 Hz, 1H, phosphaalkene C<u>H</u>), 1.64 (s, 9H, N-*t*-Bu), 1.13 (d, $^4J_{HP}$ = 1.6 Hz, 9H, phosphaalkene-*t*-Bu).

^{19}F NMR (377 MHz, 298 K, $CDCl_3$): δ −130.1 (ddd, $^3J_{FF}$ = 23 Hz, $^4J_{FF}$ = 9 Hz, $^4J_{FP}$ = 36 Hz, 2F, *o*-C_6F_5), −157.1 (t, $^3J_{FF}$ = 20 Hz, 1F, *p*-C_6F_5), −163.1 (ddd, $^3J_{FF}$ = 23 Hz, $^3J_{FF}$ = 20 Hz, $^5J_{FP}$ = 8 Hz, 2F, *m*-C_6F_5).

^{19}F{^{31}P} NMR (564 MHz, 298 K, $CDCl_3$): δ −130.2 (d, $^3J_{FF}$ = 23 Hz, 2F, *o*-C_6F_5), −157.2 (t, $^3J_{FF}$ = 20 Hz, 1F, *p*-C_6F_5), −163.1 to −163.2 (m, 2F, *m*-C_6F_5).

^{31}P NMR (243 MHz, 298 K, $CDCl_3$): δ 265.9 (doublet of quintets, $^2J_{PH}$ = 23 Hz, $^4J_{PF}$ = 36 Hz, phosphaalkene).

^{31}P{^{1}H} NMR (243 MHz, 298 K, $CDCl_3$): δ 265.9 (quintet, $^4J_{PF}$ = 36 Hz, phosphaalkene).

^{31}P{^{19}F} NMR (243 MHz, 298 K, $CDCl_3$): δ 265.9 (d, $^2J_{PH}$ = 24 Hz, phosphaalkene).

^{11}B NMR (128 MHz, 298 K, $CDCl_3$): δ −22.5 (s, borate).

^{13}C{^{1}H} NMR (101 MHz, 298 K, $CDCl_3$), partial: δ 205.4 (d, $^1J_{CP}$ = 51 Hz, phosphaalkene <u>C</u>H), 147.8 (dm, $^1J_{CF}$ ~ 241 Hz, C_6F_5), 137.4 (dm, $^1J_{CF}$ ~ 248 Hz, C_6F_5), 60.3 (s, N-<u>C</u>$(CH_3)_3$), 40.6 (d, $^2J_{CP}$ = 11 Hz, CH-<u>C</u>$(CH_3)_3$), 30.6 (d, $^3J_{CP}$ = 13 Hz, CH-C(<u>C</u>$H_3)_3$), 29.5 (s, N-C(<u>C</u>$H_3)_3$).

HRMS (DART) calcd for $[C_{22}H_{20}BF_{10}NP]^+$ ($[M+H]^+$) 530.1267, found 530.1265

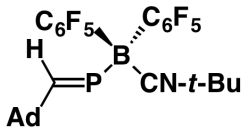

Synthesis of 4-16

In a nitrogen-filled glovebox, dimer **4-14** (21 mg, 0.02 mmol) was weighed in a 20 mL scintillation vial equipped with a magnetic stir bar and dissolved in 1.5 mL DCM. An excess of *tert*-butylisocyanide (6 mg, 0.07 mmol) was weighed in a 3 mL vial, dissolved in 0.5 mL DCM, and transferred to the solution of **4-14**. The isocyanide vial was rinsed with 2 x 0.5 mL DCM, and the rinses were added to the reaction mixture. The resulting clear, colourless solution was stirred at ambient glovebox temperature (35 °C) for 5 minutes. The volatiles were then removed *in vacuo*, and the resulting material was dissolved in 3 mL pentane and filtered. The filtrate was concentrated *in vacuo* to yield **4-16** as a faint yellow oil in 84% yield (20 mg, 0.034 mmol). Crystals suitable for X-ray diffraction studies were grown by layered diffusion of pentane into a DCM solution of **4-16** at 35 °C.

^{1}H NMR (500 MHz, 298 K, $CDCl_3$): δ 8.61 (d, $^{2}J_{HP}$ = 23.5 Hz, 1H, phosphaalkene C<u>H</u>), 2.03–1.98 (m, 3H, Ad C3), 1.74–1.70 (m, 3H, Ad C4), 1.66 (d, $^{4}J_{HP}$ = 2.5 Hz, 6H, Ad C2), 1.64 (s, 9H, N-*t*-Bu), 1.63–1.60 (m, 3H, Ad C4).

^{19}F NMR (377 MHz, 298 K, $CDCl_3$): δ −130.1 (ddd, $^{4}J_{FP}$ = 36.5 Hz, $^{3}J_{FF}$ = 23.2 Hz, $^{4}J_{FF}$ = 8.0 Hz, 2F, *o*-C_6F_5), −157.3 (t, $^{3}J_{FF}$ = 20.4 Hz, 1F, *p*-C_6F_5), −163.1 to −163.2 (m, 2F, *m*-C_6F_5).

^{31}P NMR (243 MHz, 298 K, $CDCl_3$): δ 268.3 (doublet of quintets, $^{2}J_{PH}$ = 23.8 Hz, $^{4}J_{PF}$ = 36.5 Hz, phosphaalkene).

^{31}P{^{1}H} NMR (243 MHz, 298 K, $CDCl_3$): δ 268.3 (quintet, $^{4}J_{PF}$ = 36.5 Hz, phosphaalkene).

^{11}B NMR (128 MHz, 298 K, $CDCl_3$): δ −22.5 (s, borate).

^{13}C{^{1}H} NMR (126 MHz, 298 K, $CDCl_3$), partial: δ 205.6 (d, $^{1}J_{CP}$ = 51.5 Hz, phosphaalkene <u>C</u>H), 147.7 (dm, $^{1}J_{CF}$ ~ 241 Hz, C_6F_5), 139.9 (dm, $^{1}J_{CF}$ ~ 251 Hz, C_6F_5), 137.3 (dm, $^{1}J_{CF}$ ~ 255 Hz, C_6F_5), 60.2 (s, N-<u>C</u>$(CH_3)_3$), 43.5 (d, $^{3}J_{CP}$ = 12.9 Hz, Ad C2), 42.8 (d, $^{2}J_{CP}$ = 10.3 Hz, Ad C1), 36.8 (s, Ad C4), 29.5 (s, N-C(<u>C</u>$H_3)_3$), 28.7 (d, $^{4}J_{CP}$ = 1.6 Hz, Ad C3).

HRMS (DART) calcd for $[C_{28}H_{26}BF_{10}NP]^{+}$ ($[M+H]^{+}$) 608.1736, found 608.1723.

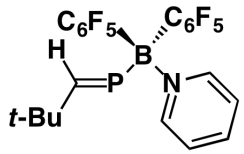

Synthesis of 4-17

In a nitrogen-filled glovebox, dimer **4-12** (18 mg, 0.02 mmol) was weighed in a 6 mL vial equipped with a magnetic stir bar and dissolved in 1.5 mL DCM. An excess of pyridine (6.2 mg, 0.08 mmol) was weighed in a 3 mL vial, dissolved in 0.5 mL DCM, and transferred to the solution of **4-12**. The pyridine vial was rinsed with 2 x 0.5 mL DCM, and the rinses were added to the reaction mixture. The resulting solution was stirred at ambient glovebox temperature (35 °C) for 1 hour. The volatiles were removed *in vacuo* and the resulting faint yellow oil was dissolved in minimal pentane and placed in a −35 °C freezer. A solid precipitated from solution, and after decanting the yellow supernatant, **4-17** was isolated as an off-white solid in 73% yield (15 mg, 0.029 mmol). Single crystals suitable for X-ray diffraction studies were grown from slow evaporation of a pentane solution of **4-17** at 35 °C.

^{1}H NMR (400 MHz, 298 K, $CDCl_3$): δ 8.92 (d, $^{3}J_{HH}$ = 5.2 Hz, 2H, py *o*-C<u>H</u>), 8.41 (d, $^{2}J_{HP}$ = 24.8 Hz, 1H, phosphaalkene C<u>H</u>), 8.16 (tt, $^{3}J_{HH}$ = 7.6 Hz, $^{4}J_{HH}$ = 1.4 Hz, 1H, py *p*-C<u>H</u>), 7.73–7.68 (m, 2H, py *m*-C<u>H</u>), 1.07 (d, $^{4}J_{HP}$ = 1.2 Hz, 9H, phosphaalkene-*t*-Bu).

^{19}F NMR (377 MHz, 298 K, $CDCl_3$): δ −129.2 to −129.4 (m, 2F, *o*-C_6F_5), −157.0 (t, $^{3}J_{FF}$ = 20.5 Hz, 1F, *p*-C_6F_5), −163.2 to −163.3 (m, 2F, *m*-C_6F_5).

^{31}P NMR (202 MHz, 298 K, $CDCl_3$): δ 271.2 (doublet of quintets, $^{2}J_{PH}$ = 25 Hz, $^{4}J_{PF}$ = 28 Hz, phosphaalkene).

^{31}P{^{1}H} NMR (202 MHz, 298 K, $CDCl_3$): δ 271.2 (quintet, $^{4}J_{PF}$ = 28 Hz, phosphaalkene).

^{11}B NMR (128 MHz, 298 K, $CDCl_3$): δ −0.8 (s, borate).

^{13}C{^{1}H} NMR (126 MHz, 298 K, $CDCl_3$), partial: δ 204.0 (d, $^{1}J_{CP}$ = 45 Hz, phosphaalkene <u>C</u>H), 147.7 (dm, $^{1}J_{CF}$ ~ 243 Hz, C_6F_5), 147.3 (d, $^{3}J_{CP}$ = 10 Hz, py *o*-<u>C</u>H), 142.1 (s, py *p*-<u>C</u>H), 139.8 (dm, $^{1}J_{CF}$ ~ 251 Hz, C_6F_5), 137.4 (dm, $^{1}J_{CF}$ ~ 247 Hz, C_6F_5), 126.2 (s, py *m*-<u>C</u>H), 40.3 (d, $^{2}J_{CP}$ = 11 Hz, phosphaalkene-<u>C</u>$(CH_3)_3$), 30.4 (d, $^{4}J_{CP}$ = 13 Hz, phosphaalkene-C(<u>C</u>$H_3)_3$).

HRMS (ESI) calcd for $[C_{22}H_{18}BF_{10}NOP]^+$ ($[M+H_3O]^+$) 543.1090, found 543.1081 *the $[M+H]^+$ ion was not observed, but the hydrated $[M+H]^+$ ion was found. The mass was calculated using the ^{10}B isotope.

4.4.3 Solid State NMR Spectroscopy

The $^{31}P\{^{1}H\}$ ssNMR spectrum of **4-12** was acquired on an Agilent DD2-700 MHz spectrometer with a 1.6 mm Double Resonance T3-HX MAS Solids Balun probe. The signal, comprised of spinning sidebands spaced at 20 kHz intervals, spans 400–30 ppm and exhibits a maximum at 254 ppm (Figure 4.18). The sideband at 185 ppm was resolved into an overlapping doublet of doublets with $^{2}J_{PP} \sim 1520$ Hz.

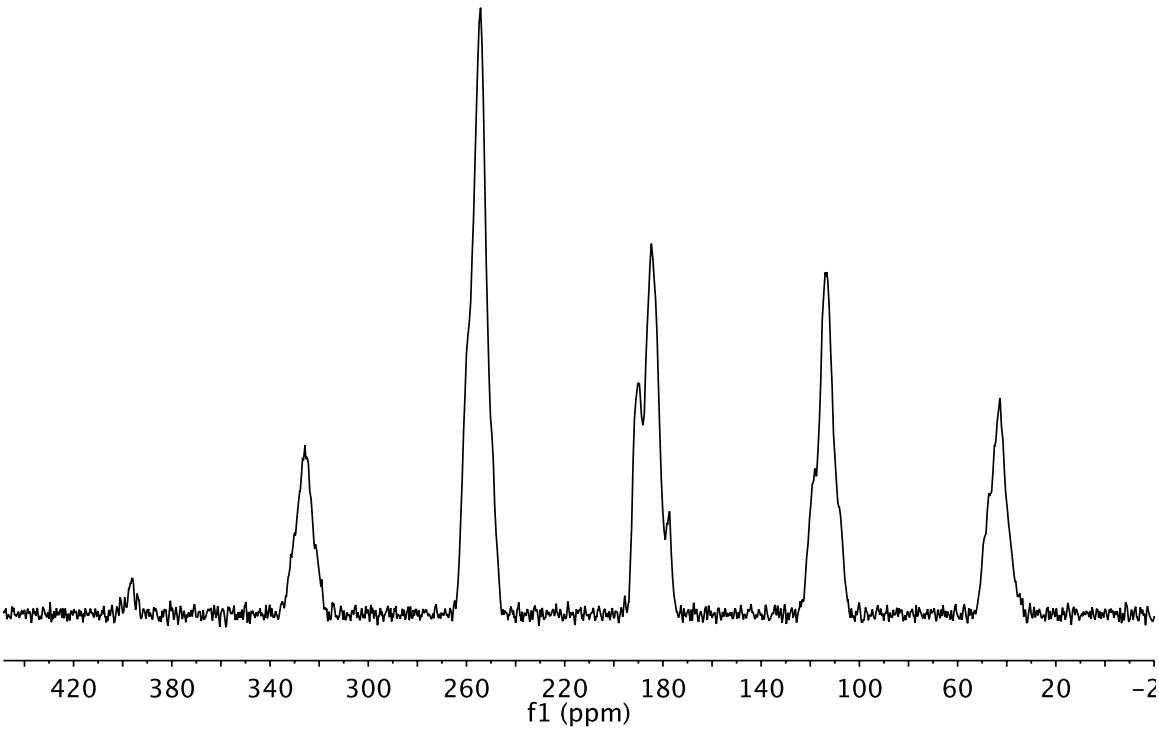

Figure 4.18 – $^{31}P\{^{1}H\}$ ssNMR (283 MHz, spinning frequency: 20 kHz) spectrum of **4-12**.

4.4.4 X-ray Crystallography

4.4.4.1 X-ray Collection and Reduction

Crystals were coated in Paratone-N oil in the glovebox, mounted on a MiTegen Micromount and placed under an N_2 stream, thus maintaining a dry, O_2-free environment for each crystal. The data were collected on a Bruker Kappa Apex II diffractometer. Data collection strategies were determined using Bruker Apex 2 software and optimized to provide >99.5% complete data to a

2θ value of at least 55°. The data were collected at 150(±2) K for all. The data integration and absorption correction were performed with the Bruker Apex 2 software package.[101]

4.4.4.2 X-ray Solution and Refinement

Non-hydrogen atomic scattering factors were taken from the literature tabulations.[102] The heavy atom positions were determined using direct methods employing the SHELX-2013 direct methods routine. The remaining non-hydrogen atoms were located from successive difference Fourier map calculations. The refinements were carried out by using full-matrix least squares techniques on F^2. All non-hydrogen atoms were assigned anisotropic temperature factors in the absence of disorder or insufficient data. In the latter cases, atoms were treated isotropically. C-bound H atoms were placed at calculated positions and allowed to ride on the carbon to which they are bonded during refinement. H-atom temperature factors were fixed at 1.20 times (central atoms) or 1.50 times (terminal CH_3 atoms) the isotropic temperature factor of the C-atom to which they are bonded. The locations of the largest peaks in the final difference Fourier map calculation as well as the magnitude of the residual electron densities in each case were of no chemical significance.

Table 4.1 – Selected crystallographic data for **4-2a**, **4-12**, and **4-14**.

	4-2a	½[**4-12**]	**4-14**·CH_2Cl_2
Formula	$C_{15}H_{29}P_3$	$C_{17}H_{10}BF_{10}P$	$C_{47}H_{34}B_2Cl_2F_{20}P_2$
Formula weight	302.29	446.03	1133.20
Crystal System	Monoclinic	Monoclinic	Monoclinic
Space group	$P2_1/c$	$P2_1/n$	$P2_1/n$
a (Å)	9.5404(7)	10.1481(9)	12.7403(8)
b (Å)	11.9679(10)	18.9650(16)	10.5722(7)
c (Å)	18.6011(11)	18.9465(15)	17.2285(9)
α (°)	90	90	90
β (°)	120.857(3)	98.799(4)	92.986(6)
γ (°)	90	90	90
V (Å^3)	1823.2(2)	3603.5(5)	2317.4(2)
Z	4	8	2
Temp. (K)	150	150	150
d_{calc} (gcm^{-1})	1.101	1.644	1.624
Abs. coeff. μ (mm^{-1})	0.312	0.252	0.326
Reflections Collected	16603	61542	37063
Data $F_o^2>3\sigma(F_o^2)$	4074	8246	5365
Variables	172	523	343
R	0.0655	0.0401	0.0634
R_w	0.1662	0.0813	0.1470
GOF	1.026	1.010	1.036

Table 4.2 – Selected crystallographic data for **4-16** and **4-17**.

	4-16·½C_5H_{12}	2[**4-17**]
Formula	$C_{30.5}H_{31}BF_{10}NP$	$C_{44}H_{30}B_2F_{20}N_2P_2$
Formula weight	643.34	1050.26
Crystal System	Triclinic	Triclinic
Space group	P-1	P-1
a (Å)	10.0406(11)	11.8016(7)
b (Å)	15.2415(15)	14.2001(9)
c (Å)	21.777(3)	14.7948(9)
α (°)	76.688(6)	68.567(3)
β (°)	78.456(5)	82.456(4)
γ (°)	71.560(5)	80.515(3)
V (Å^3)	3047.1(6)	2269.5(2)
Z	4	2
Temp. (K)	149	149
d_{calc} (gcm^{-1})	1.402	1.537
Abs. coeff. μ (mm^{-1})	0.173	0.214
Reflections Collected	10460	29012
Data $F_o^2>3\sigma(F_o^2)$	10460	10466
Variables	784	631
R	0.1038	0.0413
R_w	0.2495	0.0996
GOF	1.519	1.052

4.5 References

(1) Pitzer, K. S. *Journal of the American Chemical Society* **1948**, *70*, 2140–2145.

(2) Mulliken, R. S. *Journal of the American Chemical Society* **1950**, *72*, 4493–4503.

(3) Regitz, M.; Binger, P. *Angewandte Chemie International Edition* **1988**, *27*, 1484–1508.

(4) Dugal-Tessier, J.; Conrad, E. D.; Dake, G. R.; Gates, D. P. In *Phosphorus(III) Ligands in Homogeneous Catalysis: Design and Synthesis*; Kamer, P. C. J., Leeuwen, P. W. N. M. van, Eds.; John Wiley & Sons Ltd, 2012; pp 321–341.

(5) Gier, T. E. *Journal of the American Chemical Society* **1961**, *83*, 1769–1770.

(6) Hopkinson, M. J.; Kroto, H. W.; Nixon, J. F.; Simmons, N. P. C. *Journal of the Chemical Society, Chemical Communications* **1976**, 513–515.

(7) Märkl, G. *Angewandte Chemie International Edition* **1966**, *5*, 846–847.

(8) Dimroth, K.; Hoffmann, P. *Angewandte Chemie International Edition* **1964**, *3*, 384.

(9) Becker, G. *Zeitschrift für Anorganische und Allgemeine Chemie* **1976**, *423*, 242–254.

(10) Klebach, T. C.; Lourens, R.; Bickelhaupt, F. *Journal of the American Chemical Society* **1978**, *100*, 4886–4888.

(11) Bates, J. I.; Dugal-Tessier, J.; Gates, D. P. *Dalton Transactions* **2010**, *39*, 3151–3159.

(12) Le Floch, P. *Coordination Chemistry Reviews* **2006**, *250*, 627–681.

(13) Mathey, F. *Angewandte Chemie International Edition* **2003**, *42*, 1578–1604.

(14) Becker, G.; Gresser, G.; Uhl, W. *Zeitschrift für Naturforschung* **1981**, *36b*, 16–19.

(15) Russell, C. A.; Townsend, N. S. In *Phosphorus(III) Ligands in Homogeneous Catalysis: Design and Synthesis*; Kamer, P. C. J., Leeuwen, P. W. N. M. van, Eds.; John Wiley & Sons, Ltd., 2012; pp 343–354.

(16) Becker, G.; Schwarz, W.; Seidler, N.; Westerhausen, M. *Zeitschrift für Anorganische und Allgemeine Chemie* **1992**, *612*, 72–82.

(17) Puschmann, F. F.; Stein, D.; Heift, D.; Hendriksen, C.; Gal, Z. A.; Grützmacher, H. F.; Grützmacher, H. *Angewandte Chemie International Edition* **2011**, *50*, 8420–8423.

(18) Krummenacher, I.; Cummins, C. C. *Polyhedron* **2012**, *32*, 10–13.

(19) Jupp, A. R.; Goicoechea, J. M. *Angewandte Chemie International Edition* **2013**, *52*, 10064–10067.

(20) Jupp, A. R.; Goicoechea, J. M. *Journal of the American Chemical Society* **2013**, *135*, 19131–19134.

(21) Robinson, T. P.; Goicoechea, J. M. *Chemistry - A European Journal* **2015**, *21*, 5727–5731.

(22) Märkl, G.; Lieb, F.; Merz, A. *Angewandte Chemie International Edition* **1967**, *6*, 458–459.

(23) Märkl, G.; Lieb, F.; Merz, A. *Angewandte Chemie International Edition* **1967**, *6*, 944–945.

(24) Ashe, A. J. *Journal of the American Chemical Society* **1971**, *93*, 3293–3295.

(25) Barron, A. R.; Cowley, A. H. *Angewandte Chemie International Edition* **1987**, *26*, 907–

908.

(26) Binger, P.; Leininger, S.; Stannek, J.; Gabor, B.; Mynott, R.; Bruckmann, J.; Krüger, C. *Angewandte Chemie International Edition* **1995**, *34*, 2227–2230.

(27) Tabellion, F.; Nachbauer, A.; Leininger, S.; Peters, C.; Preuss, F.; Regitz, M. *Angewandte Chemie International Edition* **1998**, *37*, 1233–1235.

(28) Falconer, R. L.; Russell, C. A. *Coordination Chemistry Reviews* **2015**, *297–298*, 146–167.

(29) Choong, S. L.; Woodul, W. D.; Schenk, C.; Stasch, A.; Richards, A. F.; Jones, C. *Organometallics* **2011**, *30*, 5543–5550.

(30) Schmitz, M.; Göller, R.; Bergsträßer, U.; Leininger, S.; Regitz, M. *European Journal of Inorganic Chemistry* **1998**, 227–235.

(31) Ionkin, A. S.; Ignat'eva, S. N.; Arbuzov, B. A. *Russian Chemical Bulletin* **1990**, *6*, 1315.

(32) Bedford, R. B.; Hibbs, D. E.; Hill, A. F.; Hursthouse, M. B.; Malik, K. M. A.; Jones, C. *Chemical Communications* **1996**, 1895–1896.

(33) Bedford, R. B.; Hill, A. F.; Jones, C. *Angewandte Chemie International Edition* **1996**, *35*, 547–549.

(34) Bedford, R. B.; Hill, A. F.; Jones, C.; White, A. J. P.; Williams, D. J.; Wilton-Ely, J. D. E. T. *Organometallics* **1998**, *17*, 4744–4753.

(35) Greenacre, V. K.; Trathen, N.; Crossley, I. R. *Organometallics* **2015**, *34*, 2533–2542.

(36) Barnard, J. H.; Yruegas, S.; Couchman, S. A.; Wilson, D. J. D.; Dutton, J. L.; Martin, C. D. *Organometallics* **2016**, *35*, 929–931.

(37) Müller, C.; Vogt, D. *Dalton Transactions* **2007**, 5505–5523.

(38) Zhang, Y.; Tham, F. S.; Nixon, J. F.; Taylor, C.; Green, J. C.; Reed, C. A. *Angewandte Chemie International Edition* **2008**, *47*, 3801–3804.

(39) Nyulászi, L. *Chemical Reviews* **2001**, *101*, 1229–1246.

(40) Le Floch, P. In *Phosphorus-Carbon Heterocyclic Chemistry*; 2001; pp 485–533.

(41) Knoch, F.; Kremer, F.; Schmidt, U.; Zenneck, U.; Le Floch, P.; Mathey, F. *Organometallics* **1996**, *15*, 2713–2719.

(42) Breit, B.; Winde, R.; Mackewitz, T.; Paciello, R.; Harms, K. *Chemistry - A European Journal* **2001**, *7*, 3106–3121.

(43) Märkl, G.; Lieb, F. *Angewandte Chemie International Edition* **1968**, *7*, 733.

(44) Märkl, G.; Lieb, F.; Martin, C. *Tetrahedron Letters* **1971**, *12*, 1249–1252.

(45) Gleiter, R.; Lange, H.; Binger, P.; Stannek, J.; Krüger, C.; Bruckmann, J.; Zenneck, U.;

Kummer, S. *European Journal of Inorganic Chemistry* **1998**, 1619–1621.

(46) Townsend, N. S.; Green, M.; Russell, C. A. *Organometallics* **2012**, *31*, 2543–2545.

(47) Clendenning, S. B.; Gehrhus, B.; Hitchcock, P. B.; Nixon, J. F. *Chemical Communications* **1999**, *38*, 2451–2452.

(48) Renner, J.; Bergsträsser, U.; Binger, P.; Regitz, M. *Angewandte Chemie International Edition* **2003**, *42*, 1863–1866.

(49) Krein, M.; Bergsträßer, U.; Peters, C.; Ruf, S. G.; Regitz, M. *Chemical Communications* **2000**, *653*, 2015–2016.

(50) Seitz, A. E.; Eckhardt, M.; Erlebach, A.; Peresypkina, E. V; Sierka, M.; Scheer, M. *Journal of the American Chemical Society* **2016**, *138*, 10433–10436.

(51) Mahdi, T.; Heiden, Z. M.; Grimme, S.; Stephan, D. W. *Journal of the American Chemical Society* **2012**, *134*, 4088–4091.

(52) Mahdi, T.; del Castillo, J. N.; Stephan, D. W. *Organometallics* **2013**, *32*, 1971–1978.

(53) Longobardi, L. E.; Mahdi, T.; Stephan, D. W. *Dalton Transactions* **2015**, *44*, 7114–7117.

(54) Jones, C.; Waugh, M. *Dalton Transactions* **2004**, 1971–1979.

(55) Binger, P.; Stutzmann, S.; Stannek, J.; Günther, K.; Phillips, P.; Mynott, R.; Bruckmann, J.; Krüger, C. *European Journal of Inorganic Chemistry* **1999**, 763–769.

(56) Floch, P. Le. In *Topics in Heterocyclic Chemistry*; 2009; pp 147–184.

(57) Geier, S. J.; Chase, P. A.; Stephan, D. W. *Chemical Communications* **2010**, *46*, 4884–4886.

(58) Liu, Y.; Du, H. *Journal of the American Chemical Society* **2013**, *135*, 12968–12971.

(59) Chase, P. A.; Jurca, T.; Stephan, D. W. *Chemical Communications* **2008**, *2*, 1701–1703.

(60) Preuss, F.; Fuchslocher, E.; Leber, E.; Towae, W. *Zeitschrift für Naturforschung* **1989**, *44b*, 271–277.

(61) Hills, A.; Hughes, D.; Leigh, G. J.; Prieto-Alcon, R. *Journal of the Chemical Society, Dalton Transactions* **1993**, 3609–3617.

(62) Massa, W.; Wocadlo, S.; Lotz, S.; Dehnicke, K. *Zeitschrift für Anorganische und Allgemeine Chemie* **1990**, *587*, 79–88.

(63) Bowers, C. R.; Weitekamp, D. P. *Journal of the American Chemical Society* **1987**, *109*, 5541–5542.

(64) Duckett, S. B.; Mewis, R. E. *Accounts of Chemical Research* **2012**, *45*, 1247–1257.

(65) Zhivonitko, V. V.; Telkki, V. V.; Chernichenko, K.; Repo, T.; Leskela, M.; Sumerin, V.;

Koptyug, I. V. *Journal of the American Chemical Society* **2014**, *136*, 598–601.

(66) Hintermann, L.; Xiao, L.; Labonne, A. *Angewandte Chemie International Edition* **2008**, *47*, 8246–8250.

(67) Zhong, G.; Chan, B.; Radom, L. *Journal of the American Chemical Society* **2007**, *129*, 924–933.

(68) Broeckx, L. E. E.; Güven, S.; Heutz, F. J. L.; Lutz, M.; Vogt, D.; Müller, C. *Chemistry - A European Journal* **2013**, *19*, 13087–13098.

(69) Dimroth, K.; Mach, W. *Angewandte Chemie International Edition* **1968**, *7*, 461–462.

(70) Dimroth, K.; Mach, W. *Angewandte Chemie International Edition* **1968**, *7*, 460–461.

(71) Chirila, A.; Wolf, R.; Chris Slootweg, J.; Lammertsma, K. *Coordination Chemistry Reviews* **2014**, *270–271*, 57–74.

(72) Dureen, M. A.; Stephan, D. W. *Journal of the American Chemical Society* **2009**, *131*, 8396–8397.

(73) Dureen, M. A.; Brown, C. C.; Stephan, D. W. *Organometallics* **2010**, *29*, 6594–6607.

(74) Kehr, G.; Erker, G. *Chemical Communications* **2012**, *48*, 1839–1850.

(75) Kehr, G.; Erker, G. *Chemical Science* **2016**, *7*, 56–65.

(76) Esteves, P. M.; Laali, K. K. *Organometallics* **2004**, *23*, 3701–3713.

(77) Laurent, J. C. T. R. B.-S.; King, M. A.; Kroto, H. W.; Nixon, J. F.; Suffolk, R. J. *Journal of the Chemical Society, Dalton Transactions* **1983**, 755–759.

(78) Aldridge, S.; Calder, R. J.; Rossin, A.; Dickinson, A. A.; Willock, D. J.; Jones, C.; Evans, D. J.; Steed, J. W.; Light, M. E.; Coles, S. J.; Hursthouse, M. B. *Journal of the Chemical Society, Dalton Transactions* **2002**, 2020–2026.

(79) Miller, R. W.; Spencer, J. T. *Organometallics* **1996**, *15*, 4293–4300.

(80) Binger, P.; Sandmeyer, F.; Kruger, C.; Kuhnigk, J.; Goddard, R.; Erker, G. *Angewandte Chemie International Edition* **1994**, *33*, 197–198.

(81) Becker, G.; Becker, W.; Knebl, R.; Schmidt, H.; Hildenbrand, U.; Westerhausen, M. *Phosphorous and Sulfur and the Related Elements* **1987**, *30*, 349–352.

(82) Parks, D. J.; Spence, R. E. von H.; Piers, W. E. *Angewandte Chemie International Edition* **1995**, *34*, 809–811.

(83) Bedford, R. B.; Hibbs, D. E.; Hill, A. F.; Hursthouse, M. B.; Malik, K. M. A.; Jones, C. *Chemical Communications* **1996**, 1895–1896.

(84) Geier, S. J.; Gilbert, T. M.; Stephan, D. W. *Inorganic Chemistry* **2011**, *50*, 336–344.

(85) Groshens, T. J.; Higa, K. T.; Nissan, R.; Butcher, R. J.; Freyer, A. J. *Organometallics* **1993**, *12*, 2904–2910.

(86) Rodriguez, A.; Olsen, R. A.; Ghaderi, N.; Scheschkewitz, D.; Tham, F. S.; Mueller, L. J.; Bertrand, G. *Angewandte Chemie International Edition* **2004**, *43*, 4880–4883.

(87) Scheschkewitz, D.; Amii, H.; Gornitzka, H.; Schoeller, W. W.; Bourissou, D.; Bertrand, G. *Science* **2002**, *295*, 1880–1881.

(88) Rodriguez, A.; Tham, F. S.; Schoeller, W. W.; Bertrand, G. *Angewandte Chemie International Edition* **2004**, *43*, 4876–4880.

(89) Fuks, G.; Saffon, N.; Maron, L.; Bertrand, G.; Bourissou, D. *Journal of the American Chemical Society* **2009**, *131*, 13681–13689.

(90) Crabtree, R. H. *The Organometallic Chemistry of the Transition Metals*, 5th ed.; John Wiley & Sons, Inc.: Hoboken, New Jersey, 2009.

(91) Reich, H. J.; Dykstra, R. R. *Organometallics* **1994**, *13*, 4578–4585.

(92) Geier, S. J.; Gilbert, T. M.; Stephan, D. W. *Journal of the American Chemical Society* **2008**, *130*, 12632–12633.

(93) Tanur, C. A.; Stephan, D. W. *Organometallics* **2011**, *30*, 3652–3657.

(94) Liddle, S. T.; Izod, K. *Organometallics* **2004**, *23*, 5550–5559.

(95) Yamada, N.; Abe, K.; Toyota, K.; Yoshifuji, M. *Organic Letters* **2002**, *4*, 569–572.

(96) Ito, S.; Sekiguchi, S.; Yoshifuji, M. *European Journal of Organic Chemistry* **2003**, 4838–4841.

(97) Aldridge, S.; Jones, C.; Junk, P. C.; Richards, A. F.; Waugh, M. *Journal of Organometallic Chemistry* **2003**, *665*, 127–134.

(98) Magnuson, K. W.; Oshiro, S. M.; Gurr, J. R.; Yoshida, W. Y.; Gembicky, M.; Rheingold, A. L.; Hughes, R. P.; Cain, M. F. *Organometallics* **2016**, *35*, 855–859.

(99) Müller, C.; Wasserberg, D.; Weemers, J. J. M.; Pidko, E. A.; Hoffmann, S.; Lutz, M.; Spek, A. L.; Meskers, S. C. J.; Janssen, R. A. J.; van Santen, R. A.; Vogt, D. *Chemistry - A European Journal* **2007**, *13*, 4548–4559.

(100) Parks, D. J.; Piers, W. E.; Yap, G. P. A. *Organometallics* **1998**, *17*, 5492–5503.

(101) *Bruker AXS Inc.*; 2013.

(102) Cromer, D. T.; Waber, J. T. In *International Tables for X-Ray Crystallography*; Kynoch Press: Birmingham, 1974; pp 71–147.

Chapter 5
$B(C_6F_5)_3$-Mediated Reductions of Ketones and Aldehydes

5.1 Introduction

5.1.1 Classical Ketone Reductions

The widely utilized classic boron[1] and aluminum hydrides[2] offer a reliable method for carbonyl reduction and are still regularly employed in synthetic chemistry,[3] despite being stoichiometric reagents that are often used in large excess. Catalytic methods for ketone (direct and transfer) hydrogenations exploit transition metal systems based on precious metal Ru and Rh complexes, and many chiral catalysts have been applied to asymmetric reductions of prochiral substrates (Figure 5.1).[4–7] More recently, interest in reductions based on earth-abundant elements has been motivated by economic and environmental advantages. To this end, Fe, Co, and Ni-based catalysts for ketone reduction have emerged.[8–10]

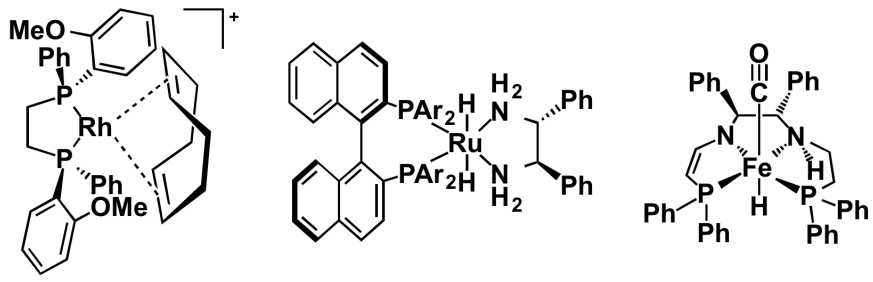

Figure 5.1 – a) Rh (Knowles), b) Ru (Noyori), and c) Fe (Morris) catalysts for the (transfer) hydrogenation of ketones.

5.1.2 FLP Reduction Chemistry

The field of frustrated Lewis pair (FLP) chemistry, as discussed in Chapter 1, has led to dramatic growth in main group hydrogenation systems.[11–13] Catalytic reductions for a myriad of unsaturated substrates including imines,[14] protected nitriles and aziridines,[15] enamines,[16] silyl enol ethers,[17,18] N-heterocycles,[19–21] olefins,[22–24] poly-arenes,[25] alkynes,[26] and most recently, ketones and aldehydes,[27,28] have been achieved using main group molecules and H_2. Efforts to extend FLP systems to encompass bases featuring oxygen donors had found limited success due to the high oxophilicity of the electrophilic boranes needed for H_2 activation, at the time when this research was conducted. Early reports from the Stephan and Erker laboratories showed that

H_2-activated phosphine-borane systems could deliver hydride to benzaldehyde, forming the corresponding alkoxide-bound phosphonium borate zwitterions;[14,29] subsequent work by Rieger and Repo showed analogous chemistry using bulky nitrogen bases (Scheme 5.1).[30] Nonetheless, computational investigations by the groups of Privalov[31] and Wang[32] suggested that ketone reductions using $B(C_6F_5)_3$ as a catalyst are energetically viable.

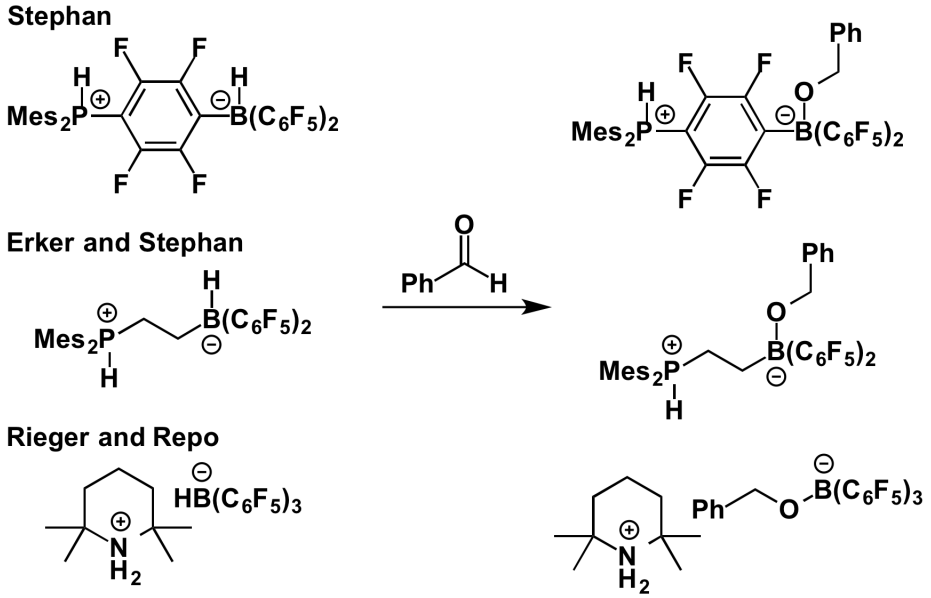

Scheme 5.1 – Examples of FLP borohydride reductions of benzaldehyde.

Repo and co-workers reported the first experimental evidence that carbonyl compounds could behave as Lewis bases capable of FLP H_2 activation.[33] Using benzophenone in combination with $B(C_6F_5)_3$ and H_2 in d_8-toluene, they observed reduction of the substrate to diphenyl(tolyl)methanes, as well as loss of HC_6F_5/DC_6F_5 and $HOB(C_6F_5)_2/DOB(C_6F_5)_2$ (Scheme 5.2). We were interested in exploring FLP carbonyl chemistry further and, in particular, whether alkyl-substituted ketones and aldehydes would behave in an analogous fashion to the aryl-substituted ketones and aldehydes reported by Repo, which underwent deoxygenation reactions. This chapter will disclose our efforts towards reducing alkyl-substituted carbonyl substrates using FLPs, as well has the syntheses of new bulky, electrophilic boranes and their behaviour in FLP chemistry.

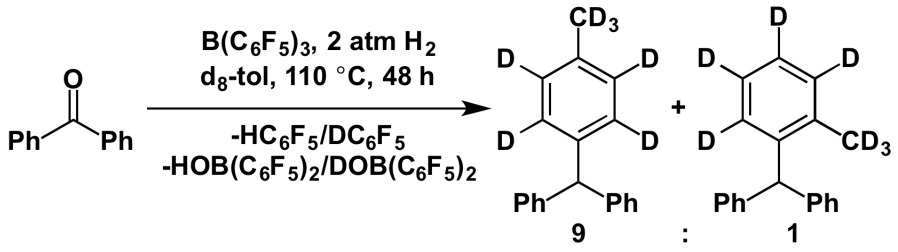

Scheme 5.2 – Initial report of the FLP-mediated reduction of carbonyl compounds.

5.2 Results and Discussion

5.2.1 Initial Reaction Screening

Initially, one equivalent of $B(C_6F_5)_3$ was combined with 4-heptanone **5-1a** in toluene. An adduct was formed at room temperature, as evidenced by a broad singlet in the ^{11}B NMR spectrum at 9.3 ppm. This mixture was heated to 110 °C under 4 atm of H_2 for 24 hours. Complete conversion of the ketone to a new boron-containing product **5-2a** with the concurrent formation of HC_6F_5 was observed. Evaporation of the volatiles followed by purification yielded product **5-2a**, which resonated as a broad singlet at 39.3 ppm in the ^{11}B NMR spectrum, and as 3 peaks at −132.3, −150.8, and −161.9 ppm in the ^{19}F NMR spectrum. These data suggested that a three-coordinate boron species had formed. The ^{1}H NMR spectrum of **5-2a**, in addition to the expected aliphatic resonances, exhibited a quintet integrating to 1H at 4.20 ppm. Collectively, these data are in agreement with previous reports of C_6F_5-substituted borinic esters[34–36] and support the formulation of product **5-2a** as $Pr_2CH–OB(C_6F_5)_2$ (Scheme 5.3). This assignment was further reinforced by treatment of **5-1a** with Piers' borane, $HB(C_6F_5)_2$;[37] this hydroboration reaction produced the same product, **5-2a**. The product **5-2a** is not sufficiently Lewis acidic to activate H_2 in conjunction with the ketone Lewis base, making this a stoichiometric reduction. The reactivity of dialkyl ketone **5-1a** stands in contrast to the previously reported FLP hydrogenation chemistry of aryl-substituted ketones, where the C−O bond is cleaved to afford a mixture of Friedel-Crafts arylation products.[33]

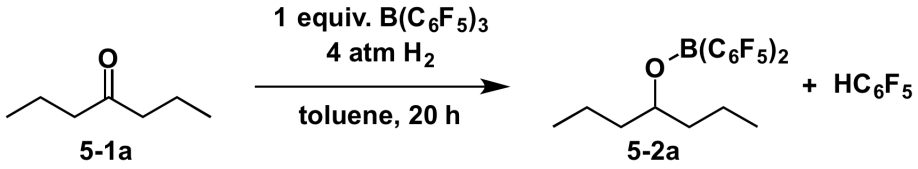

Scheme 5.3 – Reduction of **5-1a** to borinic ester **5-2a** via FLP hydrogen activation.

5.2.2 Reaction Scope

In an effort to probe the generality of this transformation, the reaction conditions were applied to a variety of alkyl-substituted ketones (Table 5.1). Diethyl ketone (**5-1b**) and acetone (**5-1c**) were found to react with $B(C_6F_5)_3$ and H_2 to produce the corresponding borinic esters **5-2b** and **5-2c**, respectively, and were isolated in high yields. Ketones bearing β-substituents were reduced (**5-1d**), and cyclic ketones were also shown to undergo the analogous reduction (**5-1e**). Substrates with one branched substituent (**5-1f** and **5-1g**) were tolerated, however for substrate **5-1h**, bearing α and α' substituents, the hydrogenation was prohibitively slow. Similarly, reduction of di-*tert*-butyl ketone (**5-1i**) was not observed. These latter observations were attributed to steric inhibition and are in accord with previous hydrogenation attempts by Repo.[33] In further support of the steric inhibition, it is interesting to note that the combination of **5-1i** with $B(C_6F_5)_3$ at room temperature does not result in adduct formation, as evidenced by the resonance at 60.5 ppm in the ^{11}B NMR spectrum. With the exception of the sterically crowded systems, reductive formation of borinic esters proved to be quite general for dialkyl ketones, proceeding to full conversion with high isolated yields.

Table 5.1 – Scope of ketone reduction using $B(C_6F_5)_3$ and H_2. NMR yields are reported, with representative isolated yields in parentheses. xx = not determined.

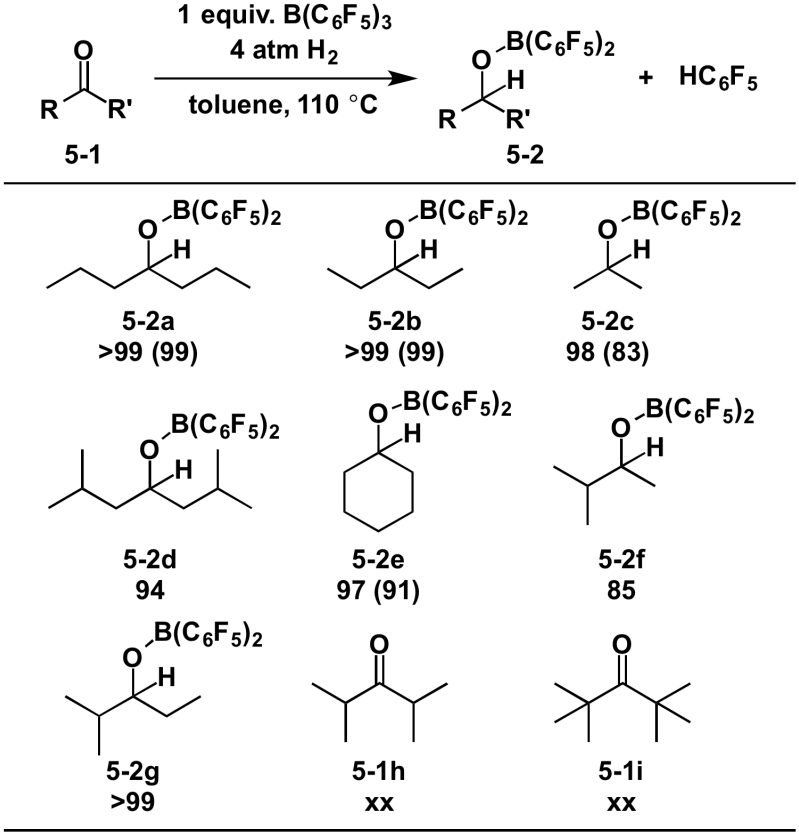

5.2.3 Mechanistic Investigations

It is evident that elevated temperatures encourage dissociation of the ketone–$B(C_6F_5)_3$ adduct. The resulting Lewis acid/base combination of $B(C_6F_5)_3$ and ketone can then act as an FLP, enabling heterolytic H_2 cleavage and generating an oxonium borohydride species of the form $[R_2C{=}O{-}H][H{-}B(C_6F_5)_3]$. Recent studies have discovered other FLP systems comprised of boranes and oxygen-based Lewis bases: the combination of $B(C_6F_5)_3$ and Et_2O was shown to activate H_2 and effect the catalytic hydrogenation of olefins,[24] and Ashley and co-workers extended this chemistry to a series of perchloroarylboranes, $B(C_6Cl_5)_n(C_6F_5)_{3-n}$ (where n = 0–3), which activate H_2 in combination with THF.[38] For the FLP reduction of carbonyl compounds, two reaction pathways were envisioned following activation of H_2 by the ketone/borane FLP (Scheme 5.4). Delivery of the hydride to the carbonyl carbon would afford the alcohol and $B(C_6F_5)_3$ *in situ*. However, $B(C_6F_5)_3$ is not stable to alcohol functionalities at the elevated temperature required to initiate the reaction with H_2, and thus subsequent protonation of a $-C_6F_5$

group on $B(C_6F_5)_3$ would generate the borinic ester (Scheme 5.4, pathway 1) with loss of HC_6F_5. An alternate pathway (Scheme 5.4, pathway 2) involves the direct protonation of a -C_6F_5 group from the anion [$HB(C_6F_5)_3$] by the acidic cation [R_2C=O–H], which would liberate HC_6F_5, ketone, and $HB(C_6F_5)_2$. Rapid ketone hydroboration would generate the borinic ester.[39]

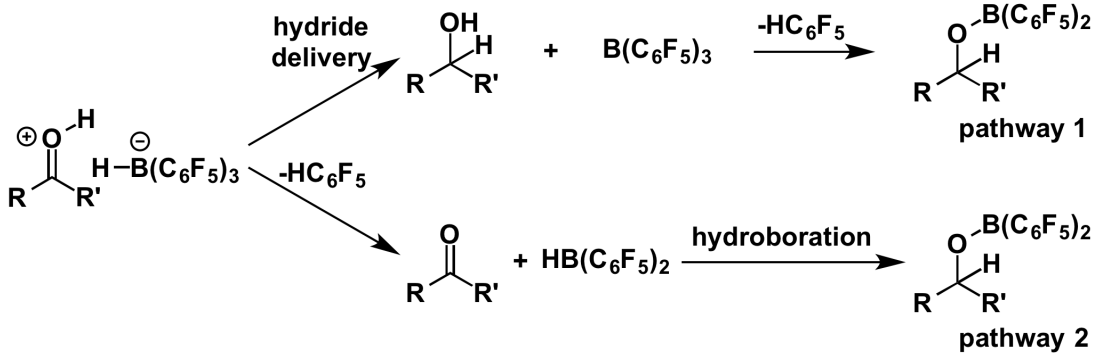

Scheme 5.4 – Possible reaction pathways for the generation of borinic esters from ketone, $B(C_6F_5)_3$, and H_2.

The mechanism was investigated by using cyclohex-2-en-1-one **5-1j** as a substrate (Scheme 5.5). If the reaction proceeded via pathway 1 (Scheme 5.4), hydride delivery would be observed after initial H_2 activation. Hydride, being a soft nucleophile, was anticipated to undergo conjugate 1,4-addition to the protonated enone. This would generate cyclohexanone in its enol form, which would then rapidly tautomerize to its keto form. The activation of a second equivalent of H_2, followed by a second hydride delivery would generate cyclohexyl borinic ester **5-2e**. If $HB(C_6F_5)_2$ is generated *in situ* (Scheme 5.4, pathway 2), the ketone was anticipated to undergo hydroboration, leaving the alkene functionality intact. Indeed, addition of $HB(C_6F_5)_2$ to **5-1j** resulted in an immediate reaction at room temperature, and in addition to the ^{11}B NMR resonance at 39.8 ppm and the three resonances at −132.7, −149.3, and −161.0 ppm in the ^{19}F NMR spectrum, olefinic resonances at 5.71 and 5.60 ppm in the ^{1}H NMR spectrum were observed (Figure 5.2b). These data led us to assign the new product as borinic ester **5-2j**. Heating this material in the presence or absence of H_2 led to degradation, and **5-2e** was not observed by multinuclear NMR spectroscopy. In contrast, treatment of **5-1j** with one equivalent of $B(C_6F_5)_3$ and H_2 results in reduction to borinic ester **5-2e**, where the enone is fully reduced (Figure 5.2a), supporting the mechanistic postulate of pathway 1. It is noteworthy that this was further

supported by the formation of borinic ester **5-2e** via direct treatment of $B(C_6F_5)_3$ with cyclohexanol in toluene at 110 °C.

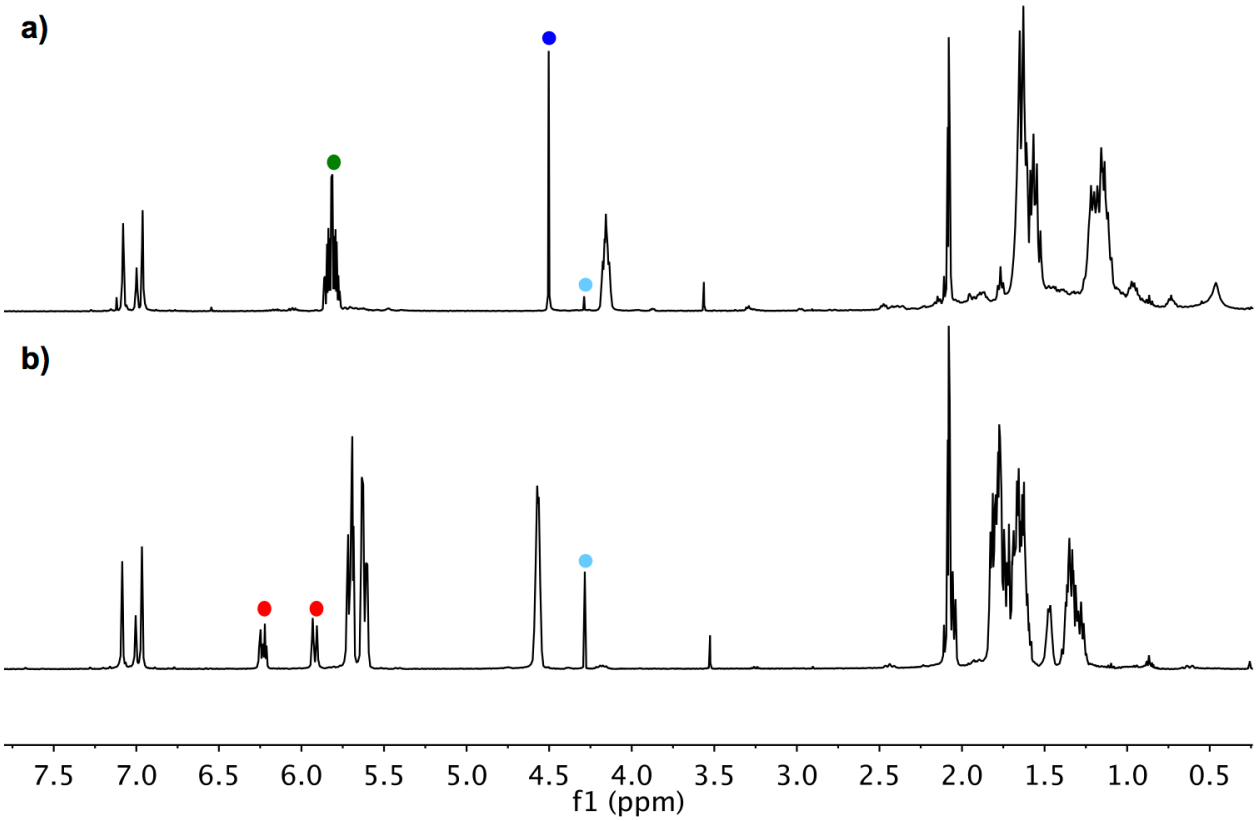

Figure 5.2 – ^{1}H NMR spectra (400 MHz, 298 K, d_8-toluene) of a) the reaction mixture for the $B(C_6F_5)_3$-mediated hydrogenation of **5-1j** yielding **5-2e**, and b) the hydroboration of **5-1j** yielding **5-2j**. Green = HC_6F_5; royal blue = H_2; light blue = DCM; red = unreacted **5-1j**.

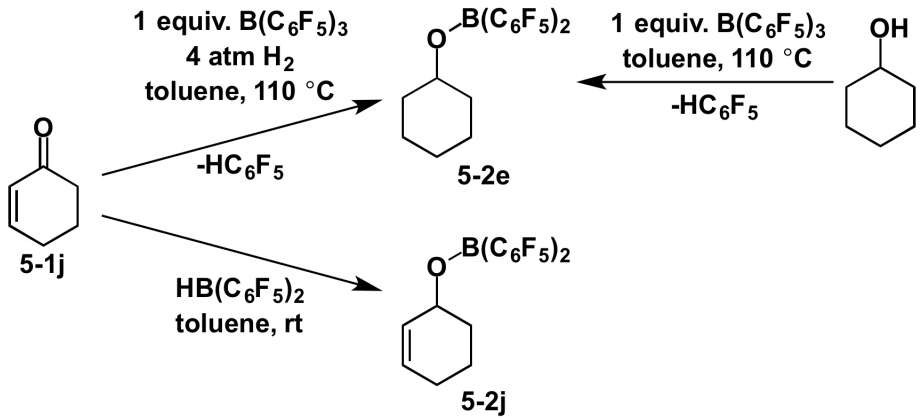

Scheme 5.5 – Hydrogenation and hydroboration of α,β-unsaturated ketone **5-1j**.

5.2.4 FLP Reductions of Aldehydes

Aliphatic aldehydes were also evaluated as substrates under similar reduction conditions. In general, complex mixtures of products were generated upon treating a variety of aldehydes with $B(C_6F_5)_3$ and H_2 in toluene at 110 °C. Efforts to isolate or purify the reaction mixtures were unsuccessful. However, in the case of aldehyde Et_2CHCHO **5-3a**, which bears an α-substituent, loss of HC_6F_5 and clean conversion to a new product **5-4a** was evident from the peak at 39.8 ppm in the ^{11}B NMR spectrum, and peaks at −131.9, −148.1, and −161.0 ppm in the ^{19}F NMR spectrum. The ^{1}H NMR spectrum of **5-4a**, while similar to the anticipated borinic ester, did not have the expected resonance in the 3.5–4 ppm range, and instead showed a new singlet at 6.37 ppm. Collectively, these data support the formulation of **5-4a** as the boron enolate product $Et_2C{=}CH(OB(C_6F_5)_2)$. In this instance, the substrate was not hydrogenated, but rather **5-3a** reacts in its enol form with $B(C_6F_5)_3$ at elevated temperature to effect the formation of **5-4a** and liberate HC_6F_5 (Scheme 5.6). Indeed, when the reaction was repeated in the absence of H_2, the same product **5-4a** was observed. Pleasingly, this reactivity is also observed with the less Lewis acidic borane BPh_3, generating enolate **5-4b** and benzene. It is interesting to note that this enol-type reactivity was not observed for any α-substituted ketones. In addition, these reactions of enols with boranes is analogous to the latter step in the mechanism of the FLP reduction of ketones described above, and further supports the proposed reaction pathway (Scheme 5.4, pathway 1).

Products **5-4a** and **5-4b** were amenable to FLP-catalyzed hydrogenation (Scheme 5.6). Using reaction conditions reported for the reduction of silyl enol ethers,[17] the substrates were treated with 20 mol% $B(C_6F_5)_3$ and the bidentate phosphine $C_{10}H_6(PPh_2)_2$ under 4 atm of H_2 at 110 °C to yield the borinic esters **5-5a** and **5-5b**, respectively.

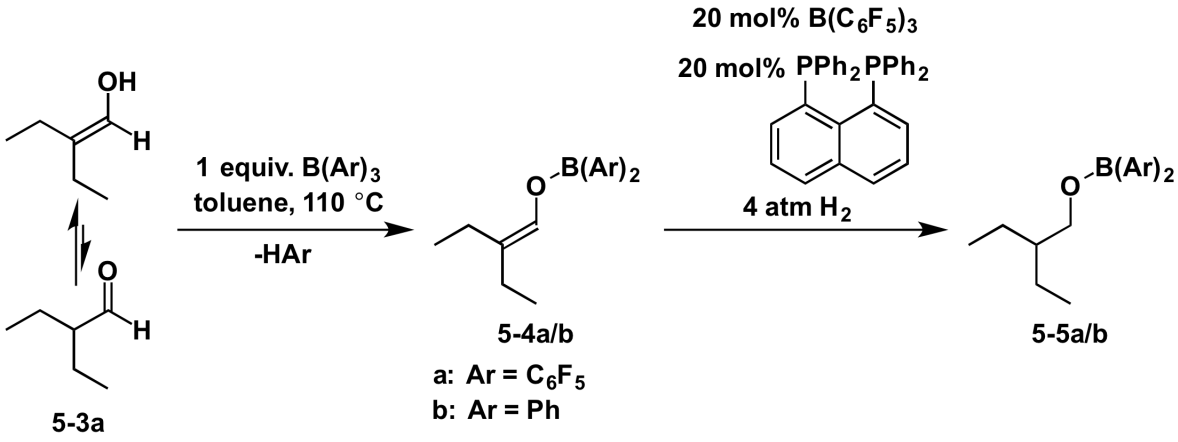

Scheme 5.6 – Synthesis of boron enolates **5-4a** and **5-4b**, and subsequent reduction to borinic esters **5-5a** and **5-5b**.

5.2.5 New Electrophilic Boranes – Efforts towards Catalytic Ketone Reduction

Catalytic ketone hydrogenation using an FLP has recently been achieved, however before the seminal reports by the Stephan[27] and Ashley[28] research groups, there was interest in modifying the existing FLP ketone hydrogenation methods to promote catalysis. Experimental observations suggested that *in situ*-generated alcohol reacts irreversibly with $B(C_6F_5)_3$, generating borinic esters which were not sufficiently Lewis acidic to activate H_2, which renders the method stoichiometric (*vide supra*). The synthesis of new boranes was undertaken with the hope that they would be sufficiently Lewis acidic to enable H_2 activation, but would be more sterically encumbered than $B(C_6F_5)_3$ to discourage B–O bond formation.

Inspiration was drawn from the works of Wang and co-workers, who had exploited fMes-substituted boranes in FLP chemistry.[40–43] The preparation of $fMes_2BPh$ **5-6** was achieved by treating $fMes_2BF$[44] with PhLi (Scheme 5.7), and the new compound was crystallographically characterized (Figure 5.3). Unfortunately, the borane **5-6** was proven too sterically hindered to activate H_2; no interaction was observed when it was combined with P(*t*-Bu)$_3$, suggesting the formation of an FLP, however exposure of this mixture to 4 atm of H_2 did not result in any observable H–H cleavage. N-benzylidene-*tert*-butylamine was also treated with a catalytic amount of **5-6**, with and without DABCO,[45] and no hydrogenation was observed under 4 atm of H_2, even after 24 hours at 110 °C. It was therefore unsurprising that **5-6** did not activate H_2 with ketones to effect carbonyl hydrogenation.

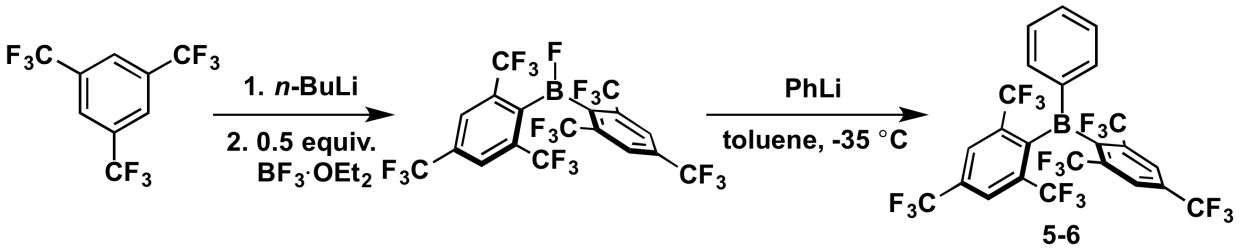

Scheme 5.7 – Synthesis of **5-6** from $fMes_2BF$.

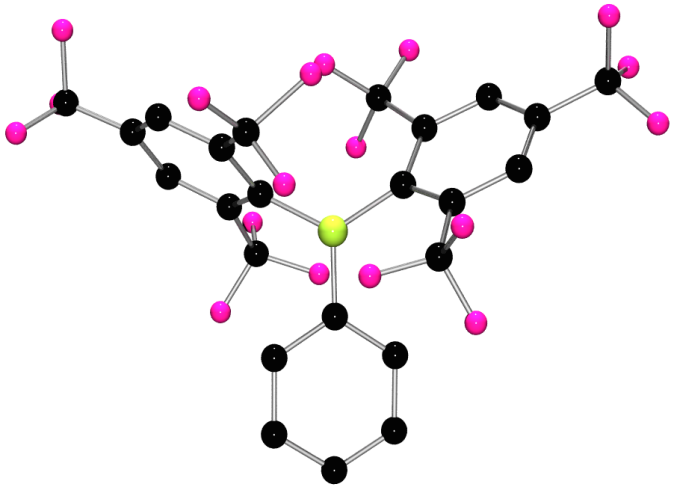

Figure 5.3 – POV-ray depiction of **5-6**, with H atoms omitted for clarity. C: black; B: yellow-green; F: pink.

Soós' borane $MesB(C_6F_5)_2$ had been demonstrated to be catalytically active (when combined with DABCO or quinuclidine) for the hydrogenation of imines, enamines, and enones.[45] The fMes analogue of Soós' borane, $fMesB(C_6F_5)_2$ **5-7**, was synthesized by treating Li(fMes) with $ClB(C_6F_5)_2$ in Et_2O. The solid state structure of **5-7** is shown in Figure 5.4. **5-7** was catalytically inactive for the hydrogenation of imines or ketones, independently or in combination with DABCO. It was also unable to cleave H_2 in concert with P(*t*-Bu)$_3$. This led to the conclusion that fMes-substituted boranes are highly sensitive to the steric constraints about the boron centre; $fMes_2BH$ is capable of activating small molecules, but $fMes_2BPh$ is not. Likewise, $MesB(C_6F_5)_2$ effects FLP-catalyzed reductions, but $fMesB(C_6F_5)_2$ does not. The close contacts between the boron centre and -CF_3 groups were noted in the solid state structures of both **5-6** and **5-7**: there is a B···F distance of 2.723(3) Å in **5-6**, and 2.523(3) Å in **5-7** (sum of the van der Waals radii = 3.37),[46] which could be preventing coordination and small molecule activation.

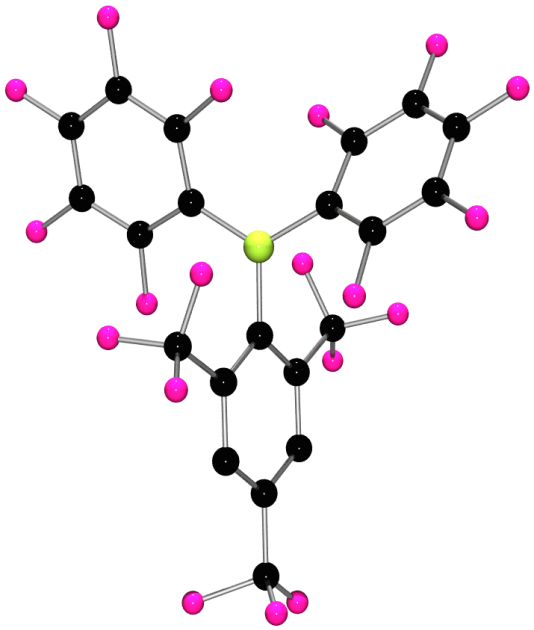

Figure 5.4 – POV-ray depiction of **5-7**, with H atoms omitted for clarity. C: black; B: yellow-green; F: pink.

5.3 Conclusions

A range of aliphatic ketones activate H_2 in the presence of $B(C_6F_5)_3$ and undergo stoichiometric reduction to give the corresponding borinic ester products and HC_6F_5. This observation stands in contrast to earlier reports of FLP hydrogenations of aryl-substituted ketones where the C−O bond is cleaved.[33] Reductions of linear aliphatic aldehydes led to complex mixtures, although **5-3a**, bearing an α-substituent, was shown to react through its enol form with $B(C_6F_5)_3$ and BPh_3, affording boron enolate products, which were amenable to further FLP-catalyzed hydrogenation. The H_2 activation achieved by the combination of aliphatic ketones and an electrophilic borane is proposed to transiently form the corresponding alcohol, which reacts further with $B(C_6F_5)_3$ to cleave a B–C bond and form a B–O bond, providing a new approach to borinic esters. Two new fMes-substituted boranes were prepared and crystallographically characterized, however they were both inactive for FLP cleavage of H_2 with phosphine Lewis bases, and were unable to catalyze the hydrogenation of ketones or imines.

5.4 Experimental Details

5.4.1 General Considerations

All reactions and workup procedures were performed under an inert atmosphere of dry N_2 using

standard Schlenk techniques or a glovebox (MBraun glovebox equipped with a −35 °C freezer). Pentane, toluene, and Et_2O (Aldrich) were dried using an Innovative Technologies solvent system. Deuterated solvents (CD_2Cl_2, d_8-toluene, C_6D_5Br) were purchased from Cambridge Isotope Laboratories, Inc. and stored over activated 4 Å molecular sieves prior to use. Ketones and aldehydes were purchased from either Sigma-Aldrich or Alfa Aesar, *n*-BuLi solution, PhLi solution, and $BF_3{\cdot}OEt_2$ were purchased from Sigma-Aldrich, $B(C_6F_5)_3$ was purchased from Boulder Scientific, fMes was purchased from TCI America, and BPh_3 was purchased from Strem. All were used without further purification. $C_{10}H_6(PPh_2)_2$,[47] $fMes_2BF$,[44] and $ClB(C_6F_5)_2$[48] were prepared according to literature procedures. Hydrogen gas (Grade 5.0) was obtained from Linde and purified through a Matheson Model 450B or Matheson Nanochem WeldAssureTM gas purifier.

NMR spectra were obtained on a Bruker Avance III 400 MHz, Varian Mercury 300 MHz, Agilent DD2 600 MHz, or Agilent DD2 500 MHz spectrometer. Spectra were referenced to residual solvent of d_8-toluene (^1H = 2.08 for methyl; ^{13}C = 20.40 for CH_3), CD_2Cl_2 (^1H = 5.32, ^{13}C = 54.0), C_6D_5Br (^1H = 7.28 ppm for meta proton; ^{13}C = 122.4 ppm for ipso carbon), or externally (^{19}F: $CFCl_3$, ^{11}B: $(Et_2O)BF_3$, ^{31}P: 85% H_3PO_4). Chemical shifts are listed in ppm and coupling constants are listed in Hz. NMR assignments are supported by additional 2D experiments. High-resolution mass spectrometry (HRMS) was performed in house.

5.4.2 Syntheses and Characterizations

In general, borinic esters and boron enolates synthesized for this communication were highly prone to decomposition upon isolation. Boron enolates have been characterized in solution, and attempts to cleanly isolate borinic ester **5-5b** were unsuccessful (*vide infra*). These materials are stable in their crude reaction mixture for days; the products that were successfully isolated were stored in a −35 °C freezer. These products are sensitive to air and moisture, and were unstable in dichloromethane (with the exception of **5-2a**).

General Synthesis – Ketone Hydrogenation (NMR scale): The ketone (0.05 mmol), $B(C_6F_5)_3$ (0.05 mmol), and 1,3,5-tri-*tert*-butylbenzene (internal standard, 0.02-0.03 mmol) were combined in 0.4 mL d_8-toluene or C_6D_5Br and transferred to a J-Young NMR tube. The tube was degassed by three freeze-pump-thaw cycles on a vacuum/H_2 Schlenk line and filled with H_2 (4 atm) at −196 °C. The tube was then heated to 110 °C until the reaction was complete, as evidenced by ^1H, ^{19}F, and ^{11}B NMR spectroscopy. NMR yields were calculated using ^1H integration and a

known amount of internal standard (1,3,5-tri-*tert*-butylbenzene). For isolation, the reaction was repeated without internal standard and, once the reaction was complete, the solvent was removed *in vacuo*, the resulting material was dissolved in pentane and filtered over Celite. The filtrate was concentrated, yielding the borinic ester product.

General Synthesis – Ketone Hydrogenation (large scale): The ketone (0.5 mmol) was quantitatively transferred to a vial containing $B(C_6F_5)_3$ (0.5 mmol) with 1 mL toluene. The resulting solution was quantitatively transferred to a 50 mL Schlenk bomb equipped with a magnetic stir bar using 3 mL toluene. The reaction vessel was degassed by three freeze-pump-thaw cycles on a vacuum/H_2 Schlenk line and filled with H_2 (4 atm) at −196 °C. The reaction was heated to 110 °C for the required reaction time, after which the volatiles were removed *in vacuo* and the resulting material was dissolved in minimal pentane and filtered over Celite. The solution was concentrated, yielding the desired products as colourless or faint yellow oils.

General Synthesis – Boron Enolate Synthesis: The aldehyde (0.05 mmol) and borane (0.05 mmol) were combined in 0.5 mL d_8-toluene or C_6D_5Br and heated to 110 °C until the reaction was complete, as evidenced by ^1H, ^{19}F (where applicable), and ^{11}B NMR spectroscopy. Isolation attempts were unsuccessful, as the materials decomposed upon concentration. They are therefore characterized from the crude reaction mixtures.

General Synthesis – Boron Enolate Hydrogenation: A crude reaction mixture containing **5-4a** or **5-4b** was added to a vial containing $B(C_6F_5)_3$ (0.01 mmol). The resulting solution was combined with $C_{10}H_6(PPh_2)_2$ (0.01 mmol) and the reaction was transferred to a J-Young NMR tube. The tube was degassed by three freeze-pump-thaw cycles on a vacuum/H_2 Schlenk line and filled with H_2 (4 atm) at −196 °C. The tube was then heated to 110 °C until the reaction was complete, as evidenced by ^1H, ^{19}F, ^{31}P, and ^{11}B NMR spectroscopy. NMR yields were calculated using ^1H integration and a known amount of internal standard (1,3,5-tri-*tert*-butylbenzene). The reaction was repeated without internal standard, and the reactions (upon completion) were concentrated, dissolved in minimal pentane and filtered over Celite to remove the phosphine. Successive washings with cold pentane yielded the pure product **5-5a** or **5-5b**.

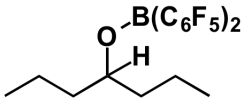

5-2a: Reaction time: 24 h. Isolated as a faint yellow oil (228 mg, 99%).

^{1}H NMR (400 MHz, 298 K, CD_2Cl_2): δ 4.21 (quintet, $^{3}J_{HH}$ = 6.0 Hz, 1H, OCH), 1.70–1.55 (m, 4H, 2xCH_2), 1.47–1.36 (m, 2H, CH_2), 1.33–1.22 (m, 2H, CH_2), 0.88 (t, $^{3}J_{HH}$ = 7.3 Hz, 6H, CH_3).

^{19}F NMR (377 MHz, 298 K, CD_2Cl_2): δ −132.3 (dd, $^{3}J_{FF}$ = 23 Hz, $^{4}J_{FF}$ = 10 Hz, 2F, *o*-C_6F_5), −150.8 (t, $^{3}J_{FF}$ = 20 Hz, 1F, *p*-C_6F_5), −161.8 to −162.0 (m, 2F, *m*-C_6F_5).

^{11}B NMR (128 MHZ, 298 K, CD_2Cl_2): δ 39.3 (br s).

^{13}C{^{1}H} NMR (101 MHz, 298 K, CD_2Cl_2), partial: δ 148.0 (dm, $^{1}J_{CF}$ ~ 249 Hz, C_6F_5), 138.0 (dm, $^{1}J_{CF}$ ~ 254 Hz, C_6F_5), 82.5 (s, OCH), 38.6 (s, CH_2), 18.7 (s, CH_2), 14.3 (s, CH_3).

HRMS (EI) calcd for $C_{19}H_{15}BF_{10}O$ 460.1056, found 460.1067.

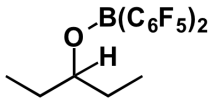

5-2b: Reaction time: 24 h. Isolated as a colourless oil (213 mg, 99%).

^{1}H NMR (300 MHz, 298 K, C_6D_5Br): δ 3.97–3.89 (m, 1H, OCH), 1.64–1.42 (m, 4H, 2xCH_2), 0.83 (t, $^{3}J_{HH}$ = 7.4 Hz, 6H, 2xCH_3).

^{19}F NMR (282 MHz, 298 K, C_6D_5Br): δ −131.4 (dd, $^{3}J_{FF}$ = 24 Hz, $^{4}J_{FF}$ = 10 Hz, 2F, *o*-C_6F_5), −149.0 (t, $^{3}J_{FF}$ = 21 Hz, 1F, *p*-C_6F_5), −160.1 to −160.3 (m, 2F, *m*-C_6F_5).

^{11}B NMR (128 MHz, 298 K, C_6D_5Br): δ 39.2 (br s).

^{13}C{^{1}H} NMR (126 MHz, 298 K, d_8-tol), partial: δ 147.7 (dm, $^{1}J_{CF}$ ~ 245 Hz, C_6F_5), 143.0 (dm, $^{1}J_{CF}$ ~ 256 Hz, C_6F_5), 137.6 (dm, $^{1}J_{CF}$ ~ 255 Hz, C_6F_5), 84.5 (s, OCH), 28.7 (s, CH_2), 9.3 (s, CH_3).

HRMS (EI) calcd for $C_{17}H_{11}BF_{10}O$ 432.0743, found 432.0727.

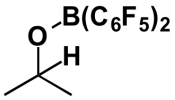

5-2c: Reaction time: 21 h. Isolated as a colourless oil (168 mg, 83%).

^{1}H NMR (400 MHz, 298 K, d_8-tol): δ 4.17 (septet, $^{3}J_{HH}$ = 6.0 Hz, 1H, OCH), 1.09 (d, $^{3}J_{HH}$ = 6.0 Hz, 6H, 2xCH_3).

^{19}F NMR (377 MHz, 298 K, d_8-tol): δ −133.0 (dd, $^{3}J_{FF}$ = 24 Hz, $^{4}J_{FF}$ = 9 Hz, 2F, *o*-C_6F_5), −149.4 (br t, $^{3}J_{FF}$ = 20 Hz, 1F, *p*-C_6F_5), −161.1 (br s, 2F, *m*-C_6F_5).

^{11}B NMR (128 MHz, 298 K, d_8-tol): δ 39.3 (br s).

^{13}C{^{1}H} NMR (100 MHz, 298 K, d_8-tol), partial: δ 74.6 (s, OCH), 24.1 (s, 2xCH_3).

HRMS (EI) calcd for $C_{15}H_7BF_{10}O$ 404.0430, found 404.0438.

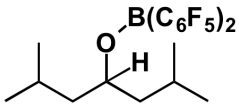

5-2d: Reaction time: 120 h. NMR yield 94%.

^{1}H NMR (400 MHz, 298 K, d_8-tol): δ 4.26 (quintet, $^3J_{HH}$ = 6.2 Hz, 1H, OCH), 1.68–1.51 (m, 4H, 2xCH_2), 1.38–1.31 (m, 2H, 2xCH), 0.79 (d, $^3J_{HH}$ = 6.5 Hz, 6H, 2xCH_3), 0.72 (d, $^3J_{HH}$ = 6.4 Hz, 6H, 2xCH_3).

^{19}F NMR (377 MHz, 298 K, d_8-tol): δ −132.2 (br s, 2F, *o*-C_6F_5), −149.3 (br s, 1F, *p*-C_6F_5), −161.1 (br s, 2F, *m*-C_6F_5).

^{11}B NMR (128 MHz, 298 K, d_8-tol): δ 39.3 (br s).

^{13}C{^{1}H} NMR (126 MHz, 298 K, d_8-tol), partial: δ 147.8 (dm, $^1J_{CF}$ ~ 240 Hz, C_6F_5), 143.1 (dm, $^1J_{CF}$ ~ 259 Hz, C_6F_5), 137.7 (dm, $^1J_{CF}$ ~ 255 Hz, C_6F_5), 79.2 (s, OCH), 45.7 (s, CH_2), 24.5 (s, CH), 22.8 (s, CH_3), 22.4 (s, CH_3).

HRMS (EI) calcd for $C_{21}H_{19}BF_{10}O$ 488.1369, found 488.1364.

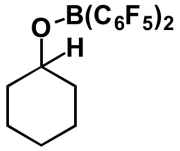

5-2e: Reaction time: 24 h. NMR yield: 97%. Isolated as a faint yellow oil (from cyclohexanone: 201 mg, 91%; from cyclohexenone: 208 mg, 94%).

^{1}H NMR (400 MHz, 298 K, C_6D_5Br): δ 4.26 (br, 1H, OCH), 1.77–1.58 (m, 6H, Cy), 1.33–1.21 (m, 4H, Cy).

^{19}F NMR (377 MHz, 298 K, C_6D_5Br): δ −131.9 (dd, $^3J_{FF}$ = 24 Hz, $^4J_{FF}$ = 10 Hz, 2F, *o*-C_6F_5), −149.5 (br s, 1F, *p*-C_6F_5), −160.7 (br s, 2F, *m*-C_6F_5).

^{11}B NMR (128 MHz, 298 K, C_6D_5Br): δ 39.1 (br s).

^{13}C{^{1}H} NMR (126 MHz, 298 K, C_6D_5Br), partial: δ 79.1 (s, OCH), 34.1 (s, CH_2), 25.3 (s, CH_2), 23.0 (s, CH_2).

HRMS (EI) calcd for $C_{18}H_{11}BF_{10}O$ 444.0743, found 444.0739.

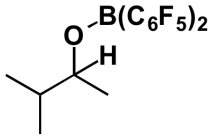

5-2f: Reaction time: 65 h. NMR yield: 85%.

^{1}H NMR (400 MHz, 298 K, d_8-tol): δ 3.92–3.86 (m, 1H, OCH), 1.58–1.47 (m, 1H, *i*-Pr CH), 1.12 (d, $^{3}J_{HH}$ = 6.3 Hz, 3H, OCH-C$\underline{H}_3$), 0.88 (d, $^{3}J_{HH}$ = 6.7 Hz, 3H, *i*-Pr CH_3), 0.78 (d, $^{3}J_{HH}$ = 6.8 Hz, 3H, *i*-Pr CH_3).

^{19}F NMR (377 MHz, 298 K, d_8-tol): δ −132.6 (dd, $^{3}J_{FF}$ = 24 Hz, $^{4}J_{FF}$ = 9 Hz, 2F, *o*-C_6F_5), −149.4 (br s, 1F, *p*-C_6F_5), −161.1 (br s, 2F, *m*-C_6F_5).

^{11}B NMR (128 MHz, 298 K, d_8-tol): δ 39.4 (br s).

^{13}C{^{1}H} NMR (101 MHz, 298 K, d_8-tol), partial: δ 147.8 (dm, $^{1}J_{CF}$ ~ 248 Hz, C_6F_5), 137.7 (dm, $^{1}J_{CF}$ ~ 256 Hz, C_6F_5), 82.9 (s, OCH), 34.3 (s, *i*-Pr CH), 19.8 (s, OCH-$\underline{C}H_3$), 18.4 (s, *i*-Pr CH_3), 16.7 (s, *i*-Pr CH_3).

HRMS (EI) calcd for $C_{17}H_{11}BF_{10}O$ 432.0743, found 432.0750.

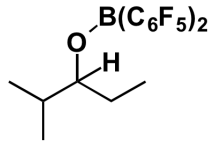

5-2g: Reaction time: 68 h. NMR yield: >99%.

^{1}H NMR (300 MHz, 298 K, d_8-tol): δ 3.74 (dt, $^{3}J_{HH}$ = 8.4, 4.7 Hz, 1H, OCH), 1.74–1.34 (m, 3H, CH_2 and *i*-Pr CH), 0.86 (d, $^{3}J_{HH}$ = 6.8 Hz, 3H, CH_3), 0.82–0.77 (m, 6H, 2xCH_3).

^{19}F NMR (377 MHz, 298 K, CD_2Cl_2): δ −132.0 (dd, $^{3}J_{FF}$ = 24 Hz, $^{4}J_{FF}$ = 9 Hz, 2F, *o*-C_6F_5), −150.9 (t, $^{3}J_{FF}$ = 21 Hz, 1F, *p*-C_6F_5), −161.9 to −162.1 (m, 2F, *m*-C_6F_5).

^{11}B NMR (96 MHz, 298 K, d_8-tol): δ 39.5 (br s).

^{13}C{^{1}H} NMR (100 MHz, 298 K, d_8-tol), partial: δ 87.9 (s, OCH), 32.2 (s, *i*-Pr CH), 26.0 (s, CH_2), 18.3 (s, CH_3), 16.8 (s, CH_3), 9.5 (s, CH_3).

HRMS (EI) calcd for $C_{18}H_{13}BF_{10}O$ 446.0900, found 446.0903.

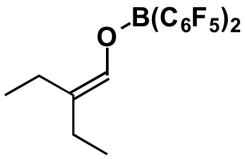

5-4a: Reaction time: 24 h. Characterized from the crude reaction mixture with HC_6F_5.

^{1}H NMR (400 MHz, 298 K, d_8-tol): δ 6.37 (s, 1H, alkene CH), 2.29 (q, $^3J_{HH}$ = 7.6 Hz, 2H, CH_2), 1.77 (qd, $^3J_{HH}$ = 7.5 Hz, $^4J_{HH}$ = 1.4 Hz, 2H, CH_2), 1.02 (t, $^3J_{HH}$ = 7.6 Hz, 3H, CH_3), 0.82 (t, $^3J_{HH}$ = 7.5 Hz, 3H, CH_3). HC_6F_5: δ 5.86-5.77 (m, 1H).

^{19}F NMR (376 MHz, 298 K, d_8-tol): δ −131.9 (d, $^3J_{FF}$ = 23 Hz, 2F, *o*-C_6F_5), −148.1 (t, $^3J_{FF}$ = 21 Hz, 1F, *p*-C_6F_5), −160.9 to −161.0 (m, 2F, *m*-C_6F_5). HC_6F_5: δ −139.2 to −139.3 (m, 2F), −154.3 (t, $^3J_{FF}$ = 20 Hz, 1F), −162.4 to −162.6 (m, 2F).

^{11}B NMR (128 MHz, 298 K, d_8-tol): δ 39.8 (br s).

^{13}C{^{1}H} NMR (100 MHz, 298 K, d_8-tol), partial: δ 148.3 (dm, $^1J_{CF}$ ~ 245 Hz, C_6F_5), 143.6 (dm, $^1J_{CF}$ ~ 254 Hz, C_6F_5), 133.6 (dm, $^1J_{CF}$ ~ 251 Hz, C_6F_5), 133.5 (s, alkene CH), 133.5 (s, quat. C), 24.3 (s, CH_2), 20.9 (s, CH_2), 12.7 (s, CH_3), 12.4 (s, CH_3). HC_6F_5, partial: δ 100.5 (td, $^2J_{CF}$ = 23 Hz, $^3J_{CF}$ = 4 Hz, CH).

HRMS (EI) calcd for $C_{18}H_{11}BF_{10}O$ 444.0743, found 444.0730.

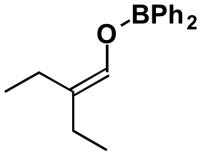

5-4b: Reaction time: 24 h. Characterized from the crude reaction mixture with C_6H_6.

^{1}H NMR (400 MHz, 298 K, d_8-tol): δ 7.73–7.71 (m, 4H, *o*-CH), 7.24–7.19 (m, 6H, *m*-CH and *p*-CH), 6.61 (br t, $^4J_{HH}$ = 1.2 Hz, 1H, alkene CH), 2.41 (q, $^3J_{HH}$ = 7.6 Hz, 2H, CH_2), 1.80 (qd, $^3J_{HH}$ = 7.4 Hz, $^4J_{HH}$ = 1.2 Hz, 2H, CH_2), 1.10 (t, $^3J_{HH}$ = 7.6 Hz, 3H, CH_3), 0.87 (t, $^3J_{HH}$ = 7.4 Hz, 3H, CH_3). C_6H_6: δ 7.12 (s).

^{11}B NMR (128 MHz, 298 K, d_8-tol): δ 45.2 (br s).

^{13}C{^{1}H} NMR (101 MHz, 298 K, d_8-tol), partial: δ 135.8 (s, alkene CH), 135.3 (s, *o*-CH), 130.8 (s, *p*-CH), 127.9 (s, *m*-CH), 127.8 (s, quat. C), 24.5 (s, CH_2), 21.0 (s, CH_2), 13.1 (s, CH_3), 12.7 (s, CH_3). C_6H_6: δ 128.5.

HRMS (EI) calcd for $C_{18}H_{21}BO$ 264.1685, found 264.1686.

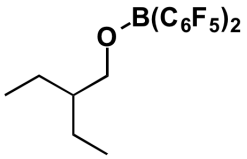

5-5a: Reaction time: 24 h. NMR yield: 79%.

^{1}H NMR (600 MHz, 298 K, d_8-tol): δ 3.88 (d, $^{3}J_{HH}$ = 4.5 Hz, 1H, OCH_2), 1.38–1.23 (m, 5H, CH and 2xCH_2), 0.77 (t, $^{3}J_{HH}$ = 7.4 Hz, 6H, 2xCH_3).

^{19}F NMR (377 MHz, 298 K, d_8-tol): δ −132.5 to −132.6 (m, 2F, *o*-C_6F_5), −148.9 (br s, 1F, *p*-C_6F_5), −160.9 (br s, 2F, *m*-C_6F_5).

^{11}B NMR (128 MHz, 298 K, d_8-tol): δ 40.0 (br s).

^{13}C{^{1}H} NMR (101 MHz, 298 K, d_8-tol), partial: δ 72.0 (s, OCH_2), 42.6 (s, CH), 23.2 (s, 2xCH_2), 11.1 (s, 2xCH_3).

HRMS (EI) calcd for $C_{18}H_{13}BF_{10}O$ 446.0900, found 446.0891.

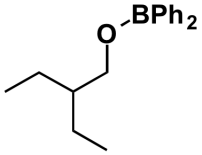

5-5b: Reaction time: 24 h. NMR yield: 70%.

^{1}H NMR (400 MHz, 298 K, d_8-tol): δ 7.67–7.64 (m, 4H, *o*-CH), 7.25–7.21 (m, 6H, *m*-CH and *p*-CH), 3.95 (d, $^{3}J_{HH}$ = 4.4 Hz, 2H, OCH_2), 1.43–1.31 (m, 5H, CH and 2xCH_2), 0.79 (t, $^{3}J_{HH}$ = 7.2 Hz, 6H, 2xCH_3).

^{11}B NMR (128 MHz, 298 K, d_8-tol): δ 45.7 (br s).

^{13}C{^{1}H} NMR (126 MHz, 298 K, d_8-tol), partial: δ 134.6 (s, *o*-CH), 130.2 (s, *p*-CH), 127.9 (s, *m*-CH), 69.6 (s, OCH_2), 43.4 (s, CH), 23.6 (s, 2xCH_2), 11.4 (s, 2xCH_3).

HRMS (EI) calcd for $C_{18}H_{23}BO$ 266.1842, found 266.1846.

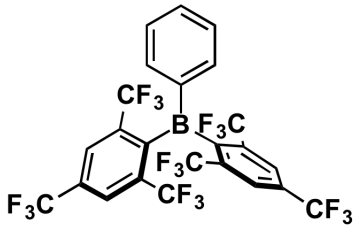

Synthesis of 5-6

fMes_2BF (148 mg, 0.25 mmol) was dissolved in 2 mL dry toluene. The resulting yellow solution was cooled to −35 °C, and PhLi (150 µL, 1.8 M solution in *n*-Bu_2O) was added drop-wise to the reaction. The solution was allowed to slowly warm to room temperature over 3 h while stirring.

The reaction mixture was filtered over Celite and the filtrate was concentrated *in vacuo*. The crude material was recrystallized from a pentane solution of **5-6** at −35 °C yielding the pure borane (124 mg, 76%).

^{1}H NMR (400 MHz, 298 K, CD_2Cl_2): δ 8.25 (s, 4H, Mes-CH), 7.60 (tt, $^{3}J_{HH}$ = 7.4 Hz, $^{4}J_{HH}$ = 1.2 Hz, 1H, *p*-Ph), 7.38 (t, $^{3}J_{HH}$ = 7.8 Hz, 2H, *m*-Ph), 7.19 (dd, $^{3}J_{HH}$ = 8.0 Hz, $^{4}J_{HH}$ = 1.2 Hz, 2H, *o*-Ph).

^{19}F NMR (377 MHz, 298 K, CD_2Cl_2): δ −53.9 (br, 6F, *o*-CF_3), −63.9 (s, 3F, *p*-CF_3).

^{11}B NMR (128 MHz, 298 K, CD_2Cl_2): δ 69.5 (br s).

^{13}C{^{1}H} NMR (101 MHz, 298 K, CD_2Cl_2), partial: δ 145.5 (br, *i*-Ph), 142.7 (br, *i*-Mes), 137.2 (s, *o*-Ph), 137.1 (br, *o*-Mes), 134.5 (s, *p*-Ph), 133.5 (q, $^{2}J_{CF}$ = 35 Hz, *p*-Mes), 128.0 (s, *m*-Ph), 127.5 (br, *m*-Mes), 123.6 (q, $^{1}J_{CF}$ = 276 Hz, *o*-CF_3), 123.1 (q, $^{1}J_{CF}$ = 274 Hz, *p*-CF_3).

Elemental analysis calcd (%) for $C_{24}H_9BF_{18}$: C 44.34; H 1.40; Found: C 44.31; H 1.81.

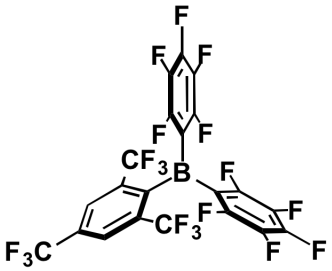

Synthesis of 5-7

fMes (82 mg, 0.29 mmol) was dissolved in 1 mL Et_2O and cooled to −35 °C. *n*-BuLi (181 μL, 1.6 M solution in hexanes) was added drop-wise to the fMes solution. This reaction was allowed to slowly warm to room temperature over 2 h while stirring. $ClB(C_6F_5)_2$ (100 mg, 0.26 mmol) was dissolved in 2 mL Et_2O and the resulting solution was cooled to −35 °C. The Li(fMes) solution was then added drop-wise to the $ClB(C_6F_5)_2$ at −35 °C. The vial containing the Li(fMes) solution was rinsed with 1 mL Et_2O. The reaction mixture slowly warmed to room temperature. After 1.5 h the solution was cloudy and a yellow-orange colour. The solution was filtered over Celite and concentrated *in vacuo*; an orange oil was isolated. The oil was triturated with pentane, and the solution was filtered over Celite. The material was recrystallized from a pentane solution of **5-7** at −35 °C yielding the pure borane (127 mg, 78% yield).

^{1}H NMR (400 MHz, 298 K, CD_2Cl_2): δ 8.17 (s, 2H, Mes-CH).

^{19}F NMR (377 MHz, 298 K, CD_2Cl_2): δ 57.1 (s, 6F, *o*-CF_3), 63.6 (s, 3F, *p*-CF_3), −127.2 (d, $^{3}J_{FF}$ = 21 Hz, 4F, *o*-C_6F_5), −143.5 (tt, $^{3}J_{FF}$ = 20 Hz, $^{4}J_{FF}$ = 7 Hz, 2F, *p*-C_6F_5), −161.1 to −161.2 (m, 4F, *m*-C_6F_5).

^{11}B NMR (128 MHz, 298 K, CD_2Cl_2): δ 59.2 (br s).

^{13}C{^{1}H} NMR (101 MHz, 298 K, CD_2Cl_2), partial: δ 149.7 (dm, $^{1}J_{CF}$ ~ 254 Hz, C_6F_5), 145.8 (dm, $^{1}J_{CF}$ ~ 262 Hz, C_6F_5), 138.1 (dm, $^{1}J_{CF}$ ~ 253 Hz, C_6F_5), 133.5 (q, $^{2}J_{CF}$ = 35 Hz, *o*-fMes), 133.1 (q, $^{2}J_{CF}$ = 33 Hz, *p*-fMes), 127.0 (br s, *m*-fMes), 124.3 (q, $^{1}J_{CF}$ = 275 Hz, *o*-CF_3), 123.1 (q, $^{1}J_{CF}$ = 274 Hz, *p*-CF_3).

Multiple attempts to obtain satisfactory elemental analysis data were unsuccessful.

5.4.3 X-ray Crystallography

5.4.3.1 X-ray Collection and Reduction

Crystals were coated in Paratone-N oil in the glovebox, mounted on a MiTegen Micromount and placed under an N_2 stream, thus maintaining a dry, O_2-free environment for each crystal. The data were collected on a Bruker Kappa Apex II diffractometer. Data collection strategies were determined using Bruker Apex 2 software and optimized to provide >99.5% complete data to a 2θ value of at least 55°. The data were collected at 150(±2) K for all. The data integration and absorption correction were performed with the Bruker Apex 2 software package.[49]

5.4.3.2 X-ray Solution and Refinement

Non-hydrogen atomic scattering factors were taken from the literature tabulations.[50] The heavy atom positions were determined using direct methods employing the SHELX-2013 direct methods routine. The remaining non-hydrogen atoms were located from successive difference Fourier map calculations. The refinements were carried out by using full-matrix least squares techniques on F^2. All non-hydrogen atoms were assigned anisotropic temperature factors in the absence of disorder or insufficient data. In the latter cases, atoms were treated isotropically. C-bound H atoms were placed at calculated positions and allowed to ride on the carbon to which they are bonded during refinement. H-atom temperature factors were fixed at 1.20 times (central atoms) or 1.50 times (terminal CH_3 atoms) the isotropic temperature factor of the C-atom to which they are bonded. The locations of the largest peaks in the final difference Fourier map calculation as well as the magnitude of the residual electron densities in each case were of no chemical significance.

Table 5.2 – Selected crystallographic data for **5-6** and **5-7**.

	5-6	**5-7**
Formula	$C_{24}H_9BF_{18}$	$C_{21}H_2BF_{19}$
Formula weight	650.12	626.04
Crystal System	Orthorhombic	Triclinic
Space group	Pbca	P-1
a (Å)	15.5600(11)	9.4993(10)
b (Å)	8.7136(6)	10.3425(12)
c (Å)	35.624(3)	12.7615(15)
α (°)	90	95.430(7)
β (°)	90	103.787(6)
γ (°)	90	117.260(6)
V ($Å^3$)	4830.1(6)	1051.8(2)
Z	8	2
Temp. (K)	150	150
d_{calc} (gcm^{-1})	1.788	1.977
Abs. coeff. μ (mm^{-1})	0.201	0.233
Reflections Collected	67817	17412
Data $F_o^2>3\sigma(F_o^2)$	4256	3704
Variables	423	382
R	0.0449	0.0455
R_w	0.0913	0.1032
GOF	1.042	1.022

5.5 References

(1) Schlesinger, H. I.; Brown, H. C.; Abraham, B.; Bond, A. C.; Davidson, N.; Finholt, A. E.; Gilbreath, J. R.; Hoekstra, H.; Horvitz, L.; Hyde, E. K.; Katz, J. J.; Knight, J.; Lad, R. A.; Mayfield, D. L.; Rapp, L.; Ritter, D. M.; Schwartz, A. M.; Sheft, I.; Tuck, L. D.; Walker, A. O. *Journal of the American Chemical Society* **1953**, *75*, 186–190.

(2) Nystrom, R. F.; Brown, W. G. *Journal of the American Chemical Society* **1947**, *69*, 1197–1199.

(3) Brown, H. C.; Ramachandran, P. V. In *Reductions in Organic Synthesis*; ACS Symposium Series; American Chemical Society, 1996; Vol. 641, p 1.

(4) Knowles, W. S. *Angewandte Chemie International Edition* **2002**, *41*, 1999.

(5) Noyori, R. *Angewandte Chemie International Edition* **2002**, *41*, 2008–2022.

(6) Noyori, R.; Ohkuma, T. *Angewandte Chemie International Edition* **2001**, *40*, 40–73.

(7) Chi, Y.; Tang, W.; Zhang, X. In *Modern Rhodium-Catalyzed Organic Reactions*; Wiley-VCH Verlag GmbH & Co. KGaA, 2005; pp 1–31.

(8) Zuo, W.; Lough, A. J.; Li, Y. F.; Morris, R. H. *Science* **2013**, *342*, 1080–1083.

(9) Fleischer, S.; Zhou, S.; Junge, K.; Beller, M. *Angewandte Chemie International Edition* **2013**, *52*, 5120–5124.

(10) Li, Y.-Y.; Yu, S.-L.; Shen, W.-Y.; Gao, J.-X. *Accounts of Chemical Research* **2015**, *48*, 2587–2598.

(11) Stephan, D. W. *Accounts of Chemical Research* **2015**, *48*, 306–316.

(12) Stephan, D. W.; Erker, G. *Angewandte Chemie International Edition* **2010**, *49*, 46–76.

(13) Stephan, D. W.; Erker, G. *Angewandte Chemie International Edition* **2015**, *54*, 6400–6441.

(14) Chase, P. A.; Welch, G. C.; Jurca, T.; Stephan, D. W. *Angewandte Chemie International Edition* **2007**, *46*, 8050–8053.

(15) Chase, P. A.; Jurca, T.; Stephan, D. W. *Chemical Communications* **2008**, *2*, 1701–1703.

(16) Spies, P.; Schwendemann, S.; Lange, S.; Kehr, G.; Fröhlich, R.; Erker, G. *Angewandte Chemie International Edition* **2008**, *47*, 7543–7546.

(17) Wang, H.; Fröhlich, R.; Kehr, G.; Erker, G. *Chemical Communications* **2008**, 5966–5968.

(18) Wei, S.; Du, H. *Journal of the American Chemical Society* **2014**.

(19) Geier, S. J.; Chase, P. A.; Stephan, D. W. *Chemical Communications* **2010**, *46*, 4884–4886.

(20) Liu, Y.; Du, H. *Journal of the American Chemical Society* **2013**, *135*, 12968–12971.

(21) Zhang, Z.; Du, H. *Angewandte Chemie International Edition* **2014**, 1–5.

(22) Greb, L.; Oña-Burgos, P.; Schirmer, B.; Grimme, S.; Stephan, D. W.; Paradies, J. *Angewandte Chemie International Edition* **2012**, *51*, 10164–10168.

(23) Greb, L.; Daniliuc, C. G.; Bergander, K.; Paradies, J. *Angewandte Chemie International Edition* **2013**, *52*, 5876–5879.

(24) Hounjet, L. J.; Bannwarth, C.; Garon, C. N.; Caputo, C. B.; Grimme, S.; Stephan, D. W.

Angewandte Chemie International Edition **2013**, *52*, 7492–7495.

(25) Segawa, Y.; Stephan, D. W. *Chemical Communications* **2012**, *48*, 11963–11965.

(26) Chernichenko, K.; Madarász, A.; Pápai, I.; Nieger, M.; Leskelä, M.; Repo, T. *Nature Chemistry* **2013**, *5*, 718–723.

(27) Mahdi, T.; Stephan, D. W. *Journal of the American Chemical Society* **2014**, *136*, 15809–15812.

(28) Scott, D. J.; Fuchter, M. J.; Ashley, A. E. *Journal of the American Chemical Society* **2014**, *136*, 15813–15816.

(29) Spies, P.; Erker, G.; Kehr, G.; Bergander, K.; Fröhlich, R.; Grimme, S.; Stephan, D. W. *Chemical Communications* **2007**, *2*, 5072–5074.

(30) Sumerin, V.; Schulz, F.; Nieger, M.; Leskelä, M.; Repo, T.; Rieger, B. *Angewandte Chemie International Edition* **2008**, *47*, 6001–6003.

(31) Nyhlén, J.; Privalov, T. *Dalton Transactions* **2009**, *25*, 5780–5786.

(32) Li, H.; Zhao, L.; Lu, G.; Huang, F.; Wang, Z.-X. *Dalton Transactions* **2010**, *39*, 5519–5526.

(33) Lindqvist, M.; Sarnela, N.; Sumerin, V.; Chernichenko, K.; Leskelä, M.; Repo, T. *Dalton Transactions* **2012**, *41*, 4310–4312.

(34) Duchateau, R.; Lancaster, S. J.; Thornton-Pett, M.; Bochmann, M. *Organometallics* **1997**, *16*, 4995–5005.

(35) Lewis, S. P.; Henderson, L. D.; Chandler, B. D.; Parvez, M.; Collins, W. E. P. S. *Journal of the American Chemical Society* **2005**, *127*, 46–47.

(36) Lewis, S. P.; Chai, J.; Collins, S.; Sciarone, T. J. J.; Henderson, L. D.; Fan, C.; Parvez, M.; Piers, W. E.; Wiley, J.; York, N. *Organometallics* **2009**, *28*, 249–263.

(37) Parks, D. J.; Spence, R. E. von H.; Piers, W. E. *Angewandte Chemie International Edition* **1995**, *34*, 809–811.

(38) Scott, D. J.; Fuchter, M. J.; Ashley, A. E. *Angewandte Chemie International Edition* **2014**, *53*, 10218–10222.

(39) Piers, W. E.; Chivers, T. *Chemical Society Reviews* **1997**, *26*, 345–354.

(40) Lu, Z.; Cheng, Z.; Chen, Z.; Weng, L.; Li, Z. H.; Wang, H. *Angewandte Chemie International Edition* **2011**, *50*, 12227–12231.

(41) Ye, H.; Lu, Z.; You, D.; Chen, Z.; Li, Z. H.; Wang, H. *Angewandte Chemie International Edition* **2012**, *51*, 12047–12050.

(42) Lu, Z.; Wang, Y.; Liu, J.; Lin, Y.; Li, Z. H.; Wang, H. *Organometallics* **2013**, 8–13.

(43) Zheng, J.; Lin, Y.-J.; Wang, H. *Dalton Transactions* **2016**, *45*, 6088–6093.

(44) Cornet, S. M.; Dillon, K. B.; Entwistle, C. D.; Fox, M. A.; Goeta, A. E.; Goodwin, H. P.; Marder, T. B.; Thompson, A. L. *Dalton Transactions* **2003**, *32*, 4395–4405.

(45) Eros, G.; Mehdi, H.; Pápai, I.; Rokob, T. A.; Király, P.; Tárkányi, G.; Soós, T. *Angewandte Chemie International Edition* **2010**, *49*, 6559–6563.

(46) Alvarez, S. *Dalton Transactions* **2013**, *42*, 8617–8636.

(47) Jackson, R. D.; James, S.; Orpen, A. G.; Pringle, P. G. *Journal of Organometallic Chemistry* **1993**, *458*, C3–C4.

(48) Parks, D. J.; Piers, W. E.; Yap, G. P. A. *Organometallics* **1998**, *17*, 5492–5503.

(49) *Bruker AXS Inc.*; 2013.

(50) Cromer, D. T.; Waber, J. T. In *International Tables for X-Ray Crystallography*; Kynoch Press: Birmingham, 1974; pp 71–147.

Chapter 6
The Synthesis and Reactivity of Neutral Borocyclic Radicals

6.1 Introduction

6.1.1 Stable Radicals – Historical Perspective and Synthetic Strategies

In 1900, Gomberg reported the reduction of triphenylmethyl chloride with Ag^0, with the goal of generating hexaphenylethane. The reduction yielded a coloured solution, which formed a stable peroxide upon exposure to air, leading Gomberg to make the controversial claim that he had generated a free radical (Scheme 6.1).[1] Although initially met with skepticism, this seminal work was eventually accepted by the scientific community and led to increased interest in free radical chemistry.[2]

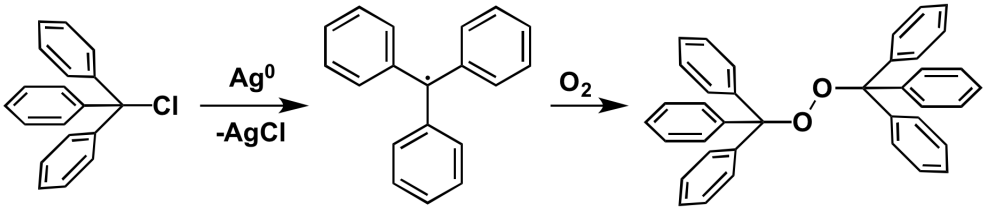

Scheme 6.1 – Gomberg's synthesis of the triphenylmethyl radical, and its subsequent oxidation.

Since Gomberg's work, chemists have been challenged to develop new strategies for the preparation of isolable radicals. Successful strategies to stabilize such species include delocalization of the unpaired electron through π-systems, and incorporating sterically demanding substituents to suppress undesired reactivity.[3] Indeed, some of the most ubiquitous examples of organic free radicals, such as nitroxyl (e.g. TEMPO), verdazyl, and phenalenyl radicals, are stabilized through π-delocalization or sterically demanding substituents (Figure 6.1).

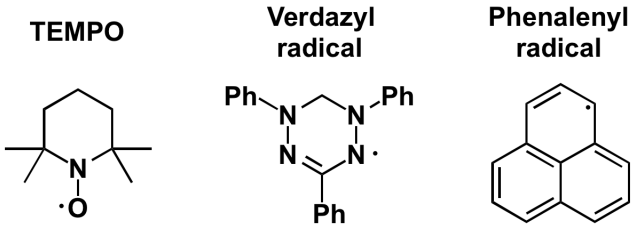

Figure 6.1 – Examples of stable organic free radicals.

For the purpose of this thesis, "persistent" radicals will be defined as those that have relatively long lifetimes under the conditions through which they were generated, and "stable" radicals as those that can be isolated and stored in the absence of air and moisture without decomposition.[4]

6.1.2 Anionic Boron Radicals

Following work by Gomberg, Schlenk, and others on carbon radicals,[2] free radicals bearing boron functionalities were examined. The triphenylboron radical anion $[BPh_3]^{\bullet-}$, which is isoelectronic with $[CPh_3]^{\bullet}$, was first prepared by reducing BPh_3 with alkali metals in 1926,[5] and was spectroscopically studied in 1970.[6] This strategy became the standard approach to synthesizing species of the type $[BR_3]^{\bullet-}$ (Scheme 6.2a).

It was not until 1986 that a boron-containing free radical was characterized in the solid state. This accomplishment was achieved by Power and co-workers,[7] more than 10 years after the solid state structures of BPh_3[8] and $BMes_3$[9] were reported, by reducing $BMes_3$ with Li^0 followed by the addition of 12-crown-4, generating the free trimesitylboron radical anion, $[BMes_3]^{\bullet-}$. Tris(pentafluorophenyl)boron radical anion $[B(C_6F_5)_3]^{\bullet-}$ has been detected by EPR spectroscopy, however it is a much more reactive molecule and its half-life is estimated to be 2 minutes at room temperature.[10] Beyond aryl-substituted boron radical anions, persistent trialkylboron radical anions $[BR_3]^{\bullet-}$ have been generated, where R = *t*-Bu or Np.[11] These radicals display much larger hyperfine coupling constants ($a(^{11}B)$ = 28–38 G) than related aryl-substituted species ($a(^{11}B)$ = 7–11 G), indicative of greater localization of the unpaired electron on the boron centre.

An example of boron radical anion chemistry particularly relevant to the research in this chapter can be found in Eaton's electrochemical reduction of ketone-ligated borinic esters (Scheme 6.2b).[12] The resultant boron radical anion was amenable to EPR spectroscopic studies, although it was not sufficiently stable to be isolated.

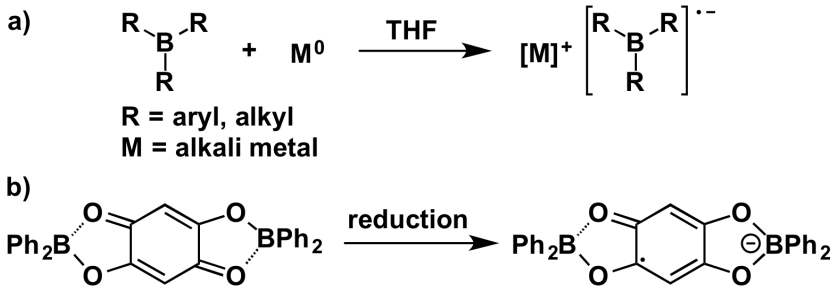

Scheme 6.2 – a) General procedure for the synthesis of boron radical anions from neutral boranes, and b) electrochemically generated heterocyclic boron radical anion.

6.1.3 Neutral Boron Radicals

6.1.3.1 Semiquinone-Based Neutral Boron Radicals

Similar to Eaton's heterocyclic boron radical anion,[12] a number of heterocyclic neutral boron radicals have been generated based on orthosemiquinone ligand scaffolds. Select examples are shown in Figure 6.2. These radicals were observed by EPR spectroscopy but were not isolated or further characterized. They were prepared by treating boronic esters with alkoxy radicals (Figure 6.2a & b),[13] oxidizing borinate esters (Figure 6.2c),[14] treating semiquinone radical and catecholate with BCl_3 (Figure 6.2d),[15] and UV irradiating diones in the presence of BPh_3 (Figure 6.2e).[16]

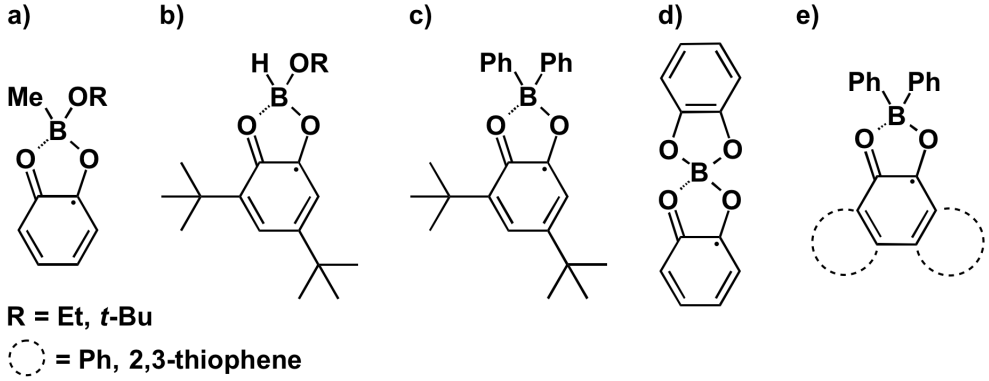

Figure 6.2 – Examples of semiquinone-based neutral boron radicals observed by EPR spectroscopy.

6.1.3.2 Persistent or Stable Neutral Boron Radicals

The chemistry of stable, neutral boron radicals is less developed than that of their anionic relatives, but in recent years several groups have contributed to this area of research (Figure 6.3). Haddon has used phenalenyl substituents to generate zwitterionic boron radicals, which he showed to have conducting properties.[17,18] The groups of Bertrand[19] and Braunschweig[20,21] have demonstrated how N-heterocyclic carbenes (NHCs) and cyclic (alkyl)(amino)carbenes (CAACs) can be used to prepare and isolate a number of neutral boron-containing radical species. Curran and Lacôte have generated persistent NHC-stabilized neutral boron radicals *in situ* for application in catalysis and organic synthesis.[22,23] Mesityl substituents on boron have enabled Gabbaï[24] to isolate an acridinyl-substituted boron free radical, and recently enabled Bourissou[25] to generate a persistent phosphine-stabilized Gomberg-type boryl radical. A more unusual example is the neutral boron radical obtained by Yamashita, Ohkoshi, and Nozaki[26] in 2012 by employing a β-diiminate ligand framework. These examples reflect the strategies outlined in section 6.1.1, whereby π-delocalization and sterically encumbered substituents facilitate free radical isolation and manipulation.

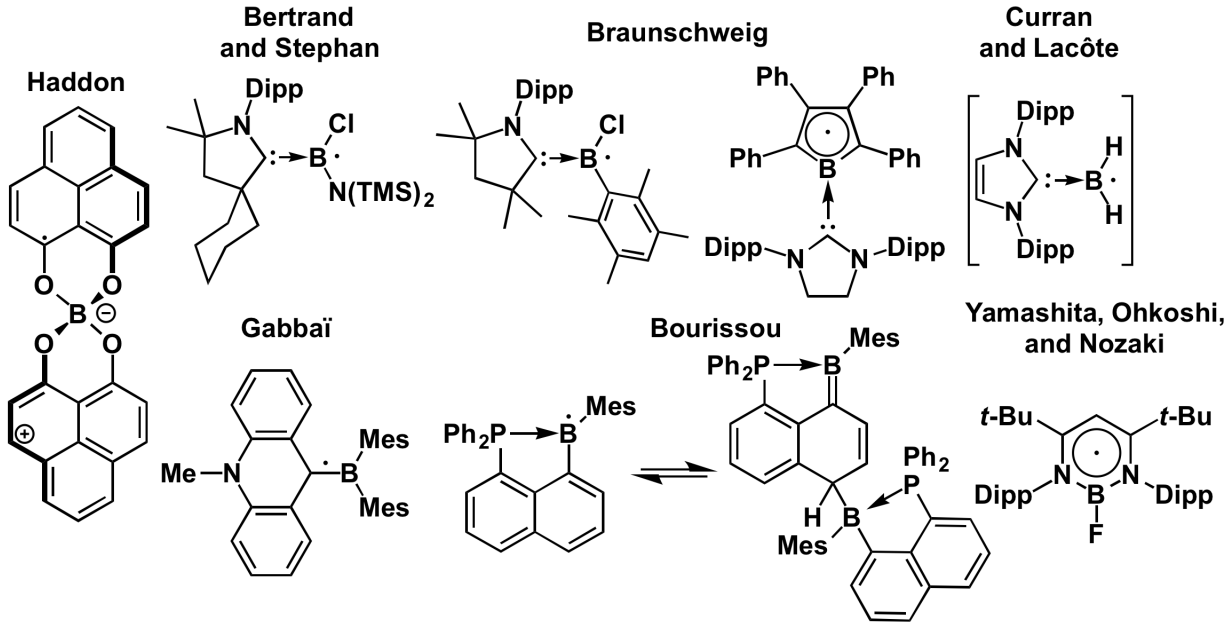

Figure 6.3 – Examples of persistent or stable neutral boron-containing free radicals.

6.1.4 Frustrated Lewis Pair Radical Processes

The topic of frustrated Lewis pairs (FLPs) has been extensively covered in Chapter 1 and in the introductions of Chapters 2, 3, and 5, however recent examples in paramagnetic FLP chemistry are particularly relevant for the research discussed in this chapter. The Stephan group reported the first "frustrated radical pair" in 2013,[27] which was accessed through the decomposition of a phosphine-alane FLP adduct of N_2O. These radical pairs were unstable and activated solvent C–H bonds to form more stable phosphonium aluminate salts (Scheme 6.3a). The Erker group has been actively exploring FLP radical chemistry, and have used intramolecular phosphine-boranes to capture NO.[28–32] They have also recently reported FLP alkene additions[33] and H_2 cleavage using TEMPO (Scheme 6.3b).[34]

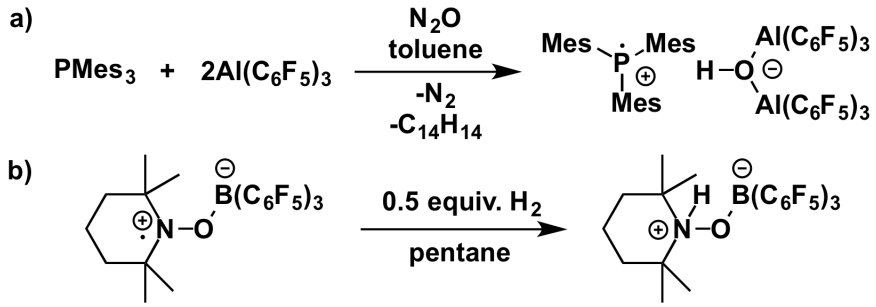

Scheme 6.3 – a) FLP activation of N_2O and *in situ* formation of a frustrated radical pair, and b) H_2 activation by mixtures of $B(C_6F_5)_3$ with TEMPO.

In this chapter, the borinic ester synthetic methodology presented in Chapter 5 will be applied to the generation of borocyclic radicals based on phenanthrenedione and pyrenedione scaffolds. The numbering systems shown in Figure 6.4 will be applied where pertinent.

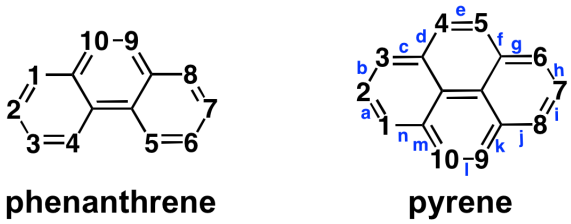

Figure 6.4 – Numbering systems for phenanthrene and pyrene.

6.2 Results and Discussion

6.2.1 Hydrogenation of Ketones with Donor Substituents

The stoichiometric reduction of ketones using $B(C_6F_5)_3$ and H_2 was previously established, as discussed in Chapter 5. The resulting borinic esters were not reliably stable once isolated, prompting the decision to test ketone substrates bearing donor groups. It was postulated that having a pendent donor group that could coordinate in an intramolecular fashion to the borinic ester might result in products that are more stable and easier to isolate. Ketones **6-1a** and **6-2a** were subjected to the optimized reaction conditions for borinic ester formation (Scheme 6.4), to investigate the stabilizing effect of both N and O donor groups. 2-Benzoylpyridine **6-1a** was found to activate H_2 in combination with $B(C_6F_5)_3$ at 110 °C, and the anticipated pyridyl-ligated borinic ester **6-1b** was generated. The NMR data for **6-1b** were consistent with similar species,[35] however the isolated yield was lower than expected (51%). The reaction was monitored by multinuclear NMR spectroscopy, and species arising from reduction of the aromatic N-heterocycle appeared to be forming, based upon resonances in the aliphatic region of the ^1H NMR spectrum. This type of $B(C_6F_5)_3$-mediated aromatic reduction was previously observed with ethyl 2-picolinate.[36] A higher isolated yield (83%) of the desired product was obtained by hydroboration of **6-1a** with $HB(C_6F_5)_2$. Substrate **6-2a**, despite being pictorially depicted as a dione, is more appropriately viewed as an α-hydroxy enone under the reaction conditions; the ^1H NMR spectrum in d_8-toluene shows a broad -OH resonance and an olefinic resonance at 6.14 ppm and 5.71 ppm, respectively. $B(C_6F_5)_3$ was observed to react with **6-2a** in the presence of H_2, yielding a new product **6-2b** with loss of HC_6F_5, however it was determined, based on the corresponding ^1H and $^{13}C\{^1H\}$ NMR spectra, that hydrogenation had not occurred. Indeed, when the reaction was repeated in the absence of H_2, the same product **6-2b** was formed. The reaction is a thermal protonation of a $-C_6F_5$ ring on $B(C_6F_5)_3$ from the enol form of **6-2a**, akin to the reactions of alcohols with $B(C_6F_5)_3$ reported in Chapter 5. Both **6-1b** and **6-2b** were amenable to single crystal X-ray diffraction studies (Figure 6.5).

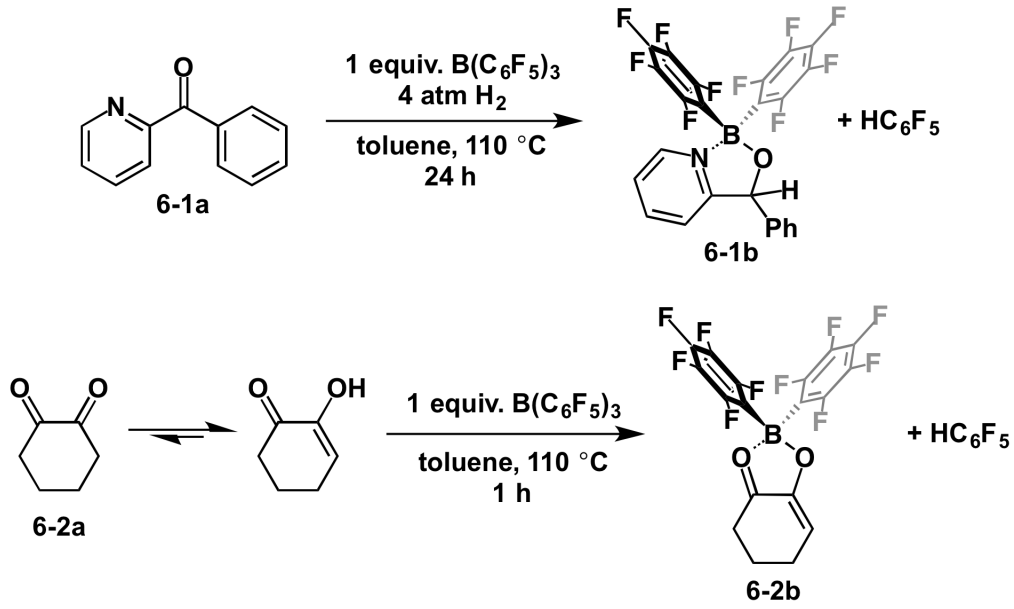

Scheme 6.4 – Reactivity of **6-1a** and **6-2a** with $B(C_6F_5)_3$.

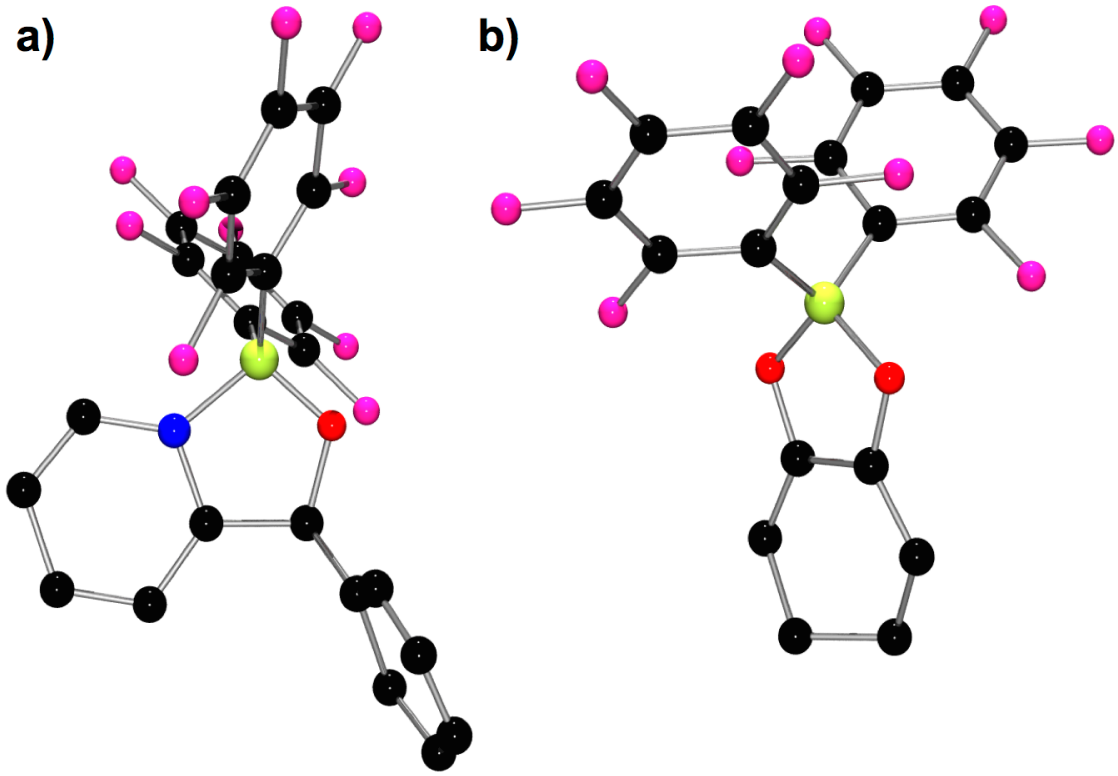

Figure 6.5 – POV-ray depictions of a) **6-1b** and b) **6-2b**, with H atoms omitted for clarity. C: black; B: yellow-green; F: pink; N: blue; O: red.

6.2.2 Synthesis, Isolation, and Characterization of Borocyclic Radicals

The over-reduction of substrate **6-1a** and the enol reactivity observed for **6-2a** led to the exploration of non-enolizable diones as substrates for FLP-mediated hydrogenations. 9,10-Phenanthrenedione **6-3a** was fortuitously chosen as a test substrate. When **6-3a** was combined with one equivalent of $B(C_6F_5)_3$ in d_8-toluene at room temperature, a dark black-red solution formed. NMR analysis of the mixture suggested that a weak adduct **6-3b** had formed, based on the very broad ^{11}B NMR resonance at ~30 ppm, although this chemical shift was found to be sensitive to small changes in environment (likely trace amount of H_2O), as the same combinations were also observed to resonate as far upfield as 24 ppm. The molecular structure of **6-3b** was confirmed crystallographically (Figure 6.7a).

When a 1:1 mixture of $B(C_6F_5)_3$ and **6-3a** in d_8-toluene was heated to 110 °C under 4 atm H_2, complete consumption of the starting materials was observed after 1 hour. Loss of HC_6F_5 was evident from the ^1H and ^{19}F NMR spectra, and the ^{11}B NMR spectrum showed no resonances. The volatiles were removed *in vacuo*, revealing a mixture of a dark green solid and a smaller amount of an off-white solid. The mixture was washed with pentane, and was taken up in $CDCl_3$. A new resonance in the ^{11}B NMR spectrum was observed at 30.2 ppm, along with three peaks in the ^{19}F NMR spectrum at −127.4, −146.5, and −160.6 ppm, as well as a very broad peak at −159.5 ppm (Figure 6.6). These data suggested the formation of a 3-coordinate boron species, although the broad resonance at −159.5 ppm was initially not understood. The ^1H NMR spectrum of the crude mixture showed three resonances at 8.74 (d), 8.28 (d), and 7.71 (m) ppm, integrating in a 1:1:2 ratio, respectively.

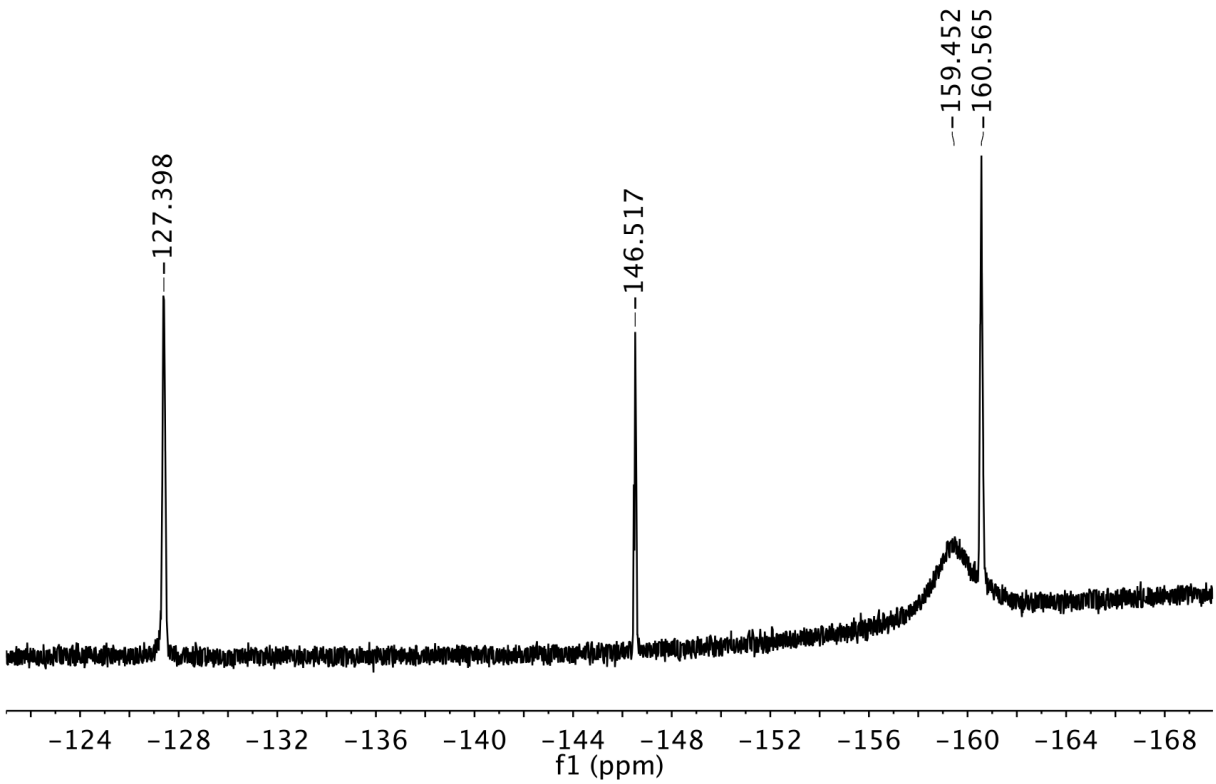

Figure 6.6 – ^{19}F NMR spectrum (377 MHz, 298 K, $CDCl_3$, baseline correction not applied) of the material isolated from the reaction of **6-3a** with $B(C_6F_5)_3$ and H_2, following a pentane wash workup.

The mixture of products was dissolved in DCM, layered with pentane, and left to equilibrate at −35 °C. Single crystals were obtained as black plates, although while mounting the crystals it was noted that there was a smaller amount of yellow microcrystalline material in the sample. X-ray diffraction studies confirmed that the black crystals contained the borocyclic radical **6-3c** (Figure 6.7b). This species qualitatively appeared to be the majority of the crude material, however developing a satisfactory purification strategy was challenging. The material was crystalline, but small amounts of the other product would always co-crystallize from solution. Various different solvent mixtures were tested (DCM/pentane, $CHCl_3$/pentane, toluene/pentane, DCM/cyclohexane, toluene/cyclohexane), and all gave similar results. After multiple attempts at selective crystallization had failed, silica gel chromatography was tested as a means of purifying the crude mixture. A small amount of material was removed from the glovebox for thin layer chromatography (TLC). Pleasingly, elution with DCM caused the dark green-black spot to

migrate from the baseline, although a small amount of **6-3a** formed on the TLC plate. The two species could be separated, and the radical **6-3c** was isolated in yields as high as 80% using column chromatography. NMR spectra from the purified material confirmed that **6-3c** is ^{1}H, ^{11}B, and ^{13}C{^{1}H} NMR silent, and shows one broad singlet in the ^{19}F NMR spectrum in CD_2Cl_2 at −159.9 ppm.

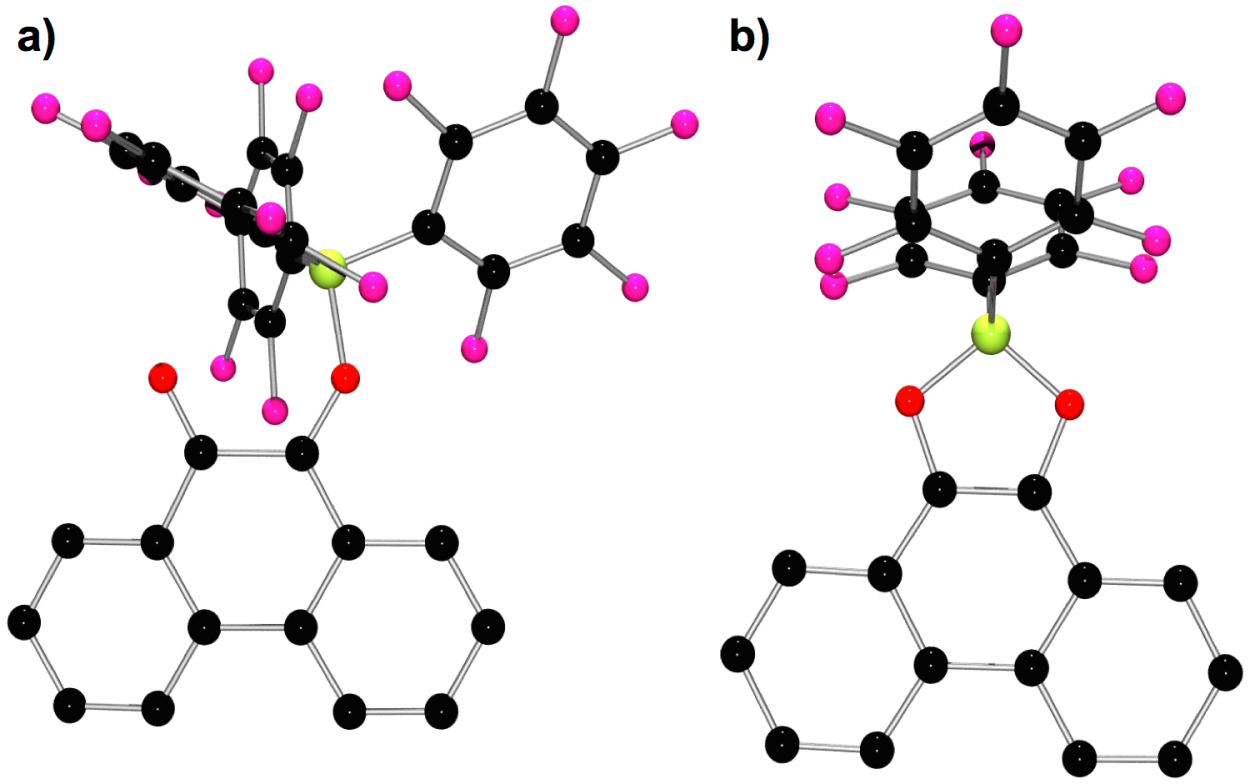

Figure 6.7 – POV-ray depiction of a) **6-3b** and b) **6-3c**, with H atoms omitted for clarity. C: black; B: yellow-green; F: pink; O: red.

The second product from the reduction of **6-3a** was sparingly soluble in DCM, which allowed a small amount of the material to be isolated. A batch of the crude reaction mixture (which contained a mixture of **6-3c** and the unknown impurity) was slurried in minimal DCM. The material was filtered through a glass frit, and cold DCM was carefully flushed through the frit to remove all traces of the radical, which was easily determined by visual inspection of the material. A small amount of a white solid was collected from the frit, dried *in vacuo*, and dissolved in CD_2Cl_2. Heteronuclear NMR data matched the resonances observed in the crude reaction mixture (*vide supra*). Mass spectrometric measurements of the sample suggested that the molecular

formula was $C_{20}H_8BF_5O_2$, which was also supported by elemental analysis. These data led to the proposal that the impurity was the C_6F_5-substituted boronic ester **6-3d** (Scheme 6.5). This was further supported by the independent synthesis of **6-3d**,[37] in which diol **6-3e** and $B(C_6F_5)_3$ were heated to 110 °C in toluene for 1 hour.

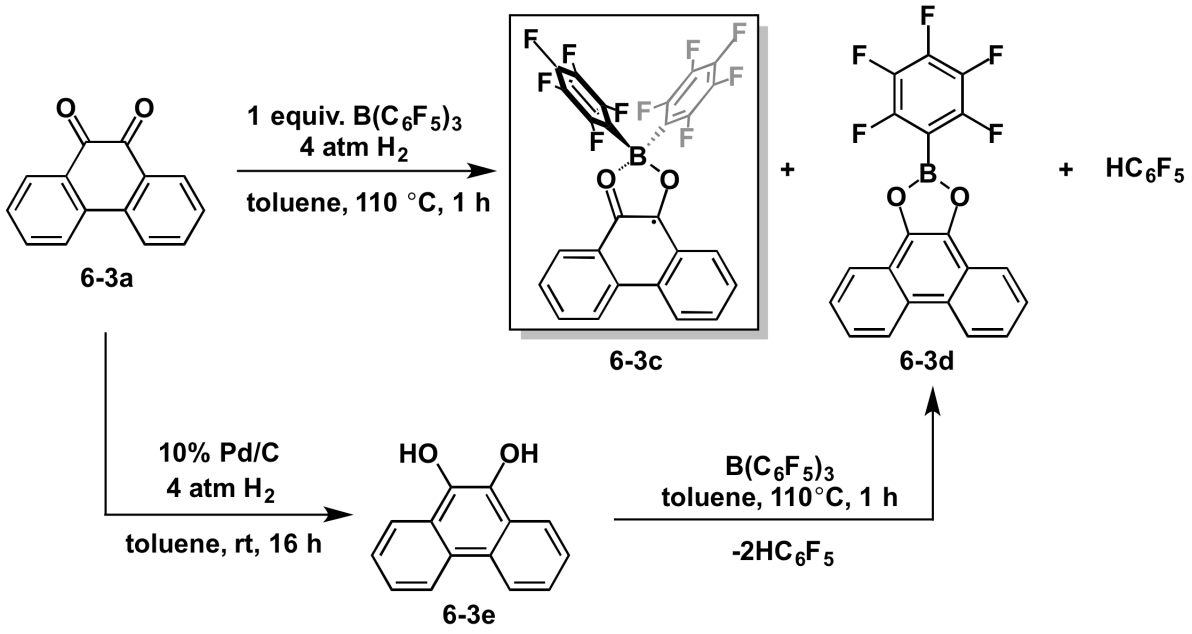

Scheme 6.5 – Hydrogenation of **6-3a** with $B(C_6F_5)_3$ and H_2 to yield a mixture of **6-3c**, **6-3d**, and HC_6F_5.

Single crystals of **6-3d** were grown, the molecular structure of which is shown in Figure 6.8. The material recrystallized as fine, colourless needles from C_6H_5Br. The solid state structure of **6-3d** is planar, and the sum of the angles about the boron centre is 360° (∠OBO = 111.9(4)°, ∠OBC = 124.0(4)° and 124.0(4)°).

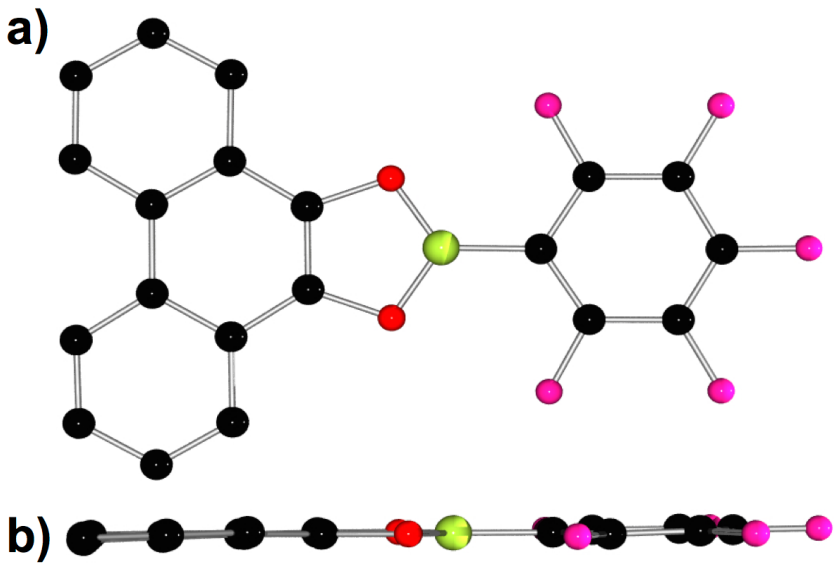

Figure 6.8 – POV-ray depiction of **6-3d**, with a) face-on and b) side-on views shown. H atoms are omitted for clarity. C: black; B: yellow-green; F: pink; O: red.

The analogous reaction with 4,5-pyrenedione **6-4a** proceeds in a similar fashion to the reduction of **6-3a** (Scheme 6.6), and a broad peak in the ^{19}F NMR spectrum at −158.3 ppm, as well as a broad singlet in the ^{1}H NMR spectrum at 6.70 ppm, were attributed to radical **6-4c**. The crude reaction mixture from the reduction of **6-4a** also contained a lesser amount of a white precipitate, which was postulated to be the C_6F_5-sbustituted pyrene boronic ester **6-4d**, although this material was less soluble in organic solvents than **6-3d**. While attempts to independently synthesize **6-4d** were unsuccessful, some of the material was isolated from the crude reaction mixture by employing the same strategy used to isolate **6-3d** from the corresponding reaction mixture. Because of its limited solubility in d_8-toluene, CD_2Cl_2, and $CDCl_3$, room temperature NMR spectroscopic data could not be obtained using these solvents. d_6-DMSO forms an adduct with **6-4d**, as evidenced by the ^{11}B NMR resonance at 10.9 ppm. Heating a d_8-toluene suspension of the material to 100 °C, however, generated a sufficiently concentrated solution to allow the ^{11}B NMR resonance of the free boronic ester to be observed at 29.7 ppm.

Radical **6-4c** was purified by column chromatography, in an analogous fashion to **6-3c**, and was isolated in 46% yield. The material is a dark navy blue colour, and single crystals were grown by slow diffusion of pentane into a DCM solution of **6-4c** at −35 °C. The solid state structure (Figure 6.9) has similar metrical parameters to that of **6-3c**. Both species are stable on

deactivated silica, they do not degrade in air (in the solid state or in solution) after 24 h, and are stable under N_2 indefinitely. Hydrolysis was observed when the products were purified on wet silica.

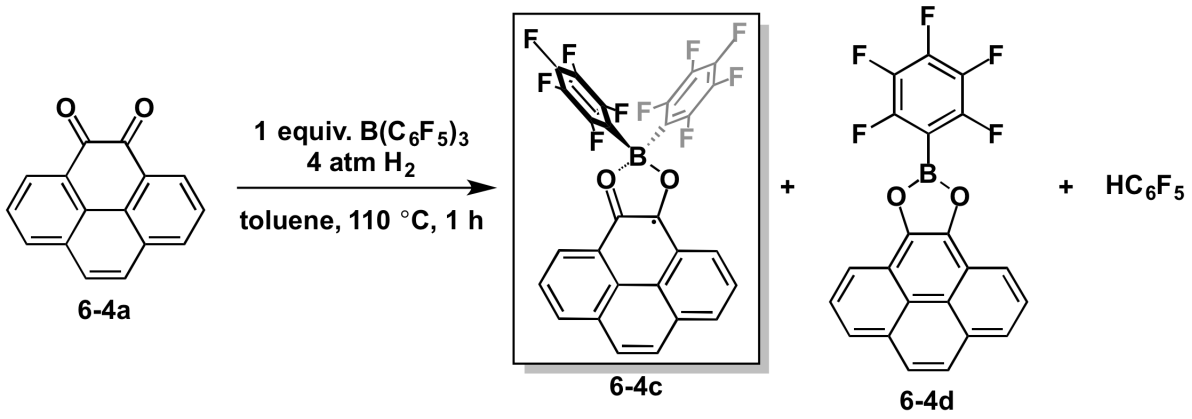

Scheme 6.6 – Synthesis of **6-4c** and **6-4d** from the reduction of **6-4a** with $B(C_6F_5)_3$ and H_2.

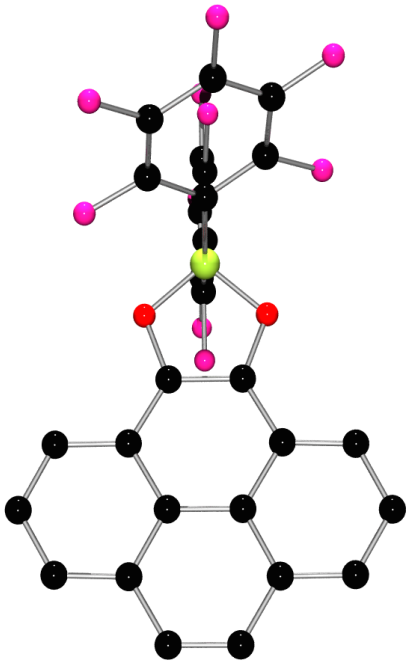

Figure 6.9 – POV-ray depiction of **6-4c**, with H atoms omitted for clarity. C: black; B: yellow-green; F: pink; O: red.

The radicals **6-3c** and **6-4c** were characterized by EPR and UV/vis spectroscopy. The corresponding EPR spectra are shown in Figure 6.10, and the absorbance spectra are shown in Figure 6.11. The EPR signal of **6-3c** suggests delocalization of the radical over the phenanthrene

backbone, with simulated hyperfine coupling constants of $a(^{11}B)$ = 2.58 G and $a(^{1}H)$ = 3.39, 0.00, 2.43, and 1.01 G. The EPR signal of **6-4c** also suggests delocalization of the radical over the pyrene backbone, with simulated hyperfine coupling constants of $a(^{11}B)$ = 2.80 G and $a(^{1}H)$ = 3.38, 0.86, 2.89, and 2.21 G. The absorbance spectrum of **6-3c** shows a λ_{abs} at 471 nm, and **6-4c** has a notable absorbance at 766 nm.

Prof. Stefan Grimme calculated the spin densities and SOMOs of the two borocyclic radicals. The spin densities are shown in Figure 6.12, and show good correlation with EPR spectroscopic studies, where the unpaired electron is delocalized over the polycyclic aromatic backbone. The spin densities at the boron centres of **6-3c** and **6-4c** were calculated to be −0.04 and −0.03 e^-, respectively, supporting the notion that the unpaired electrons in **6-3c** and **6-4c** are not localized at the boron centres but throughout the aromatic backbones.

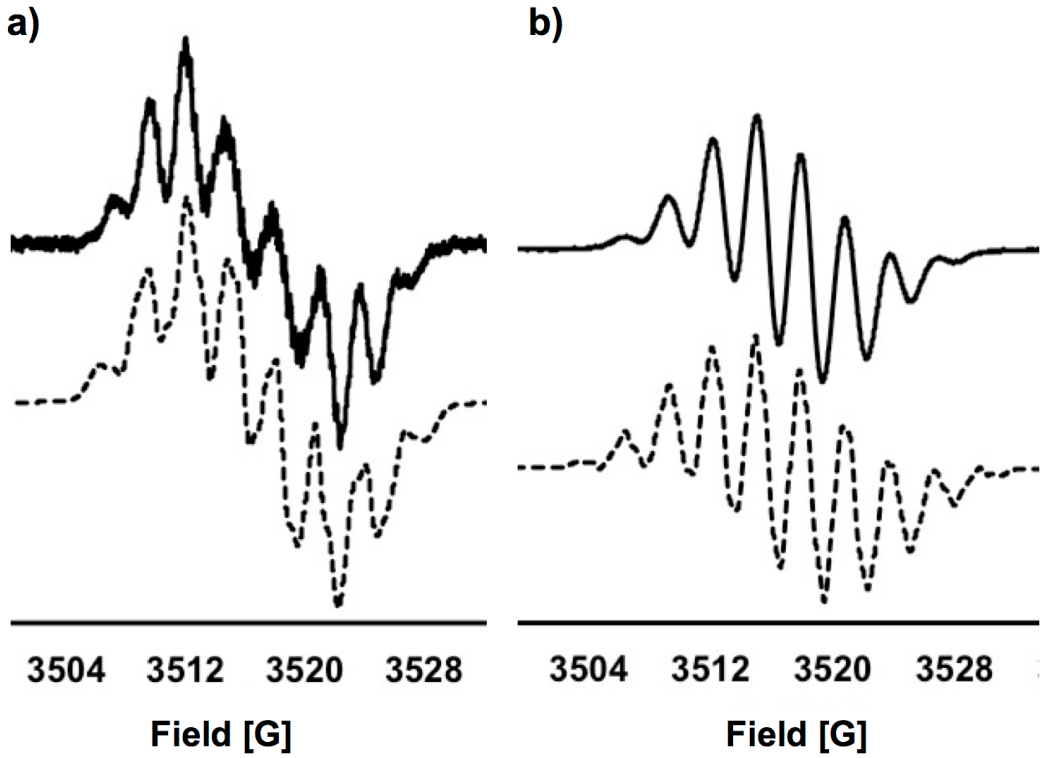

Figure 6.10 – X-band EPR spectra of a) **6-3c** (g = 2.0039) and b) **6-4c** (g = 2.0040) in toluene (observed spectrum = solid line, simulated spectrum = dashed line).

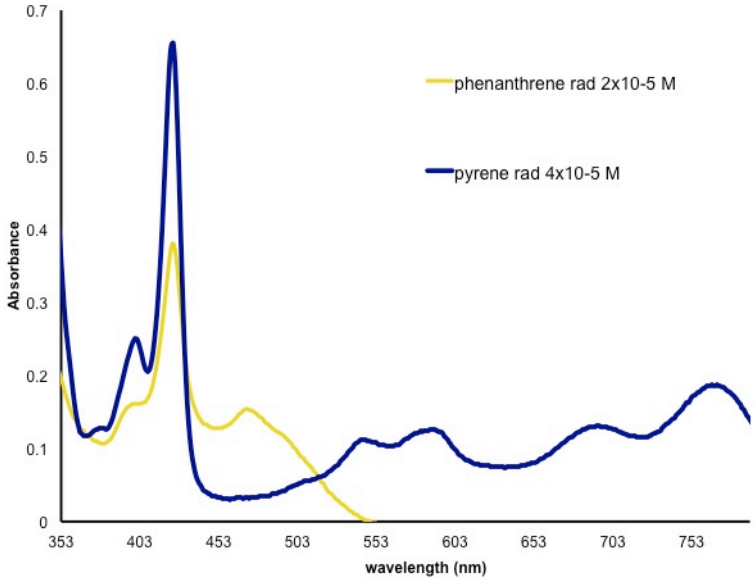

Figure 6.11 – UV/vis spectra of **6-3c** (yellow) and **6-4c** (blue) in DCM.

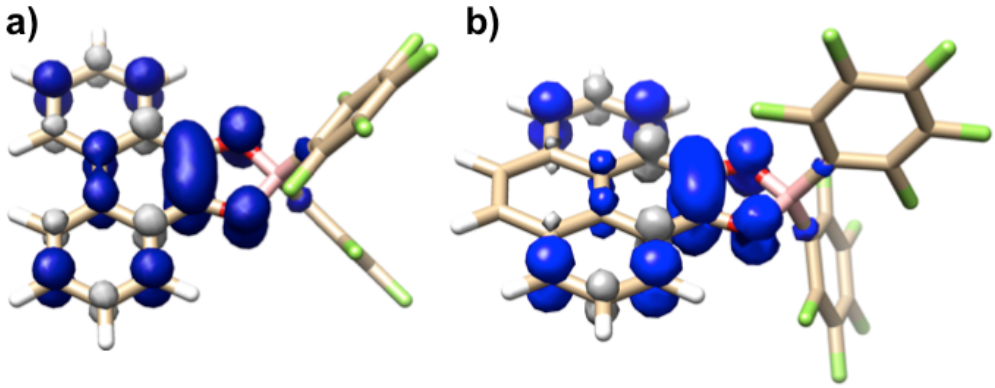

Figure 6.12 – Spin densities of a) **6-3c** and b) **6-4c**, at a contour surface value of ±0.03 au.

6.2.3 Mechanistic Proposal

The formation of boron-containing radicals **6-3c** and **6-4c** was an unexpected result, as the generation of borinic esters like **6-1b** and **6-2b** had been anticipated. Control reactions of diones **6-3a** and **6-4a** with $B(C_6F_5)_3$ in d_8-toluene, in the absence of H_2, were monitored by multinuclear NMR spectroscopy. No formation of **6-3c** or **6-4c** was detected by ^{19}F NMR spectroscopy after 1 hour at 110 ºC, and only minor degradation products had formed (small amounts of HC_6F_5 and DC_6F_5 were detected in the ^{19}F NMR spectra when the reactions were performed in the presence or absence of light). DC_6F_5 was not detected in the hydrogenation reactions of **6-3a** and **6-4a** with $B(C_6F_5)_3$, nor was decafluorobiphenyl. A report by Pampaloni in 2004 described the

Pd-catalyzed reduction of **6-3a** to **6-3e**,[37] which was the same method used to independently synthesize **6-3d** (Scheme 6.5). It was postulated that the generation of the borocyclic radicals begins with an FLP H_2 activation to reduce **6-3a** to **6-3e**. The $B(C_6F_5)_3$-catalyzed reduction of ketones was recently realized,[38,39] and under similar conditions (10 mol% $B(C_6F_5)_3$, 4 atm H_2, d_8-THF, 70 °C) it was found that the hydrogenation of **6-3a** to **6-3e** can be catalyzed, albeit slowly, by $B(C_6F_5)_3$ (Figure 6.13).

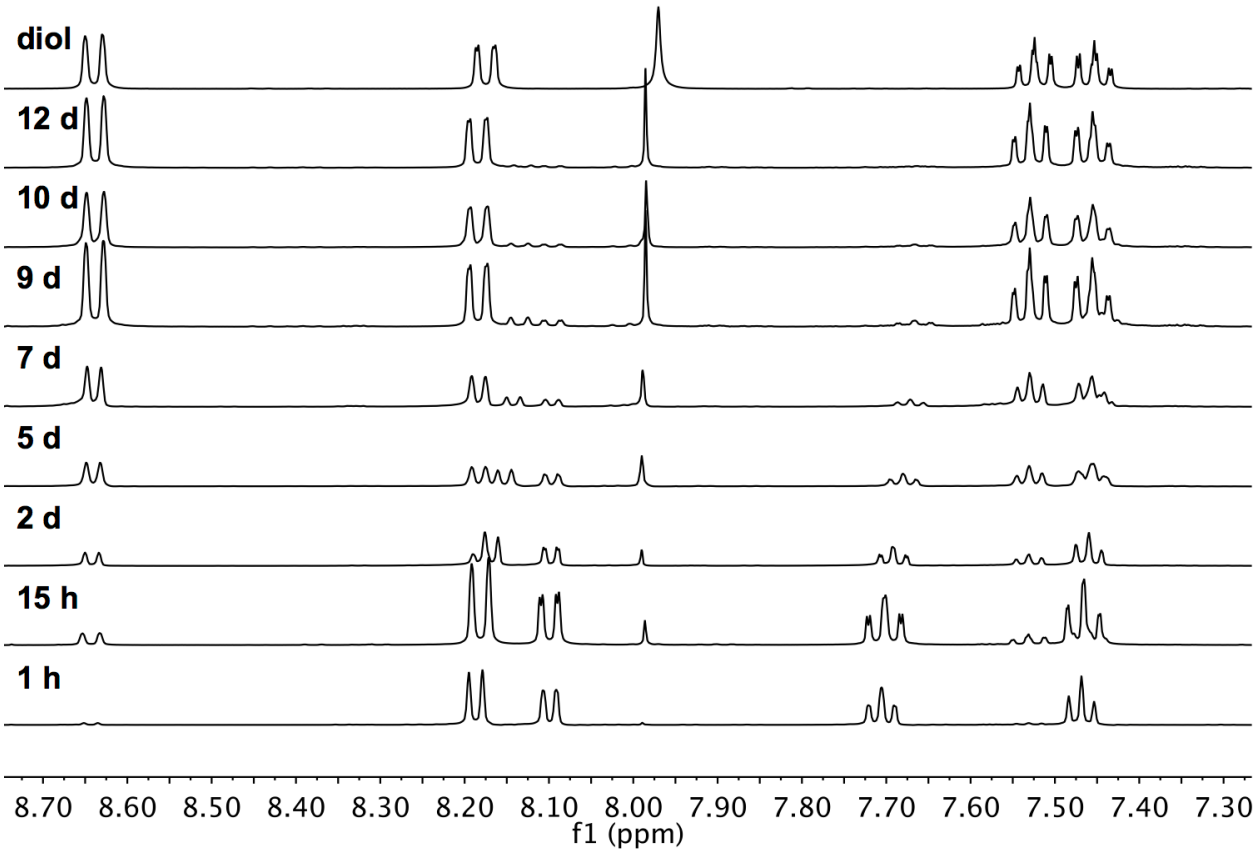

Figure 6.13 – ^{1}H NMR spectra of the catalytic reduction of **6-3a** to diol **6-3e** (500 MHz, 298 K, d_8-THF).

Two pathways to the formation of radical **6-3c** from **6-3e** were envisioned (Scheme 6.7). Pampaloni and co-workers reported that one equivalent of **6-3a** reacts with one equivalent of **6-3e** in toluene to form two equivalents of an organic radical **6-3f**.[37] This process was described as reversible based on spectroscopic evidence. **6-3f** could form *in situ*, and react further with $B(C_6F_5)_3$ to yield **6-3c** and HC_6F_5 (Scheme 6.7, pathway 1). Alternatively, it was established in Chapter 5 that alcohols react with $B(C_6F_5)_3$ at elevated temperatures to liberate HC_6F_5 and form a

B–O bond.[40] Accordingly, once **6-3e** is generated *in situ*, the $B(C_6F_5)_3$ in solution could react with the diol to form a borinic ester, with one -OH functionality remaining. This species could then release $H^{\bullet}$ to form **6-3c** (Scheme 6.7, pathway 2). The second pathway was discredited based on the observed reactivity of isolated **6-3e** with $B(C_6F_5)_3$. When combined in a 1:1 mixture in d_8-toluene at 110 °C, complete consumption of the starting materials with loss of HC_6F_5 was observed after 1 h. Boronic ester **6-3d** was the only product detected by NMR spectroscopy, and it was isolated in quantitative yield. No formation of **6-3c** was observed. It was also found that subjecting isolated **6-3f** (which is an insoluble black powder) to one equivalent of $B(C_6F_5)_3$ and heating the reaction to 110 °C for 1 h in the absence of H_2 resulted in the loss of HC_6F_5 and formation of radical **6-3c**, boronic ester **6-3d**, and a small amount of dione **6-3a**. These data support pathway 1, and also supports the reversible formation of **6-3f** from **6-3a** and **6-3e**. This mechanism was corroborated through DFT calculations performed by Prof. Stefan Grimme.[41]

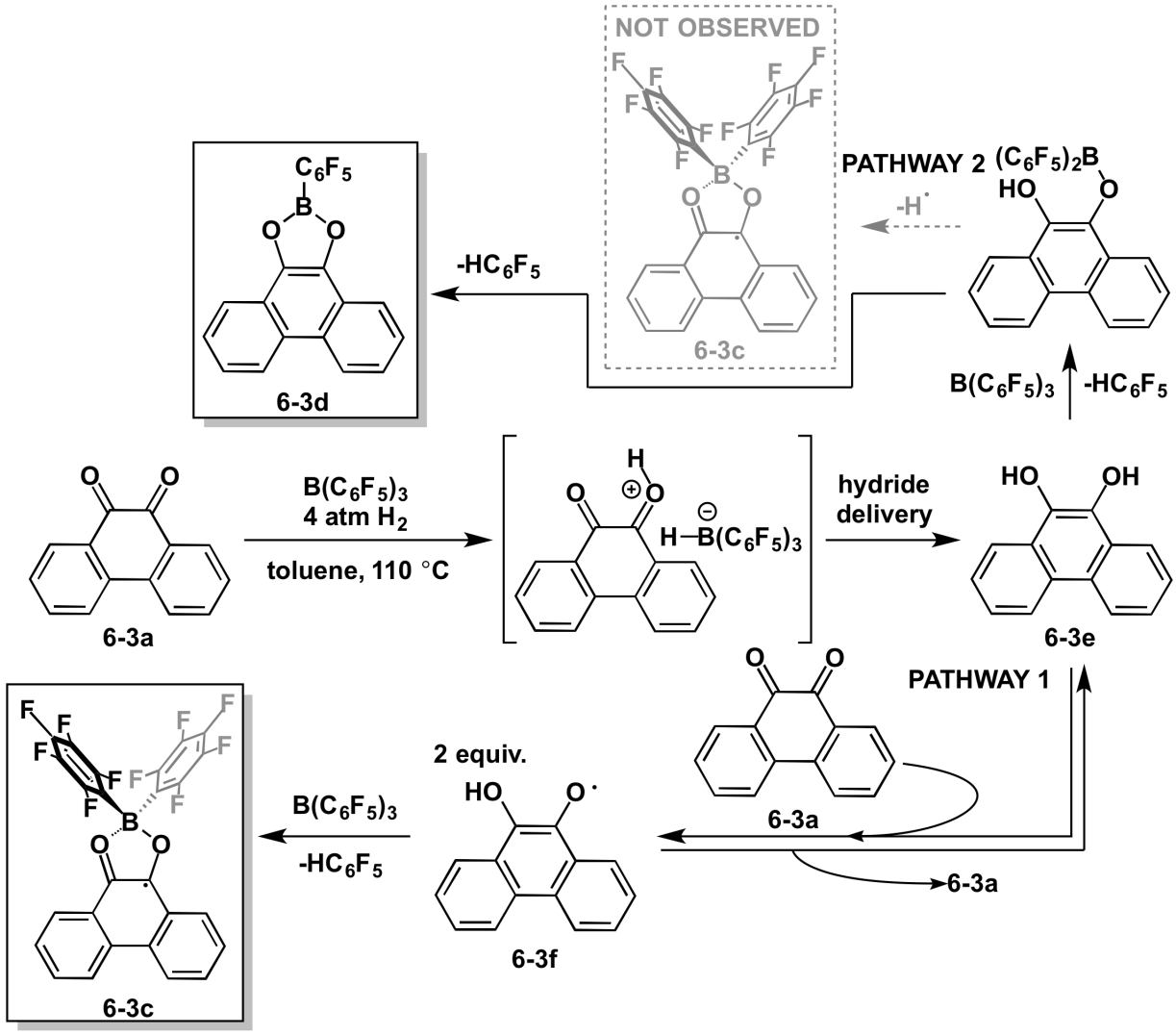

Scheme 6.7 – Mechanistic proposal for the formation of **6-3c** and **6-3d** when **6-3a** is treated with $B(C_6F_5)_3$ and H_2.

6.2.4 One-Electron Reduction Chemistry

The electrochemistry of isolated radicals **6-3c** and **6-4c** was examined, and their cyclic voltammograms are shown in Figure 6.14. A quasi-reversible reduction was observed for both systems, with $E_{1/2} = -0.27$ V vs Fc/Fc^+. Chemical reductions of the isolated borocyclic radicals were then attempted. Main group reductants, such as $PMes_3$, NPh_3, and verdazyl radicals, did not appear to react with **6-3c** or **6-4c**, as determined by multinuclear NMR spectroscopy. Efforts were then focused on $CoCp_2$, which was found to cleanly reduce the borocyclic radicals to the cobaltocenium borate salts **6-3g** and **6-4g** (Scheme 6.8). Single crystals of the pyrene borate **6-4g** were obtained, however single crystals of **6-3g** were not grown, so the analogous

decamethylcobaltocenium borate salt **6-3h** was prepared, which was recrystallized from Et_2O. The solid-state structures of **6-4g** and **6-3h** are shown in Figure 6.15. The anion of **6-3h** has B–O bond lengths of 1.497(3) and 1.500(3) Å, O–C bond lengths of 1.352(3) and 1.364(3) Å, and a C^9–C^{10} bond length of 1.356(3) Å. The anion of **6-4g** has B–O bond lengths of 1.511(4) and 1.508(4) Å, O–C bond lengths of 1.363(3) and 1.363(3) Å, and a C^4–C^5 bond length of 1.360(4) Å.

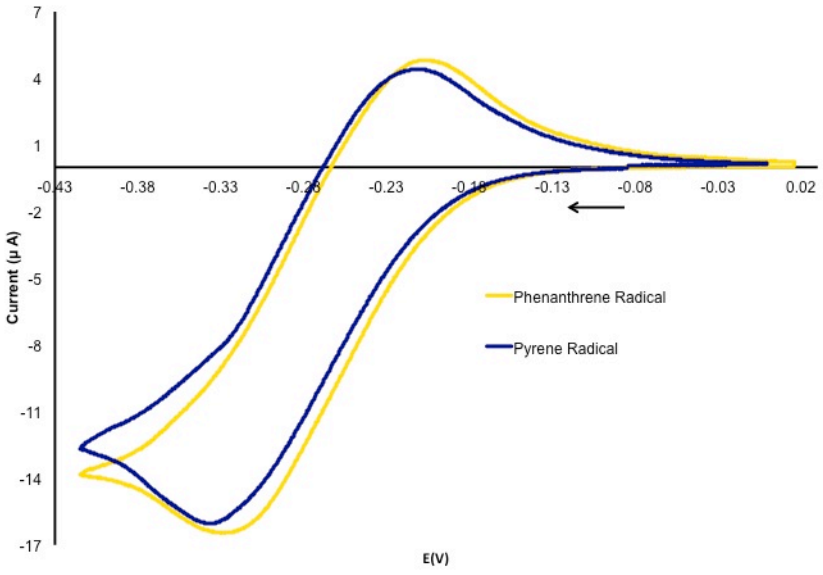

Figure 6.14 – Cyclic voltammogram of **6-3c** (yellow) and **6-4c** (blue) in DCM, referenced vs. Fc/Fc^+.

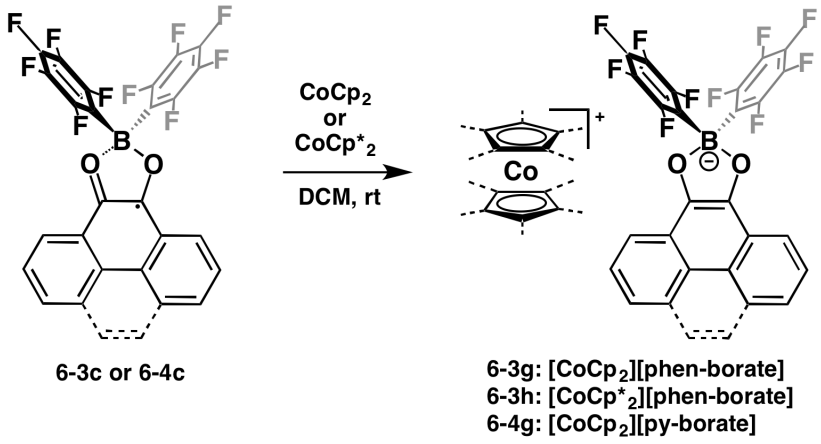

Scheme 6.8 – Chemical reduction of **6-3c** and **6-4c** using $CoCp_2$ and $CoCp^*_2$.

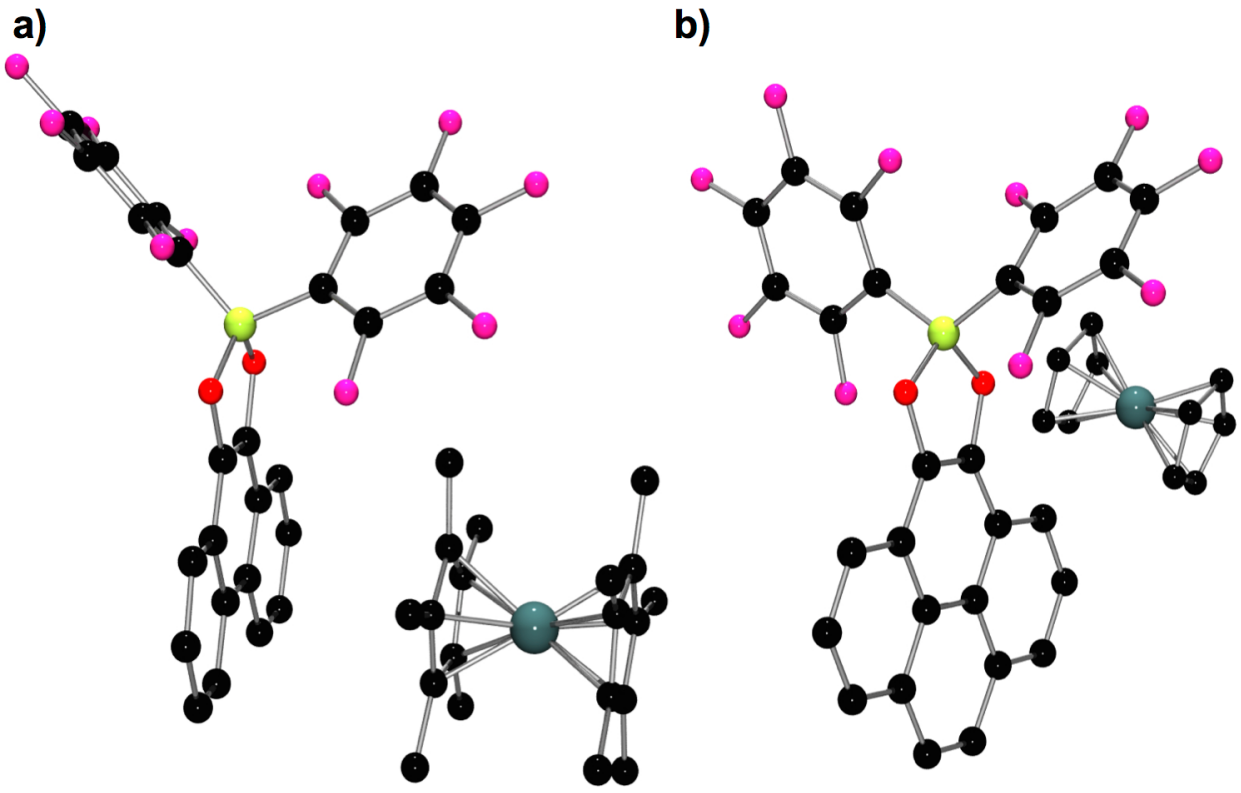

Figure 6.15 – POV-ray depiction of a) **6-3h** and b) **6-4g**, with H atoms omitted for clarity. C: black; B: yellow-green; Co: slate gray; F: pink; O: red.

6.2.5 Reactivity with Nucleophiles

6.2.5.1 Reactivity with Tertiary Phosphines

The reduction of borocyclic radicals **6-3c** and **6-4c** was attempted with $PMes_3$, due to the relative stability of its radical cation,[27] but no reaction was observed when $PMes_3$ was subjected to **6-3c** or **6-4c** in d_8-toluene. After several hours, the formation of a small amount of $HPMes_3$ was detected, which might have formed from trace amounts of water in the NMR solvent. The reactivity of other phosphines with the borocyclic radicals was then explored. Initially, **6-3c** was combined with one equivalent of P(*t*-Bu)$_3$ in CD_2Cl_2. The formation of two new species was observed by ^{31}P NMR spectroscopy: a singlet at 48.9 ppm and a doublet centered at 59.7 ppm (J = 430 Hz) that collapsed to a singlet in the $^{31}P\{^1H\}$ NMR spectrum. The reaction mixture changed from an initial dark black yellow colour to a vibrant yellow colour, and crystals grew from the NMR-scale reaction mixture. X-ray diffraction analysis of these crystals showed the molecular structure to be that of zwitterionic species **6-5a**, where the phosphine is now bound to

the 3-position of the phenanthrene backbone. The ^{31}P NMR resonance at 48.9 ppm was attributed to **6-5a**. This solid state structural confirmation, where an Ar C–H bond from the starting material is absent, supported the proposal for the identity of the second product, which resonates at 59.7 ppm in the ^{31}P NMR spectrum, as phosphonium borate salt **6-5b**. NMR spectroscopic data of other $[HP(t\text{-Bu})_3]^+$ salts,[42,43] and of isolated borate salt **6-3g**, further supported this prediction. While **6-5b** could not be cleanly isolated from the reaction mixture, single crystals of the material grew from a DCM solution of the crude reaction mixture over several months at −35 °C, and the molecular structure of **6-5b** was obtained. The overall reaction is shown in Scheme 6.9, with the solid-state structures of **6-5a** and **6-5b** shown in Figure 6.16. The solid state structure of **6-5a** revealed that the P–C^3 bond has a length of 1.826(2) Å and is bent slightly out of the plane of the phenanthrene ring, with a P–C^3–C^2–C^1 dihedral angle of 169.1(2)°.

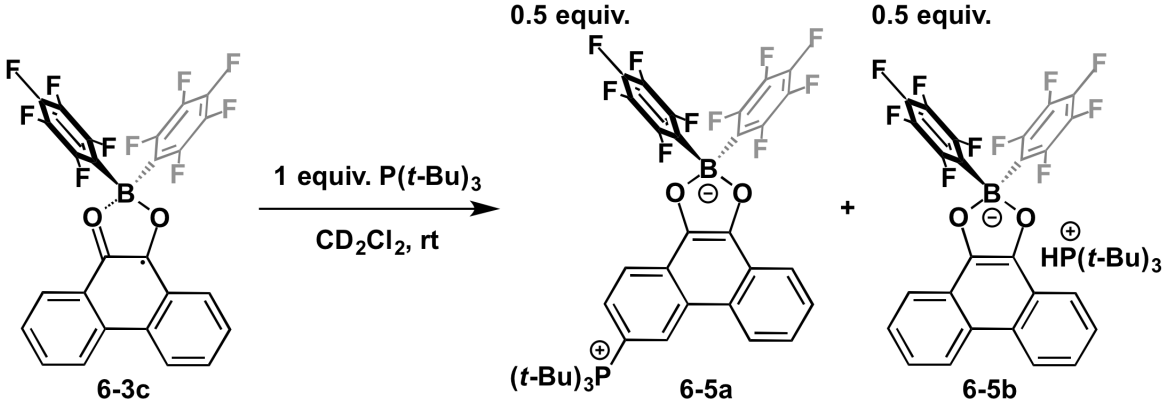

Scheme 6.9 – Reaction of **6-3c** with P(*t*-Bu)$_3$.

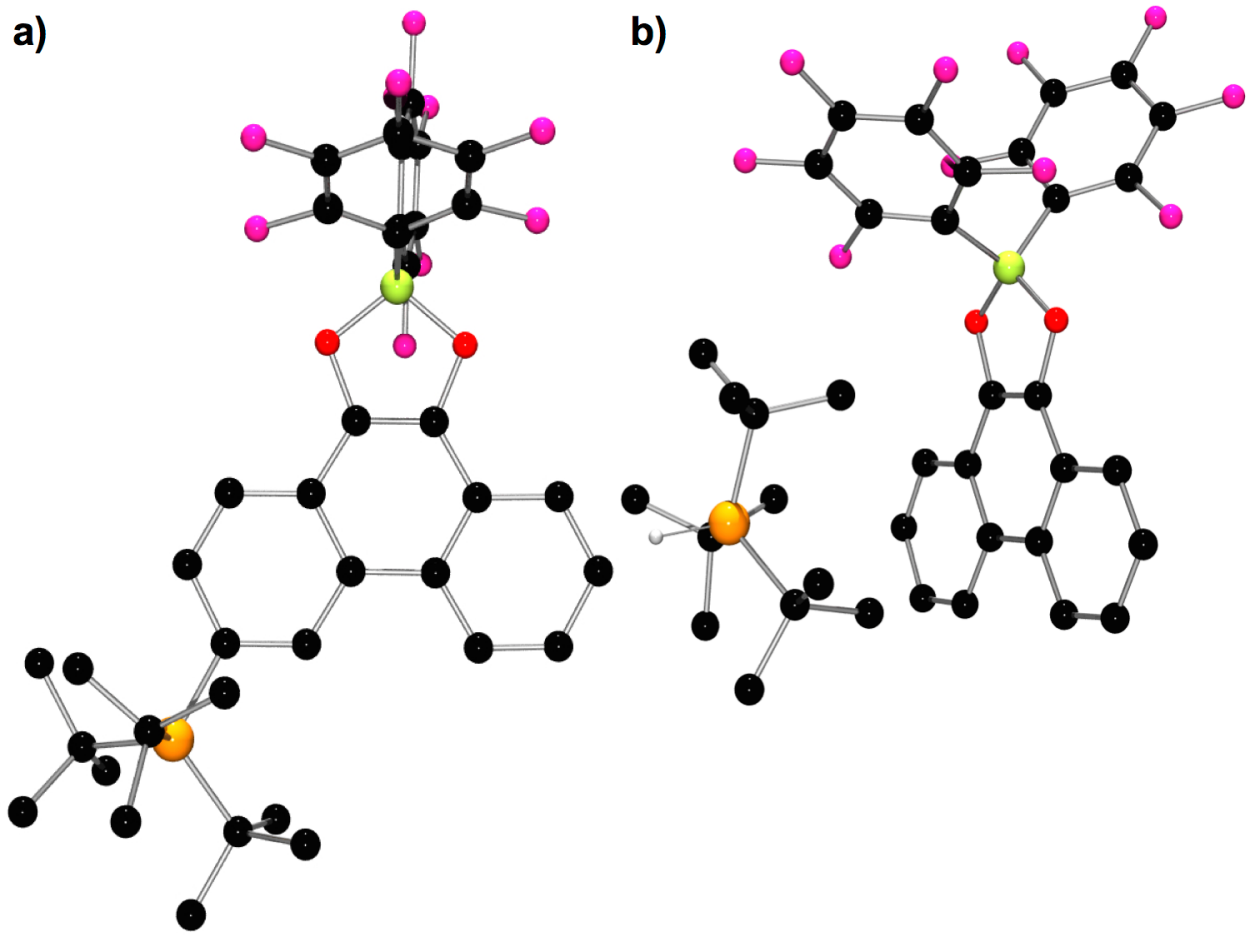

Figure 6.16 – POV-ray depiction of a) **6-5a** and b) **6-5b**, with C–H hydrogen atoms omitted for clarity. C: black; H: grey; B: yellow-green; F: pink; O: red; P: orange.

6-3c was then treated with one equivalent of PPh_3 in d_8-toluene at room temperature, to determine whether the same Ar C–H substitution would be observed with phosphines that are more weakly basic than P(*t*-Bu)$_3$. The dark black yellow solution turned a yellow-orange colour as the reaction proceeded, and the ^{31}P NMR spectrum revealed two new products, with resonances at 28.8 and 22.9 ppm, in addition to unreacted PPh_3. Unlike the reaction of **6-3c** with P(*t*-Bu)$_3$, both ^{31}P NMR resonances were singlets. The ^{11}B NMR spectrum showed two broad resonances at 29.5 ppm and 12.0 ppm. The loss of HC_6F_5 was observed by ^{19}F NMR spectroscopy, and a sparingly soluble, white precipitate formed. These data support the formation boronic ester **6-3d** in the reaction of **6-3c** with PPh_3. Red-orange crystals grew from the crude reaction mixture in the NMR tube, and X-ray diffraction analysis confirmed the identity as zwitterion **6-6a**, where PPh_3 is bound to the 1-position of the phenanthrene ring. This material gives rise to the ^{31}P NMR resonance at 28.8 ppm. The crude reaction mixture was purified by

flash column chromatography, and the two phosphorus-containing products could be cleanly separated from **6-3d**. The product that resonates at 22.9 ppm in the ^{31}P NMR spectrum was isolated as a yellow precipitate. Recrystallization from toluene afforded yellow crystals, X-ray diffraction analysis of which revealed them to contain zwitterion **6-6b**, where PPh_3 is bound to the 3-position of the phenanthrene ring. The overall reaction is shown in Scheme 6.10, with the molecular structures of **6-6a** and **6-6b** shown in Figure 6.17. It was proposed that phosphonium borate salt **6-6c** is produced from the reaction of **6-3c** with PPh_3. Unlike salt **6-5b**, however, the $[HPPh_3]^+$ cation is sufficiently acidic[44] that it protonates a -C_6F_5 ring (which most likely proceeds via proton transfer to a B-bound oxygen atom) to liberate boronic ester **6-3d**, HC_6F_5, and PPh_3. The reaction therefore consumes a substoichiometric amount of PPh_3. **6-6a** has a P–C^1 bond length of 1.800(2) Å, whereas **6-6b** has a slightly shorter P–C^3 bond length of 1.783(2) Å.

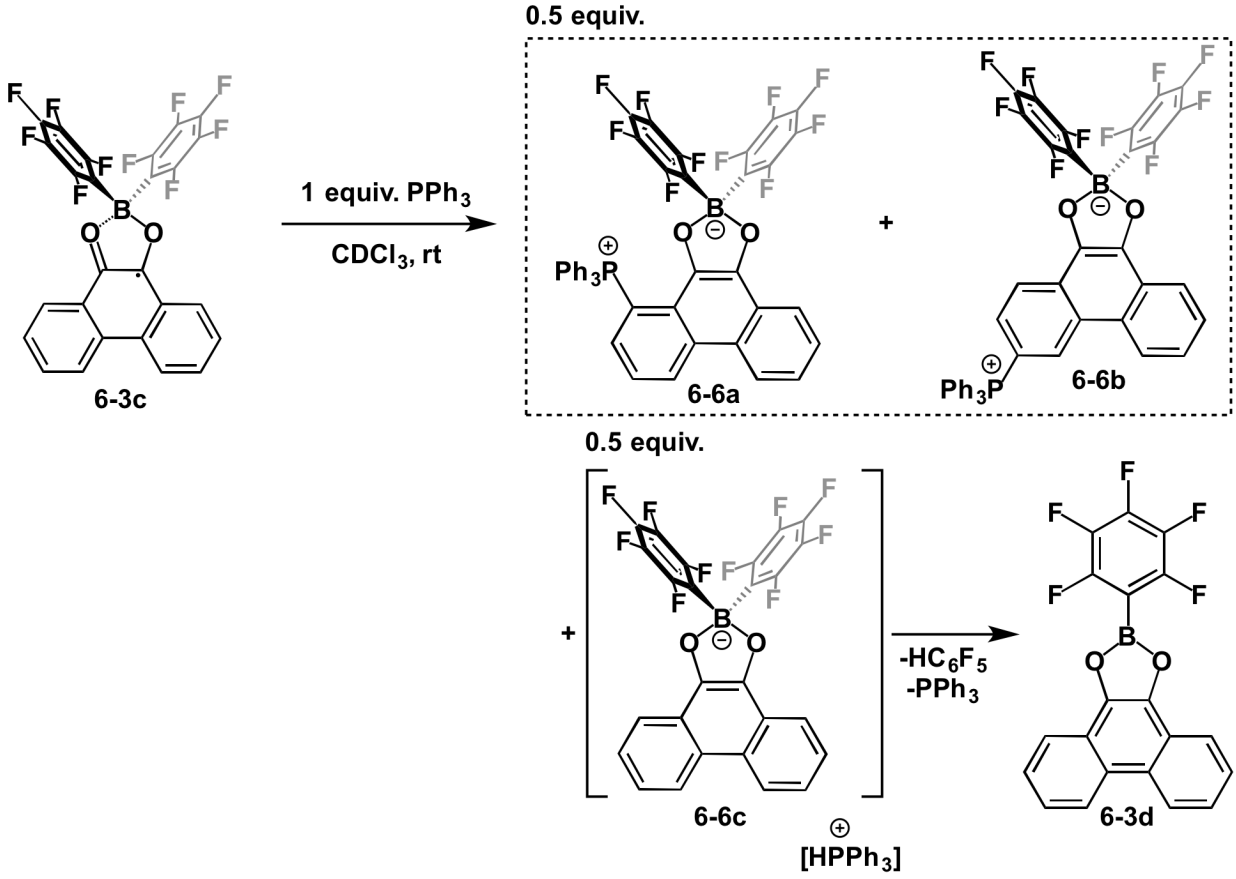

Scheme 6.10 – Reactivity of **6-3c** with PPh_3.

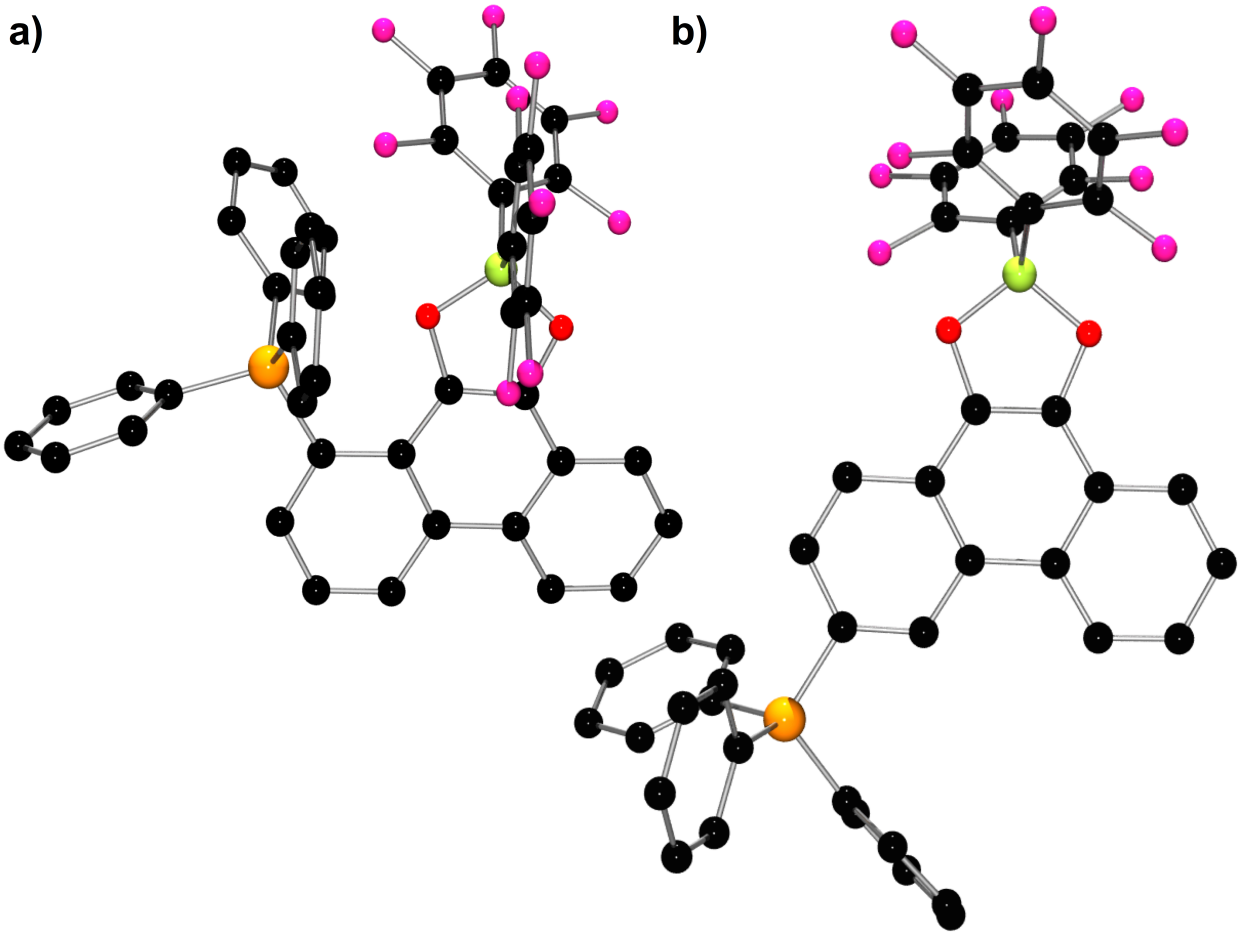

Figure 6.17 – POV-ray depictions of a) **6-6a** and b) **6-6b**, with H atoms omitted for clarity. C: black; B: yellow-green; F: pink; O: red; P: orange.

Similar chemistry was observed with radical **6-4c**. When treated with a substoichiometric amount of PPh_3, the dark black-blue $CDCl_3$ reaction mixture became viscous due to the low solubility of **6-4d** formed during the reaction, and the solution turned a raspberry colour. Loss of HC_6F_5 was observed, with concomitant formation of two new phosphorus containing products, with resonances at 28.6 and 22.2 ppm in the ^{31}P NMR spectrum. The majority of **6-4d** was removed by filtration, and the two new products were separated and purified by preparative TLC. Single crystals of both products were obtained, and X-ray diffraction analysis confirmed their identities as zwitterions **6-7a** and **6-7b**, where PPh_3 is bound at the 3-position and 1-position of the pyrene ring, respectively (Figure 6.18). Both species are very highly coloured: **6-7a** is bright orange-pink and **6-7b** is bright raspberry-pink when dissolved in various organic solvents. **6-7a** has a slightly longer P–C^3 bond length of 1.795(2) Å, compared to the P–C^1 bond length of 1.778(5) Å in **6-7b**.

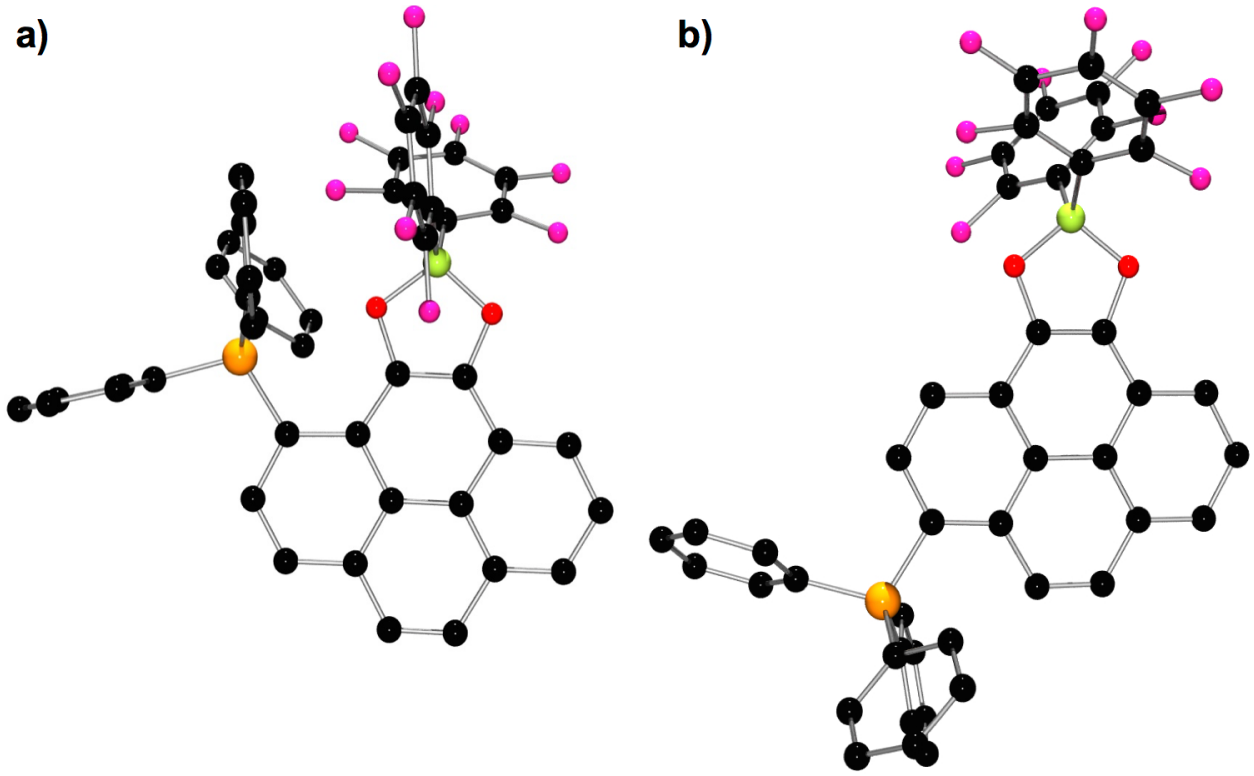

Figure 6.18 – POV-ray depictions of a) **6-7a** and b) **6-7b**, with H atoms omitted for clarity. C: black; B: yellow-green; F: pink; O: red; P: orange.

The proposed mechanism for these reactions is shown in Scheme 6.11. Radicals **6-3c** and **6-4c** are not sufficiently strong oxidants to oxidize P(*t*-Bu)$_3$ or PPh$_3$,[46] however they can be represented as zwitterionic borate radical cations. A S_NAr reaction is proposed, where the phosphine undergoes nucleophilic attack on the radical π-system. This generates a phosphonium borate zwitterionic radical intermediate, which is then deprotonated by a second equivalent of phosphine to re-aromatize the ring and induce electron transfer to a second equivalent of borocyclic radical. Positive charge can be localized at the 1- and 3-positions of both the phenanthrene and pyrene rings, which supports the distribution of regioisomeric products isolated from the reactions with PPh$_3$. This was also supported through DFT calculations of the lowest unoccupied molecular orbital of **6-3c** (Figure 6.19). The high regioselectivity for the reaction of P(*t*-Bu)$_3$ with **6-3c** is likely due to the increased steric congestion, favoring attack at the 3-position. The consumption of a second equivalent of **6-3c** in the reaction with P(*t*-Bu)$_3$ was circumvented by the addition of a stoichiometric amount of [FeCp$_2$][BF$_4$] (which is unreactive

towards **6-3c**). The solvent was changed to MeCN to ensure good solubility of the ferrocenium salt. This resulted in the formation of **6-5a**, $[HP(t\text{-}Bu)_3][BF_4]$, and $FeCp_2$.

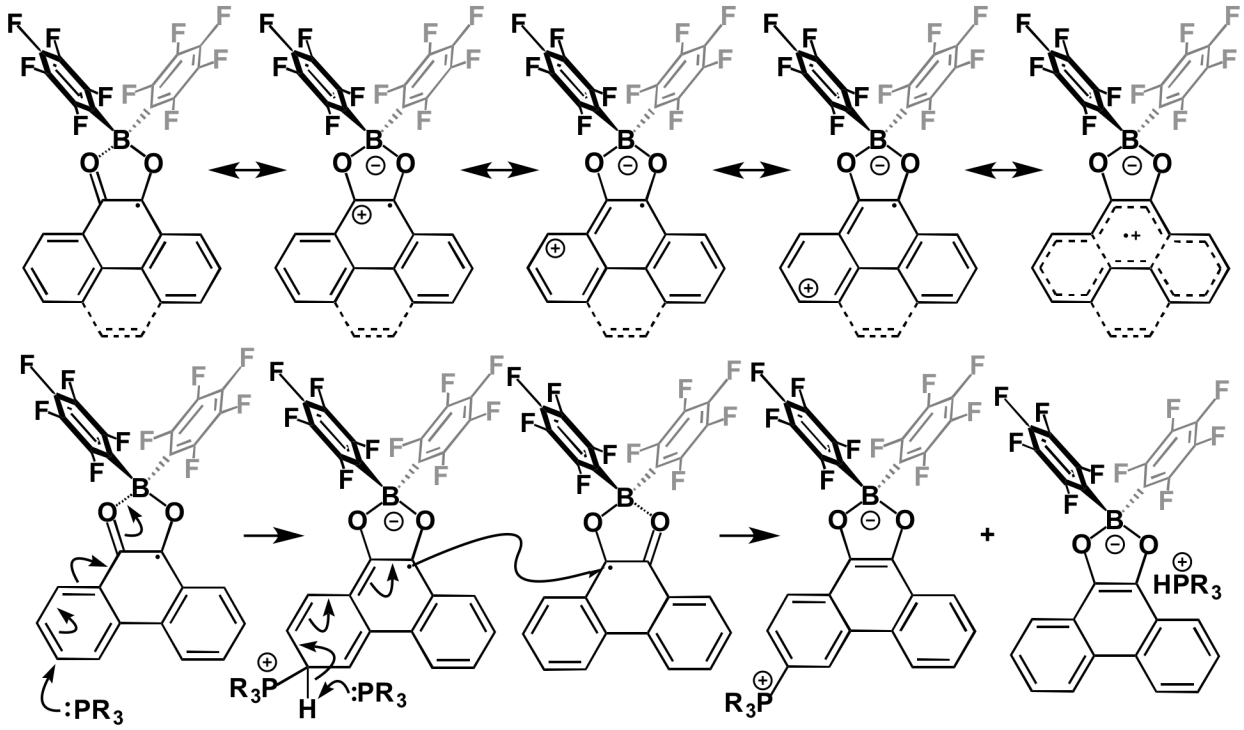

Scheme 6.11 – Resonance structures of radicals **6-3c** and **6-4c**, and the proposed mechanism for phosphine nucleophilic attack.

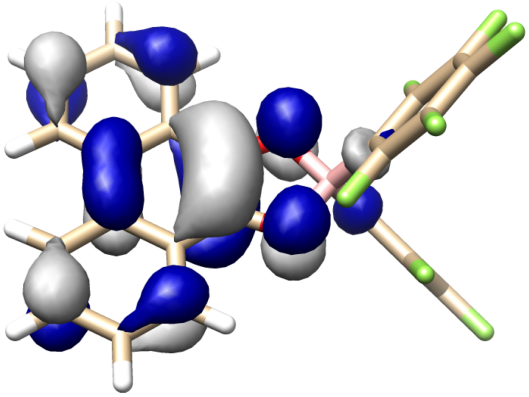

Figure 6.19 – Lowest unoccupied molecular orbital (LUMO) of **6-3c** at a contour surface value of ±0.03 au.

Both solvent and temperature were found to affect the distribution of **6-6a** and **6-6b** produced from the reaction of **6-3c** with PPh_3, and the results are summarized in Table 6.1. The barrier to

generate **6-6a** is likely larger than the barrier to generate **6-6b** for steric reasons. Raising the reaction temperature in either polar or non-polar solvents generated more of **6-6a**, resulting in poorer regioselectivity of the overall reaction. Conducting the reaction in a less polar solvent, such as C_6D_6, resulted in a larger amount of **6-6a** being formed. It was noted that isolated **6-6b** does not convert to **6-6a** when heated to 65 ºC for 24 hours, or when left in $CDCl_3$ at room temperature for 10 days, as evidenced by ^{31}P NMR spectroscopy. If the S_NAr reaction with phosphine is a) rate-limiting, and b) an equilibrium, the non-polar solvent may be stabilizing the intermediate for the generation of **6-6a** to a greater extent than the polar solvent. Further mechanistic work is required to validate this reasoning. Similar behaviour was observed in the reaction of **6-4c** with PPh_3. Variable temperature NMR spectroscopic studies on isolated **6-7a** showed that it does not convert to **6-7b**, and isolated **6-7b** does not convert into **6-7a** when heated in d_8-toluene at 110 °C for several hours.

Table 6.1 – Ratio of **6-6a** : **6-6b** for the reaction of **6-3c** with PPh_3 under various reaction conditions.*

Solvent	Temperature (°C)	6-6a : 6-6b
C_6D_6	25	1 : 3
	60	1 : 2
$CDCl_3$	25	1 : 12
	60	1 : 5

*Determined by quantitative ^{31}P NMR spectroscopy (after 48 h at 60 ºC and 96 h at 25 ºC). The $Ph_3P{=}O$ adduct of **6-3d** was detected as the reactions progressed, likely due to O_2 permeating the NMR cap.

6.2.5.2 Reactivity with Secondary Phosphines

Radical **6-4c** reacts with substoichiometric amounts of $HPPh_2$ in $CDCl_3$ (Scheme 6.12), with the loss of HC_6F_5 and the formation of boronic ester **6-4d** observed by NMR analysis of the reaction mixture. A new species **6-8a** was observed by ^{31}P NMR spectroscopy; it resonated as a doublet

centered at 5.9 ppm in the ^{31}P NMR spectrum, with $^{1}J_{PH}$ = 547 Hz. A single crystal X-ray diffraction study of **6-8a** confirmed its identity as a zwitterionic phosphonium borate (Figure 6.20), where the $HPPh_2$ substituent is bound at the 3-position of the pyrene ring. The observed regioselectivity may be due to H-bonding between the oxygen atoms and the P–H bond. Compound **6-8a** was envisioned as a precursor to the neutral phosphine-borane system **6-9a** through the loss of HC_6F_5. Small scale reactions appeared promising, where heating a sample of **6-8a** to 150 °C in C_6D_5Br for three hours led to the loss of one equivalent of HC_6F_5 and formation of a new three-coordinate boron species, as evidenced by the broad ^{11}B NMR resonance at 29.2 ppm and the ^{19}F NMR resonances at −126.3, −147.2, and −161.2 ppm. A new singlet in the ^{31}P NMR spectrum at −5.2 ppm provided additional evidence that the neutral species **6-9a** had formed, however attempts to isolate the material resulted in decomposition, and increasing the scale of the reaction (which was performed by Mr. Pavel Zatsepin) resulted in a complex product distribution.

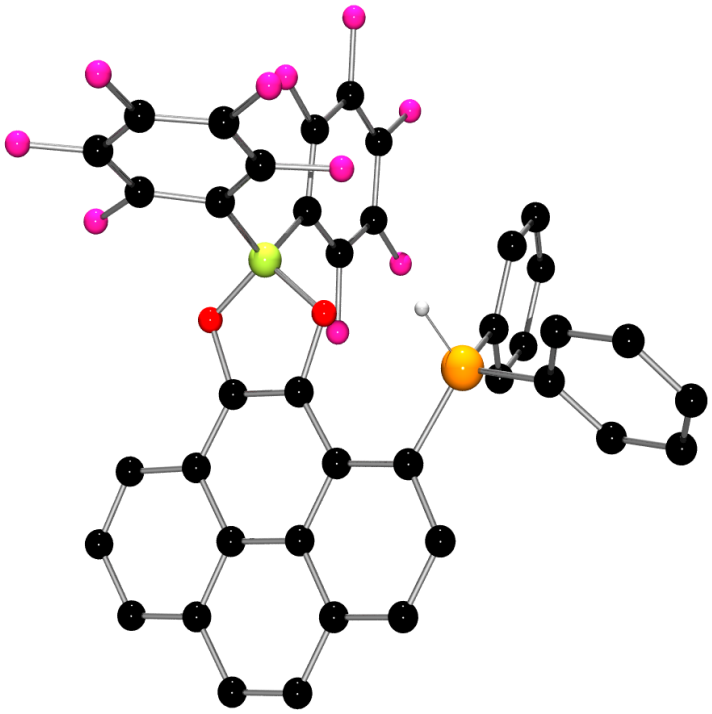

Figure 6.20 – POV-ray depiction of **6-8a**, with C–H atoms omitted for clarity. C: black; H: grey; B: yellow-green; F: pink; H: turquoise; O: red; P: orange.

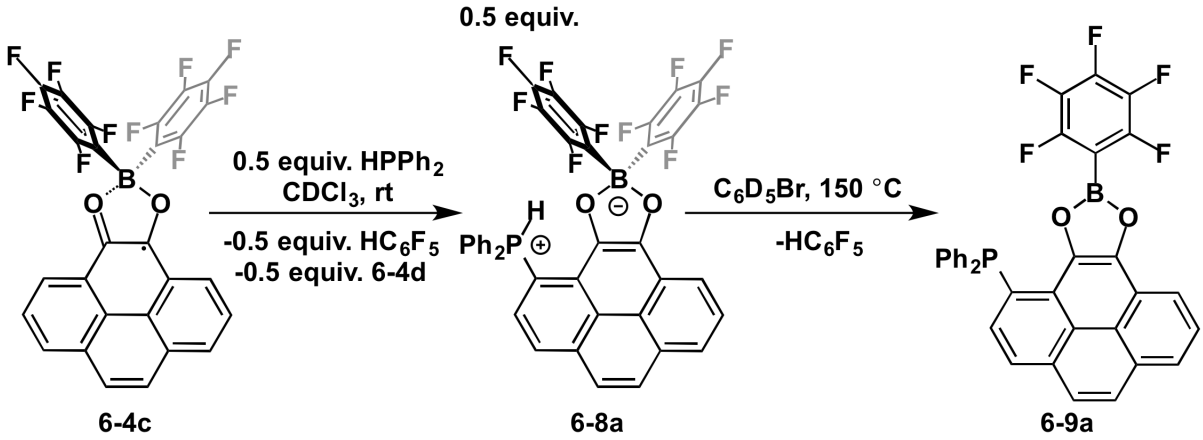

Scheme 6.12 – Formation of zwitterion **6-8a**, and subsequent thermal loss of HC_6F_5 to form **6-9a**.

6.2.5.3 Reactivity with Other Nucleophiles

The reactivity of other nucleophiles with radical **6-3c** was explored, specifically carbenes and N-heterocycles. When **6-3c** was combined with one equivalent of IMes in THF, an immediate reaction occurred and the colour of the solution turned from dark black yellow to clear orange red (Scheme 6.13). Following workup and flash column chromatography, a yellow powder was isolated and recrystallized to afford yellow blocks. X-ray diffraction analysis of the crystals confirmed the identity as zwitterionic product **6-10a** (Figure 6.21), where a new C–C bond has formed at the 3-position of the phenanthrene ring (likely due to the steric bulk of IMes). This reaction was not as clean as the reactions of **6-3c** and **6-4c** with phosphines, and unidentified impurities were detected by ^{1}H and ^{19}F NMR spectroscopy, however **6-10a** was the only zwitterionic product isolated. A byproduct of this reaction, based on the mechanism outlined in Scheme 6.11, is presumed to be $[IMesH][C_{14}H_8O_2B(C_6F_5)_2]$ **6-10b**, where the borate anion is that which is found in **6-3g**, **6-3h**, and **6-5b**.

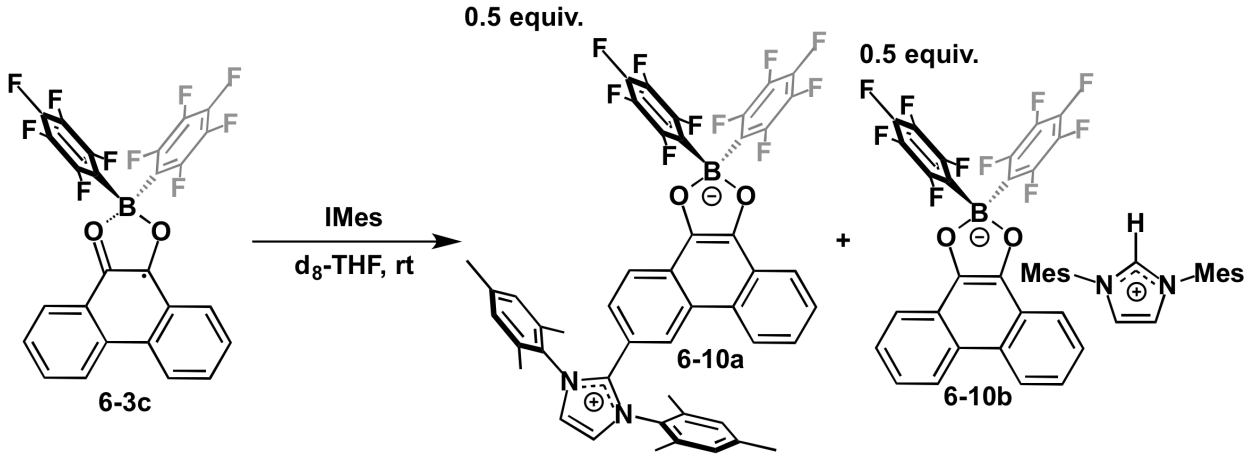

Scheme 6.13 – Reaction of **6-3c** with IMes.

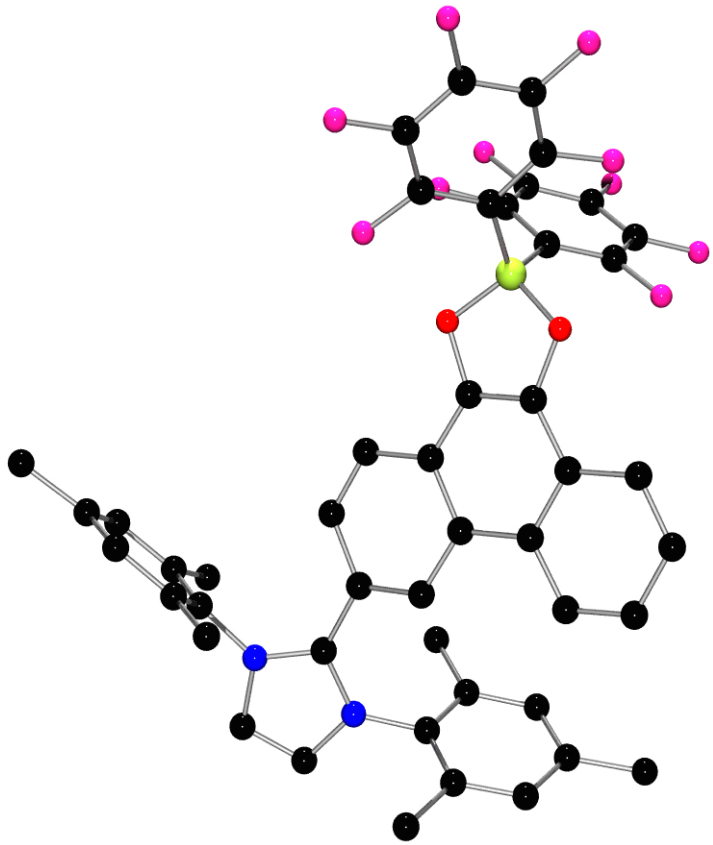

Figure 6.21 – POV-ray depiction of **6-10a**, with H atoms omitted for clarity. C: black; B: yellow-green; F: pink; N: blue; O: red.

Lastly, DMAP was investigated as a representative N-heterocycle, to determine whether this class of nucleophiles would behave in an analogous fashion to the phosphines discussed in

section 6.2.5.1. When **6-3c** was combined with one equivalent of DMAP in toluene and allowed to stir at room temperature, the solution turned a yellow colour and a large amount of a yellow-orange precipitate formed (Scheme 6.14). The precipitate was collected on a frit, dried, and dissolved in DMSO. It was immediately evident that the new product **6-11** did not have a DMAP bound to the phenanthrene backbone like the related products generated from phosphine or carbene attack. The ^{1}H NMR spectra of **6-5a**, **6-6a**, **6-6b**, and **6-10a** all show an unsymmetrical phenanthrene backbone, with 7 inequivalent Ar C–H resonances. The ^{1}H NMR spectrum of **6-11** appeared to contain two different, symmetric phenanthrene units, and two symmetric DMAP units, which was further supported by 2D NMR experiments. The ^{19}F NMR spectrum showed two equivalent -C_6F_5 rings, and two inequivalent -C_6F_5 rings. The ^{11}B NMR spectrum showed two broad resonances at 10.3 and 6.3 ppm, indicating that the product consists of two inequivalent borate centres. The material was recrystallized from a cold DCM solution, and X-ray diffraction analysis of the single crystals confirmed the solid state structure of **6-11** as a borate salt, where the cation contains a four-coordinate boron centre but is overall cationic due to the two DMAP molecules that have undergone attack at the 9- and 10-positions of the phenanthrene ring (Figure 6.22). The solid state structure of the anion has similar metrical parameters to those observed in **6-3h** and **6-5b**, however the cation features a strongly canted borate group due to the bound DMAP rings. The C–O bond lengths are 1.389(4) and 1.387(5) Å, the C^{9}–N and C^{10}–N bond lengths are 1.511(4) and 1.511(5) Å, and the C^{9}–C^{10} bond length is 1.571(5) Å, diagnostic of the single bond character, when compared to the C^{9}–C^{10} bond length of 1.356(3) Å in **6-3h** and 1.370(4) Å in **6-5b**. The ∠OCN angles are 109.5(3)° and 105.5(3)°; ∠$OC^{9}C^{14}$ and ∠$OC^{10}C^{11}$ angles are 110.0(3)° and 112.9(3)°, respectively; and ∠$NC^{9}C^{14}$ and ∠$NC^{10}C^{11}$ angles are 109.0(3)° and 109.0(3)°, respectively. The C^{14}–C^{9}–C^{10}–C^{11} dihedral angle is 36.0(4)°, the O^{1}–C^{9}–C^{10}–O^{2} dihedral angle is 37.4(3)°, and the N^{3}–C^{9}–C^{10}–N^{1} dihedral angle is 35.6(4)°. The reasoning for the observed reactivity with DMAP is not fully understood, however it is proposed that the selectivity for attack the 9- and 10- positions may be due to its small size and its propensity to react with carbonyl-type functional groups.[47]

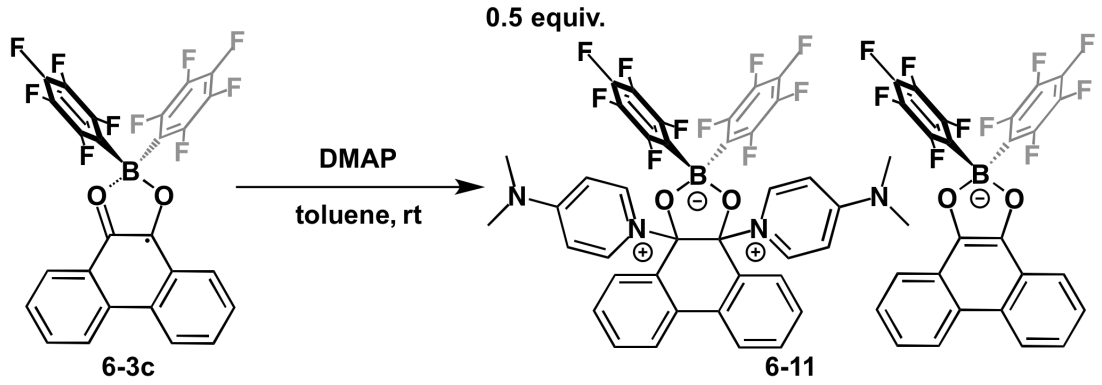

Scheme 6.14 – Reaction of **6-3c** with DMAP.

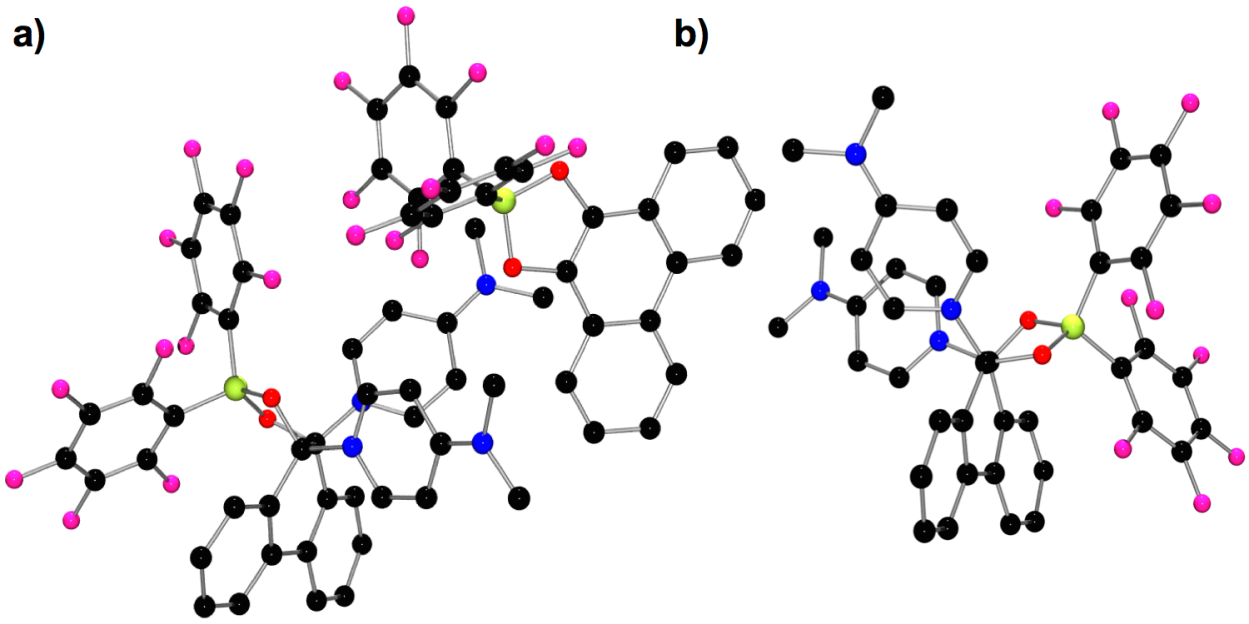

Figure 6.22 – POV-ray depiction of a) salt **6-11** and b) cation of **6-11**, with H atoms omitted for clarity. C: black; B: yellow-green; F: pink; N: blue; O: red.

6.3 Conclusions

This chapter has presented the synthesis, purification, isolation, and characterization of stable borocyclic radicals **6-3c** and **6-4c**. Potential mechanisms were investigated experimentally, which were supported through DFT studies. Electrochemical and chemical reductions of **6-3c** and **6-4c** were achieved, isolating borate salts **6-3g**, **6-3h**, and **6-4g**. The reactivity of the borocyclic radicals with various nucleophiles was investigated: they were found to undergo

nucleophilic attack when exposed to P(*t*-Bu)$_3$, PPh$_3$, IMes, and DMAP, yielding zwitterionic species and either borate salts or boronic esters **6-3d**/**6-4d**.

6.4 Experimental Details

6.4.1 General Considerations

All reactions and workup procedures were performed under an inert atmosphere of dry, oxygen-free N_2 using standard Schlenk techniques or a glovebox (MBraun, equipped with a −35 °C freezer) unless otherwise specified. Pentane, dichloromethane, and toluene (Aldrich) were dried using a Grubbs-type Innovative Technologies solvent purification system. Chloroform was dried by stirring over CaH_2 for several days followed by distillation. THF was dried by stirring over Na/benzophenone for several days, followed by vacuum transfer. Deuterated solvents (CD_2Cl_2, $CDCl_3$, d_6-DMSO, d_8-toluene, C_6D_5Br, d_8-THF) were purchased from Cambridge Isotope Laboratories, Inc. and stored over activated 4 Å molecular sieves prior to use, unless otherwise specified. 1,2-Cyclohexanedione **6-2a**, 9,10-phenanthrenequinone **6-3a**, pyrene, bis(pentamethylcyclopentadienyl)cobalt(II), Pd/C, and DMAP were purchased from Sigma-Aldrich. 2-Benzoylpyridine **6-1a** was purchased from Alfa Aesar. Bis(cyclopentadienyl)cobalt(II), P(*t*-Bu)$_3$, PPh$_3$, and IMes were purchased from Strem. All were used without further purification. B(C_6F_5)$_3$ was purchased from Boulder Scientific and sublimed under vacuum at 85 °C prior to use. 4,5-Pyrenedione **6-4a**[48] and 9,10-phenanthrenediol **6-3e**[37] were prepared according to literature procedures. Hydrogen gas (Grade 5.0) was obtained from Linde and purified through a Matheson Model 450B or Matheson Nanochem WeldAssureTM gas purifier. Thin-layer chromatography (TLC) and preparative TLC were performed on 0.5 mm EMD Silica Gel 60 F_{254} plates, with visualization of the developed plates under UV light (254 nm). Silica gel for glovebox manipulations was dried under vacuum at 150 °C. Column chromatography was performed with Silicycle Silia-P Flash Silica Gel using plastic syringes (in a glovebox) or glass columns (in air).

NMR spectra were obtained on a Bruker Avance III 400 MHz, Agilent DD2 500 MHz, or Agilent DD2 600 MHz spectrometer and spectra were referenced to residual solvent of d_8-toluene (^{1}H = 2.08 for CH_3; ^{13}C = 20.40 for CH_3), CD_2Cl_2 (^{1}H = 5.32; ^{13}C = 54.0), $CDCl_3$ (^{1}H = 7.26; ^{13}C = 77.2), d_6-DMSO (^{1}H = 2.50; ^{13}C = 39.5), d_8-THF (^{1}H = 3.58 for CH_2O; ^{13}C = 67.2 for CH_2O), or externally (^{19}F: $CFCl_3$, ^{11}B: (Et_2O)BF_3, ^{31}P: 85% H_3PO_4). Chemical shifts (δ) are

reported in ppm and coupling constants are listed in Hz. NMR assignments are supported by additional 2D experiments. Elemental analyses (C,H,N) and high resolution mass spectrometry (HRMS) were performed in house. UV/vis absorption spectra were obtained on a Varian Cary 5000 UV-vis-NIR spectrophotometer using dry dichloromethane solutions in quartz cuvettes. Electrochemistry was performed with a BASi Epsilon potentiostat. A standard three-electrode cell with a 2.0 mm diameter Pt button working electrode, a Ag/Ag^+ reference electrode, and a Pt wire counter electrode was used, with a 10 mV s^{-1} scan rate. Electrochemical measurements were conducted in a nitrogen-filled glovebox in dry dichloromethane containing 0.1 M tetrabutylammonium hexafluorophosphate as the supporting electrolyte, and were referenced against the ferrocene/ferrocenium (Fc/Fc^+) redox couple. Electron paramagnetic resonance (EPR) measurements were performed at 298 K using a Bruker ECS-EMX X-band EPR spectrometer equipped with an ER4119HS cavity. Simulations were performed using PEST WinSIM Software.

6.4.2 Syntheses and Characterizations

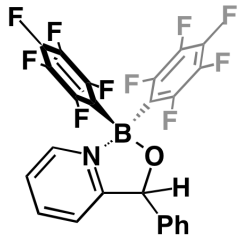

Synthesis of 6-1b

Method 1: FLP hydrogenation

In a nitrogen-filled glovebox, **6-1a** (37 mg, 0.2 mmol) was dissolved in 0.5 mL toluene and transferred to a vial containing $B(C_6F_5)_3$ (102 mg, 0.2 mmol). The vial containing the **6-1a** was washed with 2 x 0.25 mL toluene, and the washes were transferred to the reaction mixture. The resulting yellow solution was transferred to a 10 mL Schlenk bomb, and the vial was rinsed with 2 x 0.5 mL toluene, with washes transferred to the reaction vessel. The Schlenk bomb was sealed and subjected to one freeze-pump-thaw cycle, followed by addition of H_2 at −196 °C. The reaction was heated to 100 °C for 22 h. Once complete, the reaction was concentrated *in vacuo*, yielding a yellow-brown solid (crude yield: 105 mg). The solid was dissolved in toluene and filtered over a plug of silica. The filtrate was concentrated *in vacuo*, and the resulting material was purified by recrystallization from slow diffusion of pentane into a toluene solution of **6-1b** at 35 °C. Successive recrystallizations yielded the desired product in 51% yield (54 mg). Crystals

suitable for single crystal X-ray diffraction studies were grown by slow diffusion of pentane into a DCM solution of **6-1b** at −35 °C.

Method 2: Hydroboration

In a nitrogen-filled glovebox, **6-1a** (37 mg, 0.2 mmol) was dissolved in 0.5 mL toluene and transferred to a vial containing a solution of $HB(C_6F_5)_2$ (69 mg, 0.2 mmol) in 3 mL toluene, equipped with a magnetic stir bar. Upon initial addition, the solution became a homogenous yellow colour, however with stirring the colour quickly dissipated. The vial containing the **6-1a** was washed with 3 x 0.5 mL toluene, and the washes were transferred to the reaction mixture. The resulting colourless solution was stirred under a N_2 atmosphere at 35 °C. The reaction was complete after 48 h, as evidenced by ^{19}F and ^{11}B NMR spectroscopy, and so it was concentrated *in vacuo*, yielding a white solid. The solid was washed with 10 mL pentane, and the remaining material was dissolved in DCM, transferred to a tared vial, and concentrated to yield the desired product as a white solid in 83% yield (87 mg).

^{1}H NMR (500 MHz, 298 K, $CDCl_3$): δ 8.64 (d, $^3J_{HH}$ = 5.5 Hz, 1H, py *o*-C<u>H</u>), 8.07 (td, $^3J_{HH}$ = 7.8 Hz, $^4J_{HH}$ = 1.3 Hz, 1H, py *p*-C<u>H</u>), 7.65–7.62 (m, 1H, py N-CH-C<u>H</u>), 7.44–7.35 (m, 6H, C_6H_5 and py N-C-C<u>H</u>), 6.22 (s, 1H, O-C<u>H</u>).

^{19}F NMR (470 MHz, 298 K, $CDCl_3$): δ −133.9 (dd, $^3J_{FF}$ = 24.0 Hz, $^4J_{FF}$ = 9.4 Hz, 2F, *o*-C_6F_5), −135.3 (dd, $^3J_{FF}$ = 24.9 Hz, $^4J_{FF}$ = 9.4 Hz, 2F, *o*-C_6F_5), −155.7 to −155.8 (m, 1F, *p*-C_6F_5), −156.6 (t, $^3J_{FF}$ = 20.2 Hz, 1F, *p*-C_6F_5), −163.0 to −163.1 (m, 4F, *m*-C_6F_5).

^{11}B NMR (160 MHz, 298 K, $CDCl_3$): δ 6.4 (s).

^{13}C{^{1}H} NMR (126 MHz, 298 K, $CDCl_3$), partial: δ 162.0 (s, py quat. C), 148.6 (dm, $^1J_{CF}$ ~ 246 Hz, C_6F_5), 148.0 (dm, $^1J_{CF}$ ~ 240 Hz, C_6F_5), 142.5 (s, py *p*-<u>C</u>H), 141.7 (s, py *o*-<u>C</u>H), 139.5 (s, Ph quat. C), 137.4 (dm, $^1J_{CF}$ ~ 245 Hz, C_6F_5), 129.3 (s, Ph *m*-<u>C</u>H), 129.2 (s, Ph *p*-<u>C</u>H), 127.7 (s, Ph *o*-<u>C</u>H), 124.8 (s, py N-CH-<u>C</u>H), 122.1 (s, py N-C-<u>C</u>H), 82.1 (s, O-<u>C</u>H).

HRMS (DART) calcd for $[C_{24}H_{11}BF_{10}NO]^+$ ($[M+H]^+$) 530.0774, found 530.0782.

Elemental Analysis calcd (%) for $C_{24}H_{10}BF_{10}NO$: C 54.48; H 1.90; N 2.65; Found: C 54.88; H 1.53; N 2.82.

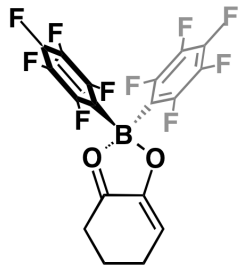

Synthesis of 6-2b

In a nitrogen-filled glovebox, **6-2a** (28 mg, 0.25 mmol) was dissolved in 0.5 mL toluene and transferred to a vial containing $B(C_6F_5)_3$ (128 mg, 0.25 mmol). The initial vial was rinsed with 0.5 mL toluene, which was transferred to the reaction mixture. The resulting yellow solution was transferred to a 10 mL Schlenk bomb equipped with a magnetic stir bar, and rinsed with 2 x 1 mL toluene. The rinses were added to the reaction flask, which was sealed and heated to 110 °C for 1 h. After 1 h the volatiles were removed *in vacuo*, and the resulting pink-brown solid was dissolved in DCM, transferred to a pre-weighed vial, and concentrated to yield the desired product (107 mg, 94%). Crystals suitable for single crystal X-ray diffraction studies were grown by slow diffusion of layered pentane into a DCM solution of **6-2b** at −35 °C.

^{1}H NMR (400 MHz, 298 K, CD_2Cl_2): δ 6.66 (t, $^3J_{HH}$ = 5.0 Hz, 1H, sp^2-C<u>H</u>), 3.06 (td, $^3J_{HH}$ = 6.8 Hz, $^4J_{HH}$ = 1.6 Hz, 2H, C(O)-C<u>H</u>$_2$), 2.65–2.60 (m, 2H, CH-C<u>H</u>$_2$), 2.18 (p, $^3J_{HH}$ = 6.4 Hz, 2H, CH_2-C<u>H</u>$_2$-CH_2).

^{19}F NMR (377 MHz, 298 K, CD_2Cl_2): δ −135.6 to −135.7 (m, 2F, *o*-C_6F_5), −156.6 to −156.7 (m, 1F, *p*-C_6F_5), −164.2 to −164.4 (m, 2F, *m*-C_6F_5).

^{11}B NMR (128 MHz, 298 K, CD_2Cl_2): δ 13.7 (s).

^{13}C{^{1}H} NMR (101 MHz, 298 K, CD_2Cl_2, partial): δ 209.5 (s, <u>C</u>=O), 154.5 (s, CH=<u>C</u>-O), 148.5 (dm, $^1J_{C\text{-}F}$ ~ 244 Hz, CF), 141.3 (dm, $^1J_{C\text{-}F}$ ~ 252 Hz, CF), 137.7 (dm, $^1J_{C\text{-}F}$ ~ 250 Hz, CF), 130.1 (s, <u>C</u>H=C-O), 31.2 (s, C(O)-<u>C</u>H$_2$), 25.1 (s, CH-<u>C</u>H$_2$), 22.6 (s, CH_2-<u>C</u>H$_2$-CH_2).

HRMS (EI) calcd for $C_{18}H_7BF_{10}O_2$ 456.0379, found 456.0381.

Elemental Analysis calcd (%) for $C_{18}H_7BF_{10}O_2$: C 47.41; H 1.55; Found: C 47.36; H 1.20.

General Procedure for the Synthesis of Radicals 6-3c and 6-4c

A solution of dione (0.75 mmol) was transferred quantitatively to a vial containing $B(C_6F_5)_3$ (384 mg, 0.75 mmol) with 3 x 2 mL toluene. The resulting dark solution was transferred to a 50 mL Schlenk bomb equipped with a magnetic stir bar. The vial was rinsed with 2 x 2 mL toluene, and the washes were transferred to the Schlenk bomb. The bomb was sealed and subjected to one

freeze-pump-thaw cycle, followed by the addition of H_2 (4 atm) at −196 °C. The bomb was heated to 110 °C for 1 h, after which the reaction was cooled to room temperature and the volatiles were removed under reduced pressure, resulting in a mixture of dark green solid (**6-3c**) or dark blue solid (**6-4c**) and white solid. The crude mixture was washed with 10 mL pentane, and the remaining material was purified by flash column chromatography (eluent = 1:1 pentane:DCM) in a nitrogen-filled glovebox. Crystals suitable for single crystal X-ray diffraction studies were grown by slow diffusion of layered pentane into a DCM solution of the radical at −35 °C.

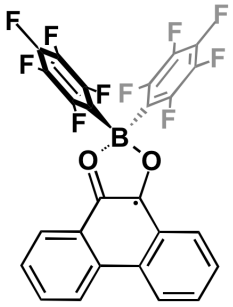

Characterization of 6-3c

Isolated in 79% yield (327 mg).

^{1}H NMR (400 MHz, 298 K, CD_2Cl_2): NMR silent.

^{19}F NMR (377 MHz, 298 K, CD_2Cl_2): δ −159.9 (br s, Ar-F).

^{11}B NMR (128 MHz, 298 K, CD_2Cl_2): NMR silent.

^{13}C{^{1}H} NMR (101 MHz, 298 K, CD_2Cl_2): NMR silent.

HRMS (DART) calcd for $[C_{26}H_8BF_{10}O_2\cdot]^+$ ($[M]^+$) 553.0458, found 553.0479.

Elemental Analysis calcd (%) $C_{26}H_8BF_{10}O_2^{\bullet}$: C 56.46; H 1.46; Found: C 57.01; H 1.53.

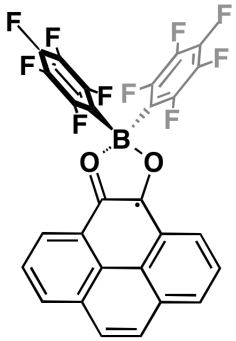

Characterization of 6-4c

Isolated in 46% yield (199 mg).

^{1}H NMR (400 MHz, 298 K, $CDCl_3$): δ 7.52 (br s, Ar-H).

^{19}F NMR (377 MHz, 298 K, $CDCl_3$): δ −158.7 (br s, Ar-F)

^{11}B NMR (128 MHz, 298 K, $CDCl_3$): NMR silent

^{13}C{^{1}H} NMR (126 MHz, 298 K, $CDCl_3$): NMR silent

HRMS (DART) calcd for $[C_{28}H_9BF_{10}O_2\cdot]^+$ ($[M+H]^+$) 578.0536, found 578.0526.

Elemental Analysis calcd (%) for $C_{28}H_8BF_{10}O_2\cdot$: C 58.27; H 1.40; Found: C 58.44; H 1.01.

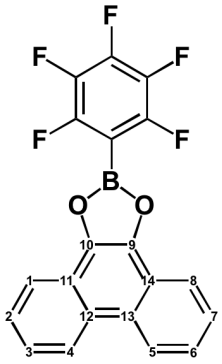

Synthesis of 6-3d

Procedure: In a nitrogen-filled glovebox, $B(C_6F_5)_3$ (154 mg, 0.3 mmol) was dissolved in 0.5 mL toluene and transferred to a vial containing **6-3e** (63 mg, 0.3 mmol). The borane vial was rinsed with 2 x 0.5 mL toluene, and the washes were added to the reaction mixture. The resulting cloudy yellow solution was transferred to a 10 mL Schlenk bomb, and the vial was rinsed with 3 x 0.5 mL toluene. The rinses were added to the Schlenk bomb, which was then sealed and heated to 110 °C for 1 h. Once the reaction was complete, the vessel was cooled to room temperature and the volatiles were removed *in vacuo*. The peach-coloured solid was washed with 3 mL pentane, which removed the coloured impurity and left a white crystalline solid. The material was dissolved in $CHCl_3$ (sparingly soluble) and transferred to a pre-weighed vial, which was then concentrated to yield the desired product in 99% yield (115 mg). Crystals suitable for single crystal X-ray diffraction studies were grown from a saturated bromobenzene solution at −35 °C.

NMR data in d_6-DMSO (DMSO adduct, as evidenced by ^{19}F and ^{11}B NMR spectra):

^{1}H NMR (400 MHz, 298 K, d_6-DMSO): δ 8.79 (d, $^{3}J_{HH}$ = 8.4 Hz, 1H, CH-1&8), 8.01 (d, $^{3}J_{HH}$ = 7.6 Hz, 1H, CH-4&5), 7.62 (t, $^{3}J_{HH}$ = 7.4 Hz, 1H, CH-3&6), 7.50 (t, $^{3}J_{HH}$ = 7.4 Hz, 1H, CH-2&7).

^{19}F NMR (377 MHz, 298 K, d_6-DMSO): δ −133.4 (dd, $^{3}J_{FF}$ = 25 Hz, $^{4}J_{FF}$ = 10 Hz, 2F, *o*-C_6F_5), −157.2 (t, $^{3}J_{FF}$ = 22 Hz, 1F, *p*-C_6F_5), −163.7 to −163.9 (m, 2F, *m*-C_6F_5).

^{11}B NMR (128 MHz, 298 K, d_6-DMSO): δ 10.6 (br s, DMSO adduct).

$^{13}C\{^{1}H\}$ NMR (126 MHz, 298 K, d_6-DMSO, partial): δ 147.4 (dm, $^{1}J_{CF}$ ~ 246 MHz, C_6F_5), 139.8 (s, C9&10), 139.6 (dm, $^{1}J_{CF}$ ~ 248 MHz, C_6F_5), 136.5 (dm, $^{1}J_{CF}$ ~ 246 MHz, C_6F_5), 126.4 (s, C3&6), 125.5 (s, C11&14), 123.5 (s, C12&13), 123.3 (s, C1&8), 123.2 (s, C2&7), 119.6 (s, C4&5).

NMR data in d_8-toluene:

^{1}H NMR (400 MHz, 298 K, d_8-tol): δ 8.37 (d, $^{3}J_{HH}$ = 8.0 Hz, 1H, C<u>H</u>-1&8), 8.22 (dd, $^{3}J_{HH}$ = 7.8 Hz, $^{4}J_{HH}$ = 1.0 Hz, 1H, C<u>H</u>-4&5), 7.44–7.40 (m, 1H, C<u>H</u>-3&6), 7.38–7.33 (m, 1H, C<u>H</u>-2&7).

^{19}F NMR (377 MHz, 298 K, d_8-tol): δ −128.2 to −128.3 (m, 2F, *o*-C_6F_5), −148.1 (tt, $^{3}J_{FF}$ = 21 Hz, $^{4}J_{FF}$ = 6 Hz, 1F, *p*-C_6F_5), −161.9 to −162.0 (m, 2F, *m*-C_6F_5).

^{11}B NMR (128 MHz, 298 K, d_8-tol): δ 29.5 (br s).

HRMS (DART) calcd for $[C_{20}H_9BF_5O_2]^+$ ($[M+H]^+$) 387.0616, found 387.0623.

Elemental Analysis calcd (%) for $C_{20}H_8BF_5O_2$: C 62.22; H 2.09; Found: C 62.00; H 1.92.

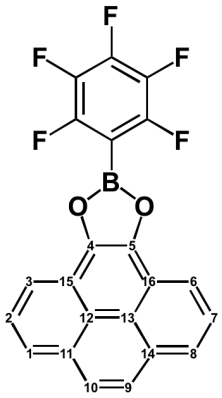

Isolation of 6-4d

The crude mixture of **6-4c** and **6-4d** obtained after hydrogenation of **6-4a** was dissolved in minimal DCM and filtered. The solid was flushed with minimal DCM to fully remove **6-4c**, yielding a small amount of **6-4d** as a white powder.

NMR data at 298 K in d_6-DMSO (DMSO adduct, as evidenced by ^{19}F and ^{11}B NMR spectra):

^{1}H NMR (400 MHz, 298 K, d_6-DMSO): δ 8.29 (dd, $^{3}J_{HH}$ = 7.6 Hz, $^{4}J_{HH}$ = 1.6 Hz, 2H, C<u>H</u>-3&6), 8.16 (s, 2H, C<u>H</u>-9&10), 8.13 (d, $^{3}J_{HH}$ = 7.2 Hz, 2H, C<u>H</u>-1&8), 8.06 (t, $^{3}J_{HH}$ = 7.6 Hz, 2H, C<u>H</u>-2&7).

^{19}F NMR (377 MHz, 298 K, d_6-DMSO): δ −133.4 (dd, $^{3}J_{FF}$ = 26 Hz, $^{4}J_{FF}$ = 9 Hz, 2F, *o*-C_6F_5), −157.2 (t, $^{3}J_{FF}$ = 21 Hz, 1F, *p*-C_6F_5), −163.7 to −163.8 (m, 2F, *m*-C_6F_5).

^{11}B NMR (128 MHz, 298 K, d_6-DMSO): δ 10.9 (br s).

$^{13}C\{^{1}H\}$ NMR (101 MHz, 298 K, d_6-DMSO), partial: δ 140.6 (s, C4&5), 131.1 (s, C11&14), 127.6 (s, C9&10), 125.8 (s, C2&7), 122.4 (s, C15&16), 122.1 (s, C1&8), 119.6 (s, C12&13), 116.7(s, C3&6).

NMR data at 373 K in d_8-toluene:

^{1}H NMR (600 MHz, 373 K, d_8-tol): δ 8.39 (d, $^{3}J_{HH}$ = 7.8 Hz, 2H, CH-3&6), 7.86 (d, $^{3}J_{HH}$ = 7.2 Hz, 2H, CH-1&8), 7.80-7.76 (m, 4H, CH-9&10 and CH-2&7).

^{19}F NMR (564 MHz, 373 K, d_8-tol): δ −128.1 to −128.2 (m, 2F, *o*-C_6F_5), −148.4 to −148.5 (m, 1F, *p*-C_6F_5), −162.1 to −162.2 (m, 2F, *m*-C_6F_5).

^{11}B NMR (192 MHz, 373 K, d_8-tol): δ 29.7 (br s).

HRMS (DART) calcd for $[C_{22}H_9BF_5O_2]^+$ $[M+H]^+$ 411.0616, found 411.0622.

Elemental Analysis calcd (%) for $C_{22}H_8BF_5O_2$: C 64.43; H 1.97; Found: C 63.39; H 1.61. Elemental analysis was consistently low on %carbon.

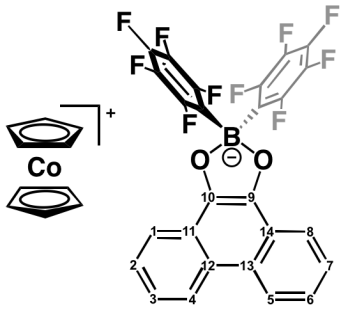

Synthesis of 6-3g

In a nitrogen-filled glovebox, radical **6-3c** (83 mg, 0.15 mmol) was weighed in a 3 mL vial, dissolved in 1.0 mL DCM, and transferred to a vial containing $CoCp_2$ (28 mg, 0.15 mmol) stirring in 1.0 mL DCM. The vial for the radical solution was rinsed with 3 x 1.0 mL DCM, and the rinses were transferred to the reaction. The resulting dark brown solution was stirred at room temperature for 1 h and then concentrated *in vacuo* to isolate the desired product in quantitative yield (117 mg).

^{1}H NMR (400 MHz, 298 K, d_6-DMSO): δ 8.70 (br s, 2H, CH-4&5), 7.95 (br s, 2H, CH-1&8), 7.52 (br s, 2H, CH-2&7), 7.38 (br s, 2H, CH-3&6), 5.60 (br s, 10 H, Cp).

^{19}F NMR (377 MHZ, 298 K, d_6-DMSO): δ −134.6 (d, $^{3}J_{FF}$ = 20 Hz, 2F, *o*-C_6F_5), −160.2 (t, $^{3}J_{FF}$ = 20 Hz, 1F, *p*-C_6F_5), −164.8 to −164.9 (m, 2F, *m*-C_6F_5).

^{11}B NMR (128 MHz, 298 K, d_6-DMSO): δ 10.1 (s).

$^{13}C\{^{1}H\}$ NMR (101 MHz, 298 K, d_6-DMSO), partial: δ147.2 (dm, $^{1}J_{CF}$ ~ 240 Hz, C_6F_5), 141.8 (s, C9&10), 138.4 (dm, $^{1}J_{CF}$ ~ 240 Hz, C_6F_5), 136.0 (dm, $^{1}J_{CF}$ ~ 238 Hz, C_6F_5), 125.6 (s, C2&8), 124.5 (s, C12&13), 123.9 (s, C11&14), 123.0 (s, C4&5), 121.8 (s, C3&6), 119.7 (s, C1&8), 86.7 (br s, Cp).

Elemental Analysis calcd (%) for $C_{36}H_{18}BCoF_{10}O_2$: C 58.25; H 2.44; Found: C 58.04; H 2.24.

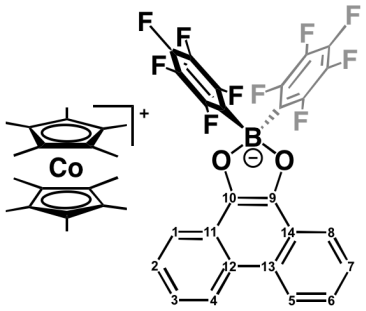

Synthesis of 6-3h

In a nitrogen-filled glovebox, radical **6-3c** (83 mg, 0.15 mmol) was dissolved in 1 mL DCM and the solution was stirred with a magnetic stir bar in a 6 mL vial. $CoCp^*_2$ (49 mg, 0.15 mmol) was dissolved in 1 mL DCM and transferred dropwise to the stirring radical solution. The vial for the Co solution was rinsed with 3 x 1 mL DCM, with the washings transferred to the reaction flask. An orange precipitate immediately began to form from the dark black-yellow solution. The reaction was stirred at room temperature for 30 min, after which the volatiles were removed *in vacuo*. The material was washed with minimal DCM, and the remaining orange solid was collected and evaporated to dryness to yield the desired product in 66% yield (87 mg). Crystals suitable for single crystal X-ray diffraction studies were grown from a saturated Et_2O solution of **6-3g** at −35 °C.

The material was air and moisture stable, therefore non-dried d_6-DMSO was used for NMR analysis.

^{1}H NMR (400 MHz, 298 K, d_6-DMSO): δ 8.68 (d, $^{3}J_{HH}$ = 8.4 Hz, 2H, C<u>H</u>-4&5), 7.90 (dd, $^{3}J_{HH}$ = 8.0 Hz, $^{4}J_{HH}$ = 1.2 Hz, 2H, C<u>H</u>-1&8), 7.49 (t, $^{3}J_{HH}$ = 7.6 Hz, 2H, C<u>H</u>-2&7), 7.38–7.33 (m, 2H, C<u>H</u>-3&6), 1.66 (s, 30H, Cp^* Me)

^{19}F NMR (377 MHz, 298 K, d_6-DMSO): δ −134.6 (dd, $^{3}J_{FF}$ = 26 Hz, $^{4}J_{FF}$ = 9 Hz, 2F, *o*-C_6F_5), −160.2 (t, $^{3}J_{FF}$ = 22 Hz, 1F, *p*-C_6F_5), −164.8 to −165.0 (m, 2F, *m*-C_6F_5).

^{11}B NMR (128 MHz, 298 K, d_6-DMSO): δ 10.0 (s).

$^{13}C\{^{1}H\}$ NMR (126 MHz, 298 K, d_6-DMSO), partial: δ 141.7 (s, C9&10), 125.5 (s, C2&7), 124.5 (s, C12&13), 123.8 (s, C11&14), 123.0 (s, C4&5), 121.8 (s, C3&6), 119.7 (s, C1&8), 93.8 (s, Cp), 7.5 (s, Cp^* Me).

Elemental Analysis calcd (%) for $C_{46}H_{38}BCoF_{10}O_2$: C 62.60; H 4.34; Found: C 62.17; H 4.21.

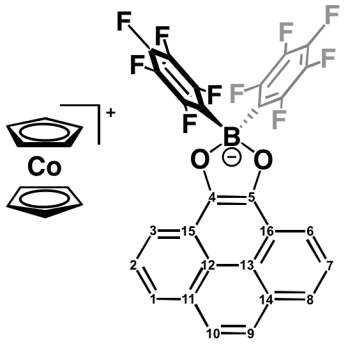

Synthesis of 6-4g

In a nitrogen-filled glovebox, radical species **6-4c** (87 mg, 0.15 mmol) was dissolved in 3 mL DCM in a 20 mL scintillation vial equipped with a magnetic stir bar. $CoCp_2$ (28 mg, 0.15 mmol) was weighed in a vial, dissolved in 1 mL DCM, and transferred to the radical solution. The $CoCp_2$ vial was rinsed with 2 x 0.5 mL DCM and the washes were transferred to the reaction. The resulting mixture was a dark black-orange colour. The reaction was allowed to stir at room temperature for 30 min, after which it was concentrated to dryness. The desired product was isolated as a metallic golden-black solid in quantitative yield (115 mg). Crystals suitable for single crystal X-ray diffraction studies were grown from a saturated Et_2O solution of **6-4g** at −35 °C.

^{1}H NMR (400 MHz, 298 K, d_6-DMSO): δ 8.20 (dd, $^{3}J_{HH}$ = 7.2 Hz, $^{4}J_{HH}$ = 1.6 Hz, 2H, C<u>H</u>-3&6), 8.08 (s, 2H, C<u>H</u>-9&10), 8.01–7.94 (m, 4H, C<u>H</u>-1&8 and C<u>H</u>-2&7), 5.77 (s, 10H, Cp).

^{19}F NMR (377 MHz, 298 K, d_6-DMSO): δ −134.5 (dd, $^{3}J_{FF}$ = 27 Hz, $^{4}J_{HH}$ = 10 Hz, 2F, *o*-C_6F_5), −160.1 (t, $^{3}J_{FF}$ = 22 Hz, 1F, *p*-C_6F_5), −164.7 to −164.9 (m, 2F, *m*-C_6F_5).

^{11}B NMR (128 MHz, 298 K, d_6-DMSO): δ 10.4 (br s).

$^{13}C\{^{1}H\}$ NMR (126 MHz, 298 K, d_6-DMSO), partial: δ 147.3 (dm, $^{1}J_{CF}$ ~ 242 Hz, C_6F_5), 142.6 (s, C4&5), 138.4 (dm, $^{1}J_{CF}$ ~ 247 Hz, C_6F_5), 136.0 (dm, $^{1}J_{CF}$ ~ 245 Hz, C_6F_5), 131.0 (s, C11&14), 127.3 (s, C9&10), 125.2 (s, C2&7), 123.1 (s, C15&16), 120.6 (s, C1&8), 118.8 (s, C12&13), 116.7 (s, C3&6), 84.6 (s, Cp).

Elemental Analysis calcd (%) for $C_{38}H_{18}BCoF_{10}O_2$: C 59.56; H 2.37; Found: C 59.72; H 2.43.

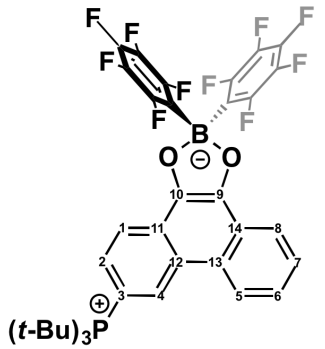

Synthesis of 6-5a

In a nitrogen-filled glovebox, P(*t*-Bu)$_3$ (30 mg, 0.15 mmol) was dissolved in 0.5 mL THF and transferred to a 20 mL scintillation vial containing **6-3c** (83 mg, 0.15 mmol). The P(*t*-Bu)$_3$ vial was rinsed with 2 x 0.5 mL THF, and the washes were added to the reaction mixture. The scintillation vial was equipped with a magnetic stir bar, capped, and stirred at ambient glovebox temperature (35 °C) for 14 h. Over the course of the reaction, the solution changed from dark black yellow to a cloudy orange suspension. The volatiles were removed *in vacuo* and the remaining material was triturated with pentane, followed by toluene, and finally DCM. NMR analysis of the 3 washes confirmed that the majority of **6-5a** was in the DCM wash. The material was removed from the glovebox, dry-packed onto Celite, and purified by flash column chromatography (100% DCM) on silica that had been pretreated with a 10% Et_3N in DCM solution. One fraction was collected, which, upon concentration, afforded a bright yellow solid. This material contained a small amount of new phosphine impurities (as determined by NMR, which appear to have formed on the column), however these were easily removed by washing the yellow solid with excess toluene. After column chromatography and toluene washes the desired product was isolated as a bright yellow solid in 66% yield (37 mg, 0.05 mmol).

^{1}H NMR (400 MHz, 298 K, CD_2Cl_2): δ 9.30 (dd, $^3J_{HP}$ = 11.4 Hz, $^4J_{HH}$ = 2.0 Hz, 1H, C<u>H</u>-4), 8.44 (d, $^3J_{HH}$ = 8.5 Hz, 1H, C<u>H</u>-8), 8.27 (dd, $^3J_{HH}$ = 8.9 Hz, $^4J_{HP}$ = 3.8 Hz, 1H, C<u>H</u>-1), 8.23–8.21 (m, 1H, C<u>H</u>-5), 7.91 (ddd, $^3J_{HH}$ = 8.9 Hz, $^3J_{HP}$ = 7.0 Hz, $^4J_{HH}$ = 2.0 Hz, 1H, C<u>H</u>-2), 7.65 (ddd, $^3J_{HH}$ = 8.1 Hz, $^3J_{HH}$ = 6.9 Hz, 1.0 Hz, 1H, C<u>H</u>-6), 7.53 (ddd, $^3J_{HH}$ = 8.4 Hz, $^3J_{HH}$ = 6.9 Hz, 1.4 Hz, 1H, C<u>H</u>-7), 1.81 (d, $^3J_{HP}$ = 14.1 Hz, 27H, P-(C(C<u>H</u>$_3$)$_3$)$_3$).

^{19}F NMR (377 MHz, 298 K, CD_2Cl_2): δ −136.0 (dd, $^3J_{FF}$ = 25 Hz, $^4J_{FF}$ = 10 Hz, 2F, *o*-C_6F_5), −161.2 (t, $^3J_{FF}$ = 20 Hz, 1F, *p*-C_6F_5), −165.9 to −166.1 (m, 2F, *m*-C_6F_5).

^{31}P{^{1}H} NMR (162 MHz, 298 K, CD_2Cl_2): δ 49.0 (s).

^{11}B NMR (128 MHz, 298 K, CD_2Cl_2): δ 10.9 (s).

$^{13}C\{^{1}H\}$ NMR (101 MHz, 298 K, CD_2Cl_2), partial: δ 149.2 (s, C9), 142.7 (s, C10), 131.6 (d, $^{2}J_{CP}$ = 6 Hz, C4), 128.6 (d, $^{2}J_{CP}$ = 6 Hz, C2), 127.5 (s, C6), 126.4 (br s, C11), 126.0 (s, C14), 125.5 (2, C13), 124.4 (s, C7), 124.3 (d, $^{3}J_{CP}$ = 11 Hz, C12), 122.3 (s, C8), 122.1 (s, C5), 122.0 (d, $^{3}J_{CP}$ = 11 Hz, C1), 105.8 (d, $^{1}J_{CP}$ = 67 Hz, C3), 41.8 (d, $^{1}J_{CP}$ = 30 Hz, P-(C(CH$_3$)$_3$)$_3$), 32.1 (s, P-(C(CH$_3$)$_3$)$_3$).

HRMS (ESI) calcd for $[C_{38}H_{35}{}^{10}BF_{10}O_2P]^+$ ($[M+H]^+$) 754.2339, found 754.2325.

Elemental Analysis calcd (%) for $C_{38}H_{34}BF_{10}O_2P$: C 60.50; H 4.54; Found: C 59.99; H 4.54.

Synthesis of 6-6a and 6-6b

In a nitrogen-filled glovebox, triphenylphosphine (43 mg, 0.16 mmol) was weighed in a vial, dissolved in 1 mL toluene, and the resulting solution was transferred to a vial containing borocyclic radical **6-3c** (150 mg, 0.27 mmol). The vial that contained the PPh_3 was rinsed with 2 x 1 mL toluene, and the washes were added to the reaction mixture. The resulting black solution was transferred to a 25 mL Schlenk bomb equipped with a magnetic stir bar. The vial that contained the reaction mixture was washed with 4 x 1 mL toluene, making the total reaction volume 7 mL. The bomb was sealed, removed from the glovebox, and heated to 60 °C for 3 d. The reaction flask was cooled to room temperature and the volatiles were removed *in vacuo*. The residual orange-yellow precipitate was stirred over ~ 10 mL pentane. After decanting the pentane wash, the residual yellow-orange material was stirred over ~ 5 mL toluene. Finally, after decanting the toluene wash, the remaining yellow material was dissolved in DCM and transferred into a vial. The toluene wash contained mostly **6-6a** with a small amount of **6-6b** and boronic ester **6-3d**. The DCM wash contained mostly **6-6b** with a small amount of **6-6a** and a very small amount of boronic ester **6-3d**. The toluene wash was purified by flash column chromatography in the glovebox, using 1:1 pentane:DCM as the eluent. **6-6a** was isolated as an orange solid (28 mg, 0.03 mmol). The DCM wash was purified by adding Et_2O to the impure material; a small amount of yellow solid did not dissolve in Et_2O, which was found to be pure **6-6b**. The Et_2O solution was left at ambient glovebox temperature (35 °C) and orange crystals grew from the solution. The mother liquor was decanted (which contained a mixture of **6-6a**, **6-6b**, and boronic ester **6-3d**), and the crystals were found to be pure **6-6b**. The pure batches of **6-6b** were combined, which is a yellow solid (75 mg, 0.09 mmol). In total, the 2 isomers were isolated in a combined yield of 93% (103 mg, 0.13 mmol). Single crystals of **6-6a** suitable for

X-ray diffraction studies grew from an NMR scale reaction in $CDCl_3$ at room temperature. Single crystals of **6-6b** were grown from a saturated toluene solution of **6-6b** at −35 °C.

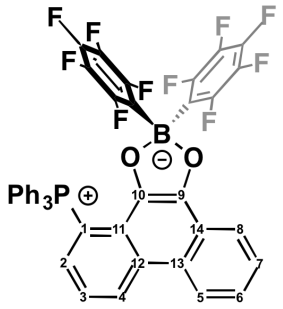

Characterization of 6-6a

^{1}H NMR (400 MHz, 298 K, d_8-THF): δ 9.24 (d, $^{3}J_{HH}$ = 8.3 Hz, 1H, C<u>H</u>-4), 8.81 (d, $^{3}J_{HH}$ = 8.4 Hz, 1H, C<u>H</u>-8), 8.15 (d, $^{3}J_{HH}$ = 7.6 Hz, 1H, C<u>H</u>-5), 7.99–6.98 (br, 15 Hz, PPh_3), 7.61–7.57 (m, 1H, C<u>H</u>-6), 7.53–7.49 (m, 1H, C<u>H</u>-7), 7.38–7.33 (m, 1H, C<u>H</u>-3), 7.22 (dd, $^{3}J_{HH}$ = 7.4 Hz, $^{3}J_{HP}$ = 17.2 Hz, 1H, C<u>H</u>-2).

^{19}F NMR (377 MHz, 298 K, d_8-THF): δ −134.3 (dd, $^{3}J_{FF}$ = 26 Hz, $^{4}J_{FF}$ = 9 Hz, 2F, *o*-C_6F_5), −163.5 (t, $^{3}J_{FF}$ = 20 Hz, 1F, *p*-C_6F_5), −167.2 to −167.3 (m, 2F, *m*-C_6F_5).

^{31}P{^{1}H} NMR (162 MHz, 298 K, d_8-THF): δ 29.0 (s).

^{11}B NMR (128 MHz, 298 K, d_8-THF): δ 10.0 (s).

^{13}C{^{1}H} NMR (126 MHz, 298 K, d_8-THF), partial: δ 149.6 (s, C9), 149.0 (dm, $^{1}J_{CF}$ ~ 241 Hz, C_6F_5), 141.3 (s, C10), 140.1 (dm, $^{1}J_{CF}$ ~ 246 Hz, C_6F_5), 138.7 (d, $^{2}J_{CP}$ = 11 Hz, C2), 137.3 (dm, $^{1}J_{CF}$ ~ 241 Hz, C_6F_5), 134.2 (br, PPh_3), 132.2 (s, C4), 129.7 (br, PPh_3), 127.6 (s, C7), 127.3 (s, C13), 126.8 (d, $^{3}J_{CP}$ = 10 Hz, C12), 126.2 (d, $^{2}J_{CP}$ = 6 Hz, C11), 125.5 (s, C14), 125.1 (br, PPh_3), 124.8 (s, C6), 124.3 (br, PPh_3), 124.1 (s, C5), 122.2 (s, C8), 120.8 (d, $^{3}J_{CP}$ = 15 Hz, C3), 106.3 (d, $^{1}J_{CP}$ = 91 Hz, C1).

HRMS (DART) calcd for $[C_{44}H_{23}BF_{10}O_2P]^+$ ($[M+H]^+$) 815.1369, found 815.1373

Elemental Analysis calcd (%) for $C_{44}H_{22}BF_{10}O_2P$: C 64.89; H 2.72; Found: C 64.50; H 2.89.

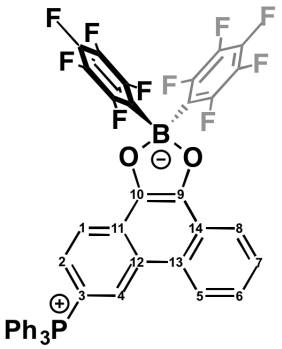

Characterization of 6-6b

^{1}H NMR (400 MHz, 298 K, $CDCl_3$): δ 8.60 (dd, $^{2}J_{HP}$ = 15.8 Hz, $^{4}J_{HH}$ = 1.7 Hz, 1H, C<u>H</u>-4), 8.41 (dd, $^{3}J_{HH}$ = 8.6 Hz, $^{4}J_{HP}$ = 4.1 Hz, 1H, C<u>H</u>-1), 8.30 (d, $^{3}J_{HH}$ = 8.1 Hz, 1H, C<u>H</u>-8), 8.02 (d, $^{3}J_{HH}$ = 8.4 Hz, 1H, C<u>H</u>-5), 7.88 (t, $^{3}J_{HH}$ = 7.3 Hz, 3H, Ph *para*-C<u>H</u>), 7.75–7.64 (m, 12H, Ph *ortho*-C<u>H</u> and *para*-C<u>H</u>), 7.55–7.51 (m, 1H, C<u>H</u>-7), 7.39 (ddd, $^{3}J_{HP}$ = 10.6 Hz, $^{3}J_{HH}$ = 8.6 Hz, $^{4}J_{HH}$ = 1.7 Hz, 1H, C<u>H</u>-2), 7.34–7.30 (m, 1H, C<u>H</u>-6).

^{19}F NMR (377 MHz, 298 K, $CDCl_3$): δ −135.2 (dd, $^{3}J_{FF}$ = 25.4 Hz, $^{4}J_{FF}$ = 9.6 Hz, 2F, *o*-C_6F_5), −160.6 (t, $^{3}J_{FF}$ = 20.4 Hz, 1F, *p*-C_6F_5), −165.4 to −165.5 (m, 2F, *m*-C_6F_5).

^{31}P{^{1}H} NMR (162 MHz, 298 K, $CDCl_3$): δ 23.7 (s).

^{11}B NMR (128 MHz, 298 K, $CDCl_3$): δ 11.1 (s).

^{13}C{^{1}H} NMR (126 MHz, 298 K, $CDCl_3$), partial: δ 150.2 (s, C9), 148.4 (dm, $^{1}J_{CF}$ ~ 243 Hz, C_6F_5), 142.8 (s, C10), 139.5 (dm, $^{1}J_{CF}$ ~ 248 Hz, C_6F_5), 137.0 (dm, $^{1}J_{CF}$ ~ 249 Hz, C_6F_5), 135.4 (d, $^{4}J_{CP}$ = 3 Hz, *p*-Ph), 134.4 (d, $^{2}J_{CP}$ = 10 Hz, *o*-Ph), 131.4 (d, $^{2}J_{CP}$ = 12 Hz, C4), 130.6 (d, $^{3}J_{CP}$ = 13 Hz, *m*-Ph), 127.0 (br s, C7 and C11), 126.7 (d, $^{2}J_{CP}$ = 11 Hz, C2), 125.4 (s, C13), 125.1 (br s, C14), 124.2 (d, $^{3}J_{CP}$ = 14 Hz, C12), 124.0 (s, C6), 123.0 (d, $^{3}J_{CP}$ = 14 Hz, C1), 122.1 (s, C5), 121.7 (s, C8), 119.5 (d, $^{1}J_{CP}$ = 90 Hz, *i*-Ph), 103.0 (d, $^{1}J_{CP}$ = 97 Hz, C3).

HRMS (ESI) calcd for $[C_{44}H_{23}BF_{10}O_2P]^+$ ($[M+H]^+$) 815.1371, found 815.1384.

Elemental Analysis calcd (%) for $C_{44}H_{22}BF_{10}O_2P$: C 64.89; H 2.72; Found: C 63.97; H 2.68. Elemental analysis was consistently low on %carbon.

Synthesis of 6-7a and 6-7b

In a nitrogen-filled glovebox, triphenylphosphine (13 mg, 0.05 mmol) was weighed in a vial, dissolved in 0.5 mL $CHCl_3$, and the resulting solution was transferred to a vial containing borocyclic radical **6-4c** (58 mg, 0.1 mmol). The vial that contained the PPh_3 was rinsed with 2 x 0.5 mL $CHCl_3$, and the washes were added to the reaction mixture. The resulting black solution was transferred to a 25 mL Schlenk bomb equipped with a magnetic stir bar. The vial that

contained the reaction mixture was washed with 2 x 0.5 mL $CHCl_3$, making the total reaction volume 2.5 mL. The bomb was sealed, removed from the glovebox, and heated to 65 °C for 36 h. The reaction flask was then cooled to room temperature and the volatiles were removed *in vacuo*. The residual pink precipitate was dissolved in DCM and transferred to a tared vial. The solution was concentrated *in vacuo*, and the dried material was stirred over ~ 6 mL pentane. The pentane was decanted, and the remaining material (crude yield: 47 mg) was purified by pTLC in air, using 30:70 hexanes:DCM as the eluent. Two bands were isolated, the less polar being **6-7a** (17 mg), which is an orange-pink solid, and the more polar being **6-7b** (15 mg), which is a deep pink solid. In total, the 2 isomers were isolated in a combined yield of 76% (32 mg, 0.04 mmol).

Single crystals of **6-7a** suitable for X-ray diffraction studies grew from an NMR scale reaction in $CDCl_3$ at room temperature. Single crystals of **6-7b** were grown from by slow diffusion of pentane into a DCM solution of **6-7b** at −35 °C.

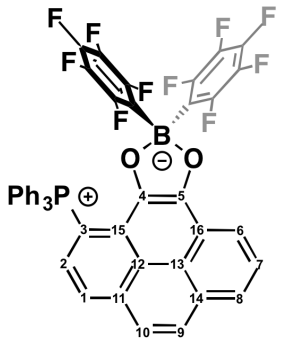

Characterization of 6-7a

^{1}H NMR (500 MHz, 298 K, $CDCl_3$): δ 8.71 (dd, $^{3}J_{HH}$ = 7.8 Hz, $^{4}J_{HH}$ = 0.8 Hz, 1H, C<u>H</u>-6), 8.31 (d, $^{3}J_{HH}$ = 9.0 Hz, 1H, C<u>H</u>-9), 8.23 (d, $^{3}J_{HH}$ = 7.5 Hz, 1H, C<u>H</u>-8), 8.13 (t, $^{3}J_{HH}$ = 7.8 Hz, 1H, C<u>H</u>-7), 8.04 (d, $^{3}J_{HH}$ = 9.0 Hz, 1H, C<u>H</u>-10), 7.77 (dd, $^{3}J_{HH}$ = 8.2 Hz, $^{4}J_{HP}$ = 2.8 Hz, 1H, C<u>H</u>-1), 7.36 (dd, $^{3}J_{HP}$ = 16.0 Hz, $^{3}J_{HH}$ = 8.0 Hz, 1H, C<u>H</u>-2), 7.89–7.19 (br, 15 H, 3xPh).

^{19}F NMR (377 MHz, 298 K, $CDCl_3$): δ −134.1 (dd, $^{3}J_{FF}$ = 25.8 Hz, $^{4}J_{FF}$ = 9.2 Hz, 2F, *o*-C_6F_5), −160.9 (t, $^{3}J_{FF}$ = 20.4 Hz, 1F, *p*-C_6F_5), −165.3 to −165.4 (m, 2F, *m*-C_6F_5).

^{31}P{^{1}H} NMR (162 MHz, 298 K, $CDCl_3$): δ 28.6 (s).

^{11}B NMR (128 MHz, 298 K, $CDCl_3$): δ 10.2 (br s).

^{13}C{^{1}H} NMR (126 MHz, 298 K, $CDCl_3$), partial: δ 149.4 (s, C5), 147.9 (dm, $^{1}J_{CF}$ ~ 242 Hz, C_6F_5), 141.5 (d, $^{3}J_{CP}$ = 3.9 Hz, C4), 139.1 (dm, $^{1}J_{CF}$ ~ 240 Hz, C_6F_5), 136.8 (d, $^{4}J_{CP}$ = 2.9 Hz, C14), 136.2 (dm, $^{1}J_{CP}$ ~ 248 Hz, C_6F_5), 133.6 (d, $^{2}J_{CP}$ = 11.2 Hz, C2), 133.0 (br s, *o*- and *p*-Ph), 132.2 (s, C9), 131.2 (d, $^{5}J_{CP}$ = 1.4 Hz, C13), 128.6 (br s, *m*-Ph), 126.6 (d, $^{5}J_{CP}$ = 1.5 Hz, C10),

126.4 (d, $^{2}J_{CP}$ = 7.3 Hz, C11), 126.3 (s, C7), 125.0 (s, C8), 122.5 (s, C12), 121.3 (s, C6), 119.6 (d, $^{3}J_{CP}$ = 11.2 Hz, C15), 119.1 (d, $^{3}J_{CP}$ = 15.0 Hz, C1), 119.0 (d, $^{4}J_{CP}$ = 1.3 Hz, C16), 97.8 (d, $^{1}J_{CP}$ = 94.4 Hz, C3).

HRMS (DART) calcd for $[C_{46}H_{23}BF_{10}O_2P]^+$ ($[M+H]^+$) 839.1369, found 839.1360.

Elemental Analysis calcd (%) for $C_{46}H_{22}BF_{10}O_2P$: C 65.90; H 2.64; Found: C 65.50; H 2.85.

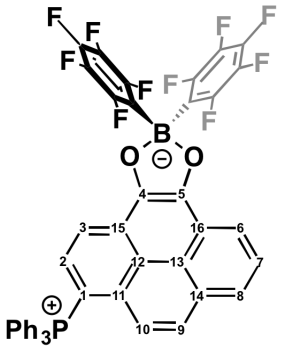

Characterization of 6-7b

^{1}H NMR (500 MHz, 298 K, $CDCl_3$): δ 8.79 (dd, $^{3}J_{HH}$ = 7.0 Hz, $^{4}J_{HH}$ = 1.5 Hz, 1H, C<u>H</u>-6), 8.42 (dd, $^{3}J_{HH}$ = 8.5 Hz, $^{4}J_{HP}$ = 3.0 Hz, 1H, C<u>H</u>-3), 8.07–8.02 (m, 2H, C<u>H</u>-7 and C<u>H</u>-8), 7.88 (d, $^{3}J_{HH}$ = 9.0 Hz, 1H, C<u>H</u>-9), 7.77–7.72 (m, 3H, *para*-C<u>H</u>), 7.63–7.59 (m, 12H, *ortho* and *meta*-C<u>H</u>), 7.46 (d, $^{3}J_{HH}$ = 9.0 Hz, 1H, C<u>H</u>-10), 7.42 (dd, $^{3}J_{HP}$ = 15.0 Hz, $^{3}J_{HH}$ = 8.5 Hz, 1H, C<u>H</u>-2).

^{19}F NMR (377 MHz, 298 K, $CDCl_3$): δ −135.1 (dd, $^{3}J_{FF}$ = 24.9 Hz, $^{4}J_{FF}$ = 10.2 Hz, 2F, *o*-C_6F_5), −160.5 (t, $^{3}J_{FF}$ = 20.2 Hz, 1F, *p*-C_6F_5), −165.3 to −165.5 (m, 2F, *m*-C_6F_5).

^{31}P{^{1}H} NMR (162 MHz, 298 K, $CDCl_3$): δ 22.3 (s).

^{11}B NMR (128 MHz, 298 K, $CDCl_3$): δ 11.4 (s).

^{13}C{^{1}H} NMR (126 MHz, 298 K, $CDCl_3$), partial: δ 150.2 (s, C5), 148.2 (dm, $^{1}J_{CF}$ ~ 244 Hz, C_6F_5), 143.7 (s, C4), 139.3 (dm, $^{1}J_{CF}$ ~ 241 Hz, C_6F_5), 136.7 (dm, $^{1}J_{CF}$ ~ 249 Hz, C_6F_5), 134.8 (d, $^{4}J_{CP}$ = 3.0 Hz, *p*-Ph), 134.7 (d, $^{2}J_{CP}$ = 8.8 Hz, C14), 134.1 (d, $^{2}J_{CP}$ = 10.2 Hz, *o*-Ph), 131.4 (d, $^{2}J_{CP}$ = 12.2 Hz, C2), 130.7 (s, C9), 130.3 (d, $^{3}J_{CP}$ = 12.7 Hz, *m*-Ph), 129.5 (s, C13), 128.1 (d, $^{4}J_{CP}$ = 2.5 Hz, C11), 126.3 (s, C7), 125.0 (s, C8), 124.0 (d, $^{3}J_{CP}$ = 8.2 Hz, C10), 123.2 (d, $^{5}J_{CP}$ = 1.4 Hz, C12), 122.2 (br s, C6), 120.3 (d, $^{1}J_{CP}$ = 88.6 Hz, *i*-Ph), 120.0 (d, $^{3}J_{CP}$ = 11.2 Hz, C15), 118.6 (d, $^{4}J_{CP}$ = 1.6 Hz, C16), 117.2 (d, $^{3}J_{CP}$ = 14.7 Hz, C3), 96.5 (d, $^{1}J_{CP}$ = 91.6 Hz, C1).

HRMS (DART) calcd for $[C_{46}H_{23}BF_{10}O_2P]^+$ ($[M+H]^+$) 839.1369, found 839.1383

Elemental Analysis calcd (%) for $C_{46}H_{22}BF_{10}O_2P$: C 65.90; H 2.64; Found: C 65.96; H 3.00.

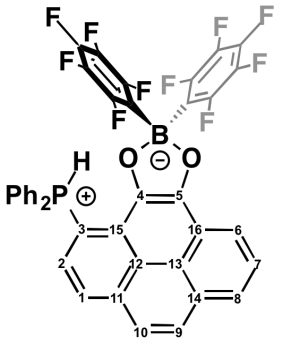

Synthesis of 6-8a

In a nitrogen-filled glovebox, diphenylphosphine (14 mg, 0.08 mmol) was weighed in a vial, dissolved in 1 mL toluene, and the resulting solution was transferred to a vial containing borocyclic radical **6-4c** (87 mg, 0.15 mmol). The vial that contained the $HPPh_2$ was rinsed with 2 x 1 mL toluene, and the washes were added to the reaction mixture. An additional 4 mL toluene was added to the reaction mixture, making the total reaction volume 7 mL. A magnetic stir bar was added to the vial, which was capped and stirred at ambient glovebox temperature (35 °C) for 5 days. The volatiles were then removed *in vacuo*. The residual pink and white precipitates were stirred over ~10 mL pentane. After decanting the pentane wash, the residual materials were stirred over ~5 mL toluene. Finally, after decanting the toluene wash, the remaining material was dissolved in DCM, filtered through a plug of silica, and transferred into a vial. The toluene and DCM washes were concentrated *in vacuo*; the DCM wash contained pure **6-8a** (22 mg) as a deep pink solid, and the toluene wash was purified by flash column chromatography (in air) using 1:1 DCM:pentane as the eluent, isolating an additional 22 mg of **6-8a**. In total, **6-8a** was isolated in 77% yield (44 mg, 0.06 mmol).

Single crystals of **6-8a** were grown from by slow diffusion of pentane into a DCM solution of **6-8a** at −35 °C.

^{1}H NMR (400 MHz, 298 K, $CDCl_3$): δ 9.87 (d, $^{1}J_{HP}$ = 549.2 Hz, 1H, P<u>H</u>), 8.75 (d, $^{3}J_{HH}$ = 8.0 Hz, 1H, C<u>H</u>-6), 8.30 (d, $^{3}J_{HH}$ = 8.8 Hz, 1H, C<u>H</u>-9), 8.22 (d, $^{3}J_{HH}$ = 7.6 Hz, 1H, C<u>H</u>-8), 8.13 (t, $^{3}J_{HH}$ = 7.6 Hz, 1H, C<u>H</u>-7), 8.03 (d, $^{3}J_{HH}$ = 8.8 Hz, 1H, C<u>H</u>-10), 7.81 (dd, $^{3}J_{HH}$ = 8.2 Hz, $^{4}J_{HP}$ = 3.0 Hz, 1H, C<u>H</u>-1), 7.71–7.66 (m, 2H, PPh_2), 7.61–7.51 (m, 8H, PPh_2), 7.42 (dd, $^{3}J_{HP}$ = 15.8 Hz, $^{3}J_{HH}$ = 8.0 Hz, 1H, C<u>H</u>-2).

^{19}F NMR (377 MHz, 298 K, $CDCl_3$): δ −135.5 (d, $^{3}J_{FF}$ = 24 Hz, 2F, *o*-C_6F_5), −160.1 (t, $^{3}J_{FF}$ = 20 Hz, 1F, *p*-C_6F_5), −164.7 to −164.9 (m, 2F, *m*-C_6F_5).

^{31}P NMR (162 MHz, 298 K, $CDCl_3$): δ 6.26 (d, $^{1}J_{PH}$ = 547 Hz, <u>P</u>H).

$^{31}P\{^{1}H\}$ NMR (162 MHz, 298 K, $CDCl_3$): δ 6.25 (s).

^{11}B NMR (128 MHz, 298 K, $CDCl_3$): δ 10.7 (s).

$^{13}C\{^{1}H\}$ NMR (126 MHz, 298 K, $CDCl_3$), partial: δ 149.1 (s, C5), 147.9 (dm, $^{1}J_{CF}$ ~ 243 Hz, C_6F_5), 142.0 (d, $^{3}J_{CP}$ = 3 Hz, C4), 139.5 (dm, $^{1}J_{CF}$ ~ 248 Hz, C_6F_5), 137.1 (d, $^{4}J_{CP}$ = 3 Hz, C11), 136.8 (dm, $^{1}J_{CF}$ ~ 250 Hz, C_6F_5), 134.4 (d, $^{4}J_{CP}$ = 3 Hz, *p*-Ph), 133.5 (d, $^{2}J_{CP}$ = 11 Hz, *o*-Ph), 132.7 (s, C9), 131.6 (d, $^{2}J_{CP}$ = 11 Hz, C2), 131.3 (d, $^{5}J_{CP}$ = 1 Hz, C14), 130.0 (d, $^{3}J_{CP}$ = 13 Hz, *m*-Ph), 126.7 (s, C7), 126.5 (d, $^{5}J_{CP}$ = 1 Hz, C10), 126.2 (d, $^{2}J_{CP}$ = 8 Hz, C15), 125.5 (s, C8), 123.0 (s, C16), 121.9 (s, C6), 119.8 (d, $^{3}J_{CP}$ = 15 Hz, C1), 119.5 (d, $^{1}J_{CP}$ = 91 Hz, *i*-Ph), 119.3 (d, $^{3}J_{CP}$ = 11 Hz, C12), 119.1 (d, $^{4}J_{CP}$ = 1 Hz, C13), 95.3 (d, $^{1}J_{CP}$ = 93 Hz, C3).

HRMS (DART) calcd for $[C_{40}H_{19}BF_{10}O_2P]^+$ ($[M+H]^+$) 763.1056, found 763.1049.

Elemental Analysis calcd (%) for $C_{40}H_{18}BF_{10}O_2P$: C 63.02; H 2.38; Found: C 62.79; H 2.33.

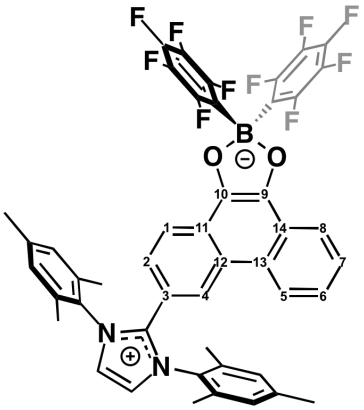

Synthesis of 6-10a

In a nitrogen-filled glovebox, IMes (46 mg, 0.15 mmol) was dissolved in 0.5 mL THF and transferred dropwise to a 20 mL scintillation vial containing a solution of **6-3c** (83 mg, 0.15 mmol) in 0.5 mL THF. The IMes vial was rinsed with 0.5 mL THF, and the wash was added to the reaction mixture. The solution immediately changed from dark black yellow to clear orange-red. The volatiles were removed immediately *in vacuo* and the remaining material was triturated with pentane, followed by toluene, Et_2O, and finally THF. The material from the THF wash was removed from the glovebox, dry-packed onto Celite, and purified by flash column chromatography (100% DCM) on silica that had been pretreated with a 10% Et_3N in DCM solution. One fraction was collected, and **6-10a** was isolated as a bright yellow solid in 68% yield (44 mg, 0.05 mmol).

^{1}H NMR (400 MHz, 298 K, d_8-THF): δ 8.19 (d, $^{4}J_{HH}$ = 1.9 Hz, 1H, C<u>H</u>-4), 8.08 (dd, $^{3}J_{HH}$ = 8.2 Hz, $^{4}J_{HH}$ = 1.3 Hz, 1H, C<u>H</u>-8), 8.05 (s, 2H, imidazole C<u>H</u>), 7.80 (d, $^{3}J_{HH}$ = 8.7 Hz, 1H,

C<u>H</u>-1), 7.79 (d, $^{3}J_{HH}$ = 8.5 Hz, 1H, C<u>H</u>-5), 7.43 (ddd, $^{3}J_{HH}$ = 8.0 Hz, 6.9 Hz, $^{4}J_{HH}$ = 1.0 Hz, 1H, C<u>H</u>-7), 7.25 (ddd, $^{3}J_{HH}$ = 8.4 Hz, 6.9 Hz, $^{4}J_{HH}$ = 1.4 Hz, 1H, C<u>H</u>-6), 7.14 (d, $^{4}J_{HH}$ = 0.4 Hz, 4H, Mes C<u>H</u>), 6.92 (dd, $^{3}J_{HH}$ = 8.7 Hz, $^{4}J_{HH}$ = 1.9 Hz, 1H, C<u>H</u>-2), 2.29 (s, 6H, Mes *p*-CH_3), 2.17 (s, 12H, Mes *o*-CH_3).

^{19}F NMR (377 MHz, 298 K, d_8-THF): δ −135.4 to −135.5 (m, 2F, *o*-C_6F_5), −163.7 (t, $^{3}J_{FF}$ = 20 Hz, 1F, *p*-C_6F_5), −167.8 to −168.0 (m, 2F, *m*-C_6F_5).

^{11}B NMR (128 MHz, 298 K, d_8-THF): δ 10.6 (s).

^{13}C{^{1}H} NMR (126 MHz, 298 K, d_8-THF), partial: δ 149.5 (s, C9), 147.4 (s, imidazole *q*-<u>C</u>), 143.7 (s, C10), 142.7 (s, Mes *o*-<u>C</u>), 135.5 (s, Mes *p*-<u>C</u>), 132.7 (s, Mes *i*-<u>C</u>), 131.3 (s, Mes *m*-<u>C</u>H), 127.0 (s, C7), 126.39 (s, C11), 126.37 (s, C13), 126.0 (s, C14), 125.9 (s, C4), 125.4 (s, imidazole <u>C</u>H), 124.3 (C12), 123.7 (s, C6), 123.2 (s, C2), 122.7 (s, C5), 122.4 (s, C8), 122.3 (s, C1), 111.9 (s, C3), 21.1 (s, Mes *p*-CH_3), 17.9 (s, Mes *o*-CH_3).

HRMS (ESI) calcd for $[C_{47}H_{32}{}^{10}BF_{10}N_2O_2]^+$ ($[M+H]^+$) 856.2428, found 856.2396.

Satisfactory elemental analysis could not be obtained after several attempts.

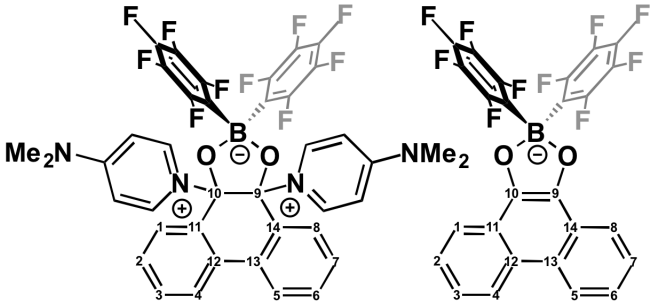

Synthesis of 6-11a

In a nitrogen-filled glovebox, radical **6-3c** (55 mg, 0.10 mmol) was weighed in a 20 mL scintillation vial equipped with a magnetic stir bar. 2 mL of toluene was added to the radical, which resulted in a very dark black-yellow solution. DMAP (12 mg, 0.10 mmol) was weighed and transferred to the solution of **6-3c** using 3 x 0.5 mL toluene. An additional 1.5 mL toluene was added to the reaction mixture. The homogeneous solution was stirred at room temperature for 48 h, during which time the reaction mixture became an orange solution with a yellow-orange precipitate. The volatiles were removed *in vacuo* revealing a yellow precipitate. Pentane (~5 mL) was added to the precipitate, which produced a suspension that was filtered through a frit. The precipitate was washed thoroughly with pentane, collected off the frit, and dried *in vacuo*. This yielded the desired product as a bright yellow solid in quantitative yield (67 mg, 0.050 mmol). Single crystals suitable for X-ray diffraction studies were grown from a saturated DCM solution of **6-11** at −35 °C.

^{1}H NMR (400 MHz, 298 K, d_6-DMSO): δ 8.68 (d, $^{3}J_{HH}$ = 8.4 Hz, 2H, anion C<u>H</u>-4&5), 8.24 (d, $^{3}J_{HH}$ = 8.1 Hz, 2H, cation C<u>H</u>-4&5), 8.09 (dd, $^{3}J_{HH}$ = 8.0 Hz, $^{4}J_{HH}$ = 2.1 Hz, 2H, cation DMAP *o*-C<u>H</u>), 7.90 (dd, $^{3}J_{HH}$ = 8.1 Hz, $^{4}J_{HH}$ = 1.4 Hz, 2H, anion C<u>H</u>-1&8), 7.56–7.48 (m, 4H, cation C<u>H</u>-3&6 and anion C<u>H</u>-2&7), 7.36 (ddd, $^{3}J_{HH}$ = 8.4, 6.8 Hz, $^{4}J_{HH}$ = 1.5 Hz, 2H, anion C<u>H</u>-3&6), 7.30–7.26 (m, 2H, cation C<u>H</u>-2&7), 7.12 (dd, $^{3}J_{HH}$ = 7.9 Hz, $^{4}J_{HH}$ = 2.2 Hz, 2H, cation DMAP *o*-C<u>H</u>), 7.09–7.03 (m, 4H, cation C<u>H</u>-1&8 and cation DMAP *m*-C<u>H</u>), 6.59 (dd, $^{3}J_{HH}$ = 8.0 Hz, $^{4}J_{HH}$ = 3.2 Hz, 2H, cation DMAP *m*-C<u>H</u>), 3.14 (s, 6H, cation NMe), 3.07 (s, 6H, cation NMe).

^{19}F NMR (377 MHz, 298 K, d_6-DMSO): δ −134.1 (d, $^{3}J_{FF}$ = 26 Hz, 2F, cation *o*-C_6F_5), −134.6 to −134.8 (m, 6F, cation *o*-C_6F_5 and anion *o*-C_6F_5), −157.4 (t, $^{3}J_{FF}$ = 22 Hz, 1F, cation *p*-C_6F_5), −160.2 (t, $^{3}J_{FF}$ = 21 Hz, 2F, anion *p*-C_6F_5), −160.6 (t, $^{3}J_{FF}$ = 21 Hz, 1F, cation *p*-C_6F_5), −163.0 to −163.2 (m, 2F, cation *m*-C_6F_5), −164.8 to −165.0 (m, 4F, anion *m*-C_6F_5), −165.7 to −165.8 (m, 2F, cation *m*-C_6F_5).

^{11}B NMR (128 MHz, 298 K, d_6-DMSO): δ 10.3 (s, anion), 6.3 (br s, cation).

^{13}C{^{1}H} NMR (126 MHz, 298 K, d_6-DMSO), partial: δ 156.2 (s, DMAP *p*-<u>C</u>), 141.8 (br s, anion C9&10), 138.2 (s, cation DMAP *o*-<u>C</u>H), 136.4 (s, cation DMAP *o*-<u>C</u>H), 132.0 (s, cation C11&14), 131.9 (s, cation C12&13), 130.8 (s, cation C3&6), 129.1 (s, cation C2&7), 128.2 (s, cation C1&8), 125.5 (br s, anion C2&7), 124.5 (br s, anion C12&13), 124.1 (s, cation C4&5), 123.9 (br s, anion C11&14), 123.0 (br s, anion C4&5), 121.8 (br s, anion C3&6), 119.7 (br s, anion C1&8), 107.7 (s, cation DMAP *m*-<u>C</u>H), 107.2 (s, cation DMAP *m*-<u>C</u>H), 97.7 (cation C9&10). N-Me ^{13}C resonances overlap with the residual solvent peak.

Elemental Analysis calcd (%) for $C_{66}H_{36}B_2F_{20}N_4O_4$: C 58.69; H 2.69; N 4.15; Found: C58.17; H 2.71; N 3.99.

6.4.3 X-ray Crystallography

6.4.3.1 X-ray Collection and Reduction

Crystals were coated in Paratone-N oil in the glovebox, mounted on a MiTegen Micromount and placed under an N_2 stream, thus maintaining a dry, O_2-free environment for each crystal. The data were collected on a Bruker Kappa Apex II diffractometer. Data collection strategies were determined using Bruker Apex 2 software and optimized to provide >99.5% complete data to a 2θ value of at least 55°. The data were collected at 150(±2) K for all. The data integration and absorption correction were performed with the Bruker Apex 2 software package.[49]

6.4.3.2 X-ray Solution and Refinement

Non-hydrogen atomic scattering factors were taken from the literature tabulations.[50] The heavy atom positions were determined using direct methods employing the SHELX-2013 direct methods routine. The remaining non-hydrogen atoms were located from successive difference Fourier map calculations. The refinements were carried out by using full-matrix least squares techniques on F^2. All non-hydrogen atoms were assigned anisotropic temperature factors in the absence of disorder or insufficient data. In the latter cases, atoms were treated isotropically. C-bound H atoms were placed at calculated positions and allowed to ride on the carbon to which they are bonded during refinement. H-atom temperature factors were fixed at 1.20 times (central and P–H atoms) or 1.50 times (terminal CH_3 atoms) the isotropic temperature factor of the C-atom to which they are bonded. The locations of the largest peaks in the final difference Fourier map calculation as well as the magnitude of the residual electron densities in each case were of no chemical significance.

Table 6.2 – Selected crystallographic data for **6-1b**, **6-2b**, and **6-3b**.

	6-1b·½CH_2Cl_2	**6-2b**	**6-3b**·CH_2Cl_2
Formula	$C_{24.5}H_{11}BClF_{10}NO$	$C_{18}H_7BF_{10}O_2$	$C_{33}H_{10}BCl_2F_{15}O_2$
Formula weight	571.60	456.05	805.15
Crystal System	Triclinic	Triclinic	Triclinic
Space group	P-1	P-1	P-1
a (Å)	7.9256(5)	9.6859(9)	10.9016(11)
b (Å)	10.4169(7)	9.9325(10)	11.8469(11)
c (Å)	15.5360(11)	11.7449(13)	11.8554(12)
α (°)	74.952(3)	90.059(6)	84.408(5)
β (°)	79.132(3)	114.275(4)	80.506(5)
γ (°)	83.786(4)	119.145(4)	88.459(5)
V (Å^3)	1214.08(14)	870.39(16)	1502.9(3)
Z	2	2	2
Temp. (K)	150	150	150
d_{calc} (gcm^{-1})	1.564	1.740	1.7791
Abs. coeff. μ (mm^{-1})	0.254	0.183	0.344
Reflections Collected	19302	13198	26267
Data $F_o^2>3\sigma(F_o^2)$	5551	3970	6897
Variables	573	280	478
R	0.0693	0.0439	0.0459
R_w	0.1911	0.1112	0.0921
GOF	1.040	1.049	1.0285

Table 6.3 – Selected crystallographic data for **6-3c**, **6-3d**, and **6-4c**.

	2[**6-3c**]	**6-3d**	**6-4c**·½CH_2Cl_2
Formula	$C_{26}H_8BF_{10}O_2^{\bullet}$	$C_{20}H_8BF_5O_2$	$C_{28.5}H_9BClF_{10}O_2^{\bullet}$
Formula weight	553.14	386.10	619.65
Crystal System	Monoclinic	Monoclinic	Orthorhombic
Space group	$P2_1/c$	$P2_1/c$	Pbcn
a (Å)	13.1078(9)	7.047(2)	17.3619(10)
b (Å)	23.2873(19)	14.854(5)	20.3198(13)
c (Å)	14.0729(9)	15.221(6)	13.4759(8)
α (°)	90	90	90
β (°)	99.581(4)	97.455(10)	90
γ (°)	90	90	90
V ($Å^3$)	4235.8(5)	1579.7(9)	4754.2(5)
Z	8	4	8
Temp. (K)	150	150	150
d_{calc} (gcm^{-1})	1.735	1.6232	1.7313
Abs. coeff. μ (mm^{-1})	0.168	0.143	0.269
Reflections Collected	29808	13656	76541
Data $F_o^2>3\sigma(F_o^2)$	7452	2748	5472
Variables	703	252	396
R	0.0871	0.0772	0.0485
R_w	0.2181	0.1990	0.0885
GOF	1.039	1.0968	1.0415

Table 6.4 – Selected crystallographic data for **6-3h**, **6-4g**, and **6-5a**.

	6-3h	**6-4g**	**6-5a**·CH_2Cl_2
Formula	$C_{46}H_{38}BCoF_{10}O_2$	$C_{38}H_{18}BCoF_{10}O_2$	$C_{39}H_{36}BCl_2F_{10}O_2P$
Formula weight	882.55	766.31	839.36
Crystal System	Monoclinic	Monoclinic	Triclinic
Space group	$P2_1/c$	C2/c	P-1
a (Å)	11.0423(8)	25.3133(18)	12.1938(19)
b (Å)	16.9039(13)	15.9662(18)	12.1954(17)
c (Å)	21.2807(14)	16.4000(13)	14.403(2)
α (°)	90	90	95.074(8)
β (°)	97.057(3)	117.857(7)	104.765(8)
γ (°)	90	90	110.310(7)
V ($Å^3$)	3942.1(5)	5860.1(10)	1905.0(5)
Z	4	8	2
Temp. (K)	150	150	150
d_{calc} (gcm^{-1})	1.4869	1.7370	1.463
Abs. coeff. μ (mm^{-1})	0.523	0.689	0.296
Reflections Collected	33408	47154	32134
Data $F_o^2>3\sigma(F_o^2)$	9073	6735	8691
Variables	540	468	496
R	0.0524	0.0470	0.0488
R_w	0.1267	0.0727	0.1124
GOF	1.0642	1.0326	1.016

Table 6.5 – Selected crystallographic data for **6-5b**, **6-6a**, and **6-6b**.

	6-5b·CH_2Cl_2	**6-6a**	**6-6b**·C_7H_8
Formula	$C_{39}H_{38}BCl_2F_{10}O_2P$	$C_{44}H_{22}BF_{10}O_2P$	$C_{51}H_{30}BF_{10}O_2P$
Formula weight	841.37	814.39	906.53
Crystal System	Orthorhombic	Triclinic	Monoclinic
Space group	Pbca	P-1	C2/c
a (Å)	20.116(6)	11.5384(9)	35.141(3)
b (Å)	16.403(3)	12.4340(10)	12.6854(11)
c (Å)	23.728(6)	14.3574(11)	19.7553(15)
α (°)	90	100.016(3)	90
β (°)	90	103.120(3)	110.047(7)
γ (°)	90	112.579(3)	90
V ($Å^3$)	7829(3)	1772.5(2)	8272.9(13)
Z	8	2	8
Temp. (K)	150	150	150
d_{calc} (gcm^{-1})	1.428	1.526	1.456
Abs. coeff. μ (mm^{-1})	0.289	0.171	0.155
Reflections Collected	38234	28943	69597
Data $F_o^2>3\sigma(F_o^2)$	8790	8107	9533
Variables	500	523	649
R	0.0606	0.0569	0.0446
R_w	0.1333	0.1442	0.1192
GOF	1.007	1.037	1.066

Table 6.6 – Selected crystallographic data for **6-10a**, **6-11** and **6-7a**.

	6-10a·CH_2Cl_2	**6-11**·$2CH_2Cl_2$	**6-7a**
Formula	$C_{48}H_{33}BCl_2F_{10}N_2O_2$	$C_{68}H_{40}B_2Cl_4F_{20}N_4O_4$	$C_{46}H_{22}BF_{10}O_2P$
Formula weight	941.47	1520.46	838.42
Crystal System	Monoclinic	Triclinic	Triclinic
Space group	$P2_1/c$	P-1	P-1
a (Å)	14.349(2)	11.331(3)	12.1499(6)
b (Å)	14.6217(18)	14.461(4)	12.2300(6)
c (Å)	21.734(3)	20.313(5)	14.2517(7)
α (°)	90	79.494(14)	67.943(3)
β (°)	103.312(7)	76.280(13)	72.004(3)
γ (°)	90	80.221(14)	68.902(3)
V ($Å^3$)	4437.3(10)	3151.3(13)	1793.79(15)
Z	4	2	2
Temp. (K)	150	150	150
d_{calc} (gcm^{-1})	1.409	1.602	1.552
Abs. coeff. μ (mm^{-1})	0.230	0.303	0.172
Reflections Collected	26972	54307	30908
Data $F_o^2>3\sigma(F_o^2)$	7823	14521	8212
Variables	614	952	541
R	0.0507	0.0804	0.0407
R_w	0.1129	0.1980	0.1149
GOF	1.018	1.037	0.893

Table 6.7 – Selected crystallographic data for **6-7b** and **6-8a**.

	6-7b·$2CH_2Cl_2$	**6-8a**·C_5H_{12}
Formula	$C_{48}H_{26}BCl_4F_{10}O_2P$	$C_{45}H_{30}BF_{10}O_2P$
Formula weight	1008.27	834.47
Crystal System	Triclinic	Triclinic
Space group	P-1	P-1
a (Å)	11.266(13)	11.9389(6)
b (Å)	14.188(16)	12.3205(7)
c (Å)	15.869(18)	13.4662(7)
α (°)	93.22(3)	75.071(3)
β (°)	109.04(3)	79.753(3)
γ (°)	106.77(5)	76.984(3)
V ($Å^3$)	2264(5)	1849.58(17)
Z	2	2
Temp. (K)	150	150
d_{calc} (gcm^{-1})	1.479	1.498
Abs. coeff. μ (mm^{-1})	0.378	0.166
Reflections Collected	13789	31790
Data $F_o^2>3\sigma(F_o^2)$	7626	8532
Variables	650	536
R	0.0810	0.0477
R_w	0.2234	0.1279
GOF	1.121	1.023

6.5 References

(1) Gomberg, M. *Journal of the American Chemical Society* **1900**, *22*, 752–757.

(2) *Stable Radicals: Fundamentals and Applied Aspects of Odd-Electron Compounds*; Hicks, R. G., Ed.; John Wiley & Sons Ltd: West Sussex, 2010.

(3) Hicks, R. G. *Organic & Biomolecular Chemistry* **2007**, *5*, 1321.

(4) Power, P. P. *Chemical Reviews* **2003**, *103*, 789–809.

(5) Krause, E.; Polack, H. *Berichte der Deutschen Chemischen Gesellschaft* **1926**, *59*, 777–

785.

(6) Leffler, J. E.; Watts, G. B.; Tanigaki, T.; Dolan, E.; Miller, D. S. *Journal of the American Chemical Society* **1970**, *92*, 6825–6830.

(7) Olmstead, M. M.; Power, P. P. *Journal of the American Chemical Society* **1986**, *108*, 4235–4236.

(8) Zettler, F.; Hausen, H. D.; Hess, H. *Journal of Organometallic Chemistry* **1974**, *107*, 832–837.

(9) Blount, J. F.; Finocchiaro, P.; Gust, D.; Mislow, K. *Journal of the American Chemical Society* **1973**, *95*, 7019–7029.

(10) Kwaan, R. J.; Harlan, C. J.; Norton, J. R. *Organometallics* **2001**, *20*, 3818–3820.

(11) Berndt, A.; Klusik, H.; Schluter, K. *Journal of Organometallic Chemistry* **1981**, *222*, 25–27.

(12) Eaton, G. R. *Inorganic Nucleus Chemistry Letters* **1972**, *8*, 643–646.

(13) Baban, J. A.; Goodchild, N. J.; Roberts, B. P. *Journal of the Chemical Society, Perkin Transactions 2* **1986**, 157–161.

(14) Stegmann, H. B.; Denninger, G.; Scheffler, K. *Tetrahedron Letters* **1979**, *20*, 3689–3690.

(15) Bubnov, N. N.; Solodovnikov, S. P.; Prokof, A. I.; Kabachnik, M. I. *Russian Chemical Reviews* **1978**, *47*, 549–571.

(16) Alberti, A.; Pedulli, G. F. *Journal of Organometallic Chemistry* **1985**, *297*, 13–19.

(17) Pal, S. K.; Itkis, M. E.; Tham, F. S.; Reed, R. W.; Oakley, R. T.; Haddon, R. C. *Science* **2005**, *309*, 281–284.

(18) Pal, S. K.; Bag, P.; Itkis, M. E.; Tham, F. S.; Haddon, R. C. *Journal of the American Chemical Society* **2014**, *136*, 14738–14741.

(19) Dahcheh, F.; Martin, D.; Stephan, D. W.; Bertrand, G. *Angewandte Chemie International Edition* **2014**, *53*, 13159–13163.

(20) Bissinger, P.; Braunschweig, H.; Damme, A.; Krummenacher, I.; Phukan, A. K.; Radacki, K.; Sugawara, S. *Angewandte Chemie International Edition* **2014**, *53*, 7360–7363.

(21) Bertermann, R.; Braunschweig, H.; Dewhurst, R. D.; Hörl, C.; Kramer, T.; Krummenacher, I. *Angewandte Chemie International Edition* **2014**, *53*, 5453–5457.

(22) Ueng, S. H.; Solovyev, A.; Yuan, X.; Geib, S. J.; Fensterbank, L.; Lacôte, E.; Malacria, M.; Newcomb, M.; Walton, J. C.; Curran, D. P. *Journal of the American Chemical Society* **2009**, *131*, 11256–11262.

(23) Curran, D. P.; Solovyev, A.; Makhlouf Brahmi, M.; Fensterbank, L.; Malacria, M.; Lacôte, E. *Angewandte Chemie International Edition* **2011**, *50*, 10294–10317.

(24) Chiu, C. W.; Gabbaï, F. P. *Angewandte Chemie International Edition* **2007**, *46*, 1723–1725.

(25) Rosenthal, A. J.; Devillard, M.; Miqueu, K.; Bouhadir, G.; Bourissou, D. *Angewandte Chemie International Edition* **2015**, *54*, 9198–9202.

(26) Aramaki, Y.; Omiya, H.; Yamashita, M.; Nakabayashi, K.; Ohkoshi, S. I.; Nozaki, K. *Journal of the American Chemical Society* **2012**, *134*, 19989–19992.

(27) Ménard, G.; Hatnean, J. A.; Cowley, H. J.; Lough, A. J.; Rawson, J. M.; Stephan, D. W. *Journal of the American Chemical Society* **2013**, *135*, 6446–6449.

(28) Cardenas, A. J. P.; Culotta, B. J.; Warren, T. H.; Grimme, S.; Stute, A.; Fröhlich, R.; Kehr, G.; Erker, G. *Angewandte Chemie International Edition* **2011**, *50*, 7567–7571.

(29) Sajid, M.; Stute, A.; Cardenas, A. J. P.; Culotta, B. J.; Hepperle, J. a M.; Warren, T. H.; Schirmer, B.; Grimme, S.; Studer, A.; Daniliuc, C. G.; Fröhlich, R.; Petersen, J. L.; Kehr, G.; Erker, G. *Journal of the American Chemical Society* **2012**, *134*, 10156–10168.

(30) Pereira, J. C. M.; Sajid, M.; Kehr, G.; Wright, A. M.; Schirmer, B.; Qu, Z.; Grimme, S.; Erker, G.; Ford, P. C. *Journal of the American Chemical Society* **2014**, *136*, 513−519.

(31) Liedtke, R.; Scheidt, F.; Ren, J.; Schirmer, B.; Cardenas, A. J. P.; Daniliuc, C. G.; Eckert, H.; Warren, T. H.; Grimme, S.; Kehr, G.; Erker, G. *Journal of the American Chemical Society* **2014**, *136*, 9014–9027.

(32) Liedtke, R.; Eller, C.; Daniliuc, C. G.; Williams, K.; Warren, T. H.; Tesch, M.; Studer, A.; Kehr, G.; Erker, G. *Organometallics* **2016**, *35*, 55–61.

(33) Türkyilmaz, F.; Kehr, G.; Li, J.; Daniliuc, C. G.; Tesch, M.; Studer, A.; Erker, G. *Angewandte Chemie International Edition* **2016**, *55*, 1470–1473.

(34) Tao, X.; Kehr, G.; Wang, X.; Daniliuc, C.; Grimme, S.; Erker, G. *Chemistry - A European Journal* **2016**, *22*, 9504–9507.

(35) Hellstrom, S. L.; Ugolotti, J.; Britovsek, G. J. P.; Jones, T. S.; White, A. J. P. *New Journal of Chemistry* **2008**, *32*, 1379–1387.

(36) Mahdi, T.; del Castillo, J. N.; Stephan, D. W. *Organometallics* **2013**, *32*, 1971–1978.

(37) Calderazzo, F.; Forte, C.; Marchetti, F.; Pampaloni, G.; Pieretti, L. *Helvetica Chimica Acta* **2004**, *87*, 781–789.

(38) Mahdi, T.; Stephan, D. W. *Journal of the American Chemical Society* **2014**, *136*, 15809–

15812.

(39) Scott, D. J.; Fuchter, M. J.; Ashley, A. E. *Journal of the American Chemical Society* **2014**, *136*, 15813–15816.

(40) Longobardi, L. E.; Tang, C.; Stephan, D. W. *Dalton Transactions* **2014**, *43*, 15723–15726.

(41) Longobardi, L. E.; Liu, L.; Grimme, S.; Stephan, D. W. *Journal of the American Chemical Society* **2016**, *138*, 2500–2503.

(42) Holthausen, M. H.; Bayne, J. M.; Mallov, I.; Dobrovetsky, R.; Stephan, D. W. *Journal of the American Chemical Society* **2015**, *137*, 7298–7301.

(43) Xu, B.-H.; Kehr, G.; Fröhlich, R.; Wibbeling, B.; Schirmer, B.; Grimme, S.; Erker, G. *Angewandte Chemie International Edition* **2011**, *50*, 7183–7186.

(44) Rahman, M. M.; Liu, H.-Y.; Eriks, K.; Prock, A.; Giering, W. P. *Organometallics* **1989**, *8*, 1–7.

(45) Uneyama, K. In *Organofluorine Chemistry*; Blackwell Publishing, 2007; pp 1–100.

(46) Sasaki, S.; Yoshifuji, M. *Current Organic Chemistry* **2007**, *11*, 17–31.

(47) Wurz, R. P. *Chemical Reviews* **2007**, *27*, 5570–5595.

(48) Venkataramana, G.; Dongare, P.; Dawe, L. N.; Thompson, D. W.; Zhao, Y.; Bodwell, G. J. *Organic Letters* **2011**, *13*, 2240–2243.

(49) *Bruker AXS Inc.*; 2013.

(50) Cromer, D. T.; Waber, J. T. In *International Tables for X-Ray Crystallography*; Kynoch Press: Birmingham, 1974; pp 71–147.

Chapter 7
Conclusion

7.1 Thesis Summary

The work presented in this thesis explored the reactivity of $B(C_6F_5)_3$ as the Lewis acidic component of a frustrated Lewis pair, in combination with novel substrates and/or Lewis basic components. A unifying theme throughout this document is the synthesis of novel main group heterocycles and their subsequent reactivity. The main observations and conclusions are summarized below:

First, *para*-methoxyanilines can act as frustrated Lewis bases. These sterically encumbered amines, in combination with $B(C_6F_5)_3$, were found to heterolytically split H_2 and undergo subsequent reduction to 7-azabicyclo[2.2.1]heptane hydridoborate salts. This was exploited to make a small family of substrates. Quinoline substrates with alkenes and alkynes tethered at the 2-position were found to preferentially undergo addition across the C–C π-bond when combined with $B(C_6F_5)_3$, instead of an aromatic reduction. Various different heterocyclic products were generated using this methodology.

N-Sulfinylamines were explored as substrates in FLP chemistry, and combinations of sterically frustrated phosphines and boranes (or alanes) were found to undergo 1,3-addition across the R–N=S=O functional group. These adducts were postulated to behave as phosphinimine-borane (or alane) adducts of sulfur monoxide, and were indeed found to transfer SO to PPh_3, Wilkinson's complex, and SIMes.

Low coordinate phosphorus compounds were evaluated as potential substrates for FLP activation. Triphosphabenzene **4-1** was found to activate H_2 without a catalyst, which was the first example of an uncatalyzed hydrogenation of an aromatic ring. The mechanism of this transformation was experimentally and computationally examined. Phosphaalkynes **4-11** and **4-13** did not behave like analogous C≡C bonds when treated with FLPs, however they were found to undergo hydroboration with $HB(C_6F_5)_2$ to yield P_2B_2 heterocycles from an unexpected regiochemical addition.

Lastly, Chapters 5 & 6 examined the reactivity of carbonyl compounds when exposed to $B(C_6F_5)_3$ and H_2. Aliphatic ketones and aldehydes were found to undergo stoichiometric

reduction to yield borinic esters, however polyaromatic diones were found to yield stable borocyclic radical species **6-3c** and **6-4c**. The mechanism of this reaction was investigated, and their reactivity with one-electron reductants was described. The boron radicals were also found to react with a variety of P-, N-, and C-based nucleophiles to furnish diamagnetic zwitterionic species.

7.2 Future Work

The work presented in this thesis is predominantly focused on the fundamental chemistry of various main group heterocycles. While preliminary reactivity has been explored, there remains a plethora of unexplored chemistry for many of these systems. Some of these avenues are currently under investigation, while others will be explored at a later date.

The aromatic reduction work presented in Chapter 2 can certainly be applied to target-oriented syntheses. It is now understood that tethered alkenes and alkynes are not tolerated for aromatic reductions of N-heterocycles, however no further substrates were explored. It is possible that other valuable organic products can be accessed by FLP aromatic reduction chemistry, as was demonstrated by Du and co-workers.[1] Additionally, the $B(C_6F_5)_3$-mediated reduction of -OMe substituents could have applications in other syntheses, where -OMe would behave as a leaving group.

Significant efforts have been made towards expanding the application of **3-4** as a source of sulfur monoxide. While it is believed to proceed through an associative mechanism, a thorough investigation of this process would provide further insight. Collaborative efforts with the Betley group at Harvard University, the Harder group at Friedrich-Alexander-Universität, and the Armstrong group at Olivet Nazarene University are ongoing, with the goal of stabilizing SO on different metal complexes or clusters. The behaviour of R-N=S=O compounds in combination with other types of Lewis acids, including fluorophosphonium cations, is currently under investigation by other students in the Stephan group.

The discovery of the unanticipated reactivity of **4-1** with H_2 has led to the systematic exploration of other uncatalyzed E–H additions (E = Sn, Ge, Si, P) to triphosphabenzene rings. This endeavor has been undertaken in collaboration with the Russell group at the University of Bristol. The reactivity of **4-1** with HD is currently being reexamined computationally by Prof.

John McGrady at the University of Oxford. The phosphaalkyne hydroboration project led to products **4-12** and **4-14**, which could potentially act as precursors to the elusive $\sigma^3\lambda^5$–phosphaalkyne, R–C≡P(BR')$_2$.[2] This will be investigated by TGA analysis. The monomeric units of **4-12** and **4-14** may also find application in coordination chemistry or FLP chemistry.

The research project pertaining to the generation and reactivity studies on boron radicals **6-3c** and **6-4c** is in its infancy. Reduction chemistry of related mono- and di-imine substrates is an ongoing project in the Stephan group. The luminescent properties of zwitterions **6-5a**–**6-11** have yet to be examined, and a collaborative effort with the Marder group at the Universität Würzburg has been established for this purpose. There is also interest in extending this method to the synthesis to 1,10-phenanthroline-5,6-dione derivatives, with the goal of ligating boron radicals to metal centres.

7.3 References

(1) Liu, Y.; Du, H. *Journal of the American Chemical Society* **2013**, *135*, 12968–12971.

(2) Regitz, M.; Binger, P. *Angewandte Chemie International Edition* **1988**, *27*, 1484–1508.

Copyright Acknowledgements